MODELLING OF TRANSIENT HEAT TRANSFER IN ANNEALING FURNACES

by

TAGELSIR MUSTAFA ABDELSALAM

A thesis submitted for the degree of Doctor of Philosophy in Chemical Engineering.

Department of Chemical Engineering,
University of Aston in Birmingham

October, 1979

MODELLING OF TRANSIENT HEAT TRANSFER IN ANNEALING FURNACES

BY

TAGELSIR MUSTAFA ABDELSALAM

A Thesis submitted for the Degree of Doctor of Philosophy in Chemical Engineering, 1979.

SYNOPSIS

This is a study of heat transfer in a lift-off furnace which is employed in the batch annealing of a stack of coils of steel strip. The objective of the project is to investigate the various factors which govern the furnace design and the heat transfer resistances, so as to reduce the time of the annealing cycle, and hence minimize the operating costs.

The work involved mathematical modelling of patterns of gas flow and modes of heat transfer. These models are: Heat conduction and its conjectures in the steel coils; Convective heat transfer in the plates separating the coils in the stack and in other parts of the furnace; and Radiative and convective heat transfer in the furnace by using the long furnace model. An important part of the project is the development of numerical methods and computations to solve the transient models.

A limited number of temperature measurements was available from experiments on a test coil in an industrial furnace. The mathematical model agreed well with these data. The model has been used to show the following characteristics of annealing furnaces, and to suggest further developments which would lead to significant savings:

. The location of the limiting temperature in a coil is nearer to the hollow core than to the outer periphery.

. Thermal expansion of the steel tends to open the coils, reduces their thermal conductivity in the radial direction, and hence prolongs the annealing cycle. Increasing the tension in the coils and/or heating from the core would overcome this heat transfer resistance.

. The shape and dimensions of the convective channels in the plates have significant effect on heat convection in the stack. An optimal design of a channel is shown to be of a width-to-height ratio equal to 9.

. Increasing the cooling rate, by using a fluidized bed instead of the normal shell and tube exchanger, would shorten the cooling time by about 15%, but increase the temperature differential in the stack.

. For a specific charge weight, a stack of different-sized coils will have a shorter annealing cycle than one of equally-sized coils, provided that production constraints allow the stacking order to be optimal.

. Recycle of hot flue gases to the firing zone of the furnace would produce a decrease in the thermal efficiency up to 30% but decreases the heating time by about 26%.

MODELLING, CONDUCTION, FURNACE, RADIATION, COMPUTATION.

بسم الله الرحمن الرحيم

IN THE NAME OF ALLAH, THE BENEFICIENT, THE MERCIFUL

ACKNOWLEDGEMENT

First of all, praise be to ALLAH, who created man with mind, and granted him knowledge.

Secondly, I wish to express my thanksgiving and gratitude to Dr. D.A. Lihou for his exceptional supervision of this work and constructive comments on the thesis.

Thirdly, I wish to extend my thanks to Dr. B. Gay for encouragement and useful suggestions.

Fourthly, I wish to acknowledge my gratitude to Wellman Incandescent Limited in recognition of cooperation and help, especially of arranging useful visits to the research centre and some steelworks of British Steel Corporation, and of allowing access to industrial information and practical data.

Finally, I wish to give my thanks to Mrs. N. Armstrong for her patient and accurate typing of this thesis.

CONTENTS

NOMENCLATURE

Symbol	Description	Units
a_g	weighting factor of grey component of gas medium	dimensionless
A	area	m^2
$B_{(n)}$	height of channels in convector plate (n)	m
C_p	specific heat	kWh/kg/K
D_2	diameter of the cover	m
D_4	outer diameter of the furnace casing	m
D_e	diameter of exhaust duct	m
D_H	hydraulic mean diameter	m
D_{hol}	diameter of central hole in convector plate	m
$DI_{(m)}$	inner diameter of coil (m)	m
$DO_{(m)}$	outer diameter of coil (m)	m
D_p	diameter of convector plate	m
D_r	diameter of refractory wall	m
E	black emissive power	kW/m^2
f	friction factor	dimensionless
F_{cor}	gas flow rate in the core of the stack	kg/h
F_{ij}	view factor between i and j	dimensionless
$F_{p(n)}$	gas flow rate in plate (n)	kg/h
F_t	total flow rate of gas	kg/h
$FG_{(m)}$	gas flow rate between the cover and coil (m)	kg/h
g	acceleration due to gravity	m/h^2
g_c	conversion factor	$kgm/N/h^2$

Symbol	Description	Units
$(\overline{GS}_1)_R$	total exchange area between the gas zone and surface zone 1 in presence of refractory	m^2
$(\overrightarrow{GS}_1)_R$	directed exchange area from gas to sink in presence of refractory	m^2
$(\overleftarrow{GS}_1)_R$	directed exchange area from sink zone 1 to gas with refractory	m^2
h	local heat transfer coefficient	$kW/m^2/K$
H	enthalpy	kW
H	incident flux	kW/m^2
H	total height of stack	m
$H_{(m)}$	height of coil (m)	m
H_e	clearance between exhaust duct and top of the cover	m
H_r	height of refractory wall	m
k	absorption coefficient of grey component	dimensionless
K	thermal conductivity	kW/m/K
L	length of convector channel	m
L_m	mean beam length of intervening gas	m
m_f	firing rate of fuel	kg/h
m_g	flow rate of combustion products	kg/h
$NC_{(n)}$	number of channels in convector plate (n)	dimensionless
p_{CO_2}	partial pressure of CO_2	atm
p_{H_2O}	partial pressure of water vapour	atm
p_t	total pressure drop in the stack	mm.w.g.
p	sum of partial pressures of CO2 and water vapour	atm

Symbol	Description	Units
q	flux density	kW/m^2
$\dot{Q}$	heat rate	kW
r	radial coordinate in the coil	m
r_H	hydraulic mean radius	m
R	radius of curvature of dished top of the cover	m
$R_{(n)}$	fraction of total gas flow passing through plate (n)	dimensionless
T	point temperature in the coil	K
T_o	datum temperature	K
T_2	cover temperature	K
T_a	ambient temperature	K
T_c	temperature of gas leaving the cooler	K
T_d	adiabatic flame temperature	K
$T_{f\ell}$	temperature of flue gases	K
T_{fn}	temperature of inert gas at the fan	K
T_{fr}	temperature of furnace gas	K
T_{gc}	temperature of gas in the central core of stack	K
$T_{gi(n)}$	temperature of gas entering plate (n)	K
T_{ij}	temperature of the coil at position ij	K
T_{tc}	temperature of the top of the cover	K
T_{tp}	temperature of the top convector plate	K
u	viscosity correction factor for convective heat transfer	dimensionless
U	overall velocity of inert gas	m/h
U	overall heat transfer coefficient	$kW/m^2/K$

Symbol	Description	Units
U	correction factor for effective conductivity in the radial direction in the coil	dimensionless
V	fan capacity	$m^3/_{min}$
W	radiosity	kW/m^2
W_i	width of convector channel at gas exit	m
W_o	width of convector channel at gas entry	m
x	proportion of excess air in the firing mixture	kg/kg
x	distance-to-diameter ratio for entry effect on convection	dimensionless
x	thickness of gap between adjacent coil laps	m
Y	correction for entry effect on convection	dimensionless
z	axial coordinate in the coil	m
α	gas absorptivity	dimensionless
β	coefficient of volumetric expansion	1/K
δ	thickness of steel sheet	m
Δ	temperature differential	K
ε	emissivity	dimensionless
η	thermal efficiency	dimensionless
μ	dynamic viscosity	kg/m/h
λ	coefficient of linear expansion of steel	1/K
ρ	reflectivity	dimensionless
ρ	density	kg/m^3
σ	Stefan Boltzmann constant	$kW/m^2/K^4$
θ	time	h
τ	transmissivity	dimensionless

Subscripts

b	bulk flow of gas
c	combustion products
f	fuel
g	gas
gs	gas property evaluated at sink temperature
i	radial position in the coil
j	axial position in the coil
k	beginning of time interval
k+1	end of time interval
m	coil number in stack (m = 1 is the bottom coil)
R	refractory
s	steel
w	wall

CHAPTER ONE

INTRODUCTION

INTRODUCTION

1.1 Furnaces in Industrial Practice

A furnace is a device in which energy is released in the form of heat and then used to raise the temperature and/or change the chemical or physical nature of the materials within its enclosure. To economize on the use of energy (eg fuel) in a furnace, both processes of energy conversion to heat and heat transfer to the sink need to be carried out with maximum thermal efficiency and as quickly as possible, while keeping the optimum balance between the two processes.

There are many types of furnaces varying in geometry and heating characteristics. Furnaces are classified according to either their purposes or their level of temperature. All types of furnaces are used in most industrial installations, from heavy ceramics and steelworks to lighter chemical process industries. High-temperature furnaces are mainly applied in ceramics, glass and steel industries. The annealing furnace, studied here, is an example of a high-temperature furnace which is classified according to its function.

Furnace technology is the concern of many engineering and scientific disciplines. The engineers' interest in furnaces is vested in their interest in the design of devices and processes which are dependent mainly on heat supply. The metallurgical industries have larger experience than many other industries which are involved in

furnace practice. Most of the modern high quality refractories and the early developments in furnace technology have been carried out in the steel industry. However, the chemical process industries have contributed largely in the recent developments of reactor furnaces and process heaters. An industrial survey of heaters for chemical reactors is given by Lihou[1], 1975.

1.2 Literature on Furnace Modelling

In a fuel-fired furnace, the process of energy transfer, from the mixture of fuel and air entering the combustion zone to the heat-sink surface disposed near the walls entails a series of complex processes. This series involves a combination of the following problems:

- fluid mechanics
- molecular and turbulent diffusion
- kinetics of chemical reaction
- radiation from gas and solid particles
- absorption of radiation by solids and gases
- reradiation from refractory surfaces
- natural and forced convection
- wall conduction, etc.

All of the above processes are not susceptible to rigorous mathematical representation. However, simplified mathematical models which are based on key factors only, can be used with the aid of computers to investigate the effects of these factors on furnace performance.

In high-temperature furnaces, like the annealing furnace, operating at more than 800°C, radiation is the dominant mode of heat transfer. Investigations of the performance of furnaces and combustion chambers is intended to provide information which gives quantitative insight to furnace design. This information, replacing the rule-of-thumb approach, would allow the calculation of local flow properties and wall heat transfer to be put on a firm quantitative basis. However, fundamental understanding of mixing and reaction processes, with detailed data, are deficient. This is because of the complexity of these processes in furnaces and combustion chambers.

There is a vast literature on radiation, but many of the exact solutions of radiative transfer are too restrictive for direct application in furnaces. Hottel and Sarofim[2] in their book "Radiative Transfer", 1967 compiled all the equations and relationships required in the modern methods of furnace design. Methods, like the zone method[3], the long furnace [4,5] and the stirred furnace[6,7] models require the calculation of the total exchange areas, if the furnace gas is assumed to be grey, or the directed flux areas otherwise. The flux method[8] of furnace design deals with modelling of radiative heat transfer through gases with surfaces providing the boundary conditions for the differential equations of heat transfer in the furnace. In the case of Monte Carlo methods[9,10] of furnace modelling, the furnace is divided into gas and surface zones and the radiative transfer between these

zones is considered as parcels of radiation moving about in a random manner; therefore, no exchange areas are evaluated. The long furnace model is discussed in detail in Chapter 3.

The methods of furnace modelling also require the calculation of the gas emissivity through the calculation of mean beam length of the gaseous medium in the furnace. Hadvig[11] developed a correlation for the gas emissivity. He plotted emissivity charts for CO_2 and H_2C partial pressure ratios of 1 and 2 on the basis of Hottel's charts[2]. He used a dimensionless absolute temperature of furnace gas and a factor which is constant for a wide range of emissivities. This gas emissivity is calculated in Chapter 6.

The phenomena of turbulent gas flow and heat transfer by radiation occur in a furnace and interact through the energy balance. Usually, isothermal physical models of furnaces are required to evaluate the convective data; however, the use of entirly mathematical models to predict furnace performance is more practical. Some researchers have used scale prediction by similarity criteria to correlate the flow patterns and combustion in the furnace[1]. When the system is highly turbulent or when the geometry of the furnace and the burner arrangment are to be developed, physical models using air or water at ambient temperature are more useful than mathematical models; although the collection of data takes more time and changing the system geometry is more laborious than changing a computer program.

Generally speaking, experimental investigation is time consuming and very expensive, especially when conducted on furnaces. This is because extensive measurements are required to cover all the factors affecting the investigated flows in the furnace. Predictive procedures can provide an alternative route to lead the development in furnace design and operation. Mathematical modelling enables the furnace performance to be estimated rapidly and reliably without using experimentation; hence avoiding the inherently large costs. Computer predictions are only valuable when their reliability has been confirmed. The reliability can be confirmed only by testing the prediction performance in practical situations. Once the validation of the computational procedure is established, then the detailed experiments can be dispensed with.

1.3 Layout of the Thesis

The thesis is concerned mainly with transient heat transfer in an annealing furnace. It starts by introducing the fundamental metallurgical aspects of steel annealing and the effect of heat on annealed steel sheets. This is shown in Chapter 2 with brief description of the lift-off cover furnace which is used in batch annealing of coils of steel strip.

In Chapter 3, the modern predictive methods of furnace modelling are presented. Detailed discussion of the long furnace model, which has been implemented in this project, is included. Also the combustion equations,

furnace temperature, fuel firing rate and the thermal efficiency are calculated.

Chapter 4 deals with patterns of gas flow in the furnace. The pressur drop in various parts of the furnace and in the convector plates are calculated. An algorithm for the computation of flow distribution between the convector plates is presented. Equations of heat convection and radial temperature profile of the gas in the plates, are developed.

The model of heat conduction in a steel coil and the correlation of effective conductivity in the radial direction in the coil have been derived in Chapter 5. Also, the numerical methods for the solution of the partial differential equations of conduction have been discussed in this Chapter.

All types of heat fluxes between the coils, the inner cover and the furnace side are shown in Chapter 6. In this chapter also, heat transfer in the core of the stack, at the top of the stack and heat exchange within the surrounding atmosphere, during cooling, are discussed.

The programming procedure for the computation of the model is outlined in Chapter 7. In Chapter 8, the results of computation are tabulated, shown as graphs and discussed. Chapter 9 summarizes the conclusions drawn from the predictive study of the model and comments on the use and practicability of these conclusions. Some

remarks on further work and devlopment in this area are mentioned in Chapter 9 as well.

CHAPTER TWO

THE ANNEALING FURNACE

THE ANNEALING FURNACE

2.1 Annealing of Steel

Annealing is one of the most important operations, in steel making, which affects the quality of the finished product, namely its ductility and surface finish. Mild steel strip, sheet or plate may be annealed to improve a particular property; for example to decrease the ductile-brittle temperature. However, the annealing treatment considered in this project is the one which is designed to make the material suitable for subsequent drawing and pressing operations.

The cold work, during the cold rolling operations, distorts the crystalline form of steel grains and hence destroys its ductility. The annealing[12] process is required to regain the lost ductility of the material. Ductility is a function of the annealing cycle and many other parameters like steel composition, hot mill rolling, amount of cold reduction, temper rolling, etc.

Annealing of steel is made by heating the metal in a controlled inert atmosphere to the recrystallization temperature, then soaking by holding at this temperature for a certain time, and finally, cooling to a temperature at which ambient air does not oxidize the steel.

The controlled inert gas is used to prevent the oxidation of steel during annealing. In some[13] annealing techniques, the inert atmosphere contains reducing gases

which help removing films of oxides formed during the treatment. In other applications, it is found possible to shorten the annealing cycle by using active gas mixtures which reduce the carbon content of mild steel.

Because the heating rate of the batch annealing furnace is relatively slow, the temperature rise does not actually affect the grain size considerably. It is the combined effect of the annealing temperature together with the soaking time that generates the required change in the metallurgical properties through controlling the extent to which the carbide particles coalesce. The annealing of steel is influenced by the quality of the ore as well as the blast furnace practice implemented in the metal making. This eventually affects the hardness and ductility of the end product.

Annealing of steel normally takes place, between its lower and upper critical temperatures of 680^{o}C and 720^{o}C respectively, to soften the steel before undergoing forming operations. Once the temperature exceeds the lower critical temperature of steel, the recrystallization of the grains starts slowly and then increases at a rate which varies with the temperature and the quality of steel. On holding at the annealing temperature for a specific time (soaking), the recrystallization will be completed. It is worth mentioning that the steel temperature should not exceed its upper critical temperature since that will upset the recrystallized structure of the metal.

Although there are some continuous annealing techniques, yet the annealing of steel is usually carried out as a batch process, in a lift-off cover furnace which will be described in the following sections of this chapter.

2.1.1 Historical Review of Lift-Off Furnace[14]

Early in the century, the bulk of tinplate and sheet was produced by hot rolling of steel bars in two-high operated mills. Then the three-high mechanized mills were developed to handle sheet bars from continuous heating furnaces with automatic discharge of hot rolled sheets. These sheets were characterized by their equiaxed structure, reduced grain size and improved drawing properties.

The conventional annealing furnace which handles the product of hand mills was of static type, and had ball races in the hearth to support and convey the load. This furnace was arranged with a cast steel dish or base. During the third decade of this century, many car and bogie type furnaces were introduced in the steel industry. These furnaces were implemented in continuous annealing of both sheet and tinplate, and resulted in substantial savings in fuel consumption as compared with the static furnaces. After that, followed the development of high-speed and large capacity mills, which produced both hot and cold rolled material in coil form. This development tendered hand mills, mechanized mills, semi-continuous

mills and their ancilliary processes obsolescent regardless of some increase in their rate. This is the stage which leads to the design and application of radiant tubes, lift-off cover furnaces adopted in the annealing of products from continuous mills either in coil or flat form, see Fig. 2.1.

2.1.2 Lift-Off Cover Furnace

The basic objectives and functions of the portable cover furnace are the following:

(i) to obtain the maximum uniformity or the minimum temperature differential through the charge during heating, soaking and cooling stages of annealing.

(ii) to carry out the annealing with full prevention of chemical reaction to preserve the clean surface finish of the material. This protection of steel is maintained by the special protective gas whose chemical composition is controlled within critical limits during heating, soaking and cooling phases of annealing.

(iii) to achieve the highest thermal efficiency in relation to the prescribed annealing cycle, variations in loading and type of charge.

(iv) to conduce an effective degree of automatic control of load temperature and pressure requirements of the furnace.

For coil annealing in lift-off furnaces, the load is usually arranged in tight coils of 1.8-2.2

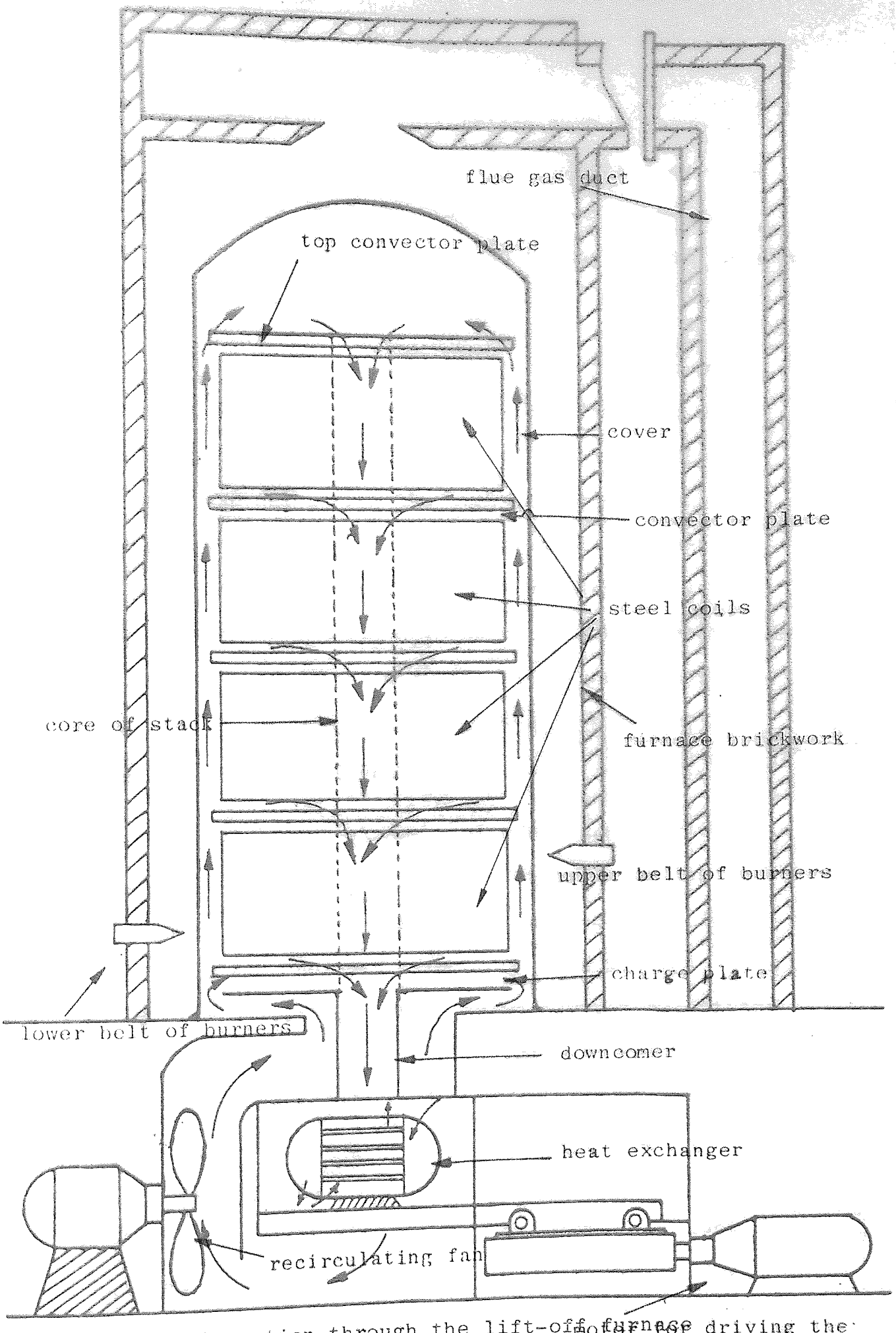

Figure 2.1 - A section through the lift-off furnace

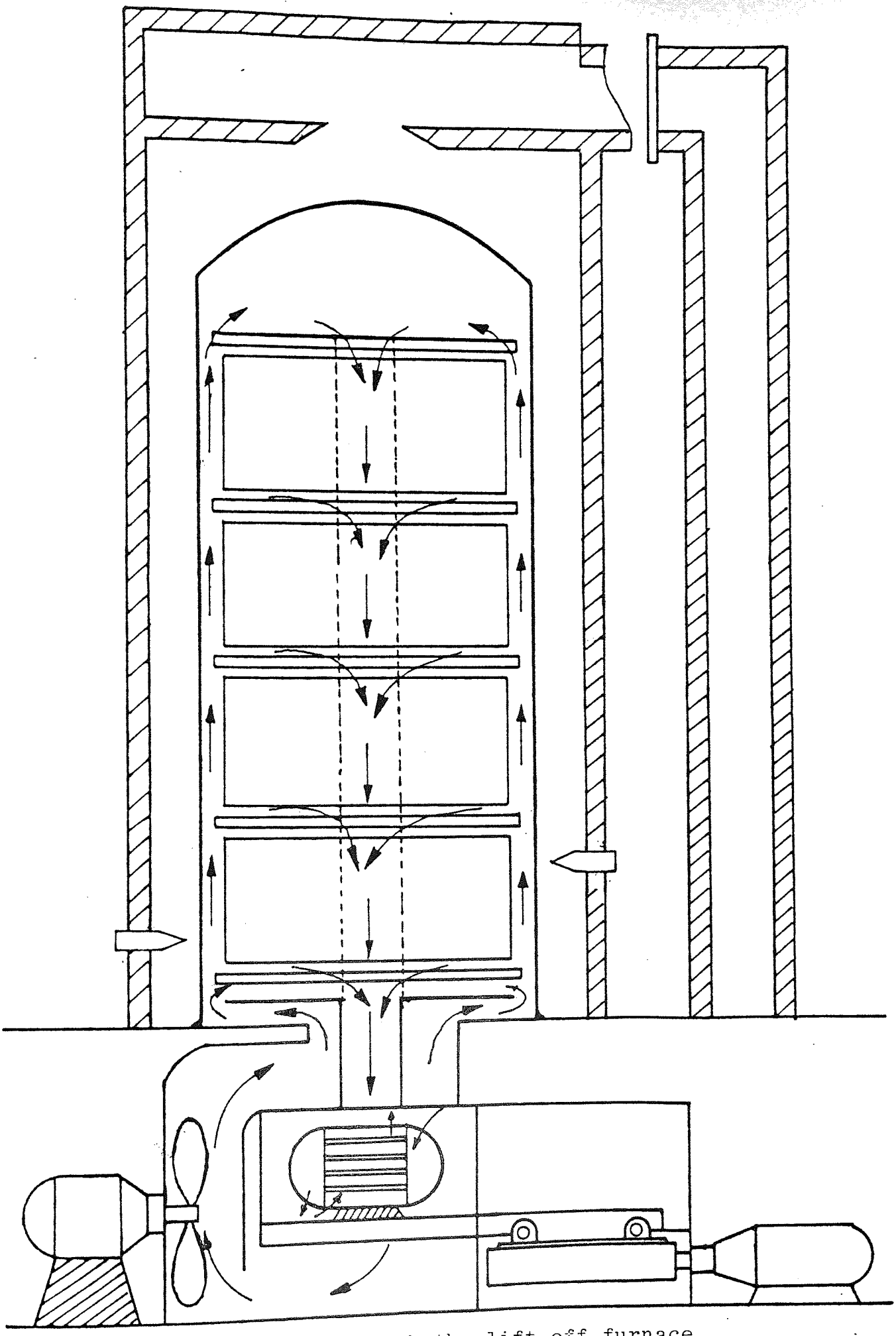

Figure 2.1 - A section through the lift-off furnace

metres diameter and 0.9-1.1 metres high. Three or four coils are stacked on each other with convector plates situated between them; different types of convector plates are usually put at the bottom (charge plate) and the top of the stack.

The open coil process of annealing is an outstanding development in steel production. In this process, the tight coil is opened automatically by thermal expansion from the tight diameter of about 1.8 metres to a final diameter of up to 2.3 metres. This expansion leaves gas spaces between the laps so that when the coil is annealed, it is subsequently recoiled to the tight diameter after annealing.

2.1.3 Types of Firing

During the development of continuous strip mills, the type of fuel available for annealing in the integrated steel plant is coke oven gas. The following are the main methods of fuel firing:

(i) Direct firing: This may be carried out either by firing on the burner horizontally to splash plates, or as in the case of single stack furnace, with single or multiple burner zones, the firing is tangential around the inner cover.

(ii) Semi-direct firing: For burners of radiant bowl type, the combustion is completed before the gaseous products are discharged vertically through the burner orifice, thus avoiding direct impingement

on the inner cover.

(iii) Radiant firing: The radiant tube is used for both single and multi-stack furnaces. This development emanated from the early parabolic tubes arranged in the vertical walls of the furnace to the O tubes implemented in single stack furnaces.

2.1.4 Convection Technique

In the early annealing processes, the progressive heating of the coil from one lamination to another, drastically limited the capacity or output of the process. It was realized later that a considerably accelerated rate of heating could be achieved by heating in a direct line of conductivity from the edge of the lamination axially to the centre. To attain this condition, the concept of convector plates was brought about. The insertion of convector plates between the coils of the stack promotes the circulation of the special gas in the stack, improves the contact between the gas and the steel to enhance convective heat transfer, and provides direct-line from edge to centre in the laps. This technique increases the annealing rate by two to three times that of direct radiation and convection from the side periphery of the stack.

For the treatment of coils of heavy weight and large dimensions (e.g. 2.2 metres diameter and 4.5 metres stacking height), the high velocity recirculating

systen was developed. The basic features of this system of convection are the following:

(i) a recirculating fan of the centrifugal type driven by a large motor of about 15hp.

(ii) a heat transfer medium, in the form of a convector plate, designed to direct the gas flow at high velocity and to shift the transmission of heat towards the coil edges.

(iii) an energy conversion unit or diffuser device. This is a circular base plate supported by a ring of diffuser blades. The diffuser plate receives the gas from the fan and delivers it to a narrow annular channel between the cylindrical inner cover and the stack of coils.

In addition to the convector plates between the coils, the cover or orifice plate is placed on the top of the stack to regulate the gas flow. Fusible and expandable orifice plates have been devised to restrict the flow at maximum density and to increase it as the temperature rises and the density falls. The optimal rate of gas flow is the mass flow rate. Several attempts were made to restrict the flow in the initial stage of heating when the density of the gas is maximum and involves high power demand; but these were abandoned in view of practical difficulties of maintenance. Also, it must be stated that the bulk, the shape, the dimensions and the contour of the load have significant effect on the flow path of the circulating gas.

2.1.5 Inner Cover

All lift-off furnaces use an inner cover to shield the effective load and the protective gas from the furnace gases during heating and from the ambient atmosphere during cooling. Inner covers are made of material which generally lies between mild steel and heat resistant steel of 25% Cr and 12% Ni. The latter has a much increased life time of about 10 years, but it is three times more expensive than mild steel. However, the life time of mild steel could be extended by using a protective coating like aluminium spraying.

In the annealing furnace, the inner cover has the following functions:

(i) A heat exchanger to transfer heat between the stack and the surrounding combustion products during heating cycle or atmospheric air during cooling cycle. This heat exchange is effected directly by radiation and indirectly through the high velocity recirculating gas.

(ii) It serves to protect the special gas surrounding the load from contamination with the surrounding atmosphere.

(iii) It extracts heat from the circulating gas during cooling by natural or forced convection.

2.1.6 Protective Atmosphere

The provision of special atmosphere is usually used to prevent oxidation and discolouration of steel during the annealing process. A deoxidizing gas is made by partial combustion of coke oven, town gas or propane which yields a gas composed of about 10% CO, 5% CO_2, hydrogen and water vapour. This gas gives full protection during annealing without affecting the surface finish of steel.

The gas which is often used is composed of nitrogen and about 5% hydrogen. With the growing requisite of oxygen in integrated steel-works, the general practice is to use the residual nitrogen derived from this process, and after ratification and elimination of oxygen traces add the necessary hydrogen produced from an ammonia cracking plant. This gas is non-toxic and non-explosive, and produces steel sheets with good surface finish.

2.1.7 Furnace Refractory

The type of refractory material used for inner lining of furnace wall is of great significance. The essential characteristics of furnace wall are the following:

(i) low density so as to lessen the overall weight of the portable cover furnace and hence reduce the lifting load.

(ii) high insulating properties to limit the heat losses and allow minimum wall thickness. This also minimizes the lifting power.

(iii) the refractory must be burned in a kiln at a temperature substantially higher than the temperature attained in the furnace to prevent after-shrinkage and resultant gas leakage which could seriously impair the operating efficiency of the furnace.

Special lightweight refractories have been developed to meet the above requirements. These are the hot face refractory bricks of density less than $0.45 g/cm^3$. Usually, the hot face refractory walls are backed by lower temperature insulating materials between the wall and the outer steel casing. Presumably this insulating material is of asbestos construction.

2.1.8 Thermal Efficiency

This term is often confused or misunderstood when associated with annealing. The real function of the annealing furnace, apart from the subsequent cooling phase, is to heat the charge from the ambient temperature to the prescribed annealing temperature with minimum temperature differential throughout the load. This is the point in the annealing cycle at which the heating is finished and the soak or holding stage commences. So the thermal efficiency of the furnace during this heating phase

could be defined as the heat input to the steel charge divided by the total heat released by the fuel; this efficiency is expressed as a percentage. Nevertheless, the thermal efficiency of the furnace is sometimes given in therms per ton of heated steel. A few years ago, a thermal efficiency of 20 therms per ton or 30-35% was common practice. Nowadays, the improvements in insulation, recuperation, combustion control and gas circulation resulted in thermal efficiency of 6-7 therms per ton or 70-60%. This high efficiency yields considerable savings in the operating costs of annealing installations of lift-off furnaces.

2.1.9 Cooling Techniques

At the end of soaking, the required metallurgical effects of annealing would be imparted on the steel, and the load must be cooled, in the same protective gas, before exposure to ambient atmosphere. The temperature of steel must be brought down to about 180^{o}C where no oxidation could take place.

Many methods have been used to advance the cooling of the charge within the inner cover so as to maximize the effective use of the bases. Several attempts were made to use cooling water, but have proved to be defective because the water causes distortion of the inner cover as well as discolouration or blueing of the exposed surfaces of the

coils. The most suitable cooling is by the protective gas which is drawn from within the inner cover, passed through shell and tube coolers and recirculated to the charge. Although this method accelerates the cooling rate considerably, yet it involves large capital and operating costs incurred in the permanent circulating system installed in each base.

The cooling rate could be accelerated further by using a portable cooling hood, which provides an annular duct around the inner cover. The hood is supplied with a large volume fan at the top to induce air between the cooling hood and the outer surface of the inner cover. The induced air promotes the forced convection currents to extract heat from the inner cover at fairly accelerated rate as compared with radiation and free convection cooling. This technique reduces the cooling time by about 30%.

The cooling and reloading of the furnace requires about double the time needed for preheating and soaking; therefore it is conventional to provide 2-3 bases per furnace for either single or multistacks. It is found that accelerated cooling rates reduce this ratio to an average of 2½ bases per active furnace stack.

2.1.10 Stacking Strategy

The first annealing furnace was designed to receive a charge of steel coils having diameters of

up to 1.2 metres and a stacking height of 2.3 metres. Cover type furnaces have also been developed for more than one stack on the same base. So bases have been designed to accommodate from two to eight stacks of coils; but the general practice in multi-stack bases has four stacks of total weight of 300 tons.

The question of whether to use single or multi-stack bases is more-or-less controversial; however, there are some arguments behind each system. The advantages of single stack installations are the following:

(a) the furnace is light and hence small lifting capacity and lighter building requirements would suffice.

(b) there is no need for deep basement below the floor level.

(c) there is greater flexibility of loading.

The positive arguements for multistack furnaces are the following:

(a) it reduces the capital cost when large tonnage of one particular grade of material is to be annealed.

(b) it reduces the operating labour cost.

(c) it requires less instrumentation.

CHAPTER THREE

THE FURNACE DESIGN MODEL

THE FURNACE DESIGN MODEL

3.1 Methods of Furnace Design

The practice in furnace design does not depend on generalizations resulting from well-controlled experiments of full-scale or reasonably large-scale performance. This is because of the high cost incurred in furnace experimentation. Alternatively, simple predictive models[2] have been used, and they show good success in the following fields:

(a) The applications to those furnace design problems in which the prediction of detailed flux density pattern over the surface of the sink is relatively less important than the prediction of the total energy transfer.

(b) Keeping satisfactory assumptions for flow and combustion, simplified and reasonable patterns of flow and of combustion progress in the furnace gases together with temperature gradients in the gas and temperature variation over the surfaces, in radiative equilibrium, give performance predictions, which are close to reality.

The main objectives of the fuel-fired furnace are the combustion of fuel in air and the energy transfer from the combustion products to the stock. The furnace may be designed so as to allow the burning of the fuel to be completed before the heat transfer begins. In this case, it is required to design a combustion chamber followed by a heat transfer section. On the other hand, the furnace may be designed to

combine the combustion of the fueland the heat transfer in the same chamber. The latter can possibly be followed by a secondary section of heat transfer if the sink temperature is justifiably low. The choice between these two extremes depends on the size of the operation, quality of the fuel, the ease of design and the total cost of the furnace.

The process of heat transfer from the fuel and air entering the furnace to the heat-sink surface disposed on the walls involves a combination of problems in fluid mechanics, molecular and turbulent flow, chemical reaction, radiation from solid surfaces and from gases, absorption by particles and gases, reradiation from refractory walls, free and forced convection, thermal conduction, etc. The analysis of these aspects of transfer entails rigorous mathematical representation and tedious numerical calculations, which require machine computation.

3.1.1 Long Furnace Model

The long furnace design model[15] is characterized by combustion at one end of the furnace, plug flow of the combustion gases with traverse mixing and negligible radiative transfer along the direction of the gas flow. In case of the lift-off cover furnace, the firing zone is at the bottom of the furnace; the combustion products rise in the annular space between the refractory wall and the inner cover, and the flue gases are discharged through the roof of the furnace.

Assumptions:

(a) The adiabatic flame temperature is achieved at the burner's zone because the combustion occurs very rapidly as compared with the total gas resistance time.
(b) The furnace is very long in the direction of the gas flow (axial direction in the case of the lift-off furnace) as opposed to its width; the radiative flux in this direction is negligible. Thus there is only transverse radiation.
(c) There is negligible backmixing in the combustion gases; however, the gas at any flow cross-section is homogeneous and isothermal.

Following the above assumptions, the local flux density in the sink at the downstream of the gas flow could be expressed in terms of the local gas and sink temperatures, the shape of the local cross-section and the disposition of sink and refractory surfaces. Hence the flux density from the gas to the sink is the function[2] $q_{g \rightarrow 1} = \Psi(T_g, T_1, A_1)$ where T_g and T_1 are the gas and sink temperatures respectively, and A_1 is the surface area of the sink per unit length of the furnace, which is a measure of the shape of cross-section at the specific length x. Similarly, the local external heat losses to the surroundings at temperature T_o are functions of the gas temperature T_g and A_R, which is a unit-length surface area of the refractory periphery from which the losses dissipate. Hence $q_{go} = \Psi(T_g, A_R)$ where q_{go} is the flux density from the

gas to the surroundings.

Equating the total heat losses and the heat flux received by the sink to the net heat flux from the combustion products, and integrating between the burner's end to a length x where the gases cool from T_{gin} to T_g, the following relation is obtained.

$$x = \int_{H_{in}}^{H} \frac{-dH}{A_1 * q_{g \rightleftharpoons 1} + A_R * q_{go}} \qquad (3\text{-}1)$$

where H, $q_{g \rightleftharpoons 1}$ and q_{go} are all dependent on T_g. H_{in} is the enthalpy of the combustion products at the burner zone and H is their enthalpy at temperature T_g such that, $dH = m_g \, Cp_c dT$ where m_g is the rate of air and fuel fired in kg/h and Cp_c is the specific heat of the combustion gases.

The net flux from the furnace gases is the following

$$\dot{Q}_{g,net} = m_{g*} \, (H_{in} - H) \qquad (3\text{-}2)$$

If the combustion gases are assumed grey, their emissivity is equal to their absorptivity taken at the sink temperature i.e., $\varepsilon_g = \alpha_{g1}$. Thus, the net rate of radiative heat transfer to the sink is given by Hottel and Sarofim[2] as follows

$$\dot{Q}_{g \rightleftharpoons 1} = q_{g \rightleftharpoons 1} * A * x = (\overline{GS}_1)_R \, (E_g - E_1) \qquad (3\text{-}3)$$

where E_g and E_1 are the black emissive powers of the gas and the sink respectively. $(\overline{GS}_1)_R$ is the total gas-sink exchange area in the presence of refractory.

If the gases are non-grey ($\varepsilon_g \neq \alpha_{g1}$), two directed areas, one based on the gas emissivity and the other on the gas absorptivity, need to be evaluated and used instead of $(\overline{GS}_1)_R$. Hottel and Sarofim[2] show that $\overrightarrow{GS}_1$ is inversely proportional to the gas temperature T_g, and $\overleftarrow{GS}_1$ is inversely proportional to the sink temperature T_1 such that: $\overrightarrow{GS}_1 * T_g = \overleftarrow{GS}_1 * T_1$. Hence equation (3-3) becomes the following

$$\dot{Q}_{g \rightleftharpoons 1} = (\overrightarrow{GS}_1)_R * \left(\frac{1-k^3}{1-k^4}\right) * (E_g - E_1) \qquad (3\text{-}4)$$

where $k = T_1/T_g$ and $(\overrightarrow{GS}_1)_R$ is the total exchange area from the gas zone to the sink with allowance for refractory. $(\overrightarrow{GS}_1)_R$ will be fully discussed later in chapter 6.

The flux density of the heat losses to the surroundings is given by equation (14-23) in Hottel and Sarofim[2] as follows

$$q_{go} = (T_g - T_o) / \left(\frac{1}{h_{ci}} + \frac{1}{U_{io}}\right) \qquad (3\text{-}5)$$

where h_{ci} is the heat transfer coefficient of the gas to the refractory inside, and U_{io} is the overall heat transfer coefficient from the refractory outside to the furnace surroundings at temperature T_o.

For the annealing furnace, all the heat transfer fluxes from the furnace gas to the steel load , via the cover and the inert gas, will be dealt with later in Chapter 6.

The load temperature at the burner end can be controlled by various techniques. The choice of an efficient control depends on the nature of the furnace operation in the first place. The following are some of these techniques:

(a) Using small convective transfer coefficient; this can be done by reducing the firing rate, which itself is a disadvantage.

(b) Adjustment of excess air: If the excess air is increased, the flame temperature will be reduced and so is the furnace thermal efficiency. This may also advance the oxidation of the cover.

(c) Recycle of combustion products: The recycling of flue gas to the burner discharge point reduces the combustion temperature. This could be determined by monitoring the recycle ratio.

Some other methods are cited in the literature[2].

Applications of Long Furnace Model[1]

Gill et al[4] implemented the plug flow, long furnace design model in a pulverised coal-fired test furnace. The results predicted too rapid combustion, too sharp radiation peak with axial distance and insufficient heat transfer.

A modified version of the long furnace design was used by Lucas and Lockett[5] to correlate the performance of the firing tube of a gas-fired shell boiler. In this case the radiation along the gas flow was neglected whereas radial temperature gradients were taken into consideration and the combustion was assumed to continue down the firing tube.

Hadvig[11] developed a correlation of effective gas temperature, of the exit gas temperature and of the rate of heat transfer by radiation and convection with the inlet gas temperature or the adiabatic flame temperature as argument. This correlation was based on the assumption of black walls, grey gas and no axial radiation. Hadvig tested his correlation by a water-cooled combustion chamber and two power station boilers.

Other researchers[1] have verified the application of the long furnace model to indirectly fired air heaters, self-recuperative burners and single-ended radiant tubes.

3.2 Furnace Fuel

In integrated steelworks, the available fuel for the annealing furnace is coke oven gas. Nevertheless, natural gas may be the suitable fuel for some annealing installations. The combustion calculations in this thesis are based on natural gas from the North Sea. The informations and data on natural gas were obtained from the British Gas Data Book[16].

The data of the approximate long-term composition of liquefied natural gas (LNG) in Cheshire is used in the following calculations. The gas composition in volume percent is as follows:

CH_4	97.5%
C_2H_6	1.8%
C_3H_8	0.2%
N_2	0.5%

The average molecular weight of this gas is 16.41 and its ideal gas density at 288K is 0.694kg/m^3.

If ideal gas behaviour is assumed to hold, the molar composition will be the same as the composition by volume.

For LNG of Cheshire:

The gross calorific value = 38.23 MJ/m^3 = 10.62 kWh/m^3.

The net calorific value = 34.44 MJ/m^3 = 9.57 kWh/m^3

During the combustion all the components of the fuel gas, except nitrogen, undergo combustion reaction as follows:

$$CH_4 + 2O_2 \rightarrow CO_2 + 2H_2O \qquad (3\text{-}6)$$

$$C_2H_6 + 3\tfrac{1}{2}O_2 \rightarrow 2CO_2 + 3H_2O \qquad (3\text{-}7)$$

$$C_3H_3 + 5O_2 \rightarrow 3CO_2 + 4H_2O \qquad (3\text{-}8)$$

From the above combustion equations, the stoichiometric amount of air necessary for the complete combustion of unit volume of fuel is 9.66 volumes. The fuel in the theoretical combustion mixture is given[16] as 9.38%, and the theoretical composition of the waste gases is the following:

N_2	70.74	(volume %)
H_2O	18.86	(")
CO_2	9.56	(")
Inerts (argon)	0.84	(")

The volumes of theoretical combustion products per volume of fuel are given[16] as follows:

N_2	7.55	(volumes/volume of fuel)
H_2O	2.01	(" " ")
CO_2	1.02	(" " ")
Inerts	0.09	(" " ")

From the ideal equation, the kmols of flue gases per kmol of fuel are calculated as 10.66kmols/kmol fuel. Assuming 10% excess air and using the molecular weights of the gas components and their compositions, the mean molecular weight of combustion products is obtained as 27.76. Hence there will be 18.05kg of flue gases per kg of fuel.

The mean specific heat of the combustion mixture is correlated from the specific heats of the components and their compositions in a polynomial, which is a function of the absolute temperature of the gas as:

$$Cp_c(T) = a + bT + cT^2 + dT^3 \quad kWh/kg/K \qquad (3\text{-}9)$$

where $a = 2.972 * 10^{-4}$

$b = 2.303 * 10^{-8}$

$c = 1.721 * 10^{-11}$

$d = -5.819 * 10^{-5}$

3.3 Combustion Calculations

Basis: 1 kg fuel

Assume that the combustion mixture enters the firing zone at 300K. The ideal density of the mixture at 300K is 0.666kg/m^3. Hence the net calorific value of the fuel is 14.369kWh/kg. The specific heat of the fuel at 300K is computed as $Cp_c(300) = 5.85 * 10^{-4}$ kWh/kg/K. The sensible heat associated with 1kg fuel at 300K is then 0.175 kWh/kg fuel. The total heat (sensible + calorific value) in 1kg fuel at 300K is 14.544 kWh/kg fuel. The specific heat of air at 300K is calculated as $2.785 * 10^{-4}$ kWh/kg/K. The sensible heat in 1kg air is 0.0836 kWh/kg.

Assume there are x kmols excess air per kmol of stoichiometric air such that the total air in the firing mixture is 17.05*(1+x) kg/kg fuel. Hence the sensible heat associated with the incoming air is 1.425*(1+x) kWh/kg fuel.

The total heat input to the furnace is composed of the heat liberated by the combustion of the fuel in air. So, the total heat given by the combustion mixture is calculated as 15.969 + 1.425*x kWh/kg fuel.

3.3.1 Adiabatic Flame Temperature

This is the ideal flame temperature[17] which can be determined by assuming:

(a) complete oxidation of reactive components of the fuel by the exact stoichiometric air,

(b) perfect mixing of the fuel and the air,
(c) instantaneous combustion of gases so that no heat losses occur during burning. Generally the flame temperature attained by the combustion of the fuel is governed by the following factors:
(a) the burner design which affects the rate of the combustion reaction.
(b) excess air over the stoichiometric amount, since this affects the amount of nitrogen to which part of the heat is imparted.
(c) the effective calorific value which depends on the actual temperature, which in turn governs the equilibrium of the reaction.
(d) the temperature of the fuel and air prior to combustion, because the sensible heat of the reactants must be added to the calorific value for calculating the total heat available in the combustion mixture.

The total mass of the firing mixture is m_g = 1 + 17.05*(1+x) kg/kg fuel. The specific heat of the combustion products is given by equation (3-9) as $Cp_c(Td)$ where Td is the adiabatic flame temperature in degree K. Heat balance: The heat given to the combustion products is equal to the heat liberated from the firing mixture. Therefore;

$$(1 + 17.05 * (1+x)) * Cp_c(Td) * Td = 15.969 + 1.425 * x \qquad (3\text{-}10)$$

This is a non-linear equation in Td which could be solved iteratively by Newton-Raphson method or any other technique.

3.3.2 Emissivity of Combustion Gases

The stoichiometric calculations of the combustion equations (3-6) - (3-8), result in the following composition of the combustion products after neglecting the inert component:

N_2	7.85	kmol/kmol fuel
H_2O	2.01	" " "
CO_2	1.02	" " "
Total	10.88	" " "

The emissivity of the gases is dependent on the partial pressures of CO_2 and H_2O.

To allow for the x kmol excess air per kmol stoichiometric air, the above composition is modified to the following:

N_2	7.85 * (1+x)	kmol/kmol fuel
CO_2	1.02	" " "
H_2O	2.01	" " "
O_2	2.02 * x	" " "
	10.88 + 9.87 * x	

The partial pressure of carbon dioxide is

$$p_{CO_2} = \frac{1.02}{10.88 + 9.87 * x} \text{ (atm)} \qquad (3\text{-}11)$$

The ratio of water vapour to carbon dioxide is 1.97, therefore, the total pressure is given by:

$$P = 2.97 * p_{CO_2} \text{ (atm)} \qquad (3\text{-}12)$$

Since the radiation in the gas medium is not parallel and the various beams travel different distances through the medium, a mean beam length, which is dependent on the geometry and the attenuation of the gas is usually used. This is calculated from[18]

$$L_m = 3.5 \frac{V}{A} \qquad (3\text{-}13)$$

where V is the volume occupied by the gas and A is the surface in contact with the gas. For the arrangement of the annealing lift-off cover furnace, the mean beam length becomes

$$L_m = \frac{3.5}{4} (D_3 - D_1) \qquad (3\text{-}14)$$

where D_1 is the diameter of the cover and D_3 the diameter of the refractory:

The emissivity of the gas is calculated using Hadvig's correlation[11] as follows:

$$\varepsilon_g = (2.7 - Td/1000) * f(RO) \qquad (3\text{-}15)$$

where the argument $RO = L_m * P$ (m.atm)

3.3.3 Calculation of Furnace Temperature

The furnace temperature is the temperature of the combustion products after leaving the firing zone which is different from the adiabatic flame temperature.

This temperature is measured in practice by a thermocouple and used as a control for the heating cycle. The following calculation of this temperature is based on the heat transfer between the refractory wall, the furnace gases, the inner cover and the thermocouple.

View Factors:

Let the subscript 1 indicate the outer surface of the cover, 2 denote the thermocouple and 3 denote the refractory wall.

Because the surface area of the thermocouple is negligible when compared with those of the cover and the refractory wall, then $A_2 = 0$ and the view factor from the thermocouple to itself F_{22} is zero. Since the outer surface of the cover is convex, then the view factor from the cover to itself F_{11} is zero also. The view factor from any point on the refractory wall to the cover is the same as that from all other points on the refractory surface to the cover. Since the thermocouple could be considered as a point on the refractory wall, then the view factor from the thermocouple to the cover is equal to the view factor from the refractory wall to the cover.

Hence $F_{21} = F_{31}$ (3-16a)

Generally $\sum_j F_{ij} = 1$ (3-16b)

So $F_{12} + F_{13} = 1$ (3-16c)

since $F_{11} = 0$

From the reciprocosity Law

$$A_i F_{ij} = A_j F_{ji} \qquad (3\text{-}16d)$$

$$F_{12} = \frac{A_2 F_{21}}{A_1} = 0 \qquad (3\text{-}16e)$$

because $A_2 = 0$

By equations (3-16c) and (3-16e)

$$F_{13} = 1 \qquad (3\text{-}16f)$$

Again by (3-16d),

$$F_{31} = \frac{A_1 F_{13}}{A_3} = \frac{A_1}{A_3}$$

Hence $$F_{31} = F_{21} = \frac{D_1}{D_3} \qquad (3\text{-}16g)$$

By equations (3-16b), (3-16g) and $F_{22} = 0$

$$F_{23} = 1 - F_{21} = \frac{D_3 - D_1}{D_3} \qquad (3\text{-}16h)$$

From equation (3-16d)

$$F_{32} = \frac{A_2 F_{23}}{A_3} = 0 \qquad (3\text{-}16i)$$

because A_2 is zero. Therefore, equations (3-16b) and (3-16g) will give F_{33} as follows:

$$F_{33} = 1 - F_{31} = \frac{D_3 - D_1}{D_3} \qquad (316j)$$

Heat Balance:

The radiation interchanged between the surfaces of the refractory, the cover and the thermocouple is attenuated by the absorbing gas which, by virtue of its temperature, radiates heat to these surfaces. The emissivity of the gas ε_g is calculated before by equation (3-15) and its emissive power is $E_g = \sigma T_g^4$ where T_g is the gas temperature and σ is Stefan-Boltzmann constant. The transmissivity of the gas medium between any pair of these surfaces is assumed to be of a single value obtained by $\tau = 1 - \varepsilon_g$.

Let the black emissive powers of the cover and the thermocouple be $E_1 = \sigma T_1^4$ and $E_2 = \sigma T_2^4$ where T_1 and T_2 are the absolute temperatures of the cover and the thermocouple respectively. If W_1, W_2 and W_3 are the radiosities of the cover, the thermocouple and the refractory wall respectively, then equation (4-37) given by Gray[18] and Miiller

$$W_i = \varepsilon_i E_i + \rho_i \tau \sum_{j=1}^{n} W_j F_{ij} + \rho_i \varepsilon_g E_g$$

will result in the following set of equations:

$$W_1 = \varepsilon_1 E_1 + \rho_1 ((W_1 F_{11} + W_2 F_{12} + W_3 F_{13})\tau + \varepsilon_g E_g) \quad (3\text{-}17a)$$

$$W_2 = \varepsilon_2 E_2 + \rho_2 ((W_1 F_{21} + W_2 F_{22} + W_3 F_{23})\tau + \varepsilon_g E_g) + h_o (T_g - T_2) \quad (3\text{-}17b)$$

$$W_3 = \varepsilon_3 E_3 + \rho_3 ((W_1 F_{31} + W_2 F_{32} + W_3 F_{33})\tau + \varepsilon_g E_g) + h_w (T_g - T_3) \quad (3\text{-}17c)$$

where h_w and h_o are the convective heat transfer coefficients from the gas to the refractory wall and the thermocouple surface respectively; ε is the emissivity, ρ is the reflectivity and the subscripts 1, 2 and 3 stand for the cover, the thermocouple and the refractory respectively.

According to equations (3-16a - j), the view factors $F_{11} = 0$, $F_{12} = 0$, $F_{32} = 0$ and $F_{13} = 1$. The refractory wall is adiabatic and so $\varepsilon_3 = 0$ and $\rho_3 = 1$. If the thermocouple is assumed to be adiabatic, then $\varepsilon_2 = 0$ and $\rho_2 = 1$. Therefore, equations (3-17a - c) become the following:

$$W_1 = \varepsilon_1 E_1 + (1-\varepsilon_1)((1-\varepsilon_g)W_3 + \varepsilon_g E_g) \qquad (3\text{-}18a)$$

$$W_2 = (1-\varepsilon_g)(W_1 F_{21} + W_3 F_{23}) + \varepsilon_g E_g + h_o(T_g - T_2) \qquad (3\text{-}18b)$$

$$W_3 = (1-\varepsilon_g)(W_1 F_{31} + W_3 F_{33}) + \varepsilon_g E_g + h_w(T_g - T_3) \qquad (3\text{-}18c)$$

The convective transfer terms in equations (3-18b) and (3-18c) are assumed negligible and they are discarded. This leaves the final form of the radiosity equations as follows:

$$W_1 = \varepsilon_1 E_1 + (1-\varepsilon_1)((1-\varepsilon_g)W_3 + \varepsilon_g E_g) \qquad (3\text{-}19)$$

$$W_2 = (1-\varepsilon_g)(W_1 F_{21} + W_3 F_{23}) + \varepsilon_g E_g \qquad (3\text{-}20)$$

$$W_3 = (1-\varepsilon_g)(W_1 F_{31} + W_3 F_{33}) + \varepsilon_g E_g \qquad (3\text{-}21)$$

For adiabatic surfaces, all the radiosity, the incident flux and the emissive power are equal; thus $W = H = E$. The emissive power of the gas can be

evaluated at the adiabatic flame temperature where $T_g = T_d$. Equations (3-19) and (3-21) are solved simultaneously for W_1 and W_3 which are then substituted in equation (3-20) to solve for W_2. Finally, the temperature of the furnace gas, which is measured by the thermocouple, is calculated here by this equation:

$$T_2 = \sqrt[4]{W_2/\sigma} \qquad (3\text{-}22)$$

3.3.4 Firing Rate

The rate at which the fuel is fired in the furnace is calculated from the heat balance over the whole furnace. The heat liberated by the combustion of the fuel is consumed in heating the steel load and the inert gas circulating under the cover. Some of this heat is lost with the flue gases leaving the furnace at the top; also there are some losses by convection to the ambient atmosphere through the roof and the side walls of the furnace.

Let m_f kg/h be the rate of fuel firing,

$\dot{Q}_{in}$ kW be the rate of total heat liberated per kg of fuel,

$\dot{Q}_s$ kW be the rate of heat taken by the stack of steel coils

$\dot{Q}_g$ kW be the rate of heat taken by the inert gas,

L_r kW be the rate of heat loss through the roof of the furnace,

L_s kW be the rate of heat loss through the side walls of the furnace

L_f kW be the rate of heat lost with the flue gases.

From equation (3-10), the heat liberated by combustion per kg fuel is .

$$\dot{Q}_{in} = 15.969 + 1.425*x \qquad (3-23)$$

The top loss through the furnace roof is calculated by

$$L_r = \frac{\pi}{4} D_3^2 h_R (T_{fg} - 350) \qquad (3-24)$$

where D_3 is the inner diameter of the furnace wall, h_R is the conductive heat transfer coefficient of the refractory in $kW/m^2/K$ and T_{fg} is the absolute temperature of the flue gases.

The loss through the side wall is calculated by

$$L_s = \pi*D_4 H_f * h_R * \left(\frac{T_d + T_{fg}}{2} - 350\right) \qquad (3-25)$$

where D_4 is the outer diameter of the furnace casing and H_f is its total height.

$$L_f = m_f*(1 + 17.05*(1+x))*Cp_c(T_{fg})*T_{fg} \qquad (3-26)$$

where $Cp_c(T_{fg})$ is the specific heat of the combustion products given by equation (3-9) and evaluated at T_{fg}.

Heat balance: Heat input = Heat Output

$$m_f * \dot{Q}_{in} = \dot{Q}_s + \dot{Q}_g + L_s + L_r + L_f \qquad (3\text{-}27)$$

$$m_f * \dot{Q}_{in} = \dot{Q}_s + \dot{Q}_g + L_s + L_r + m_f*(1+17.05*(1+x))*Cp_c(T_{fg})*T_{fg}$$

The firing rate is then given by

$$m_f = \frac{\dot{Q}_s + \dot{Q}_g + L_s + L_r}{\dot{Q}_{in} - (1 + 17.05*(1+x))*Cp_c(T_{fg})*T_{fg}} \qquad (3\text{-}28)$$

3.3.5 Thermal Efficiency

The thermal efficiency is defined here as the useful heat, the heat taken by the load to effect the process heating, divided by the total heat produced by the combustion of the fuel provided. This efficiency is expressed as a percentage. Hence,

$$\eta = \frac{\dot{Q}_s}{m_f * \dot{Q}_{in}} * 100 \qquad (3\text{-}29)$$

CHAPTER FOUR

MODELLING OF FLOW DISTRIBUTION AND CONVECTION IN CONVECTOR PLATES

MODELLING OF FLOW DISTRIBUTION AND CONVECTION IN CONVECTOR PLATES

4.1 Gas Flow Distribution

The insertion of convector plates between the coils in an annealing furnace is intended to improve the heat transmission between the inert gas and the charge. These plates, which are inserted between the stack coils, are designed with converging channels which are separated by steel vanes on both sides of the plate. When the inert gas enters the plate from the annulus between the cover and the stack, these channels direct the flow of the gas towards the core of the stack. Because the channels are converging towards the core of the coil, they promote the contact between the gas and the edge of the coil; and hence advance the heat trnasfer from the edges of the steel laps, axially, into the centre of the coil.

The inert gas is drawn into the stack by a centrifugal fan which is situated in the base of the furnace and driven by a large electric motor. As the gas rises up through the annular space between the coils and the inner cover, some of it passes through the convector plates between the steel coils. The distribution of the gas flow between the plates is governed by the pressure drop in the stack with the static pressure at the diffuser plate as a datum. The total mass of the gas circulating in the system is dependent on the volumetric capacity of the fan, Vm^3/min and the density of the gas which is a function of its temperature at the fan.

To investigate the distribution of gas flow between the plates, it is required to find the mathematical models which describe the pressure drop in the annulus between the cover and the stack, in the channels of the convector plates and in the central core of the stack.

4.1.1 P.D. in the Channels of Convector Plate:

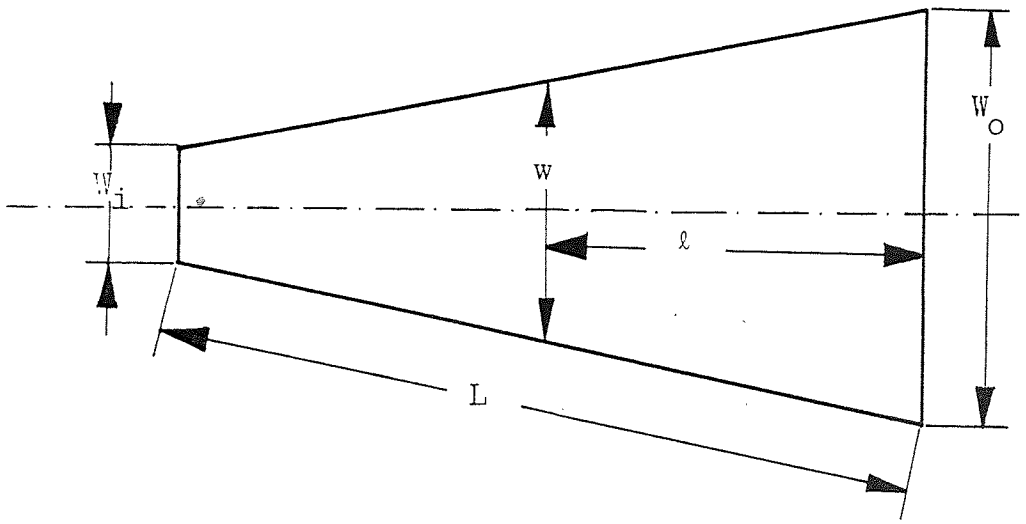

All dimensions in metres

Figure 4.1

Let the subscript n designate the coil number in the stack such that n = 1 is the subscript for the bottom coil. Fig. 4.1 represents a typical converging convective channel generated by coil (n) and the vanes of the convector plate (n). The length of the channel L is the difference between the outer and inner diameters of coil (n). Let the depth of the channel be B(n), and assume that B(n) is the same for

all the NC(n) channels of plate (n). W_i and W_o are the inner and outer widths of the channel.

From equation (6.2e) of McAdams[19], the Fanning equation can be written as follows:

$$-dp = \frac{fU^2\rho_g}{2g_c r_H} d\ell \qquad (4.1)$$

where f is the dimensionless friction factor

ρ_g is the density of the inert gas

U is the local gas velocity

r_H is the hydraulic mean radius

g_c is the conversion factor

$d\ell$ is the differential of the channel length

and dp is the differential of the pressure drop.

Applying similarity of triangles in Fig. 4.1 and differentiating, the following is obtained:

$$d\ell = - \frac{L}{W_o - W_i} dw \qquad (4.2)$$

The gas velocity at the distance ℓ from the entry of the channel is then calculated from the volumetric capacity of the fan as follows:

$$U = \frac{V}{60} * \frac{1}{NC(n)*B(n)*w} * \frac{T_{gi}(n)}{T_{fn}} \qquad (4.3)$$

where $T_{gi}(n)$ is the temperature of the gas entering plate (n), and T_{fn} is the temperature of the gas in the fan.

Assuming that the inert gas follows ideal gas behaviour, its density is calculated from the ideal gas equation as follows:

$$\rho_g = 341.4/T_{gi}(n) \qquad (4.4)$$

The hydraulic mean radius is defined as the surface area occupied by the gas divided by its perimeter. Thus

$$r_H = \frac{w * B(n)}{2*(w + B(n))} \qquad (4.5)$$

Substitution of equations (4.2) - (4.5) in the Fanning equation (4.1) gives the following:

$$-dp = \frac{0.0237}{g_c} * \left(\frac{V}{NC(n)*B(n)*T_{fn}}\right)^2 * \frac{T_{gi}(n)}{W_o - W_i} * fL * \frac{w+B(n)}{B(n)w^3}\, dw \qquad (4.6)$$

Integrating and rearranging, the pressure drop becomes the following:

$$-\Delta p = 1.864 * 10^{-9} * \frac{f*L}{W_i} * \left(1 + \frac{W_o}{W_i} + \frac{2W_o}{B(n)}\right) * \left(\frac{V}{NC(n)*B(n)W_o}\right)^2 * \frac{T_{gi}(n)}{(T_{fn})^2} \qquad (4.7)$$

If one velocity head loss is allowed for the entry effect, the pressure drop will then become the following:

$$-\Delta p_{cc} = EA_{(n)} * T_{gi}(n)/(T_{fn})^2 \quad \text{(mm.w.g)} \qquad (4.8)$$

where $-\Delta p_{cc}$ is the pressure drop in the convective channel and

$$EA(n) = 1.864 * 10^{-9} * (1 + \frac{fL}{W_i} * (1 + \frac{W_o}{W_i} + \frac{2W_o}{B(n)})) * \left(\frac{V}{NC_{(n)} * B_{(n)} W_o}\right)^2 \qquad (4.9)$$

4.1.2 P.D. in the Annulus between the Cover and the Stack

The frictional pressure drop under the inner cover could be proven negligible for the order of the fan capacity and stacking height. Nevertheless, the convector plates have larger diameters than those of steel coils, and this develops a permanent pressure drop of N_{vh} velocity heads becuase of the contraction at plate (n) which is situated between coils (n) and (n+1).

Spiers[20] in Table 82 expressed the pressure drop due to sudden contraction as a relationship of the number of velocity heads with the hydraulic mean diameter between coil (n) and the cover and that between the convector plate and the cover as follows:

$$N_{vh} = \left(\left(\frac{d_{H1}}{d_{H2}}\right)^4 - 1\right)\left(1 - \left(\frac{d_{H2}}{d_{H1}}\right)^2\right)/0.36 \qquad (4.10)$$

where the hydraulic mean diameters are given by $d_{H1} = D_2 - DO_{(n)}$ and $d_{H2} = D_2 - D_4$; and D_2 is the diameter of the cover, D_4 is that of the convector plate and $DO_{(n)}$ is the outer diameter of the coil (n).

One velocity head of pressur drop in the annular space could be evaluated at the fan temperature as follows:

$$\frac{\rho_g U^2}{2g_c} = \frac{341.4}{T_{gi(n)}} * \left(\frac{V}{60} * \frac{4}{\pi(D_2^2 - DO_{(n)}^2)} * \frac{T_{gi(n)}}{T_{fn}}\right)^2 / 2g_c$$

Therefore, the pressure drop under the cover at plate (n) is the following:

$$-\Delta p_{AG} = EB_{(n-1)} * T_{gi(n)}/T_{fn}^2 \qquad (4.11)$$

where

$$EB(n-1) = 6.043 * 10^{-9} * N_{vh} * \left(\frac{V}{D_2^2 - (DO_{(n)})^2}\right)^2 \qquad (4.12)$$

and $-\Delta p_{AG}$ is the pressure drop in the annulus.

4.1.3 P.D. in the Core of the Stack

The inert gas leaves the convector plates, accumulates in the core of the stack and flows downwards to the base of the furnace. When the gas passes plate (n) flowing downward, it develops a pressure drop which could be calculated from the Fanning equation as follows:

$$-\Delta p = \frac{fU^2 \rho_{g*} H}{2g_c r_H} \qquad (4.13)$$

where the hydraulic mean radius is given by $\frac{DI_{(n)}}{4}$ such that $DI_{(n)}$ is the inner diameter of the coil (n), and H is the height from the base of the stack to the bottom of coil (n).

If T_{gc} is the temperature of the gas in the core at plate (n), the pressure drop will be the following:

$$-\Delta p = fH \frac{4}{DI_{(n)}} * \frac{341.4}{T_{gc}} * \frac{1}{2g_c} \left(\frac{V}{60} * \frac{4}{\pi (DI_{(n)})^2} * \frac{T_{gc}}{T_{fn}}\right)^2$$

So the pressure drop in the core of stack is as follows:

$$-\Delta p_{cs} = EC_{(n)} * \frac{T_{gc}}{(T_{fn})^2} \qquad (4.14)$$

where

$$EC_{(n)} = 2.417 * 10^{-8} * f*H*V^2/(DI_{(n)})^5 \qquad (4.15)$$

4.1.4 P.D. in the Holes of Convector Plates:

The holes in the centre of convector plates are usually less in diameter than the central core of the coils. Hence, the gas flowing through these holes produces a permanent pressure drop of M_{vh} velocity heads. Again, applying Spier's correlation for the number of velocity heads due to sudden contraction, M_{vh} is calculated as follows:

$$M_{vh} = (d_H^4 - 1) * (1 - d_H^2)/0.36 \qquad (4.16)$$

where $d_H = DI_{(n)}/D_{hol}$ and D_{hol} is the diameter of the plate hole.

The pressure drop in the hole will therefore be given by the following:

$$-\Delta p_H = ED * \frac{T_{gc}}{(T_{fn})^2} \qquad (4.17)$$

where

$$ED = 6.043 * 10^{-9} * M_{vh} * \frac{V^2}{(DI_{(n)})^4} \qquad (4.18)$$

4.1.5 Algorithm for Calculating the Flow Distribution

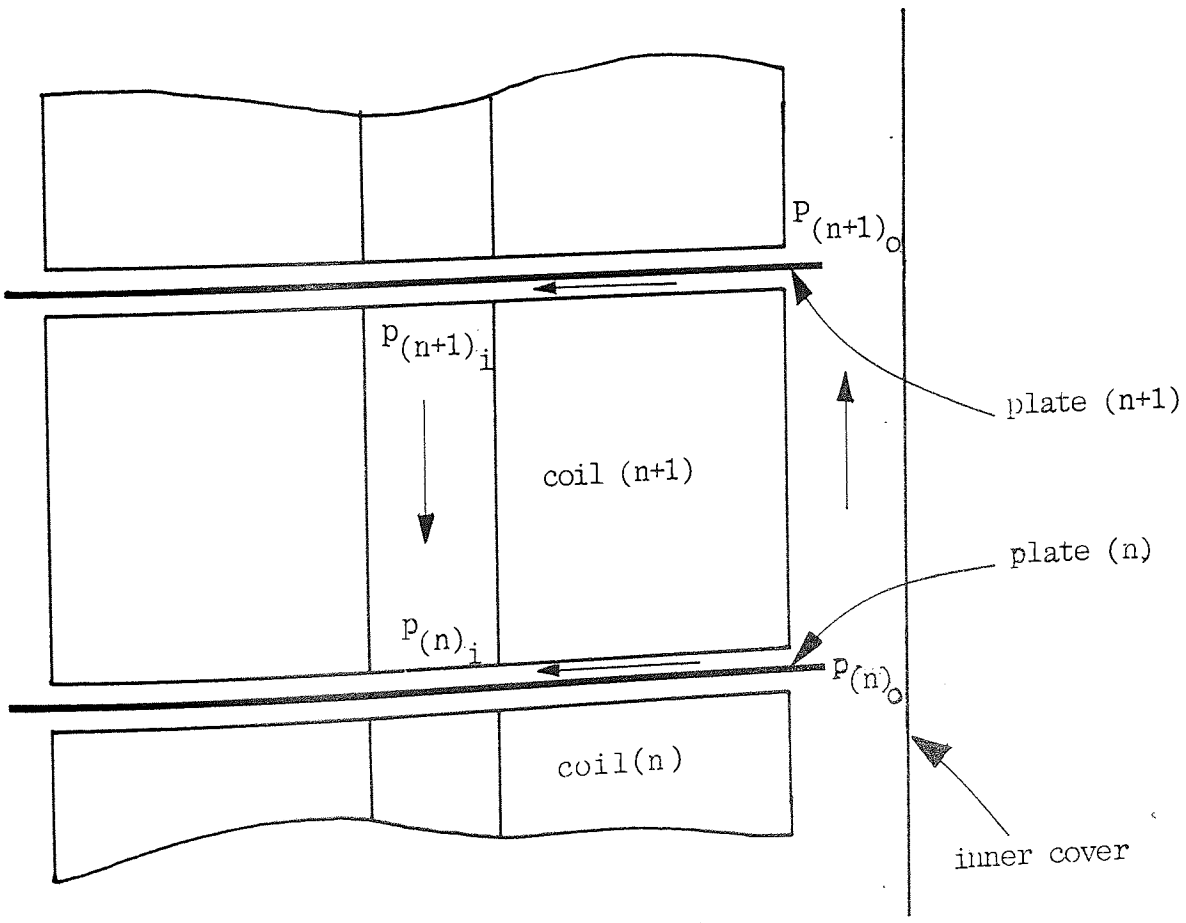

Figure 4.2

The algorithm of calculating the fractions of the the gas flow passing through each convector plate will be derived on the basis of pressure drop as shown diagramatically in Fig. 4.2.

Let $R_{(n)}$ be the fraction of the total gas flow which passes through plate (n). From Fig. 4.2, the pressure drop in the annular gap between the cover and the stack at coil (n + 1) is expressed as follows:

$$p_{(n)o} - p_{(n+1)o} = \Delta p_{AG} * (R_{(n+1)})^2 \qquad (4.19a)$$

The square of the fraction accounts for the square of flow in the velocity head or the Fanning equation.

The pressure drop in the channels of the convector plate above coil (n+1), could be written as follows:

$$p_{(n+1)o} - p_{(n+1)i} = \Delta p_{cc} * (R_{(n+1)})^2 \qquad (4.19b)$$

Similarly, the pressure drop in the core of the steel coils becomes;

$$p_{(n+1)_i} - p_{(n)i} = \Delta p_{cs} * (R_{(n+1)})^2 \qquad (4.19c)$$

The summation of equations (4.19a-c) gives the pressure drop across plate (n) as follows:

$$p_{(n)o} - p_{(n)i} = (\Delta p_{AG} + \Delta p_{cc} + \Delta p_{cs}) * (R_{(n+1)})^2 \qquad (4.20)$$

But the actual pressure drop along plate (n) due to the loss in the convective channels could be expressed as follows:

$$p_{(n)o} - p_{(n)i} = EA_{(n)} * \frac{T_{gi(n)}}{(T_{fn})^2} * (R_{(n)})^2 \qquad (4.21)$$

By guessing a value for $R_{(n+1)}$, equations (4.20) and (4.21) could be solved simultaneously for $R_{(n)}$. This is valid for the top plate only. For the second plate from the top and further downward, there is an additional term due to the pressure loss over the upper plate or plates. This is expressed by a cummulative fraction calcualated as;

$$R_c = R_{(Np)} + R_{(Np-1)} + \ldots + R_{(n)} \qquad (4.22)$$

where N_p is the total number of convector plates. Therefore, the pressure drop in the holes of a plate, or plates, is given by the following:

$$-\Delta p_{hol} = ED * \frac{T_{gc}}{(T_{gn})^2} * (R_c)^2 \qquad (4.23)$$

If the convector plates are numbered from the bottom, with the diffuser plate as 1, upward until the top plate N_p, the algorithm for calculating the distribution of the gas flow between the plates is obtained as follows:

For the top plate, $n = N_p$

$$R_{(n-1)} = R_{(n)} * \sqrt{\frac{(\Delta p_{cc} + \Delta p_{AG} + \Delta p_{cs}) * (T_{fn})^2}{EA_{(n-1)} * T_{gi(n-1)}}} \qquad (4.24)$$

When $n < N_p - 1$

$$R_{(n)} = \left(\frac{S_{cc} + S_{AG} + S_{cs}}{EA_{(n)} * T_{gi(n)}}\right)^{\frac{1}{2}} \qquad (4.25)$$

such that $S_{cc} = EA_{(n+1)} * T_{gi(n+1)} * (R_{(n+1)})^2$

$S_{AG} = EB_{(n-1)} * T_{gi(n-1)} * (R_{cum})^2$

$S_{cs} = (EC_{(n)} * (R_{cum})^2 + ED * R_c^2) * T_{gc}$

where $R_{cum} = R_c + R_{(n+1)}$.

This is an iterative calculation which converges when the sum of the fractions equals unity within tolerable error, i.e. $\sum_{n=1}^{N_p} R_{(n)} = 1$

Knowing the fractions of the gas flow going into each convector plate, the corresponding flow rate in that plate is then calculated as

$$F_{p(n)} = R_{(n)} * F_t \qquad (4.26a)$$

where F_t is the total flow given by

$$F_t = 20480 * \frac{V}{T_{fn}} \quad (kg/h) \qquad (4.26b)$$

4.1.6 Total Pressure Drop in the Stack

This is the total pressure loss between the entry of the gas to the stack at the diffuser plate and the gas return to the basement via the downcomer. This is the summation of the pressure drop across all the convector plates, through the annulus between the cover and the coils, and along the central core of the stack. This is expressed mathematically as follows:

$$p_t = (\Delta p_{cc} + \Delta p_{AG} + \Delta p_{cs})_{n=N_p} + \sum_{n=1}^{N_{p-1}} (S_{cc} + S_{AG} + S_{cs}) \quad (4.27)$$

This pressure drop is expressed in mm.w.g.

4.2 Heat Transfer in Convector Channels

The heat is transferred in the channels of the convector plate mainly by forced convection, because the inert gas attains turbulent flow in the channel. Other modes of heat transfer by conduction and radiation are neglected in the following analysis because of the poor contact at the ends of the coil laps, and the negligible emissivity of the inert gas respectively.

Since the channel is converging towards the centre of the stack, the heat transfer coefficient of forced convection is high at the entry of the channel, falling to a steady value some distance downstream of the gas flow. In a circular pipe, this distance is 24 diameters[21], and the entry effect is expressed by a scaling factor Y which is derived as a function of the distance-to-diameter ratio.

With reference to Fig. 1, let D_H be the hydraulic mean diameter of the channel where

$$D_H = \frac{2\ B_{(n)} * w}{B_{(n)} + w}$$

$$\text{Therefore, } w = \frac{D_H * B_{(n)}}{2*B_{(n)} - D_H}$$

$$\text{But } w = W_o - \frac{\ell * (W_o - W_i)}{L}$$

Differentiating and rearranging gives the following equation:

$$\frac{d\ell}{D_H} = \frac{-L}{2(W_o - W_i)} * \left(\frac{1}{D_H} + \frac{1}{2B_{(m)} - D_H} + \frac{2\,B_{(n)}}{(2B_{(n)} - D_H)^2}\right) dD_H$$

Let the distance-to-diameter ratio be x, then

$$x = \int_o^{\ell} \frac{d\ell}{D_H} = \frac{L}{2(W_o - W_i)} * \left(\ell n \left(\frac{W_o}{w}\right) + \frac{1}{B_{(n)}} (W_o - w)\right) \qquad (4.28)$$

The length of the channel L is based on the larger diameter D_{max} such that $L = \frac{D_{max} - DI_{(n)}}{2}$ where D_{max} is $DO_{(n)}$ or $DO_{(n+1)}$ whichever is larger. Similarly, $w = W_i + \frac{2*z * (W_o - W_i)}{D_{max} - DI_{(n)}}$ where z is the distance from the inner end of the channel to the position of width w.

The correction of entry effect is given as a factor Y which is plotted versus the distance-to-diameter ratio in Engineering Science Data[21]. Curves (4) and (5) shown in the above reference for sharp-edged entry or orifice plate are correlated, in this work, by the following relationship:

$$Y = 0.418 + 0.204 * \ell n(x) \quad \text{for} \quad 1 < x < 24$$

and $Y = 1$ for $x \geq 24$

At the entry of the channel, $W_o >> B_{(n)}$ and hence the hydraulic mean diameter approximates to the following: $D_H = 2*B_{(n)}$. Thus at the outer periphery of the convector channel

$$x = \frac{10^{-2}}{4*B_{(n)}} \quad , \quad taking\ \ell = 5\ mm.$$

During cooling, the convective heat transfer coefficient is reduced by $(\mu_w/\mu_b)^{0.18}$ where μ_w is the absolute viscosity of the wall and μ_b is that of the bulk of the gas flow[21]. In case of nitrogen being the inert gas, the above ratio could be expressed in terms of temperatures as $\Psi = (T_b/T_w)^{0.49}$ where the subscripts w and b denote the wall and bulk flow respectively.

The temperature of the wall T_w at radius r, is calculated at the beginning of the time interval as the average of the temperature of the top end of coil (n) at radius r, and that of the bottom end of coil (n+1) at the same radius.

Applying the Dittus-Boetler equation[19], the heat transfer coefficient of forced convection will be obtained from the following equation:

$$\frac{h_c D}{k} = \frac{0.023}{Y} \Psi R_e^{.8} P_r^{.4} \qquad (4.29)$$

where R_e and P_r are Reynolds and Prandtl numbers respectively.

The mass velocity through the $NC_{(n)}$ channels of plate (n) is given by

$$G = F_{p(n)} * \frac{1}{NC_{(n)}*B_{(n)}*w} \qquad (4.30a)$$

and

$$R_e = \frac{GD_H}{\mu} = \frac{2 * F_{p(n)}}{\mu*NC_{(n)}*(B_{(n)}+w)} \qquad (4.30b)$$

where $F_{p(n)}$ is the gas flow rate in plate (n).

$$P_r = C_{pg} * \mu_g / K_g \qquad (4.30c)$$

Substituting from equations (4.30a-c) in equation (4.29), the heat transfer coefficient becomes the following

$$h_c = 0.023 \frac{\Psi}{Y} * \frac{(B_{(n)}+w)^{0.2}}{B_{(n)}*w} * \left(\frac{F_{p(n)}}{NC_{(n)}}\right)^{0.8} * \frac{C_{pg}^{0.4} K_g^{0.6}}{\mu_g^{0.4}} \qquad (4.31)$$

4.3 The Gas Temperature Profile in Convector Channel

The nitrogen gas enters the convector plate (n) from the annulus between the cover and the stack at a temperature $T_{gi(n)}$. As the gas flows in the channels of the plate, its temperature changes with the radial position along the channel. The derivation of the profile of this temperature, with radius as argument, is based on the heat balance between the gas and the ends of coils.

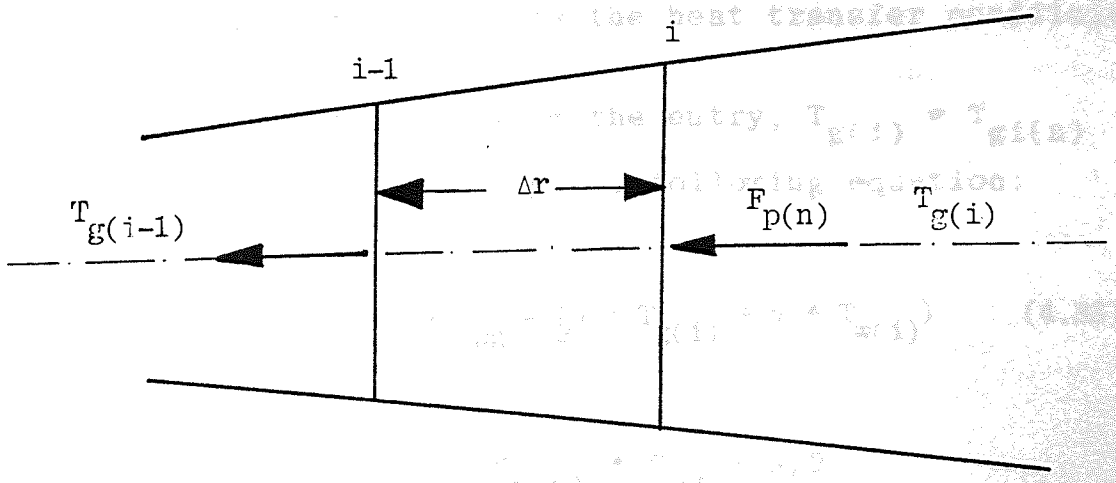

Figure 4.3

Let $T_{w(i)}$ be the average wall temperature of the two ends of the coils above and below the convector plate (n) at radius r. This wall temperature is calculated at the beginning of the time interval. $T_{g(i)}$ and $T_{g(i-1)}$ are respectively the temperatures entering and leaving the increment of the channel of length Δr, see Fig. 4.3.

The heat balance over the increment in the channel between i and i-1 is expressed by equating the heat released from the gas due to its temperature change from $T_{g(i)}$ to $T_{g(i-1)}$, to the heat input to the increment of the coils' ends between radii r + Δr and r. This is written mathematically as follows:

$$F_{p(n)} * C_{pg} * (T_{g(i)} - T_{g(i-1)}) = A_c * h_c * (T_{gm} - T_{w(i)}) \qquad (4.32)$$

where $A_c = 2\pi(2r\Delta r - (\Delta r)^2)$ which accounts for the two surfaces above and below the convector plate, $T_{gm} = \frac{1}{2}(T_{g(i)} + T_{g(i-1)})$, C_{pg} is the specific heat capacity of the gas evaluated at $T_{g(i)}$, $F_{p(n)}$ is the flow rate of the gas in convector plate (n) and h_c is the heat transfer coefficient.

Therefore, starting from the entry, $T_{g(i)} = T_{gi(n)}$ and $T_{g(i-1)}$ is then given by the following equation:

$$T_{g(i-1)} = \frac{1}{\beta}\left((F_{p(n)} * C_{pg} - \frac{\alpha}{2}) * T_{g(i)} + \alpha * T_{w(i)}\right) \qquad (4.33)$$

where

$$\alpha = A_c * h_c \text{ and } \beta = F_{p(n)} * C_{pg} + \alpha/2$$

CHAPTER FIVE

TRANSIENT CONDUCTION IN A COIL

TRANSIENT CONDUCTION IN A COIL

5.1 The Conduction Model

Since the steel coils are axially symmetrical, only half of a vertical section through a diameter of the coil will be considered. Heat flow in the direction of the tangential coordinates is taken as zero. In the model, the thermophysical properties of the steel coils are independent of temperature, which varies widely throughout the annealing cycle. These properties are correlated as polynomials of absolute temperature.

To derive the model of heat conduction in the coil, consider a cylindrical element of thickness δr at radius r from the centre of the coil, and of length δz at height z above the bottom of the coil as shown in Fig. 5.1

Assumptions:

1. The thermal conductivity of the coil in the axial direction is the same as that of steel, and expressed as a polynomial of the temperature at the centre of the element. Although there may be an axial temperature gradiant across the element, it is assumed that $\delta K_s/\delta z = 0$; where K_s is the thermal conductivity of steel, z and r are the axial and radial coordinates in the coil respectively.

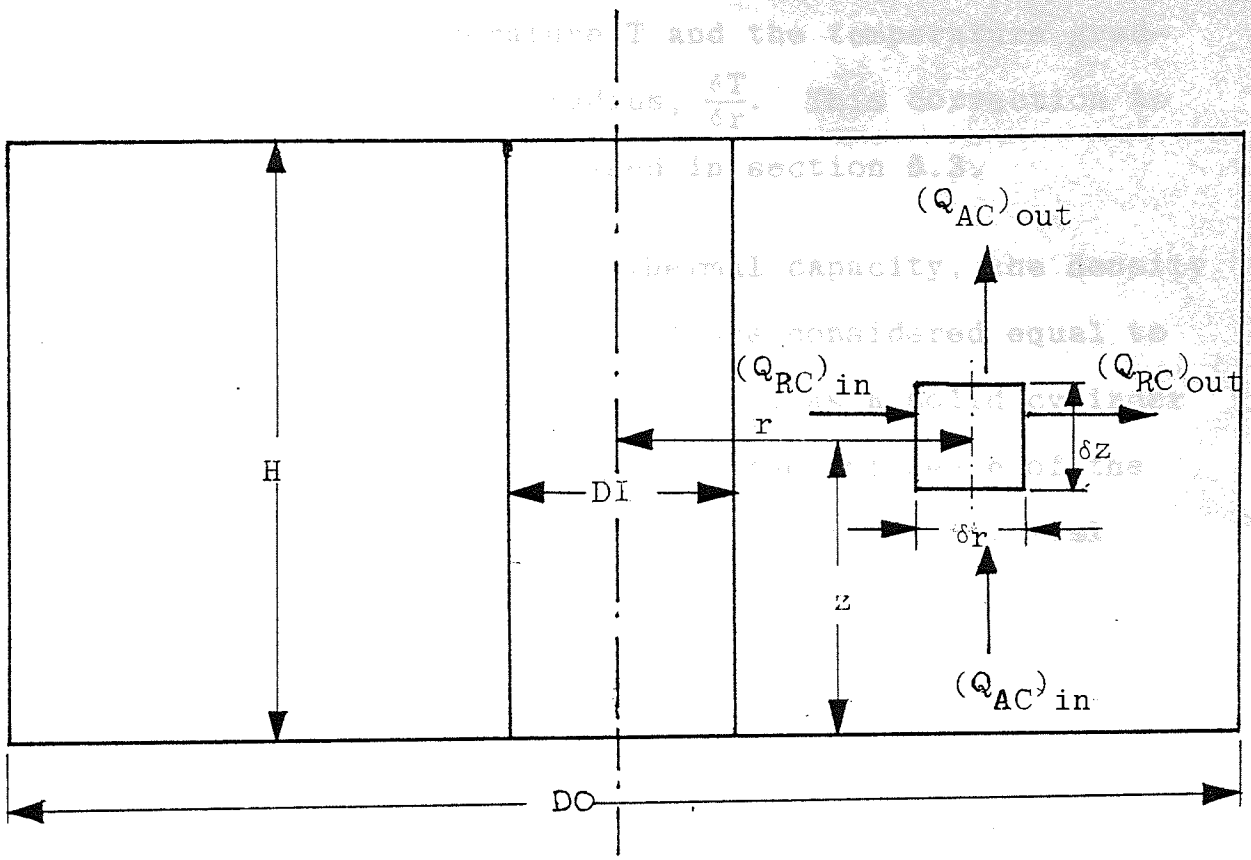

Figure 5.1

Vertical section through a diameter of the coil with the incremental elements on one half of the coil

2. Since the thickness of the steel strip may not be constant throughout the coil, and because the thermal expansion of steel may change the width of the gaps between adjacent laps in the coil, there may be an extra resistance against heat conduction in the radial direction of the coil. For this reason, an effective thermal conductivity in the radial direction K_r is expressed in terms of steel conductivity K_s multiplied by a correction factor which accounts for the extra resistance. Hence,

$$K_r = U * K_s \qquad (5.1)$$

where U is the correction factor which is a function of the radius r, the temperature T and the temperature gradient with respect to this radius, $\frac{\delta T}{\delta r}$. This correction to radial conductivity is discussed in section 5.3.

3. When calculating mass and thermal capacity, the density and the specific heat of the coil are considered equal to those of steel; i.e. treating the coil as a solid cylinder of steel. This effectively ignores the influence of the gaps between adjacent laps of steel, on those physical properties.

Heat Balance

The transient heat balance over the cylindrical element is:

Heat Input - Heat Output = Heat Accumulation

According to assumptions (2) and (3), the heat is transferred in the coil by axial and radial conduction only. Therefore,

$$(Q_{RC_{in}}) + (Q_{AC})_{in} - (Q_{RC})_{out} - (Q_{AC})_{out} = Q_{ACC} \qquad (5.2)$$

where the subscripts RC and AC indicate radial and axial conduction, respectively; and

$$(Q_{RC})_{in} = 2\pi r\delta z \left(-UK_s\frac{\delta T}{\delta r} - \frac{\delta}{\delta r}\left(-UK_s\frac{\delta T}{\delta r}\right)\frac{\delta r}{2}\right)$$

$$(Q_{AC})_{in} = 2\pi r\delta r \left(-K_s\frac{\delta T}{\delta z} - \frac{\delta}{\delta z}\left(-K_s\frac{\delta T}{\delta z}\right)\frac{\delta z}{2}\right)$$

$$(Q_{RC})_{out} = 2\pi(r+\delta r)\delta z(-UK_s \frac{\delta T}{\delta r} + \frac{\delta}{\delta r}(-UK_s \frac{\delta T}{\delta r})\frac{\delta r}{2})$$

$$(Q_{AC})_{out} = 2\pi r\delta r\,(-K_s \frac{\delta T}{\delta z} + \frac{\delta}{\delta z}(-K_s \frac{\delta T}{\delta z})\frac{\delta z}{2})$$

$$Q_{ACC} = 2\pi r\delta r\delta z \frac{\delta}{\delta\theta}(\rho_s C_{p_s} T)$$

But

$$\frac{\delta}{\delta\theta}(\rho_s C_{p_s} T) = \frac{\delta}{\delta T}(\rho_s C_{p_s} T)\cdot\frac{\delta T}{\delta\theta}$$

Hence,

$$Q_{ACC} = 2\pi r\,\delta\, r\delta z\,(\rho_s C_{p_s} + T\frac{\delta}{\delta T}(\rho_s C_{p_s}))\frac{\delta T}{\delta\theta}$$

where ρ_s and C_{p_s} are the density and the specific heat of the coil respectively, and θ is time.

After substitution in equation (5.2), rearranging and taking limits as $\delta r \to 0$, the model of heat conduction in the coil becomes as follows:

$$\alpha_s\,(\frac{\partial^2 T}{\partial z^2} + U\frac{\partial^2 T}{\partial r^2} + (\frac{U}{r} + \frac{\partial U}{\partial r})\cdot\frac{\partial T}{\partial r}) = \frac{\partial T}{\partial\theta} \qquad (5.3a)$$

where

$$\alpha_s = \frac{K_s}{\rho_s C_{p_s} + T\frac{\partial}{\partial T}(\rho_s C_{p_s})} \qquad (5.3b)$$

At time $\theta = 0$, the temperature everywhere in the coil is T_o.

5.2 Boundary Conditions

There are three transfer boundaries of the coil:

1. The outer periphery of the coil facing the inner

cover. The heat transfer at this boundary is effected by the following modes:

(a) Radiative transfer between the cover and the outer periphery of the coil with the inert gas as a transparent medium.

(b) Convection from the inert gas flowing in the annulus between the cover and the periphery of the coil.

2. The bottom and top ends of the coil where the convector plates are placed to allow forced convection between the coil ends and the circulating inert gas flowing inward through the convector channels. Conduction through the vanes of the plate also contributes a little to the heat transfer at these end boundaries.

3. In the inner core at the centre of the stack, the inert gas flows downward towards the base of the furnace. In this zone, heat is exchanged between the gas and the inner surface of the coils by forced convection.

Assumptions:

1. The inert gas circulating under the cover is mainly composed of nitrogen with very little content of CO_2 and no water vapour; hence its emissivity is negligible. So the radiation exchange between this gas and the outer surface of the coil is ignored.

2. In the convector plates at the ends of the coil, the convective transfer is considered as the controlling mode of heat transfer. Heat conduction from the convector

plate via the vanes to the coil ends is neglected due to the small dimensions of the vanes and the poor contact between the vanes and the coil ends.

Generally, all the above boundary conditions of this system are of the following type[22]:

$$K_e * \frac{\partial T}{\partial x} = q_x \qquad (5.4)$$

where K_e is the effective thermal conductivity and q_x is the local heat flux through the bundary in the direction of the x-coordinate.

The boundary conditions, at the different locations in the coil surface are derived in the light of the above assumptions as follows:

(a) Outer Periphery of the Coil:

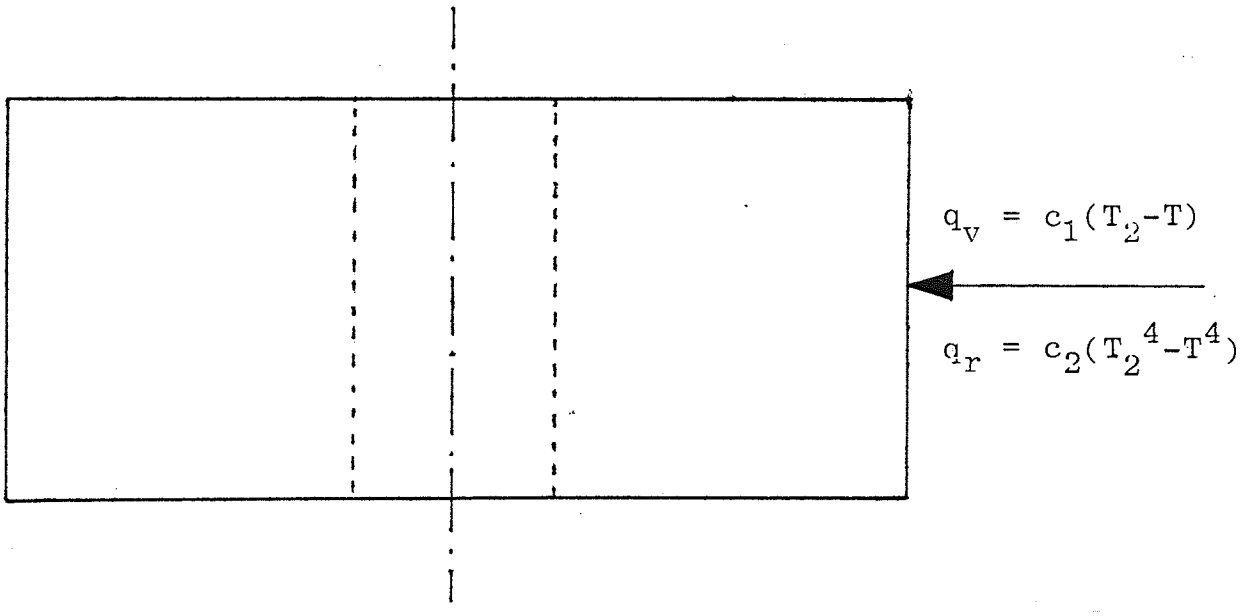

Outer peripheral heat flux

The heat balance at this boundary of the coil gives the following equation:

$$UK_s \frac{\partial T}{\partial r} = q_v + q_r = C_1*(T_2-T) + C_2(T_2^4 - T^4) \qquad (5.5)$$

where q_v and q_r are the convective and the radiative fluxes to the outer periphery of the coil respectively; T_2 is the cover temperature and the factors C_1 and C_2 are defined in Chapter 6.

For the solution of the conduction equation (5.3a) when coupled with equation (5.5), the following approximation[23] is used to evaluate $T_2^4 - T^4$:

$$T_2^4 - T^4 = T_2^4 + 3P^4 - 4P^3T \qquad (5.6)$$

where P is the value of the coil surface temperature at the beginning of the time interval. After substitution in the conduction model, it becomes the following:

$$UK_s \frac{\partial T}{\partial r} = -E_o * T + q_o \qquad (5.7a)$$

where

$$E_o = C_1 + 4 * C_2 * P^3 \qquad (5.7b)$$

and

$$q_o = C_1 * T_2 + C_2 (T_2^4 + 3P^4) \qquad (5.7c)$$

(b) Lower End of the Coil

The heat balance at the convector plate below the coil gives the following formula:

$$K_s * \frac{\delta T}{\delta z} = h_c * (T_{gb} - T) \qquad (5.8)$$

where h_c is the convective heat transfer coefficient in the convector plate and T_{gb} is the temperature of the gas in the convective channels below the coil.

(c) Upper End of the Coil:

Similarly, the heat balance at the plate above the coil results in this equation:

$$K_s \frac{\delta T}{\delta z} = - h_c (T - T_{gt}) \qquad (5.9)$$

where T_{gt} is the gas temperature in the convector plate above the coil and h_c as above.

(d) Inner Surface of the Coil:

The heat balance in the core gives the following:

$$UK_s \frac{\delta T}{\delta r} = - h_{cr} (T_{gc} - T) \qquad (5.10)$$

where h_{cr} is the convective heat transfer coefficient in the core of the stack and T_{gc} is the temperature of the gas flowing down to the basement.

5.3 Effective Radial Conductivity

Since the thickness of steel sheet may not be constant over its entire width, the wraping of the steel sheet into coil form may create some gaps between the laps of the coil. These initial gaps are assumed negligible insofar as the resistance to heat transfer is concerned. However, a positive temperature gradient in the radial direction might cause the coil laps to separate and allow the inert gas to fill the gaps between them. This separation resulting from the thermal influence cannot be ignored. Hence the local thermal conductivity of the coil in the radial direction becomes less than that of solid steel.

In view of the assumption stated above, it can be proved that if there is no positive temperature gradient, the laps will not open. The reason for this is that, in the absence of radial positive temperature gradient, the steel sheet expands in the same proportion as the radii of the inner and outer surfaces of the laps increase.

5.3.1 Correlation of Separation with Temperature Gradient

Fig. 5.2a shows adjacent laps touching each other at the initial temperature T_o, where r is the radius and δ is the initial thickness of the steel sheet. So the radii of the inner and outer surfaces of the laps, r_1 and r_2 respectively, are defined as follows:

$$r_1 = r - \delta \qquad (5.11a)$$

$$r_2 = r + \delta \qquad (5.11b)$$

Fig. 5.2b shows the same laps at a higher temperature T. At this temperature the thickness of the sheet expands from δ to δ' and if there is a positive gradient, the laps open to create a gap of thickness x. Similarly, the inner and outer radii of the laps become r_1' and r_2' respectively. The following relationships are obtained from the linear thermal expansion and equations (5.11a) and (5.11b):

$$r_1' = (r - \delta)\ (1 + \lambda_s(T - \delta \frac{\delta T}{\delta r} - T_o)) \qquad (5.12a)$$

$$r_2' = (r+\delta)\ (1 + \lambda_s(T + \delta \frac{\delta T}{\delta r} - T_o)) \qquad (5.12b)$$

$$\delta' = \delta(1 + \lambda_s(T - T_o)) \qquad (5.12c)$$

where λ_s is the coefficient of linear expansion of steel which is a function of temperature[24] as shown in Appendix (A-3).

Also from Fig. 5.2b, it can be shown that

$$x = r_2' - r_1' - 2\delta' \qquad (5.13)$$

Hence, from equations (5.12a-c) and (5.13), the width of the gap relative to the steel sheet thickness at T_o, can be expressed in terms of temperature gradient with respect to radius as follows:

$$\frac{x}{\delta} = r\ \lambda_s \frac{\delta T}{\delta r} \qquad (5.14)$$

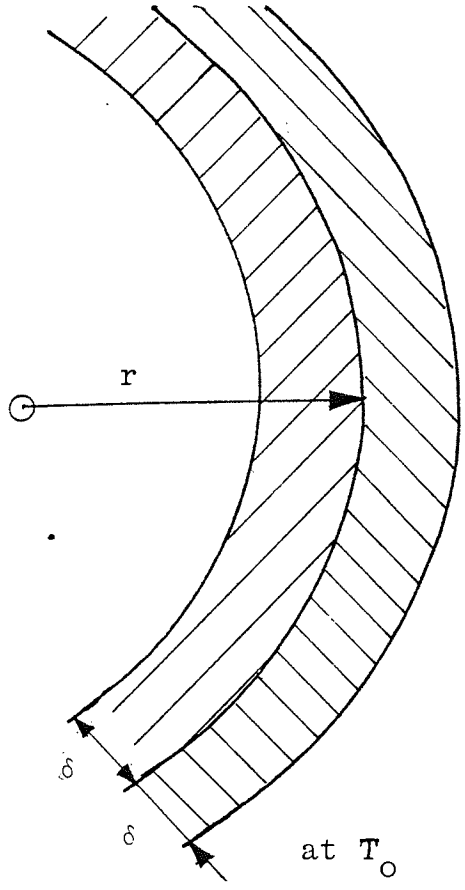

Figure 5.2a

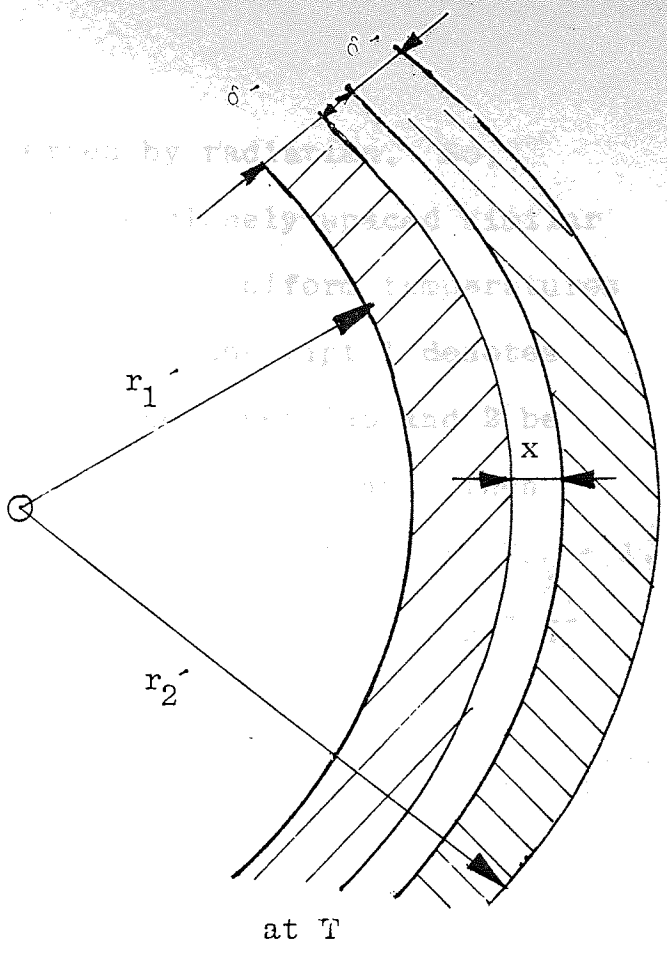

Figure 5.2b

$T > T_o$

Horizontal section through part of two adjacent laps of a coil.

Fig. a: the coil laps touching each other

Fig. b: the coil laps separated

5.3.2 Heat Transfer between Steel Laps

When the laps open, the inert gas fills the gap created between them. So the coefficient of conductive transfer in the gas gap will be $h_g = \frac{K_g}{x}$ where K_g is the thermal conductivity of the inert gas which is correlated as a polynomial of temperature[24] as in Appendix (B-1). Similarly, the conductive coefficient of the steel lap is given by

$$h_s = K_s/\delta$$

Heat is also tranferred by radiation. So, consider the steel laps to be closely spaced similar cylinders of areas A_1 and A_2 at uniform temperatures T and T + Δ respectively. The subscript 1 denotes the outer convex surface of the inner lap and 2 be the inner concave surface of the outer lap. Then the view factor $F_{11} = 0$; and from $\sum_{j=1}^{n} F_{ij} = 1$, $F_{12} = 1$. From the reciprocosity law $A_i F_{ij} = A_j F_{ji}$, $F_{21} = \frac{A_1}{A_2}$ and $F_{22} = 1 - \frac{A_1}{A_2}$.

Applying equation (3-6b) from Hottel and Sarofim[2] for surface 2, the following is obtained:

$$\frac{W_2 - \varepsilon_2 E_2}{\rho_2} = \int_{A_1} W_1 dF_{21} + \int_{A_2} W_2 dF_{22}$$

By integration and substitution for view factors from above, the following equation is obtained.

$$\frac{W_2 - \varepsilon_2 E_2}{\rho_2} = \frac{W_1 A_1}{A_2} + W_2 \left(1 - \frac{A_1}{A_2}\right) \qquad (5.15a)$$

Similarly, the application of the same equation (3.6b) for surface A_1 results in the following:

$$\frac{W_1 - \varepsilon_1 E_1}{\rho_1} = W_2 \qquad (5.15b)$$

where W_1, W_2 are the radiosities; E_1, E_2 are the emissive powers; ρ_1, ρ_2 are the reflectivies; and ε_1, ε_2 are the emissivities of surfaces 1 and 2 respectively.

The radiosity of surface 1, W_1 is calculated from the simultaneous solution of equations (5.15a) and (5.15b) as follows:

$$W_1 = \frac{A_1\varepsilon_1(1-\varepsilon_2)E_1 + A_2\varepsilon_2(E_2+\varepsilon_1(E_1-E_2))}{A_2\varepsilon_2 + A_1\varepsilon_1(1-\varepsilon_2)} \qquad (5.16)$$

The net radiant flux density from the surface is given by Hottel and Sarofin[2] in equation (3-4) as:

$$q_{net} = \frac{\varepsilon}{\rho}(E-W)$$

In case of the flux density from surface A_1, W_1 is substituted from equation (5.16) in the above expression to give the net flux density as follows:

$$q_{1,\ net} = \frac{E_1 - E_2}{\frac{1}{\varepsilon_1} + \frac{A_1}{A_2}(\frac{1}{\varepsilon_2} - 1)} \qquad (5.17)$$

Since the surface areas A_1 and A_2 are nearly equal and the gap between them is negligibly small as compared with the diameters of the laps, then $A_1 \sim A_2$ and $\varepsilon_1 \sim \varepsilon_2$ and hence,

$$q_{1,net} = \frac{\varepsilon_1}{2-\varepsilon_1}(E_1 - E_2) \qquad (5.18)$$

The emissive powers are given by:

$$E_1 = \sigma(T+\Delta)^4 \quad \text{and} \quad E_2 = \sigma T^4$$

where Δ is the temperature difference between the two surfaces 1 and 2. Therefore,

$$q_{1,net} = \frac{\varepsilon_1 \sigma}{2-\varepsilon_1} * ((T+\Delta)^4 - T^4) \qquad (5.19)$$

By the expansion of the difference $(T+\Delta)^4 - T^4$, equation (5.19) becomes the following:

$$q_{1,net} = \frac{\varepsilon_1 \sigma \Delta T^3}{2 - \varepsilon_1} (4 + 6 \frac{\Delta}{T} + 4 (\frac{\Delta}{T})^2 + (\frac{\Delta}{T})^3)$$

The terms containing $\frac{\Delta}{T}$ are neglected because $\frac{\Delta}{T}$ is expected to be very small in the order of 10^{-3}. Thus the radiative heat transfer coefficient, which is the quotient of the flux density divided by the temperature difference , is obtained as follows:

$$h_r = \frac{4 \varepsilon_1 \sigma T^3}{2-\varepsilon_1} \qquad (5.20)$$

5.3.3 Correction Factor for Radial Conductivity

The various heat transfer coefficients, derived above, are additive. The effective thermal conductivity in the radial direction is expressed as $U*K_s$ where K_s is the thermal conductivity of steel and U is the correction for the radial direction in the coil, which accounts for the extra heat transfer resistances. Thus, the effective conduction resistance becomes:

$$R_e = \frac{\delta + x}{U*K_s} = \frac{\delta(1 + x/\delta)}{U*K_s} \qquad (5.21)$$

Similarly, the heat transfer resistance due to the conduction and radiation in the gap is given by:

$$R_g = \frac{1}{h_g+h_r} = \frac{1}{K_g/x+h_r} = \frac{x}{K_g} * \frac{1}{1+\frac{x}{K_g}h_r} \qquad (5.22)$$

But $R_e = R_s + R_g$ where R_s is the resistence of conduction in the steel metal, $\frac{\delta}{K_s}$. Therefore,

$$\frac{\delta(1+x/\delta)}{U*K_s} = \frac{\delta}{K_s} + \frac{x}{K_g} * \frac{1}{1+\frac{x}{K_g}h_r} \qquad (5.23)$$

Dividing by δ/K_s, the above equation becomes the following:

$$\frac{1+x/\delta}{U} = 1 + \frac{x}{\delta} * \frac{K_s}{K_g} * (1 + \frac{xh_r}{K_g})^{-1} \qquad (5.24)$$

For T = 800K and a gap of thickness $x = 6*10^{-3}$mm, the term for the radiation contribution is calculated as $\frac{xh_r}{K_g} \sim 4*10^{-4}$, which is very small, and hence the radiation in the gap is negligible in comparison with the conduction through the nitrogen which fills the gap.

The thickness of the steel strip is about 3mm; so $\frac{x}{\delta} \sim 2*10^{-3}$ and hence $1 + \frac{x}{\delta} \sim 1$. Therefore, equation (5.24) reduces to the following approximation.

$$\frac{1}{U} = 1 + \frac{x}{\delta} * \frac{K_s}{K_g} \qquad (5.25)$$

By the substitution of $\frac{x}{\delta}$ from equation (5.14), the correction factor for radial conductivity would be obtained from the following equation:

$$\frac{1}{U} = 1 + r * \frac{K_s \lambda_s}{K_g} * \frac{\delta T}{\delta r} \qquad (5.26)$$

5.4 Numerical Solution of the Conduction Model

The partial differential equation, which defines the transient heat conduction inside the coil and satisfies the boundary conditions given in section (5.2), is solved numerically by finite difference methods. Two numerical methods were suggested and both tested with a one-coil furnace and nominal boundary conditions[25]. These tests were designed to investigate the effect of these numerical solutions on the temperature profile in the coil and the types of the boundary fluxes. The performance of the numerical techniques was measured by the stability of the solution, the criteria for convergence, the accuracy, the truncation errors and the behaviour at the boundary conditions[26] of this particular problem. The results are shown in Chapter (8).

The methods tested are the Barakat[27] and ADI[28]. The ADI method was found to be more suitable for the solution of conduction in this specific application, and it is used for the solution of the heat conduction model

for this type of annealing furnace.

5.4.1 Barakat Method

This is an explicit finite difference technique which assumes two different solutions, X_{ij}^{k+1} and Y_{ij}^{k+1} for the transient conduction equation. The two solutions are multi-level finite difference representation of the system equation. Both solutions satisfy the conduction model as well as the initial and boundary conditions of the system. The final solution of the problem is then obtained from the arithmatic mean of the two solutions.

The finite difference approximation applied by this method is based on the average of the finite difference, taken over one space interval, at the beginning of the time interval and the finite difference, taken over one space interval, at the end of the time interval. Thus, the derivatives are expressed as shown in the following diagram:

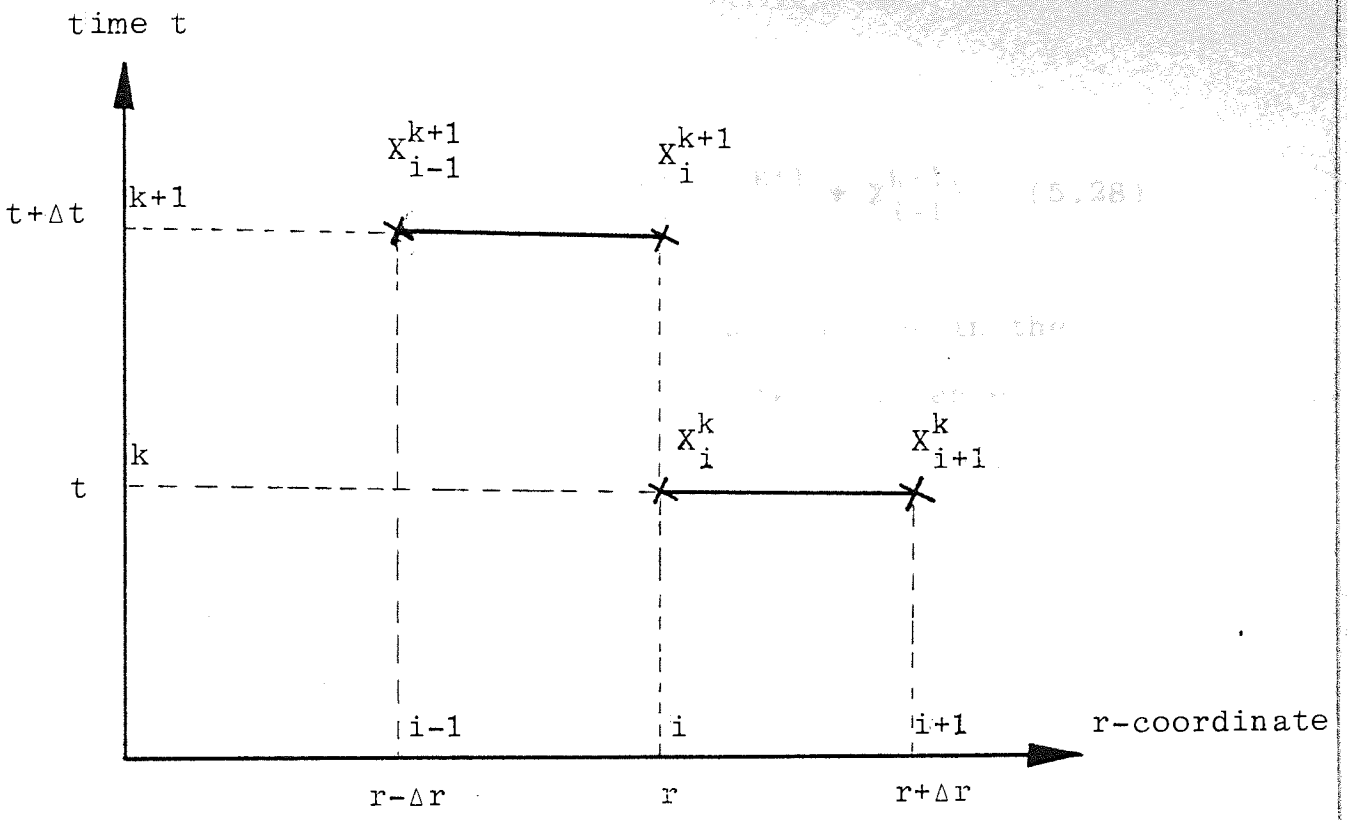

The first derivative of X_i^{k+1} with respect to r is given by:

$$\frac{\partial X_i^{k+1}}{\partial r} = \frac{1}{2}\left(\frac{X_{i+1}^k - X_i^k}{\Delta r} + \frac{X_i^{k+1} - X_{i-1}^{k+1}}{\Delta r}\right)$$

Therefore,

$$\frac{\partial X_i^{k+1}}{\partial r} = \frac{1}{2*\Delta r}\left(X_{i+1}^k - X_i^k + X_i^{k+1} - X_{i-1}^{k+1}\right) \qquad (5.27)$$

The second derivative of X_i^{k+1} with respect to r is obtained as follows:

$$\frac{\partial^2 X_i^{k+1}}{\partial r^2} = \frac{1}{\Delta r}\left(\frac{X_{i+1}^k - X_i^k}{\Delta r} - \frac{X_i^{k+1} - X_{i-1}^{k+1}}{\Delta r}\right)$$

Hence,

$$\frac{\partial^2 X_i^{k+1}}{\partial r^2} = \frac{1}{(\Delta r)^2}\left(X_{i+1}^{k} - X_i^{k} - X_i^{k+1} + X_{i-1}^{k+1}\right) \quad (5.28)$$

After substituting for all the derivatives in the conduction equation by their finite difference approximations, the first solution of the heat conduction in the coil results in the following lower tridiagonal matrix:

$$\begin{bmatrix} a_{11} & 0 & 0 & 0 & - & - & 0 \\ a_{21} & a_{22} & 0 & 0 & & & 0 \\ a_{31} & a_{32} & a_{33} & 0 & & & 0 \\ 0 & a_{42} & a_{43} & a_{44} & & & 0 \\ - & - & - & - & - & - & - \\ - & - & - & - & - & - & - \\ - & - & - & - & - & - & - \\ 0 & 0 & 0 & - & a_{n-2n} & a_{n-1n} & a_{nn} \end{bmatrix} * \begin{bmatrix} x_1 \\ x_2 \\ - \\ - \\ - \\ - \\ - \\ x_n \end{bmatrix} = \begin{bmatrix} e_1 \\ e_2 \\ - \\ - \\ - \\ - \\ - \\ e_n \end{bmatrix} \quad (5.29)$$

This matrix is solved by Gauss elimination technique.

In the case of the second solution, the derivatives are obtained from the following representation:

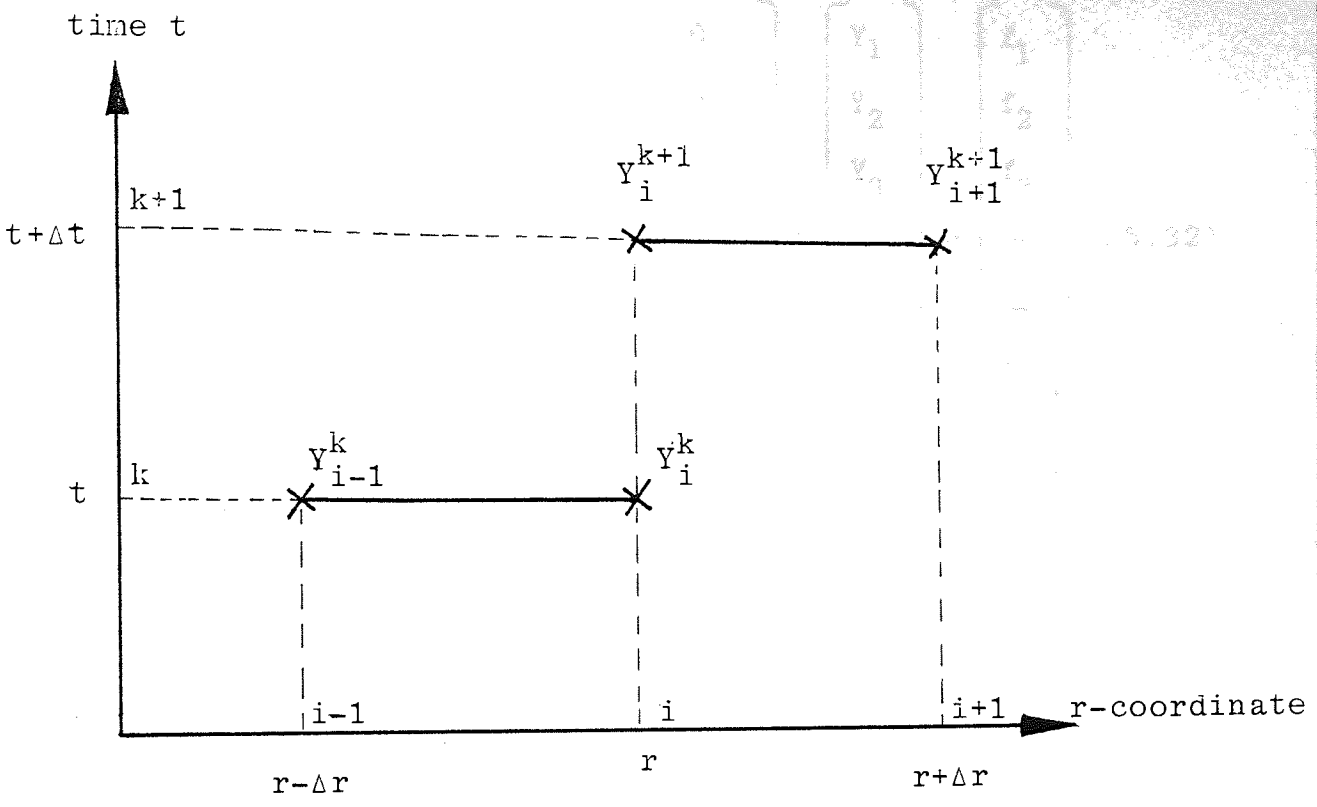

The first derivative of Y_i^{k+1} with respect to r is obtained by the same procedure, as follows:

$$\frac{\partial Y_i^{k+1}}{\partial r} = \frac{1}{2*\Delta r}\left(Y_{i+1}^{k+1} - Y_i^{k+1} + Y_i^{k} - Y_{i-1}^{k}\right) \qquad (5.30)$$

and the second derivative as:

$$\frac{\partial^2 Y_i^{k+1}}{\partial r^2} = \frac{1}{(\Delta r)^2}\left(Y_{i+1}^{k+1} - Y_i^{k+1} - Y_i^{k} + Y_{i-1}^{k}\right) \qquad (5.31)$$

For the equation of heat conduction in the coil, the second solution obtained by applying the Barakat method would result in an upper tridiagonal matrix of the following form:

$$\begin{bmatrix} b_{11} & b_{12} & b_{13} & 0 & 0 & - & 0 \\ 0 & b_{22} & b_{23} & b_{24} & 0 & - & 0 \\ 0 & 0 & b_{33} & b_{34} & b_{35} & - & 0 \\ - & - & - & - & - & - & - \\ - & - & - & - & - & - & - \\ & & & & & b_{n-1n-1} & b_{n-1n} \\ 0 & 0 & - & - & - & 0 & b_{nn} \end{bmatrix} * \begin{bmatrix} Y_1 \\ Y_2 \\ Y_3 \\ - \\ - \\ Y_{n-1} \\ Y_n \end{bmatrix} = \begin{bmatrix} f_1 \\ f_2 \\ f_3 \\ - \\ - \\ f_{n-1} \\ f_n \end{bmatrix} \qquad (5.32)$$

This matrix is also solved by Gauss elimination. The matrices (a), (b), (e) and (f) in equations (5.29) and (5.32) depend on temperature and boundary conditions. They are evaluated at the beginning of the time interval and considered as constant for the solution of the two matrices in these equations.

The final solution of the temperature distribution in the coil is computed from the arithmatic average of the two solutions as follows:

$$T_i^{k+1} = \frac{1}{2} (X_i^{k+1} + Y_i^{k+1}) \qquad (5.33)$$

5.4.2 ADI Method

This is the Alternating Direction Implicit method[28]. It is a finite difference approximation technique which entails cyclic applications of a one-dimensional Crank-Nicolson[29] differencing procedure to one spatial coordinate after another. The one-dimensional application of Crank-Nicolson to the first

coordinate produces a first estimate of the solution, the application to the second spatial coordinate produces a second estimate, and so on until the Crank-Nicolson technique is applied to the last coordinate which gives the final solution of the system.

The finite difference approximation of the derivatives implemented by this method is the same as that of Crank-Nicolson which is taken over two coordinate intervals as follows:

$$\frac{\partial T_{ij}}{\partial x} = \frac{T_{i+1j} - T_{i-1j}}{2 * \Delta x}$$

and

$$\frac{\partial^2 T_{ij}}{\partial x^2} = \frac{T_{i+1j} - 2 * T_{ij} + T_{i-1j}}{(\Delta x)^2}$$

For conduction in two space dimensions like

$$\frac{\partial T}{\partial \theta} = \alpha\left(\frac{\partial^2 T}{\partial x^2} + \frac{\partial^2 T}{\partial y^2}\right)$$

the ADI formulation generates one estimate and a final solution as follows:

$$E_{ij} - T_{ij}^k = \alpha * \Delta\theta * \left(\frac{\partial^2}{\partial x^2}\left(\frac{E_{ij} + T_{ij}^k}{2}\right) + \frac{\partial^2}{\partial y^2} T_{ij}^k\right) \qquad (5.34)$$

and

$$T_{ij}^{k+1} - E_{ij} = \alpha * \Delta\theta * \frac{\partial^2}{\partial y^2}\left(\frac{T_{ij}^{k+1} - T_{ij}^k}{2}\right) \qquad (5.35)$$

where E_{ij} is the estimate and the subscripts k and k+1 denote the beginning and the end of the time interval respectively; and $\Delta\theta$ is the time interval. Thus, T_{ij}^{k+1} is the final solution of the temperature distribution in the coil.

5.4.3 ADI Formulation of Annealing Conduction Model

The formula of transient heat conduction in the coil given by equation (5.3a) could be written in the following form:

$$\frac{\partial T_{ij}}{\partial \theta} = a_1 \frac{\partial^2 T_{ij}}{\partial z^2} + a_2 \frac{\partial^2 T_{ij}}{\partial r^2} + a_3 \frac{\partial T_{ij}}{\partial r} \qquad (5.36)$$

where $a_1 = \alpha_s$

$a_2 = \alpha_s * U$

$a_3 = \alpha_s * (\frac{U}{r} + \frac{\partial U}{\partial r})$

α_s is defined by equation (5.3b), θ is the time and z and r are the axial and radial coordinates respectively. The subscripts i and j denote the radial and axial positions in the grid, respectively.

The ADI application to equation (5.36) gives the following:

$$E_{ij} - P_{ij} = a_1 * \frac{\Delta\theta}{2} * (\frac{\partial^2 E_{ij}}{\partial z^2} + \frac{\partial^2 P_{ij}}{\partial z^2}) + a_2 * \Delta\theta * \frac{\partial^2 P_{ij}}{\partial r^2} + a_3 * \Delta\theta * \frac{\partial P_{ij}}{\partial r} \qquad (5.37)$$

$$T_{ij}-E_{ij} = a_2 * \frac{\Delta\theta}{2} * \left(\frac{\partial^2 T_{ij}}{\partial r^2} - \frac{\partial^2 P_{ij}}{\partial r^2}\right) + a_3 * \frac{\Delta\theta}{2} * \left(\frac{\partial T_{ij}}{\partial r} - \frac{\partial P_{ij}}{\partial r}\right) \qquad (5.38)$$

where P_{ij} is the value of the temperature profile in the coil at the beginning of the time interval, E_{ij} is its estimate and T_{ij} is its final solution.

After the substitution for the derivatives by their finite difference approximations, the general form of the above equations in ADI notations becomes the following:

$$-\frac{\alpha_1}{2} * E_{ij-1} + (1+\alpha_1)*E_{ij} - \frac{\alpha_1}{2} * E_{ij+1} = (1-\alpha_1-2\alpha_1)P_{ij}$$

$$+ \frac{\alpha_1}{2} * (P_{ij+1} + P_{ij-1}) + (\alpha_2+\alpha_3)P_{i+1j} + (\alpha_2-\alpha_3)P_{i-1j} \qquad (5.39)$$

and

$$\frac{\alpha_3-\alpha_2}{2} * T_{i-1j} + (1+\alpha_2)*T_{ij} - \frac{\alpha_2+\alpha_3}{2} * T_{i+1j} = E_{ij} + \alpha_2 * P_{ij}$$

$$- \frac{\alpha_2+\alpha_3}{2} * P_{i+1j} + \frac{\alpha_3-\alpha_2}{2} * P_{i-1j} \qquad (5.40)$$

where $\alpha_1 = a_1 * \Delta\theta/(\Delta z)^2$

$\alpha_2 = a_2 * \Delta\theta/(\Delta r)^2$

$\alpha_3 = a_3 * \Delta\theta/(2 * \Delta r)$

Each of equations (5.39) and (5.40) results in a tri-diagonal matrix which is solved by Gauss elimination. The solution of equation (5.39) gives the estimate of the temperature profile, and the final solution is obtained by solving equation (5.40).

5.4.4 ADI Working Equations for the Boundary Conditions

All the first derivatives of temperature with respect to radial or axial position which appear in the heat balance at the boundary conditions are represented by finite difference over two space intervals. This representation of the derivatives generates fictitious terms which must be evaluated and substituted in the general ADI expressions of heat conduction in the coil, equations (5.39) and (5.40). This manipulation of the equations at the boundary conditions will produce the working equation for the numerical solution at the specific boundary as follows:

(a) At the outer periphery of the coil:

The finite difference representation of heat transfer at this boundary gives the fictitious temperature as follows:

$$T_{i+1j} = T_{i-1j} - \varepsilon * T_{ij} + Q_{out} \qquad (5.41a)$$

where $$\varepsilon = \frac{2*\Delta r}{U*K_s} * E_o \qquad (5.41b)$$

and $$Q_{out} = \frac{2*\Delta r}{UK_s} * q_o \qquad (5.41c)$$

E_o and q_o are defined by equations (5.7b) and (5.7c). The substitution for T_{i+1j} from (5.41a) in equations (5.39) and (5.40) gives the following working equations for this boundary:

$$-\frac{\alpha_1}{2}E_{ij-1} + (1+\alpha_1)E_{ij} - \frac{\alpha_1}{2}E_{ij+1} = (1-\alpha_1-2\alpha_2-(\alpha_2+\alpha_3)*\varepsilon)*P_{ij}$$

$$+\frac{\alpha_1}{2}(P_{ij+1} + P_{ij-1}) + 2\alpha_2 P_{i-1j} + (\alpha_2+\alpha_3)*Q_{out} \qquad (5.42)$$

and

$$-\alpha_2 T_{i-1j} + (1+\alpha_2 + \frac{\alpha_2+\alpha_3}{2} * \varepsilon)T_{ij} = E_{ij} + (\alpha_2 + \frac{\alpha_2+\alpha_3}{2} *\varepsilon)P_{ij}$$

$$-\alpha_2 P_{i-1j} \qquad (5.43)$$

(b) At the inner boundary of the coil:

The finite difference form of equation (5.10) is as follows:

$$T_{i-1j} = T_{i+1j} - \beta*T_{ij} + \beta*T_{gc} \qquad (5.44a)$$

where $$\beta = \frac{2*\Delta r*h_{cr}}{U*K_s} \qquad (5.44b)$$

The temperature T_{i-1j} is fictitious which must be substituted for in equations (5.39) and (5.40)to obtain the working equations as follows:

$$-\frac{\alpha_1}{2}E_{ij-1} + (1+\alpha_1)*E_{ij} - \frac{\alpha_1}{2}E_{ij+1} = (1-\alpha_1-2\alpha_2-(\alpha_2-\alpha_3)*\beta)P_{ij}$$

$$+\frac{\alpha_1}{2} * (P_{ij+1} + P_{ij-1}) + (\alpha_2+\alpha_3)*\beta*T_{gc} \qquad (5.45)$$

and

$$(1+\alpha_2 + \frac{\alpha_2-\alpha_3}{2} *\beta)*T_{ij} - \alpha_2 T_{i+1j} = E_{ij} + (\alpha_2 + \frac{\alpha_2-\alpha_3}{2} *\beta)*P_{ij}$$

$$-\alpha_2 P_{i+1j} \qquad (5.46)$$

(c) Lower end of the coil:

The expression of equation (5.8) in finite difference approximation results in the following fictitious term:

$$T_{ij-1} = T_{ij+1} - \gamma * T_{ij} + \gamma * T_{gb} \qquad (5.47a)$$

where $\gamma = \frac{2*\Delta z}{U*K_s} * h_c$ (5.47b)

When this fictitious temperature is substituted in equation (5.39) and (5.40), the working equations become:

$$(1+\alpha_1+\frac{\alpha_1}{2}*\gamma)*E_{ij} - \alpha_1*E_{ij+1} = (1-\alpha_1-2\alpha_2-\frac{\alpha_1}{2}*\gamma)P_{ij}$$

$$+(\alpha_2+\alpha_3)*P_{i+1j} + (\alpha_2-\alpha_3)*P_{i-1j} + \alpha_1 P_{ij+1} + \alpha_1*\gamma*T_{gb} \qquad (5.48)$$

and

$$\frac{\alpha_3-\alpha_2}{2} * T_{i-1j} + (1+\alpha_2)*T_{ij} - \frac{\alpha_2+\alpha_3}{2} * T_{i+1j} = E_{ij} + \alpha_2 P_{ij}$$

$$- \frac{\alpha_2+\alpha_3}{2} * P_{i+1j} + \frac{\alpha_2-\alpha_3}{2} * P_{i-1j} \qquad (5.49)$$

(d) Upper end of the coil:

When equation (5.9) is expressed in finite difference approximation, the following equation is obtained:

$$T_{ij+1} = T_{ij-1} - \gamma * T_{ij} + \gamma * T_{gt} \qquad (5.50)$$

where γ is defined by equation (5.47b). T_{ij+1} is fictitious and hence is substituted in the general

working equations (5.39) and (5.40) where the following are the resulting equations:

$$-\alpha_1 E_{ij-1} + (1+\alpha_1+\frac{\alpha_1}{2}*\gamma)*E_{ij} = (1-\alpha_1-2\alpha_2-\frac{\alpha_1}{2}*\gamma)*P_{ij}$$

$$+(\alpha_2+\alpha_3)*P_{i+1j} + (\alpha_2-\alpha_3)*P_{i-1j} + \alpha_1 P_{ij-1} + \alpha_1*\gamma*T_{gt} \qquad (5.51)$$

and

$$\frac{\alpha_3-\alpha_2}{2} * T_{i-1j} + (1+\alpha_2)*T_{ij} - \frac{\alpha_2+\alpha_3}{2} * T_{i+1j} = E_{ij}+\alpha_2 P_{ij}$$

$$-\frac{\alpha_2+\alpha_3}{2} * P_{i+1j} + \frac{\alpha_3-\alpha_2}{2} * P_{i-1j} \qquad (5.52)$$

In the case of the top coil in the stack, the upper end of the top coil receives radiation from the top of the cover as well as convection from the gas in the top convector plate. Hence equation (5.9) is no longer valid, and instead the heat balance gives the following equation:

$$K_s \frac{\partial T}{\partial z} = q_t = k_1 * (T_{tc} - T) + k_2 * (T_{tc}^4 - T^4) \qquad (5.53)$$

where T_{tc} is the temperature of the cover above the top convector plate, k_1 is an overall convective coefficient for heat transfer between the cover top and the upper end of the top coil via the top convector plate. Both k_1 and k_2 are calculated in Chapter 6. The finite difference representation of this equation is the following:

$$T_{ij+1} = T_{ij-1} + Q_{top} \qquad (5.54a)$$

$$(1+\alpha_2+\frac{\alpha_2-\alpha_3}{2}*\beta)*T_{ij}-\alpha_2\,T_{i+1j} = E_{ij}+(\alpha_2+\frac{\alpha_2-\alpha_3}{2}*\beta)*P_{ij}$$

$$-\alpha_2 P_{i+1j} \qquad (5.58)$$

(ii) At the upper end of the inner surface of the coil, the fictitious terms are T_{i-1j} and T_{ij+1} which are given by equations (5.44a) and (5.50) respectively. The working equations at this boundary will then become the following:

$$-\alpha_1 E_{ij-1} + (1+\alpha_1+\frac{\alpha_1}{2}*\gamma)*E_{ij} = (1-\alpha_1-2\alpha_2 - \frac{\alpha_1}{2}*\gamma -$$

$$(\alpha_2-\alpha_3)*\beta)*P_{ij} + \alpha_1*P_{ij-1} + 2\alpha_2*P_{i+1j} + \alpha_1*\beta*T_{gt}$$

$$+ (\alpha_2-\alpha_3)*\beta*T_{gc} \qquad (5.59)$$

and

$$(1+\alpha_2 + \frac{\alpha_2-\alpha_3}{2}*\beta)*T_{ij} - \alpha_2*T_{i+1j} = E_{ij} + (\alpha_2 + \frac{\alpha_2-\alpha_3}{2}*\beta)*P_{ij}$$

$$-\alpha_2 P_{i+1j} \qquad (5.60)$$

In case of the top coil in the stack, the working equations become as follows:

$$-\alpha_1 E_{ij-1} + (1+\alpha_1)E_{ij} = (1-\alpha_1-2\alpha_2-(\alpha_2-\alpha_3)*\beta)*P_{ij} + \alpha_1*P_{ij-1}$$

$$+2\alpha_2 P_{i+1j} + (\alpha_2-\alpha_3)*\beta*T_{gc} + \alpha_1 * Q_{top} \qquad (5.61)$$

and

$$(1+\alpha_2 + \frac{\alpha_2-\alpha_3}{2}*\beta)*T_{ij}-\alpha_2*T_{i+1j} = E_{ij} + (\alpha_2 + \frac{\alpha_2-\alpha_3}{2}*\beta)*P_{ij}$$

$$-\alpha_2 * P_{i+1j} \qquad (5.62)$$

(iii) At the lower end of the outer periphery of the coil, there are two fictitious temperatures T_{i+1j} and T_{ij-1} expressed by equations (5.41a) and (5.47a) respectively. When T_{i+1j} and T_{ij-1} are substituted in equations (5.39) and (5.40), they give the following:

$$(1+\alpha_1 + \frac{\alpha_1}{2} *\gamma)*E_{ij} - \alpha_1 E_{ij+1} = (1-\alpha_1-2\alpha_2 - \frac{\alpha_1}{2} *\gamma-(\alpha_2+\alpha_3)*\varepsilon)*P_{ij}$$

$$+\alpha_1 *P_{ij+1} + 2\alpha_2 *P_{i-1j} + \alpha_1 *\gamma* T_{gb} + (\alpha_2+\alpha_3)* Q_{out} \quad (5.63)$$

and

$$-\alpha_2 T_{i-1j}+(1+\alpha_2 + \frac{\alpha_2+\alpha_3}{2} *\varepsilon)*T_{ij} = E_{ij}+(\alpha_2 + \frac{\alpha_2+\alpha_3}{2} *\varepsilon)*$$

$$P_{ij} - \alpha_2 P_{i-1j} \quad (5.64)$$

(iv) At the upper boundary of the outer surface of the coil, the working equations are obtained by substituting for the fictitious temperatures T_{i+1j} and T_{ij+1}, from equations (5.41a) and (5.50) respectively, in the general equations (5.39) and (5.40); the following equations are obtained:

$$-\alpha_1 E_{ij}+(1+\alpha_1 + \frac{\alpha_1}{2} *\gamma)*E_{ij} = (1-\alpha_1-2\alpha_2 - \frac{\alpha_1}{2} *\gamma - (\alpha_2+\alpha_3)*\varepsilon)*P_{ij}$$

$$+ 2\alpha_2 P_{i-1j} + \alpha_1 P_{ij-1} + \alpha_1 *\gamma* T_{gt} + (\alpha_2+\alpha_3)* Q_{out} \quad (5.65)$$

and

$$\alpha_2 T_{i-1j} + (1+\alpha_2 + \frac{\alpha_2+\alpha_3}{2} * \varepsilon) * T_{ij} = E_{ij} + (\alpha_2 + \frac{\alpha_2+\alpha_3}{2} * \varepsilon) * P_{ij} - \alpha_2 * P_{i-1j} \quad (5.66)$$

For the special case of the top coil in the stack, the working equations become the following:

$$-\alpha_1 E_{ij-1} + (1+\alpha_1) * E_{ij} = (1-\alpha_1-2\alpha_2-(\alpha_2+\alpha_3)*\varepsilon) * P_{ij} + \alpha_1 P_{ij-1} + 2\alpha_2 * P_{i-1j} + \alpha_1 * Q_{top} + (\alpha_2+\alpha_3) * Q_{out} \quad (5.67)$$

and

$$(1+\alpha_2 + \frac{\alpha_2+\alpha_3}{2} * \varepsilon) * T_{ij} - \alpha_2 T_{i-1j} = E_{ij} + (\alpha_2 + \frac{\alpha_2+\alpha_3}{2} * \varepsilon) * P_{ij} - \alpha_2 P_{i-1j} \quad (5.68)$$

CHAPTER SIX

HEAT TRANSER FLUXES IN THE FURNACE

HEAT TRANSFER FLUXES IN THE FURNACE

For the annealing of steel coils, the heat is transmitted from the furnace side, via the combustion products, to the inner cover, through the inert gas to the steel charge. During cooling, heat is extracted from the steel ccoils by the inert gas directly to the cooler in the basement; also some heat is transferred to the ambient air by radiation and convection through the inner cover. In this chapter, the various heating and cooling fluxes will be discussed. All the heat fluxes will be treated as fluxes transmitted away from the coil surface, and they will be based on unit peripheral area of the coil.

6.1 Heat Transfer Between the Coil and the Cover

Heat is exchanged between the coil periphery and the inner face of the cover by radiation; and since the inert gas circulates between them, there is also convective heat transfer by free and forced gas currents. Consider the coil (m) to be of height H(m) and outer and inner diameters DO(m) and DI(m) respectively.

6.1.1 Radiative Flux

Consider a unit height of the furnace. Then the peripheral area of the outer surface of the coil (m)

is $A_1 = \pi * DO(m)$ and that of the inner surface of the cover is $A_2 = \pi * D_2$ where D_2 is the diameter of the cover.

Let F_{12} be the view factor from the outer periphery of the coil which falls directly on the inner side of the cover. Hence, F_{21} is the view factor from the inner surface of the cover to the outer side of the coil. By the reciprocosity law[18], the direct exchange areas are related to the view factors and the surface areas as follows:

$$\overline{12} = A_1 * F_{12} = A_2 * F_{21} = \overline{21}$$

where $\overline{12}$ is the direct exchange area from the surface 1 to surface 2. The outer area of the coil is convex, hence $F_{11} = 0$

$$\text{Since } \sum_{i=1}^{n} F_{1i} = 1, \text{ then } F_{12} = 1$$

But from the reciprocosity law:

$$F_{21} = \frac{A_1}{A_2} * F_{12} = DO(m)/D_2$$

Therefore,

$$\overline{12} = A_2 * F_{21} = A_1 \qquad (6.1)$$

Equation (3.23) from Hottel and Sarofim[2], 1967 for the three-zone enclosures is used here to calculate the heat flux from the coil surface to the inner side of the cover. In this case,

the direct exchange area between the coil surface and the refractory wall $\overline{1r}$, and that between the inner side of the cover and refractory $\overline{2r}$, are both zero since neither of them sees the refractory. Hence, the above mentioned equation is written as follows:

$$\dot{Q}_{1\rightleftharpoons 2} = \frac{E_1 - E_2}{\frac{\rho_1}{A_1\varepsilon_1} + \frac{\rho_2}{A_2\varepsilon_2} + \frac{1}{\overline{12}}} \qquad (6.2)$$

Where $\dot{Q}_{1\rightleftharpoons 2}$ is the heat flux from the coil side to the inner surface of the cover, ε_1 and ε_2 are the emissivities, ρ_1 and ρ_2 are the reflectivities and the subscripts 1 and 2 designate the outer periphery of the coil and the inner surface of the cover respectively. Because the surfaces are opaque and assumed to be grey, $\rho_1 = 1-\varepsilon_1$ and $\rho_2 = 1-\varepsilon_2$. The emissive powers E_1 and E_2 are calculated by the Stefan-Botlzmann[11] equation as $E_1 = \sigma * T_1^4$ and $E_2 = \sigma * T_2^4$ where T_1 and T_2 are the temperatures of the coil surface and the cover respectively. T_1 is taken as the value of the surface temperature at the beginning of the time interval. The constant σ is given[24] as

$$\sigma = 5.67 * 10^{-11} \text{ kW/m}^2/\text{K}^4.$$

So, the radiative flux per unit peripheral area of the coil becomes the following:

$$\dot{Q}_{1\rightleftharpoons 2} = C_2 * (T_1^4 - T_2^4) \qquad (6.3a)$$

where

$$C_2 = \frac{5.67 * 10^{-11}}{1 + \frac{1-\varepsilon_1}{\varepsilon_1} * \frac{DO_{(m)}}{D_2} + \frac{1-\varepsilon_2}{\varepsilon_2}} \qquad (6.3b)$$

6.1.2 Forced Convection

The flow distribution of the nitrogen between the convector plates results in the minimum flow passing through the top plate. The diameter of the convector plate is always larger than that of the coil; this enhances the convective heat transfer with the inert gas crossing the convector plate while it flows upwards between the coils and the cover. Assuming that about 10% of the total gas flow, calculated by equation (4.26b), passes through the top plate, the Reynolds number is found to be greater than 2500. Hence, turbulent flow of nitrogen is assumed everywhere in the furnace.

For fully developed turbulence in smooth pipes, McAdams[19] shows that the following Dittus and Boetler equation is applicable:

$$Nu = \frac{0.023}{Y} R_e^{0.8} Pr^n \qquad (6.4)$$

where Y is the scaling factor for entry effect, the Prandtl number Pr is evaluated at the temperature

of the bulk flow and the exponent n is given as $n = 0.4$ for heating and $n = 0.3$ for cooling.

In the annular gap between the coils and the cover, the viscosity effect at the gas-coil surface cancels the effect of viscosity at the gas-cover surface when using the overall heat transfer coefficient.

Let h_1 be the local heat transfer coefficient at the outer surface of the coil and h_2 be the local heat transfer coefficient at the inner side of the cover. If C_1 is assumed as the overall heat transfer coefficient between the cover and the coil, then:

$$C_1 dA = h_1 * dA_1 = h_2 * dA_2 = \frac{dQ}{d\theta} = \text{constant.}$$

where $dA = dA_1 + dA_2 = \pi(D_2 + DO_{(m)})$. Therefore,

$$C_1 = \frac{D_2}{D_2 + DO_{(m)}} * h_2 \qquad (6.5)$$

The convective heat transfer coefficient h_2 is calculated from equation (6.4) as follows:

$$h_2 = \frac{0.023}{Y} \left(\frac{GD_H}{\mu_g}\right)^{.8} * \left(\frac{C_{p_g}\ \mu_g}{K_g}\right)^{.4} * \frac{K_g}{D_H} \qquad (6.6a)$$

where the hydraulic mean diameter is $D_H = D_2 - DO_{(m)}$ and $G = \frac{4}{\pi} * \frac{FG_{(m)}}{D_2^2 - (DO_{(m)})^2}$, such that $FG_{(m)}$ is the

gas flow rate in the annulus between the cover and coil (m). Hence,

$$h_2 = \frac{0.0279}{Y} * \left(\frac{FG_{(m)}}{D_2+DO_{(m)}}\right)^{.8} * \frac{1}{D_2-DO_{(m)}} * \left(\frac{C_{p_g}^{0.4} K_g^{0.6}}{\mu_g^{0.4}}\right) \qquad (6.6b)$$

After substitution in equation (6.5), C_1 becomes the following:

$$C_1 = \frac{0.0279}{Y} * \frac{(FG_{(m)})^{0.8}}{(D_2+DO_{(m)})^{1.8}} * \frac{D_2}{D_2-DO_{(m)}} * \left(\frac{C_{p_g}^{0.4} K_g^{0.6}}{\mu_g^{0.4}}\right) \qquad (6.7)$$

where the gas properties C_{p_g}, μ_g and K_g are evaluated at the temperature of the gas at the beginning of the height increment Δz in the annulus.

Thus the forced convective flux from the outer side of the coil per unit peripheral area is calculated by the following:

$$\dot{Q}_{1\rightarrow 2} = C_1 * (T_1 - T_2) \qquad (6.8)$$

where C_1 is calculated by equation (6.7).

6.1.3 Free Convection

The contribution of the natural convection currents to the heat transfer between the coil and the cover is expected to be small in comparison with forced convection and radiation. McAdams[19] in equation 7.9b gives the general formula for free convection as follows:

$$\frac{hx}{K} = c\left(\frac{x}{L}\right)^{1/9} (Gr * Pr)^{n} \qquad (6.9a)$$

where x is the gap between the cover and the coil, and the Grashof number is given by

$$Gr = x^{3}\rho_{g}^{2}g\beta\Delta T/\mu_{g}^{2} \qquad (6.9b)$$

The values of the coefficient c and the index n depend on the value of Gr. The coefficient of the volumentric expansion is calculated from the reciprocal of the average temperature, $\beta = \frac{1}{T_m}$ where $T_m = (T_1+T_2)/2$. The physical properties of the inert gas ρ_g, C_{p_g}, μ_g and K_g are evaluated at T_m.

For typical coil and cover diameters of 1.8 and 2.4 metres respectively, x = 0.3 metre. Assume T_1 = 500K and T_2 = 700K. So T_m = 600K and ΔT = 200K. Therefore, Gr = $6.78 * 10^{6}$.

According to McAdams[19] for the above value of Gr, c = 0.071 and n = $1/3$. Therefore,

$$\frac{hx}{K} = 0.071 * \left(\frac{x}{L}\right)^{1/9} (Gr * Pr)^{1/3} \qquad (6.10)$$

Thus, the heat flux from the coil surface to the cover due to free convection is given by the following equation:

$$\dot{Q}_{1\rightleftharpoons 2} = C_o*(T_1-T_2)^{1/3}/(T_1-T_2) \qquad (6.11a)$$

where

$$C_o = 3488 * \left(\frac{D_2-DO_{(m)}}{2*H_c}\right)^{1/9} * \left(\frac{C_{p_g} K_g^2}{\mu_g}\right)^{1/3} \qquad (6.11b)$$

H_c being the total height of the straight side of the cover.

The calculation of the heat flux for T_1 = 500K and T_2 = 700K resulted in a free convection flux less than 1% of the forced convective flux, and even less than 0.03% of the radiative flux. For this reason, the natural convection term is ignored in the solution of this annealing problem.

6.2 The Profile of Nitrogen Temperature in the Annulus between the Cover and the Stack

The local heat transfer coefficient between the inner surface of the cover and the gas in the annular gap is calculated from equation (6.5) as

$$h_2 = \frac{DO_{(m)} + D_2}{D_2} * C_1 \qquad (6.12)$$

Let the temperature of nitrogen change from $T_{g_{j-1}}$ to T_{g_j} as it flows upward across an incremental height Δz. The transient heat balance over this height Δz is as follows:

Heat Input - Heat Output = Heat Accumulation

$$\pi \cdot \Delta z \cdot h_2 (D_2 * (T_2 - T_{g_j}) - DO_{(m)} * (T_{g_j} - T_1)) = FG_{(m)} \, C_{p_g} * \Delta z * \frac{dT_{g_j}}{dz}$$

By integrating between zero and Δz from $T_{g_{j-1}}$ to T_{gj}, the gas temperature T_{g_j} at height z is obtained as follows:

$$T_{g_j} = \frac{D_2 * T_2 + DO_{(m)} * T_1}{D_2 + DO_{(m)}} * (1 - \frac{1}{\alpha_A}) + \frac{T_{g_{j-1}}}{\alpha_A} \qquad (6.13a)$$

where

$$\alpha_A = \exp\left(\frac{\pi * (D_2 + DO_{(m)})^2 * \Delta z * C_1}{D_2 * FG_{(m)} * C_{p_g}}\right) \qquad (6.13b)$$

C_{p_g} is the specific heat of the inert gas evaluated at the gas temperature at height $(z-\Delta z)$, $T_{g_{j-1}}$.

6.3 Heat Transfer Between the Cover and the Furnace

The heat evolved by the combustion of the fuel in the furnace is transferred from the combustion products to the outer surface of the cover. This heat is transmitted by radiation and convection.

Let the refractory wall be of diameter D_r, the temperature of the furnace gas be T_{fr} and m_f kg/h be the rate at which the gaseous fuel is fed to the burners.

6.3.1 Radiative Flux

The combustion gases in the furnace are non-greay; but they can be reasonably represented by a weighted average of one clear and one grey components[2]. Let the emissivity of the gas be designated by ε_g, the absorption coefficient of the grey component by k and the weighting factor of the grey component by a_g. If L_m is the mean beam length of the gas and P is the sum of partial pressures of carbon dioxide and water vapour in the furnace gas; then the product $RO = L_m * P$ is used as an argument in Hadvig's correlation to calculate the weighting factor of the grey gas component as follows: Calculate the gas emissivity from one mean beam length as follows:

$$\varepsilon_{g1} = a_g(1-e^{-RO*k}) \qquad (6.14a)$$

Also calculate this emissivity at twice the mean beam length as follows:

$$\varepsilon_{g2} = a_g(1-e^{-2*RO*k}) \qquad (6.14b)$$

Then, the weighting factor is calculated from the simultaneous solution of these two equations as follows:

$$a_g = \frac{\varepsilon_{g1}}{2 - \varepsilon_{g2}/\varepsilon_{g1}} \qquad (6.14c)$$

For the calculation of the net radiative exchange rate between the furnace gas and the outer surface of the cover $\dot{Q}_{g\rightarrow 2}$, the directed flux area, $(\overrightarrow{GS_1})_R$ must be implemented. Because the gas is not grey, $\varepsilon_g \neq \alpha_{gs}$ and $(\overrightarrow{GS_1})_R$ is based on the emissivity ε_g which is different from $(\overleftarrow{GS_1})$ that is based on α_{gs}.

Hottel and Sarofim[2] in 'Radiative Transfer' and McAdams[19] in 'Heat Transmission' expressed this directed area as follows:

$$\frac{1}{(\overrightarrow{GS_1})_R} = \frac{1}{a_g A_2}\left(\frac{1}{\varepsilon_3} - 1\right) + \frac{1}{\varepsilon_g}\left(A_2 + \frac{A_r}{1 + \dfrac{\varepsilon_g}{(a_g-\varepsilon_g)*F_{r2}}}\right)^{-1} \qquad (6.15a)$$

where ε_3 is the emissivity of the outer side of the cover. This emissivity is assumed to be 30% higher than the emissivity of the inner surface of the cover such that

$$\varepsilon_3 = 1.3\ \varepsilon_2 \qquad (6.15b)$$

The view factor F_{r2} from the refractory surface to the outer side of the cover is given by D_r/D_2 where D_r is the diameter of the refractory wall.

But all the fluxes are based on unit pheripheral area of the coil; thus the term $\frac{\text{Coil Area}}{(\overrightarrow{GS_1})_R}$ is required. Since $\frac{\text{Coil Area}}{\text{Cover Area}} = \frac{\text{Coil Area}}{A_2} = \frac{DO_{(m)}}{D_2}$, then $\frac{\text{Coil Area}}{(\overrightarrow{GS_1})_R} = \frac{DO_{(m)} * A_2}{D_2 * (\overrightarrow{GS_1})_R}$. Therefore,

$$\frac{\text{Coil Area}}{(\overrightarrow{GS_1})_R} = \frac{DO_{(m)}}{D_2} \left(\frac{\frac{1}{\varepsilon_3} - 1}{a_g} + \frac{1}{\varepsilon_g} \left(1 + \frac{A_r/A_2}{\frac{D_2 * \varepsilon_g}{D_r(a_g - \varepsilon_g)}}\right)\right)^{-1} \qquad (6.16)$$

Hottel and Sarofim[2] modified the grey surface model to suit the real system by using the inverse proportionality of the directed flux areas $(\overrightarrow{GS_1})_R$ and $(\overleftarrow{GS_1})_R$ with the temperatures T_{fr} and T_2 respectively; where T_{fr} is the gas temperature and T_2 the sink temperature. So, the net radiative rate between the furnace gas and the cover becomes the following:

$$\dot{Q}_{g \rightleftharpoons 2} = (\overrightarrow{GS_1})_R \left(\frac{1-k^3}{1-k^4}\right) \sigma \left(T_{fr}^4 - T_2^4\right) \qquad (6.17)$$

where $k = \frac{T_2}{T_{fr}}$.

Therefore, from equations (6.16) and (6.17), the net radiative transfer from the gas to the cover per unit area of the coil becomes the following:

$$\dot{Q}_{g \rightleftharpoons 2} = C_4 * T_{fr} * (T_{fr}^3 - T_2^3) \qquad (6.18a)$$

where the term C_4 is calculated as follows:

$$C_4 = \sigma\left(\frac{1-k^3}{1-k^4}\right) * \frac{D_2}{DO_{(m)}} * \left(\frac{1-\varepsilon_3}{a_g\varepsilon_3} + \frac{1}{\varepsilon_g}\left(1 + \frac{A_r/A_2}{1+D_2\varepsilon_g/D_r/(a_g-\varepsilon_g)}\right)^{-1}\right)^{-1} \qquad (6.18b)$$

ε_3 is calculated by equation (6.15b)

The temperature profile of the furnace gas is fitted as a linear function of height between the burner's zone, where T_{fr} is taken as the adiabatic flame temperature, and the exhaust duct at which T_{fr} is equal to the flue gas temperature T_{fl}.

6.3.2 Convective Flux

The flow rate of the combustion gas in the annular gap between the cover and the refractory wall is the same as the sum of the fuel and the air feed rate. If x is the proportion of excess air defined as kg per kg stoichiometric air, then the flow rate of the combustion gas is given by

$$m_g = m_f*(1 + 17.05 * (1 + x)) \text{ kg/h} \qquad (6.19)$$

where m_f is the rate of fuel firing; see Chapter (3.3.1).

The convective heat transfer coefficient is given by Dittus Boelter equation as follows:

$$\frac{hD_H}{K} = 0.023\ Re^{.8}\ Pr^{.4}$$

The Reynolds number is calculated by:

$$Re = \frac{4}{\pi} * \frac{m_g}{(D_r+D_2)\mu_g}$$

and Prandtl number by

$$Pr = C_{p_g} \mu_g / K_g$$

Then, the heat transfer coefficient is obtained by substitution in Dittus Boetler equation as follows:

$$h = \frac{0.0279}{(D_r-D_2)} * \left(\frac{m_g}{D_r+D_2}\right)^{.8} * \left(\frac{C_{p_g}^{.4} K_g^{.6}}{\mu_g^{.4}}\right) \qquad (6.20)$$

The heat transfer flux to the cover due to the forced convection of the furnace gas is calculated per unit peripheral area of the coil as follows:

$$\dot{Q}_{g \rightleftharpoons 2} = C_3 * (T_{fr} - T_2) \qquad (6.21a)$$

where

$$C_3 = \frac{0.0279\ D_2}{DO_{(m)} * (D_r-D_2)} * \left(\frac{m_g}{D_r+D_2}\right)^{.8} \left(\frac{C_{p_g}^{.4} K_g^{.6}}{\mu_g^{.4}}\right) \qquad (6.21b)$$

6.4 Solution of Cover Temperature with the Flux from the Furnace Gas

Over each time interval, a steady state solution for the cover temperature is calculated and used in computing the heat flux included in the boundary conditions of the

coil. This solution is obtained from the balance of heat transfer fluxes. The heat flux received by the cover from the furnace gas is passed to the outer periphery of the coil. Hence,

$$\dot{Q}_{g\rightleftharpoons 2}\Big|_{rad} + \dot{Q}_{g\rightleftharpoons 2}\Big|_{con} = F_{in}$$

$$\dot{Q}_{1\rightleftharpoons 2}\Big|_{rad} + \dot{Q}_{1\rightleftharpoons 2}\Big|_{con} = F_{out}$$

Apply Newton-Raphson iterations to solve for the cover temperature. Let E be the computational error given by $E = F_{in} - F_{out}$.

Then

$$T_2 = T_2 - E/\frac{\delta E}{\delta T_2} \qquad (6.22)$$

The solution converges when the absolute value of $E/\frac{\delta E}{\delta T_2}$ satisfies a certain tolerence.

The derivative $\frac{\delta E}{\delta T_2}$ is calculated as follows:

$$\frac{\delta E}{\delta T_2} = \frac{\delta F_{in}}{\delta T_2} - \frac{\delta F_{out}}{\delta T_2}$$

Therefore,

$$\frac{\delta E}{\delta T_2} = C_1+C_3-3C_4*T_{fr}*T_2^2+4C_2*T_2^3-(C_3-4C_4*T_{fr}^3+C_4*T_2^3)\ \frac{\delta T_{fr}}{\delta T_2} \qquad (6.23a)$$

The derivative of the furnace temperature with respect to the cover temperature, $\frac{\delta T_{fr}}{\delta T_2}$ is calculated from the heat balance over an incremental height Δz in the annulus between the cover and the refractory as follows:

$$\frac{\delta T_{fr}}{\delta T_{gj}} = - \frac{FG_{(m)} * C_{p_g}}{m_g * C_{p_c}} \qquad (6.23b)$$

where $FG_{(m)}$ is the nitrogen flow rate in the annulus between the cover and coil (m), m_g is the mass rate of the furnace gases calculated by equation (6.19); C_{p_g} and C_{p_c} are the specific heats of the inert gas and the combustion products respectively.

By differentiating equation (6.13a) with respect to the cover temperature T_2, the following is obtained:

$$\frac{\delta T_{gj}}{\delta T_2} = \frac{D_2}{D_2+DO_{(m)}} * (1 - \frac{1}{\alpha_A})$$

where α_A is given by equation (6.13b). But

$$\frac{\delta T_{fr}}{\delta T_2} = \frac{\delta T_{gj}}{\delta T_2} * \frac{\delta T_{fr}}{\delta T_{gj}}$$

Therefore,

$$\frac{\delta T_{fr}}{\delta T_2} = \frac{-D_2 * FG_{(m)} * C_{p_g}}{(D_2+DO_{(m)}) * m_g * C_{p_c}} * (1 - {}^1/\alpha_A) \qquad (6.23c)$$

By substituting in equation (6.23a), the derivative $\frac{\delta E}{\delta T_2}$ is obtained and equation (6.22) is solved to find the value of the cover temperature, T_2.

6.5 Heat Transfer Between the Cover and the Ambient Atmosphere

This heat transfer takes place during the cooling cycle after the portable furnace is lifted off and the heat is allowed to escape from the outer surface of the cover to the surrounding atmosphere. Heat is mainly transmitted by radiation and natural convection. In this case, there is no forced convective transfer.

6.5.1 Radiation Loss

The surface area of the surroundings is assumed to be very large. Because the outer surface of the cover is convex, the view factor F_{22} is zero. Therefore, the direct exchange area between the cover and the surroundings is A_2. The emissivity of the outer surface of the cover is calculated by equation (6.15b). So the radiative heat loss is given by:

$$\dot{Q}_{2\rightleftarrows a} = 1.3\sigma\varepsilon_2 A_2(T_2^4 - T_a^4)$$

where T_a is the ambient temperature. The radiative heat flux per unit peripheral area of the coil becomes the following:

$$\dot{Q}_{2\rightleftarrows a} = C_6 * (T_2^4 - T_a^4) \qquad (6.24a)$$

where $C_6 = 1.3\sigma\varepsilon_2 D_2/DO_{(m)}$ (6.24b)

6.5.2 Heat Loss by Natural Convection

As mentioned in section 6.1.3, the equation to be used for free convection depends on the magnitude of the product Gr*Pr, which determines the type of flow. High values designate a turbulent boundary layer.

For the calculation of Gr*Pr, the physical properties are taken at the arithmatic mean temperature $T_m = \frac{T_2+T_a}{2}$, where T_2 is taken as the cover temperature at the beginning of the height increment Δz.

Assume T_a = 300K, T_2 = 500K, hence T_m = 400K. Thus for a typical cover height of 4.5 metres, the product Gr*Pr is calculated as 9.65×10^{11}. Hence, the surrounding boundary layer of atmospheric air is turbulent and the natural convection transfer coefficient is obtained from McAdams[19] 'Heat Transmission' equation (7.4a) as follows:

$$\frac{hL}{K_f} = 0.13\left(\frac{L^3 \rho_f^2 g \beta_f \Delta T}{\mu_f^2} \left(\frac{C_p \mu}{K}\right)_f\right)^{1/3} \qquad (6.25a)$$

From the ideal gas equation, the density ρ_f is given by $\frac{341.37}{T_m}$ kg/m^3. After substitution and rearrangement the free convective coefficient is:

$$h = \frac{13.59}{T_m} * \left(\frac{K_f^2 C_{pf}}{\mu_f}\right)^{1/3} * (T_2-T_a)^{1/3} \qquad (6.25b)$$

Thus, the natural convective flux based on unit peripheral area of the coil becomes the following:

$$\dot{Q}_{2\rightleftharpoons a} = C_5(T_2-T_a)^{4/3} \qquad (6.26a)$$

where

$$C_5 = \frac{13.59}{T_m} * \frac{D_2}{DO_{(m)}} * \left(\frac{K_f^2 C_{pf}}{\mu_f}\right)^{1/3} \qquad (6.26b)$$

6.6 Solution of the Cover Temperature with the Atmospheric Flux

To solve for the cover temperature, consider the flux from the coil through the nitrogen to the cover F_1 to dissipate as a flux F_3 leaving the outer surface of the cover to the surrounding atmosphere. If E is considered as a computational error defined by $E = F_1-F_3$, then the cover temperature could be solved iteratively by applying the Newton-Raphson method.

$$F_1 = C_1*(T_1-T_2) + C_2*(T_1^4-T_2^4)$$

$$F_3 = C_5*(T_2-T_a)^{4/3} + C_6(T_2^4-T_a^4)$$

The solution will be obtained by the following:

$$T_2 = T_2 - E/\frac{\delta E}{\delta T_2} \qquad (6.27)$$

when the absolute value of $E/\frac{\delta E}{\delta T_2}$ becomes less or equal to a specified tolerance.

6.7 Heat Transfer in the Core of the Stack

The inert gas flowing in the convector plates between the coils converges to the centre of the stack where it accumulates and flows downward towards the basement. During its flow in the core of the stack, the gas exchanges heat with the inner surfaces of the coils. This heat is transmitted by convection only. This is because there are negligible free convective currents in this locality in the furnace and the radiative transfer is deemed negligible because the emissivity of the inert gas is negligible.

6.7.1 Coefficient of Forced Convection

If the orifice in the convector plate is less than the inner diameters of the coils, there will be an enhancement of the forced convection in the core of the stack. If x is considered as the height-to-diameter ratio, the enhancement factor will be given[21] by

$$Y = 0.409 + 0.186 \ln (x) \quad \text{for } x \geq 0.4$$

and $$Y = 0.25 \quad \text{for } x < 0.4$$

If the orifice of the convector plate has the same diameter as the core of stack, the enhancement factor will be unity.

If the temperature of the gas is less than the temperature of the coil surface, there must be a viscosity correction factor expressed by $u = (T_{gc}/T_w)^{0.49}$

where T_{gc} and T_w are the gas and wall temperatures respectively. T_w is evaluated at the beginning of the time interval as the arithmatic mean of the wall temperatures at the beginning and end of the height increment Δz.

Let H_c be the height at any position in the core starting from the level of the top plate as a datum and updating downwards until the lower surface of the bottom coil. Let F_{cor} be the mass flow rate of the gas in the core in kg/h updated in the same way.

The forced convective heat transfer coefficient is calculated from the Dittus Boetler equation as follows:

$$Nu = 0.023\ Re^{0.8}\ Pr^{0.4}$$

where Nu, Re and Pr are respectively the Nusselt, the Reynolds and the Prandtl numbers of the inert gas.

$$Nu = \frac{h_{cr} * DI_{(m)}}{K_g}$$

$$Re = \frac{DI_{(m)} * G}{\mu_g} = \frac{4F_{cor}}{\pi \mu_g * DI_{(m)}}$$

$$Pr = C_{p_g}\ \mu_g / K_g$$

where K_g is the thermal conductivity of nitrogen, and h_{cr} is the heat transfer coefficient in the core of the stack. Therefore,

$$h_{cr} = \frac{0.0279*u*(F_{cor})^{0.8}}{Y*(DI_{(m)})^{1.8}} * \frac{C_{p_g}^{0.4} K_g^{0.6}}{\mu_g^{0.4}} \qquad (6.28)$$

6.7.2 Temperature Profile of the Gas in the Core

Let F_{co} be the mass flow rate of the gas in the core entering the centre of coil (m) at temperature T_{co}. Also, F_{go} is the mass flow rate of the gas from plate (m+1) passing into the centre of coil (m) at temperature T_{go}. Then the mass rate of the gas leaving the centre of coil (m) will be F_{c1} at temperature T_{c1} as shown in Fig. 6.1. The temperature of the gas leaving the coil (m), T_{c1} is calculated from the heat balance as follows:

$$F_{co}*C_{p_g}(T_{co})*T_{co} + F_{go}*C_{p_g}(T_{go})*T_{go}$$

$$= F_{c1}*C_{p_g}(T_{c1})*T_{c1} + \pi*DI_{(m)}*H_{(m)}*h_{cr}*(\frac{T_{co}+T_{c1}}{2} - T_{wm}) \qquad (6.29)$$

where T_{wm} is the average temperature of the inner surface of coil (m). Equation (6.29) is solved for T_{c1} since all the other terms are known.

To calculate the temperature of the gas in the core at any height z from the base of coil (m), the following heat balance is used:
Heat lost from the gas over a height increment Δz is equal to the heat gained by that incremental height of the coil. Let $T_{gc(j)}$ be the temperature of the gas at position z in coil (m) and $T_{gc(j+1)}$ be the temperature

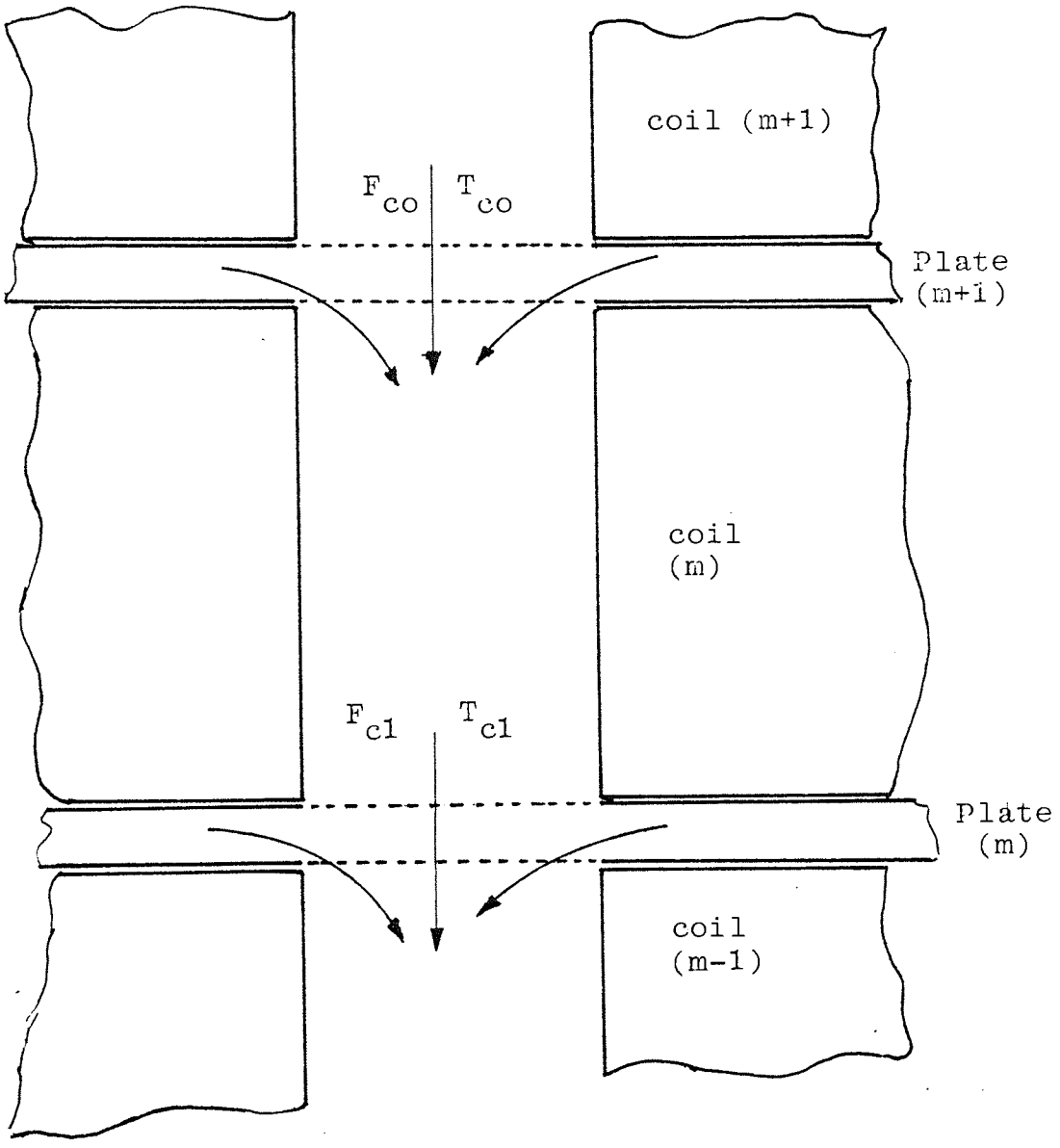

Figure 6.1

The flow of inert gas in the convector plates and the core of the stack

at $z + \Delta z$. Then,

$$F_{cor} * C_{p_g} (T_{gc(j+1)}) * (T_{gc(j+1)} - T_{gc(j)})$$

$$= \pi * DI_{(m)} * \Delta z * h_{cr} * \left(\frac{T_{gc(j+1)} + T_{gc(j)}}{2} - T_w\right) \quad (6.30)$$

where T_w is evaluated at the beginning of the time interval as the arithmatic mean of the wall temperatures at z and $z + \Delta z$. Equation (6.30) is to be solved for $T_{gc(j)}$ since $T_{gc(j+1)}$ is known from the upper height increment.

6.8 Heat Transfer at the Top of the Stack

Heat is transferred between the gas in the convector plates and the ends of the steel coils by forced convection. This is not the case for the top convector plate above the top coil, because the heat radiation from the cover top to the top plate becomes the dominant mode of heat transfer. For this reason, the heat transfer between this plate and the top coil needs special consideration.

It is assumed that the top convector plate has a uniform temperature T_{tp} which is calculated on the basis of radial distribution of the boundary temperature of the upper surface of the top coil. This assumption may not introduce a serious error because the radial conduction tends to equalize any temperature difference over the radial elements used in the analysis of heat transfer. Since the radiative flux is the controlling term of heat transfer in this plate, T_{tp} is computed from the fourth power mean of radial

temperatures of the upper end of the top coil. The areas of the top plate which do not see the end of the coil directly are assumed to be radiatively adiabatic like refractory surfaces. From the weighted average of temperatures at all radial positions of the upper surface of the top coil, the fourth-order mean temperature is calculated as follows:

$$T_{tp} = \left(\frac{4}{DO_{(m)}^{2}-DI_{(m)}^{2}} * \left(\frac{DI_{(m)}^{2}}{4} * T_t^4(1) + \sum_{i=2}^{i=IL-1} 2r*\Delta r*Tt(i)^4\right)\right)^{\frac{1}{4}} \quad (6.31)$$

where Tt(i) is the temperature of the upper surface of the top coil at radius r evaluated at the beginning of the time interval. The index i signifies the grid point at radial position r and IL signifies the outer peripheral surface of the coil while the index 1 signifies the inner surface of the coil.

6.8.1 Radiative Flux between the Cover Top and the Top Plate

Denote the surface area of the upper end of the top coil by A_1 where $A_1 = \frac{\pi}{4}(DO_{(m)}^{2} - DI_{(m)}^{2})$. Let A_3 denote the difference between the area of the top plate and A_1. Therefore,

$$A_3 = \frac{\pi}{4}(D_p^{2}-DO_{(m)}^{2} + DI_{(m)}^{2})$$

where D_p is the diameter of the convector plate.

Let A_2 be the area of the cover top which receives radiation directly from the top plate. Let H_d be the

height of the dished top of the cover and H_s be the height of the straight edge above the top plate as shown in Fig. 6.2.

Let R be the radius of curvature of the dished part of the cover which is calculated from:

$$R^2 = \left(\frac{D_2}{2}\right)^2 + (R - H_d)^2$$

Therefore, the surface area of the dished top of the cover, is calculated as follows:

$$2\pi * R * H_d = \pi\left(\frac{D_2^2}{4} + H_d^2\right) = \frac{\pi}{4}\left(D_2^2 + 4H_d^2\right)$$

The surface area of the straight part of the cover above the top plate is $\pi * D_2 * H_s$. Hence the total area of the cover which exchanges radiation with the top plate is given by:

$$A_2 = \frac{\pi}{4}\left(D_2^2 + 4 * H_d^2 + 4 * D_2 * H_s\right) \qquad (6.32a)$$

Since the end surface of the top coil A_1 cannot see itself nor the area A_3 of the top plate, then the view factors $F_{11} = F_{13} = 0$. From $\sum_j F_{ij} = 1$, the view factor $F_{12} = 1$. Therefore, the direct exchange area $\overline{12} = A_1$. To calculate the total exchange area, the area A_3 is assumed radiatively adiabatic similar to refractory surfaces.

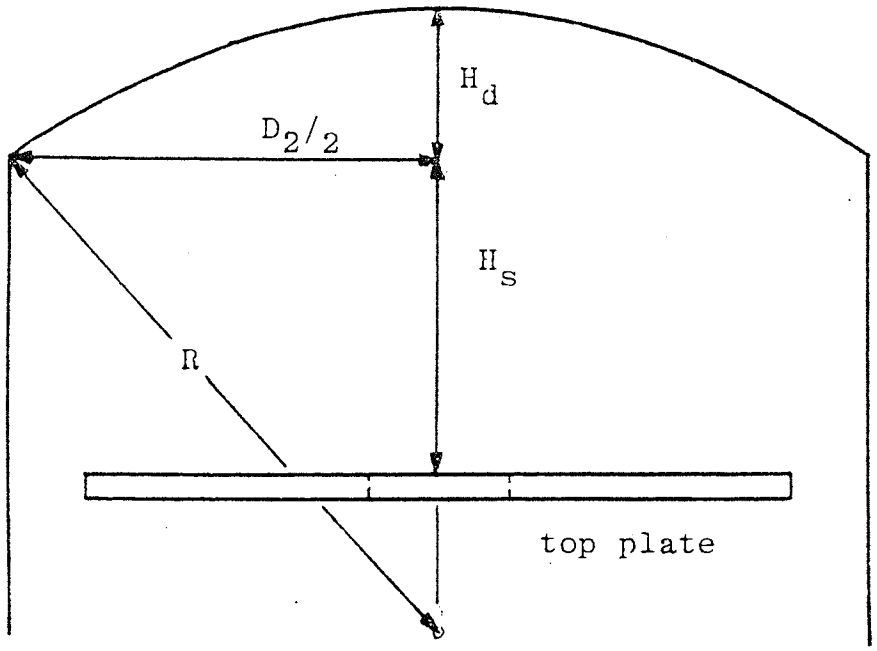

Figure 6.1

The top of the cover

From McAdams[19] 'Heat Transmission' equations over (4.32) and (4.33), the reciprocal of the total exchange area is given by:

$$\frac{1}{\overline{S_1 S_2}} = \frac{1-\varepsilon_1}{A_1\varepsilon_1} + \frac{1-\varepsilon_2}{A_2\varepsilon_2} + \frac{1}{\overline{12} - \frac{\overline{13}*\overline{23}}{\overline{33}-A_3}}$$

but $\overline{13} = 0$; therefore,

$$\frac{1}{\overline{S_1 S_2}} = \frac{1}{A_1}\left(\frac{1}{\varepsilon_1} + \frac{A_1}{A_2} * \frac{1-\varepsilon_2}{\varepsilon_2}\right)$$

or

$$\overline{S_1 S_2} = A_1 / \left(\frac{1}{\varepsilon_1} + \frac{A_1}{A_2} * \frac{1-\varepsilon_2}{\varepsilon_2}\right)$$

The total exchange area per unit end area of the top coil becomes the following:

$$\overline{S_1 S_2} = 1 / \left(\frac{1}{\varepsilon_1} + \frac{A_1}{A_2} * \frac{1-\varepsilon_2}{\varepsilon_2}\right) \qquad (6.32b)$$

where ε_1 and ε_2 are the emissivities of the convector plate and the inner surface of the cover, respectively.

Thus the radiative transfer flux from the cover to the top plate is the following:

$$q_{tr} = \alpha_r * (T_{tc}^4 - T_{tp}^4) \qquad (6.32c)$$

$$\text{where } \alpha_r = \sigma / ({}^1/\varepsilon_1 + A_1/A_2 * (1-\varepsilon_2)/\varepsilon_2) \qquad (6.32d)$$

and T_{tc} is the temperature of the top end of the cover and σ is the Stefan-Boltzmann constant.

6.8.2 Free Convective Flux Between the Cover Top and the Top Plate

Although the radiative transfer is the dominant term of heat transfer between the top convector plate and the top of the cover, nonetheless, the natural convective currents of the inert gas have some contribution to the heat transfer in this zone.

Let h' and h'' be the local convective heat transfer coefficients between the inert gas and the top convector plate, and that between the inner surface of the top of the cover and the gas, respectively. If A is taken as the overall heat transfer area, then the overall heat transfer coefficient h_n is given by the following relationship:

$$h_n dA = h' dA_1 = h'' dA_2$$

where

$$A = A_1 + A_2 = \frac{\pi}{4}(D_p^2 + D_2^2 + 4H_d^2 + 4D_2 H_s)$$

The correlation of the heat transfer coefficient by natural convection is given by McAdams[19] as follows:

$$\frac{h'x}{K_f} = c\left(\frac{x^3 \rho_f^2 g \beta_f \Delta T}{\mu_f^2}\left(\frac{C_p \mu}{K}\right)_f\right)^n$$

If the clearance between the top convector plate and the top of the cover is assumed to be 0.15 metre, and the temperatures of the cover top and the top plate are taken as 700K and 500K respectively, the value of Grashof number becomes $1.1 * 10^7$. Thus, the boundary layer lies in the turbulent region. Hence, the above equation becomes the following:

$$\frac{h'x}{K_f} = 0.075 \left(\frac{x^3 \rho_f^2 g \beta_f \Delta T \, C_p \mu}{\mu_f^2 \left(\frac{}{K}\right)_f}\right)^{1/3}$$

Therefore, the individual heat transfer coefficient is obtained as follows:

$$h' = 0.075\left((\rho_f^2 g \beta_f) \left(\frac{C_p K^2}{\mu}\right)_f (T_{tc}-T_{tp})\right)^{1/3}$$

But $\rho_f = \frac{341.37}{T_m}$, $g = 9.81 \text{ m/s}^2$ and

$T_m = (T_{tc}+T_{tp})/2$; therefore,

$$h' = \frac{120.16}{T_m}\left(\left(\frac{C_p K^2}{\mu}\right)_f (T_{tc}-T_{tp})\right)^{1/3} \qquad (6.33a)$$

Since the overall convective heat transfer coefficient is given by:

$$h_n = h' dA_2/dA$$

$$h_n = h'(D_2^2+4H_d^2+4D_2H_s)/(D_p^2+D_2^2+4H_d^2+4D_2H_s)$$

Thus, the natural convective flux per unit area of the upper surface of the top coil is given by the following equation:

$$q_{tn} = \alpha_n (T_{tc} - T_{tp})^{4/3} \qquad (6.33b)$$

where

$$\alpha_n = \frac{153.0\ (D_2^2 + 4H_d^2 + 4D_2H_s)}{(DO_{(m)}^2 - DI_{(m)}^2)(D_p^2 + D_2^2 + 4H_d^2 + 4D_2H_s)T_m} \left(\frac{C_p K^2}{\mu}\right)_f^{1/3} \qquad (6.33c)$$

The physical properties of the inert gas C_{pf}, μ_f and K_f are evaluated at the mean temperature T_m.

6.8.3 Radiative Transfer between the Top of the Cover and the Atmosphere

The total area of the cover above the level of the top convector plate, A_2 which exchanges heat radiation with the top plate is calculated by equation (6.32a). The outer surface of the cover is considered to have an emissivity which is 30% higher than the emissivity of its inner surface, given by equation (6.15b). Therefore, the flux of radiative transfer per unit peripheral area of the top coil is computed as follows:

$$q_{ta} = \nu_r (T_a^4 - T_{tc}^4) \qquad (6.34a)$$

where

$$\nu_r = 1.3\sigma\varepsilon_2\ A_2/A_1$$

and T_a is the atmospheric temperature.

6.8.4 Natural Convection Between the Cover Top and the Atmosphere

If the dished top of the cover is considered as a plate facing upwards under turbulent currents, then equation (7.8) of McAdams[19] 'Heat Transmission' could be used as follows:

$$\frac{h_a L_f}{K_f} = 0.14 * \left(\frac{L^3 \rho_f^2 g \beta \Delta T}{\mu_f^2} * \left(\frac{C_p \mu}{K}\right)_f\right)^{1/3}$$

Following the same manipulation as in Section (6.7.2), above, the coefficient of natural convection will be obtained as follows:

$$h_a = \frac{224.29}{T_m} * \left(\frac{C_p K^2}{\mu}\right)^{1/3} (T_a - T_{tc})^{1/3} \qquad (6.35a)$$

where $T_m = (T_{tc} + T_a)/2$

The natural convective flux per unit area of the end surface of the top coil becomes the following:

$$q_{na} = \nu_a (T_a - T_c)^{4/3} \qquad (6.35b)$$

where

$$\nu_a = \frac{224.29 * D_2}{(DO_{(m)}^2 - DI_{(m)}^2) * T_m} * \left(\frac{C_p K^2}{\mu}\right)_f^{1/3}$$

where C_{pf}, μ_f and K_f are the specific heat, the viscosity and the thermal conductivity of the atmospheric air

respectively. All these properties are evaluated at the mean temperature T_m.

6.8.5 Solution of Temperature of the Cover Top and the Atmospheric Flux

For the solution of the cover temperature above the top plate T_{tc}, it is considered that the flux reaching the top of the cover from the top plate leaves the cover top to the surrounding atmosphere. These fluxes are given by the following:

$$F_1 = \alpha_r(T_{tp}^4 - T_{tc}^4) + \alpha_n(T_{tp} - T_{tc})^{4/3} \qquad (6.36a)$$

$$F_2 = \nu_r(T_{tc}^4 - T_a^4) + \nu_a(T_{tc} - T_a)^{4/3} \qquad (6.36b)$$

T_{tc} is computed by iterationsusing the Newton-Raphson technique. Let E be the computing error which tends to zero when the solution for T_{tc} converges, such that $E = F_1 - F_2$. The working equation for the iterations of T_{tc} is the following:

$$T_{tc} = T_{tc} - E/\frac{\delta E}{\delta T_{tc}} \qquad (6.37)$$

The iterations converge to the solution for T_{tc} when the absolute discrepancy $E/\frac{\delta E}{\delta T_{tc}}$ satisfies a specific tolerance.

6.8.6 Heat Transfer Between the Flue Gases and the Cover Top

As the combustion products of the furnace leave the burner zone, they rise up in the annulus between the cover and the refractory wall giving heat to the cover surface. These gases accumulate above the cover where they are driven into an exhaust duct of diameter D_e and of certain clearance above the cover top. The flue gases transmit heat to the cover top by radiation and convection.

6.8.6.1 Forced Convective Transfer

At the perimeter edges of the cover top, the flue gases undergo sudden change in direction causing the convective heat transfer coefficient to be enhanced.

Let the clearance between the exhaust duct and the cover top be H_e; the flow area will be $A_e = \pi * D_e * H_e$.

Consider the clearance between the exhaust duct and the cover top as a compact heat exchanger. The hydraulic mean diameter is given by equation (11.4) in McAdams[19] 'Heat Transmission' as $D_H = 4A_eL/A$ where A is the heat transfer area and L is the flow path length. Since the flue gases flow towards the centre of the cover, then $L = D_2/2$ and $A = \pi D_2^2/4$. Therefore, the hydraulic mean

diameter becomes:

$$D_H = 8*H_e*D_e/D_2 \qquad (6.38a)$$

The heat transfer coefficient of forced convection will be calculated from the Dittus Boetler equation:

$$\frac{h\,D_H}{K} = 0.023\,\left(\frac{D_H G}{\mu}\right)_f^{0.8}\left(\frac{C_p \mu}{K}\right)^{0.4}$$

The total gas flow is given by equation (6.19) as :

$$m_g = (1 + 17.05*(1+x))m_f$$

where x is the proportion of excess air, in kg per kg of the stoichiometric air. After substitution and rearrangement, the heat transfer coefficient will be

$$h = 0.0184\,\left(\frac{m_g^{0.8}}{D_2^{1.4} D_e^{0.2} H_e^{0.2}}\right)\left(\frac{C_p^{0.4}\, K^{0.6}}{\mu^{0.4}}\right)_f \qquad (6.38b)$$

The convective heat flux per unit peripheral area of the top coil is computed as follows:

$$q_{ev} = \alpha_{ev}(T_{f\ell} - T_{tc}) \qquad (6.38c)$$

where $\alpha_{ev} = D_2^2 h/(DO_{(m)}^2 - DI_{(m)}^2)$

and $T_{f\ell}$ is the temperature of the flue gases.

6.8.6.2 Radiative Flux

For the calculation of the view factor between the refractory and the cover top, the duct of the flue gases will be ignored. Aslo the annular space between the cylindrical refractory and the ends of the straight edges of the cover will be assumed hypothetically closed. This ficticious partition is assumed to reflect all the radiation incident on it; this reflection takes place in reality except that the refractory below the level of the cover top is the actual reflecting medium rather than the hypothetical partition.

Let the refractory lining above the furnace base be of height H_r and its inner diameter be D_r. If H_2 is the height of the straight side of the cover, the area of the refractory above the level of the top convector plate will be the following:

$$A_r = \frac{\pi}{4} D_r^2 + \pi D_r(H_r+H_s-H_2) \qquad (6.39a)$$

The area of the annular gap between the cover and the refractory wall is $\frac{\pi}{4}(D_r^2-D_2^2)$.

Since the outer surface of the cover is convex, then the view factor to itself is $F_{22} = 0$ and the view factor from the cover to the refractory is $F_{2r} = 1$. So, the view factor from the refractory

to the cover is calculated from $A_2F_{2r} = A_rF_{r2}$ so that $F_{r2} = \frac{A_2}{A_r}$. Therefore,

$$F_{r2} = \frac{D_2^2 + 4H_d^2 + 4*D_2*H_s}{2D_r^2+4*D_r(H_r+H_s-H_2)-D_2^2} \qquad (6.39b)$$

For the calculation of the mean beam length of the gas volume, consider the space between the outer side of the cover top and the refractory roof as a clearance between two infinite parallel planes. The mean beam length of such planes is given by Hottel and Sarofim[2] 'Radiative Transfer' table 7.3 as 1.76 times the distance between the planes. Therefore,

$$L_m = 1.76 * (D_r-D_2)/2 \qquad (6.39c)$$

The emissivity of the flue gases is then calculated by Hadvig's correlation, f (RO) as follows:

$$\varepsilon_g = (2.7 - T_{f\ell}/1000)f(RO) \qquad (6.39d)$$

where $RO = P*L_m$ and P is the total pressure of the carbon dioxide and water vapour in the flue gases. The directed exchange area $(\overrightarrow{GS_1})_R$ between the cover and the furnace gas is given by equation (6.15a). Since the furnace gas is represented by one clear and one grey component, the weighting factor is calculated by equation (6.14c) as:

$$a_g = \frac{\varepsilon_{g1}}{2-\varepsilon_{g2}/\varepsilon_{g1}}$$

where ε_{g1} and ε_{g2} are emissivities of the flue gas evaluated by Hadvig's correlation at one beam length and at twice the beam length respecitvely.

Let R_a be the ratio of the end area of the top coil to the directed exchange area $\overrightarrow{(GS_1)}_R$ such that R_a = end area/$\overrightarrow{(GS_1)}_R$. But, the ratio of the end area of the top coil to that area of the part of the cover above the level of the top plate is:

$$\frac{\text{end area}}{A_2} = \frac{DO_{(m)}^2 - DI_{(m)}^2}{D_2^2 + 4H_d^2 + 4D_2H_s}$$

$$\text{or} \quad \text{end area} = \frac{A_2(DO_{(m)}^2 - DI_{(m)}^2)}{D_2^2 + 4H_d^2 + 4D_2H_s}$$

Substituting for $\overrightarrow{(GS_1)}_R$ from equation (6.15a) and using the above expression for the end of the coil, the ratio R_a becomes the following:

$$R_a = \frac{\text{End Area}}{\overrightarrow{(GS_1)}_R} = \frac{DO_{(m)}^2 - DI_{(m)}^2}{D_2^2 + 4H_d^2 + 4D_2H_s} * \left(\frac{1-1.3\varepsilon_2}{1.3A_2\varepsilon_2 a_g} + \frac{1}{\varepsilon_g}\left(1 + \frac{A_r/A_2}{1 + \frac{\varepsilon_g}{a_g - \varepsilon_g} * \frac{1}{F_{r2}}}\right)^{-1}\right) \qquad (6.39e)$$

As shown in section (6.3), the net radiative transfer rate between the flue gases and the cover for the modified grey surface model with real gas is obtained by using the inverse proportionality of the directed flux areas $(\overrightarrow{GS_1})_R$ and $(\overrightarrow{GS_1})_R$ with temperatures $T_{f\ell}$ and T_2 respectively, as expressed by equation (6.17) as follows:

$$\dot{Q}_{g \rightleftharpoons 2} = (\overrightarrow{GS_1})_R \left(\frac{1-k^3}{1-k^4}\right) \sigma \left(T_{f\ell}^4 - T_{tc}^4\right)$$

where $k = T_2/T_{f\ell}$. Therefore, the net radiative rate per unit peripheral area of the top coil becomes the following:

$$q_{er} = \alpha_{er} T_{f\ell}\left(T_{f\ell}^3 - T_{tc}^3\right) \qquad (6.40a)$$

where

$$\alpha_{er} = \frac{\sigma(D_2^2 + 4H_d^2 + 4D_2H_s)}{DO_{(m)}^2 - DI_{(m)}^2} * \left(\frac{1 \div 1.3\varepsilon_2}{1.3A_2\varepsilon_2 a_g} + \frac{1}{\varepsilon_g}\left(1 + \frac{A_r/A_2}{1 + \frac{\varepsilon_g}{a_g - \varepsilon_g} * \frac{1}{F_{r2}}}\right)^{-1}\right)^{-1} \qquad (6.40b)$$

where A_2, A_r and F_{r2} are given by equations (6.32a), (6.39a) and (6.39b) respectively.

6.8.7 Solution of the Temperature of the Cover Top and the Flux from the Flue Gas

The incoming flux from the furnace flue gases is calculated by the following:

$$F_3 = \alpha_{ev}(T_{f\ell}-T_{tc}) + \alpha_{er}T_{fl}(T_{f\ell}^{3}-T_{tc}^{3})$$

The flux from the cover top to the top convector plate is given by the following:

$$F_1 = \alpha_r(T_{tc}^{4}-T_{tp}^{4}) + \alpha_n(T_{tc}-T_{tp})^{4/3}$$

Let E be a computational error where $E = F_3-F_1$. Applying the Newton-Raphson iterative method, the temperature of the top of the cover is calculated as follows:

$$T_{tc} = T_{tc} - E/\frac{\delta E}{\delta T_{tc}}$$

which converges when a specific tolerance in the absolute value of $E/\frac{\delta E}{\delta T_{tc}}$ is achieved.

6.9 Heat Transfer in the Cooler

After the soaking cycle, the steel is cooled down to about 180^{o}C before it is exposed to the atmospheric air. Heat is taken from the load by the inert gas and then removed from the gas by the cooler in the basement. The cooler is normally a shell and tube heat exchanger; however, the advantages and the disadvantages of other types of heat

transfer equipment, like fluidized bed, are being considered to reduce the length of the cooling cycle. In this work, the performance of a fluidized bed cooler is comapred with that of a shell and tube heat exchanger. Results are discussed in Chapter 8.

The inert gas is drawn from the stack via the downcomer by the centrifugal fan, and then driven into the exchanger at an angle to its tubes. This kind of gas flow past a bank of tubes makes the use of finned tubes in the heat exchanger disadvantageous for this particular application. For this case, the prediction of the performance of the heat exchanger is very difficult if not impossible. Hence, the cooler performance is predicted, from performance charts, as a relationship between the rate of heat removed and the temperature of the inert gas at its entry to the downcomer. These performance charts were based on a fan capacity of $10,000 ft^3/min$ and nominal temperature and flow rate of cooling water.

In the case of the fluidized bed, the performance is predicted from graphs of thermal performance characteristics. These graphs were based on a fraction of the hot inert gas, about 40-60% flowing through the fluidized bed. Nominal flow rate and temperature of cooling water were also used. The performance of the fluidized bed cooler is correlated as a relationship between the rate of heat removal and the temperature of the inert gas entering the basement.

In this manipulation, the change in the gas temperature between the gas entry into the downcomer and its entry

into the cooler is neglected. The effect of the heat, provided by the mechanical movement of the fan, on the temperature of the gas entering the cooler is also ignored. Therefore, the temperature of the gas entering the downcomer is considered equal to the temperature of the gas entering the cooler.

The rate of heat removal by the shell and tube heat exchanger was fitted from the performance graphs by a linear relationship as follows:

$$Q_{st} = 0.938T_h - 278.64 \text{ (kW)} \qquad (6.41a)$$

where T_h, is the temperature of the gas entering the cooler.

For the fluidized bed, the heat removal rate was correlated, from the characteristics curves in Fig. 8.7. by a polynomial in T_h as follows:

$$Q_{fb} = -567.1 + 2.167*T_h - 1.182*10^{-3}*T_h^2 + 4.07*10^{-7}T_h^3 \text{ (kW)} \qquad (6.41b)$$

Let V be the volumetric capacity of the fan m^3/min. Assuming the inert gas to follow ideal gas behaviour, the density of the gas becomes $\rho_g = 341.37/T_c (kg/m^3)$ where T_c is the temperature of the gas leaving the cooler. From the heat balance over the cooler, the heat lost by the gas is equal to the heat removed by the cooler. Therefore:

$$V\rho_g C_{p_g} (T_h - T_c) = Q \qquad (6.42)$$

where Q is either Q_{st} or Q_{fb}, for the shell and tube exchanger or the fluidized bed, respectively. Since, the specific heat of the gas is a function of temperature, as shown by Appendix (B.2), then

$$Q = 20483.4*V*\left(\frac{2.93*10^{-4}}{T_c} - 3.4*10^{-8} + 7.22*10^{-11} - 3.79*10^{-14}*T_c^{\,2} + 8.05*10^{-18}*T_c^{\,3}\right)*(T_h-T_c) \quad (6.43)$$

Equation (6.43) is solved by the Newton-Raphson method to calculate the temperature of the gas leaving the cooler and entering the charge plate.

CHAPTER SEVEN

COMPUTATIONS

COMPUTATIONS

7.1 Introduction

All the computations in this research were carried out on the ICL computer of the University of Aston in Birmingham. This computer uses the 1904S system which is controlled by the permanently active program, GEORGE 3, which controls the running of programs, scheduling of jobs, etc. This system has multiaccess from MOP, teletypes and VDUs as well as remote job entry.

The programs have been writeen in ICL 1900 FORTRAN which corresponds to the standard version of FORTRAN (ANSI X3.9 - 1966) which is published by the American National Standards Institute. UAFORTRAN system is a comprehensive FORTRAN capability allowing both full access to the facilities provided by the ICL 1900 Extended FORTRAN and a wide scale interaction with the GEORGE operating system.

7.2 Computational Test of Numerical Methods

Two separate programs were developed to solve the conduction model given by equation (5.3a), one of them implements the Barakat method and called BRK, and the other called ADI uses the ADI technique. Both programs were written to solve the system of partial differential equations for a furnace having one test coil with nominal boundary conditions.

Each test program is composed of a main segment which reads the coil data and initial values of temperatures, initializes variables and arrays, calculates the coefficents and independent terms of the model matrix, applies the numerical technique to solve the temperature distribution in the coil and prints out the results. Beside the main segment, each program contains a number of subroutines to calculate the effective radial conductivity, the physical properties of steel and inert gas, the minimum and maximum temperatures in the coil and the average temperature of the coil. In the case of the ADI test program, there are two additional subroutines for the solution of the tri-diagonal matrices of the estimate and the final solution of the temperature distribution in the coil. Both subroutines implement the Gauss elimination method of matrix solution.

The two test programs were developed to compare the performance of theBarakat and ADI numerical methods, when applied to the solution of the conduction model of transient heat transfer in annealing of steel coils by the lift-off furnace. This study covers the effect of the type of numerical solution, the comparison of radial and axial heat fluxes and their contribution to the annealing, and the computational efficiency of the numerical methods. The results of this study are shown in Chapter 8.

7.3 Annealing Furnace Program

The tests of the numerical methods showed that the ADI method is more advantageous, for the solution of heat conduction in the annealing furance, than the Barakat method. For this reason, the program for the solution of transient heat transfer in the annealing lift-off furnace was based on the ADI technique for the solution of the partial differential equations of conduction in the steel coils.

The main characteristics of the annealing furnace program are the following:

(i) The program accepts any set of data which is stored in the sepaprate data file without the need to change the original program.

(ii) It can work with any number of coils in the stack.

(iii) It accepts variations in the dimensions of the convective channels in the convector plates.

(iv) It is possible to use the program with either a shell and tube heat exchanger or a fluidized bed or any other type of cooler so-long-as the relationship between the cooler performance and the gas temperature is provided.

(v) It contains a flag which shifts the control from preheating to soaking to cooling, consecutively.

(vi) The fuel data is based on natural gas; however, the program accepts changes in the percentage of excess air and hence computes various adiabatic flame temperatures.

(vii) This program comprises about 1500 statements; nevertheless, it is not a big program as far as the storing capacity is concerned, requiring a core of only 22K in the computer storage.

(viii) The execution of the program is very fast, it takes less than 300 mills (3 minutes) for a run of four coil stacks of about 90 tons of steel for the whole annealing cycle, which is about 75 hours, using half-hour intervals of time. This includes the time for printing out the results for every half hour interval.

This program of the annealing furnace is composed of the subroutines described below.

7.3.1 Main Program

The main segment performs the following functions:

(i) It explains the different notations and variables used in the whole program.

(ii) It reads from the data file, the dimensions of the cover, the furnace wall, the convector plates and steel coils as well as the control temperatures, the emissivities of the cover and the coils, and the temperature of the furnace flue gases.

(iii) It initializes the temperatures, the variables and paramters used throughout the program.

(iv) It calculates the weight of the coils and prints out the stack data as well as the information about the channels of the covector plates.

(v) It calculates the adiabatic flame temperature of the furnace based on the percentage of the excess air given in the data file.

(vi) It calls the relevant subroutine to calculate the firing rate of fuel and the temperature of the furace gas leaving the firing zone.

(vii) It computes the profile of the temperature of the furnace gas with respect to the furnace height.

(viii) It calls the subroutine which computes the flow distribution of the inert gas between the convector plates and the total pressure drop in the stack.

(ix) It calls the subprogram which calculates the temperature distribution and the profile of heat transfer coefficient in the channels of the convector plates.

(x) It calculates the coefficients of the partial differential equations of heat conduction in the coil.

(xi) It calls the subroutines for the solution of the peripheral heat flux, of the heat transfer in

the core of the stack, of the heat convection at the ends of coils and of the heat transfer at the top of the furnace, to calculate the coefficients of the conduction model at the boundaries of the steel coils.

(xii) It calls Gauss elimination routines which solve the ADI matrices to calculate the estimate and the final solution of the temperature distribution in the steel coils.

(xiii) It calculates the routines which find the minimum and maximum temperatures in the coils as well as the overall mean temperature of the stack.

(xiv) It prints out the temperature distribution together with the limiting temperatures in each coil and the overall mean temperature of the stack over each time interval. It also prints the time elapsed for each phase of annealing (heating, soaking and cooling), and the output rate in terms of "tons/hour".

7.3.2 Gauss Elimination Routines

These are two subroutines ESTMTRIDIAG and TEMPTRIDIAG which use values of matrices of coefficients and constant terms from the main program to solve for the estimate and the final solution of the temperature distribution in the coil, respectively. Both subroutines are executed once for each coil over every time interval.

7.3.3 Space and Time Parameters

This is a subprogram which calculates the terms contained in the coefficients of the matrices of the differential equation of conduction, which depend on the physical properties of steel and the increments of axial and radial dimensions of the coil, together with the size of time interval; but they are independent of temperature. This subroutine uses a flag which tests whether the coil is tight or allowed to open. In the latter case, the subroutine calls the routine of the effective radial conductivity and implements the correction factor for conduction in the radial direction of the coil. This routine is called for every grid point in each coil over each time interval.

7.3.4 Radial Conductivity

The subroutine RADCOND is executed only when the coil opens by thermal expansion and the inert gas is allowed to enter between the steel laps. In this subprogram the correction factor for radial conductivity in the coil, which is expressed by equation (5.26), is computed in terms of radius, temperature and temperature gradient at the mean radius of radial elements, both evaluated at the beginning of the time interval. This is executed for every grid point in each coil over each interval of time.

7.3.5 Gas Flow Distribution

This program uses the data of the convective channels in the convector plates, the stack data and the fan capacity to calculate the pressure drop in various parts of the stack and hence the fractions of the inert gas flowing through each of the convector plates. The program also calculates the flow rate of the gas in the plates and the total pressure drop in the stack. This program is executed only once for the whole stack every time interval.

7.3.6 Convection Subroutine

The subroutine CONVECTORS solve for the radial temperature distribution of the inert gas and the radial profile of the convective heat transfer coefficient in the channels of the convector plate. This calculation is based on a marching technique starting with the temperature of the gas entering the convector plate and updating towards the centre of the plate. This routine is executed once per convector plate for every interval of time.

7.3.7 The Furnace Firing

The FIRING subroutine computes the temperature of the furnace gas after the combustion takes place in the burners. This temperature is measured, in practice, by a thermocouple which protrudes through

the brickwork of the furnace near the burner belt. The computation of the temperature which this thermocouple would indicate, is based on radiative transfer between the furnace gas, the cover, the refractory wall and the thermocouple surface, neglecting other modes of heat transfer. The subprogram also calculates the rate of heat losses from the side walls and the roof of the furance, and the rate of heat loss with the flue gases leaving the furnace from the top. From the rate of heat losses, the rate of heat picked by the steel and the inert gas, and the rate of heat provided by the combustion of the fuel, the rate of fuel firing in the furnace is calculated. The program also computes the thermal efficiency of the furnace as a percentage of heat taken by the steel coils to the total heat provided by the fuel firing in the furnace. This program is called once every time interval.

7.3.8 The Core of the Stack

In this program, the profile of the convective heat transfer coefficient in the centre of the coils with respect to height is calculated. The program calculates the profile of the gas temperature in the core of the stack from the heat balance over incremental height in the core of the stack. The temperature of the inert gas at the level of the lower end of the bottom coil is considered equal to the temperature

of the gas entering the basement of the furnace. This subroutine is called once for every interval of time.

7.3.9 Solution of Peripheral Heat Fluxes

The subroutine COVER solves the heat transfer fluxes at the outer periphery of the coil to calculate the temperature of the cover for every height increment of the coil. This temperature is solved by iterations using the Newton-Raphson technique. The subroutine also calculates the temperature of the inert gas in the annular gap between the coil and the cover for the same height increment. This subprogram is called for each height increment in each coil over every interval of time.

7.3.10 Subroutine TOPLATE

This program solves the model of heat conduction with the boundary heat fluxes at the top of the stack of coils. It calculates the heat transfer fluxes between the cover top and the top convector plate, between the cover top and the furnace gas and, for the cooling cycle, between the atmospheric air and the top of the cover. The temperature of the top of the cover is calculated by an iterative solution of heat fluxes. The value obtained for this temperature is used in the main segment of the whole program to compute the coefficients and

constant terms of the conduction equations at the upper end of the top coil. This temperature of the top of the cover is computed for every time interval.

7.3.11 Newton-Raphson Routines

Two routines of Newton-Raphson iterative technique are used to carry out the iterations for the solution of the cover temperature. The routines are called from the subroutine COVER. One of the routines finds the solution of the cover temperature during the heating and soaking cycles while the other computes this temperature during the cooling cylce of annealing. One of the two routines must be called whenever the subroutine COVER is called.

7.3.12 Subroutine RADATA

This is a routine which uses Hadvig's correlation to calculate the emissivity of the combustion products. The routine also calculates the weighting factor of the grey components of the gas. These parameters are used to calculate the temperature-independent terms in the coefficient of the radiative flux which is calculated in the subroutine COVER. This routine is called whenever the subroutine COVER is executed.

7.3.13 Physical and Transport Properties

The annealing program has a number of segments which calculate the physical properties of steel; for example, thermal conductivity, the volumetric thermal capacity, the coefficient of linear expansion and the volumetric enthalphy. Other subroutines calculate some functions of the physical and transport properties of the inert gas which are used in the equations of convective heat transfer coefficients, computed in other subroutines. In addition to that, there are subprograms for the computation of the specific heat and thermal conductivity of the inert gas as well as those for the combustion products. All the physical and transport properties and the functions of these properties are calculated as polynomials of temperature based on the value of the temperature at the beginning of the time interval.

7.3.14 Limiting and Mean Tempeartures

The subroutine TLIMIT selects, from the final solution of the temperature distribution in the coil at the end of every time interval, the minimum and maximum temperatures in each coil. The subroutine has a flag which directs the control to search for the minimum or the maximum temperatures in the grid according to the value of the flag prescribed by the CALL statement in the main program.

The subroutine TMEAN calculates the overall average temperature of the stack of coils. This average temperature is computed from the arithmatic mean of the distribution of temperature with respect to the axial and the radial coordinates in the coil, for all the steel coils in the furnace.

Each of these routines is called once for every interval of time.

7.4 The Logic Routine of Annealing Program

The execution of the program for the solution of the annealing furnace follows a logical routine which is outlined in Fig. 7.1 and described in the following steps:

Step 1: The program starts by reading the data from the data file and initializing the variables and identifiers in the source program. It also calculates the initial values of the parameters like the enthalpy of the steel coils and the inert gas at the value of their temperatures at the beginning of the first time interval, considered here as 300K.

Step 2: Calculation of the adiabatic flame temperature, the firing rate of the fuel, the temperature of the furnace gas leaving the burners and the profile of the furnace temperature with furnace height.

Step 3: Solution of the flow distribution of the inert gas between the convector plates. It also computes the

profiles of gas temperature and heat transfer coefficient in the core of the stack and in all the convector plates.

Step 4: Computation of heat transfer fluxes at all the boundary conditions of the coil.

Step 5: Calculation of all elements in the matrices of coefficients and independent terms of the conduction equations of the estimate and the final solution of the temperature distribution in the coil.

Steps 4 and 5 are repeated for all the grid points of each coil in the stack.

Steps 2 to 5 are repeated for all intervals of time until the end of the heating cycle.

Step 6: At the end of the heating cycle, stop firing and fix the temperature of the combustion products at its value at the end of the previous time interval. Start soaking with this furnace temperature.

Steps 2 to 6 are repeated until the end of the soaking cycle.

Step 7: Solution of heat transfer in the cooler and the calculation of the temperature of the gas entering the stack.

Step 8: Lift off the portable furnace and set the profile of the temperature of the gas surrounding the outer surface of the cover at a constant value equal to the ambient temperature of the atmosphere.

All the steps from 3 onward, excpet step 6, are repeated until the cooling cycle finishes.

Step 9: Print out the results and end.

It must be empahsized that steps 4 and 5 are repeated for all the points in the space grid of each coil for every time interval.

The overall flowchart and the listing of the program are shown in Appendixes C,D and those of the flow distribution, the convection in convector plates and in the core of the stack, the firing computation, the solution of peripheral heat fluxes and the solution of heat fluxes at the top of the furnace are shown in Appendix C.

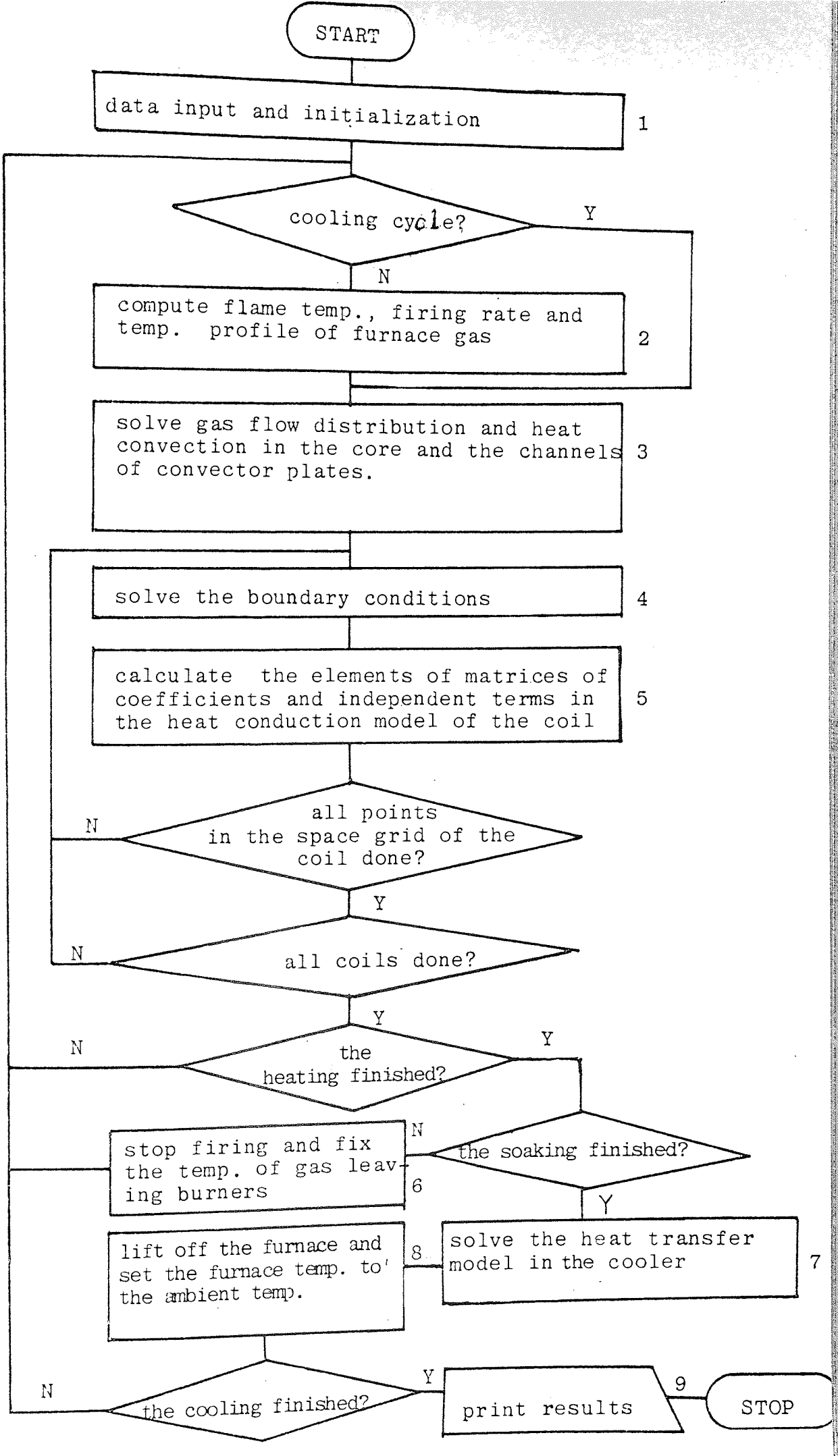
START
data input and initialization
1
cooling cycle?
Y
N
compute flame temp., firing rate and temp. profile of furnace gas
2
solve gas flow distribution and heat convection in the core and the channels of convector plates.
3
solve the boundary conditions
4
calculate the elements of matrices of coefficients and independent terms in the heat conduction model of the coil
5
all points in the space grid of the coil done?
N
Y
all coils done?
N
Y
the heating finished?
N
Y
the soaking finished?
N
Y
stop firing and fix the temp. of gas leaving burners
6
solve the heat transfer model in the cooler
7
lift off the furnace and set the furnace temp. to the ambient temp.
8
the cooling finished?
N
Y
print results
9
STOP

CHAPTER EIGHT

RESULTS AND DISCUSSIONS

RESULTS AND DISCUSSIONS

8.1 Comparisons of Numerical Methods

To study the effect of numerical techniques on the solution of the mathematical model of heat transfer in the annealing furnace, the Barakat and th ADI method of finite difference approximation were used to solve the model of heat conduction in a coil[25]. A reduced model of a furnace with one test coil was used. Typical furnace data and boundary conditions were used to test the numerical methods and to investigate the effect of the axial and radial heat fluxes on the heating cycle. The heating cycle is defined here by the time taken to heat the coil from 300K until the minimum temperature everywhere in the coil becomes greater than or equal to 900K. Computer programs for each finite difference approximation method were developed in FORTRAN and run on the ICL computer, 1904S system. The results fall in two categories, the performance of the numerical techniques on the model and the effect of radial, as opposed to axial heating in the coil.

8.1.1 Performance of Numerical Methods

(i) The computing time for one iteration showed that the program of the Barakat method is slightly faster than that of the ADI method; ie the Barakat calculation needs less computing time on the machine than the ADI method.

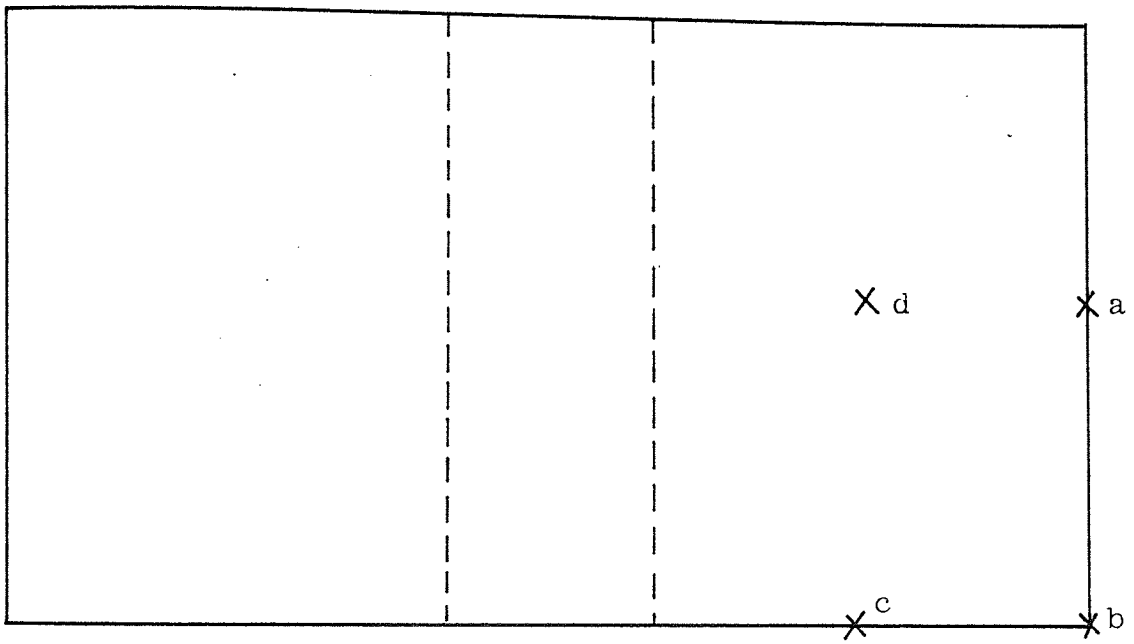

Figure 8.1

The selected points in the coil whose temperature profiles are used to investigate the effect of the size of the time interval on the accuracy of the solution. Figures 8.2a-d represents the temperature profiles of these points as follows:

point (a) - is shown in Fig. 8.2a

point (b) - is shown in Fig. 8.2b

point (c) - is shown in Fig. 8.2c

point (d) - is shown in Fig. 8.2d

(ii) The sensitivity of the methods to the courseness of space grid was tested by running the two programs for the same conditions, but with various axial and radial space intervals. The results obtained showed identical locations of the predicted minimum and maximum temperatures in the coil.

(iii) The effect of the size of time interval on the accuracy of the method calculations was investigated by running the two programs with identical time intervals up to five hours, so as to avoid the effect of the initial conditions and to select a more representative performance of each method. From thereon, RUN 1 continued for a single time interval of one hour from five to six hours, while RUN 2 continued with twenty intervals of 0.05 hours from five to six hours. The most enlightening comparisons are shown by the temperature profiles of the selected points in the coil shown in Fig. 8.1. These comparisons show the following:

(a) At the outer periphery of the coil, Fig. 8.2a and Fig. 8.2b showed that the Barakat prediciton started with a discrepancy which disappeared towards the end of the sixth hour. This discrepancy is defined by the difference between the temperature profile with the one-hour interval and the more precise profile obtained by the 0.05 hour intervals. For the case of the ADI method, the discrepancy started with a very small value

developed for some time and then disappeared by the end of the hour.

(b) From Fig. 8.2c, the temperature profile with coarse interval of time, for both theADI and the Barakat methods, started to deviate from the profile obtained with the more precise time interval. This deviation developed with time and attained its maximum value at the end of the hour. However, the deviation in the case of the ADI method is less than that of the Barakat method. This shows that the performance of the methods at the centre of the bottom end of the coil, where heat convection from the gas in the convector plate is the dominant heating flux, was poorer than anywhere else in the coil.

(c) At the middle point in the coil, as shown by Fig. 8.2d, both the ADI and the Barakat predictions showed results similar to those in Fig. 8.2c. But, the deviations at this location are smaller than those at the central point of the bottom end of the coil.

(d) Comparisons (a) to (c) show that the boundary conditions at the outer periphery of the coil, where radiation is the dominant mode of heat transfer, have less effect on the performance of these numerical techniques than the effect of the boundary conditions at the endsof the coil,

where the convector plates are situated. They also show that the accuracy of the ADI method is always less-affected by the size of the time interval than the Barakat method.

(iv) The profile of the minimum temperature in the coil obtained by the ADI calculation is more consistent with measured data than the profile predicted by the Barakat method. See Fig. 8.3.

8.1.2 Effect of Axial and Radial Heating

The effect of axial and radial heating fluxes on the heating cycle, as predicted by the two numerical methods is as follows:

(a) The results in Table 8.1 show that the Barakat predictions of the maximum temperature in the coil, at the end of the heating cycle for different heating fluxes, were almost identical, lying between 951K and 959K. On the other-hand, the values given by the ADI for the maximum temperature with different heating fluxes, have considerable variations, 904K to 964K. This means that the ADI is more sensitive to the amount of heat flux than the Barakat method, especially at the ends of the coil.

(b) Table 8.1 also shows that the Barakat method gave longer heating times than the ADI method, except with a cover temperature of 1000K and

typical convective heat transfer coefficients in the convector plates. Both methods predicted almost identical values for the minimum temperature in the coil at the end of the heating cycle.

(c) The heating cycle for a tight coil, which is similar to a hollow solid cylinder of steel, was computed by both methods. This was compared with the heating cycle of a coil which opens by thermal expansion in order to investigate the effect of coil opening on the heating rate. The ADI method showed a reduction in the cycle time from 77 to 42 hours, whereas the Barakat method showed a negligible reduction from 75 to 72 hours. This means that the Barakat method is less sensitive to the effect of the coil opening by thermal expansion than the ADI method which responded very clearly to the reduction in thermal conductivity caused by the opening of the coil.

(d) Table 8.1 shows that a cover temperature of 1000K would produce less heating time than a cover temperature of 900K or 1050K for both methods with various axial heating fluxes.

8.2 Test of the Mathematical Model

A test coil of steel was prepared with nine thermocouples fitted as shown in Fig. 8.4, and used in an industrial furnace to measure the temperature at these points during

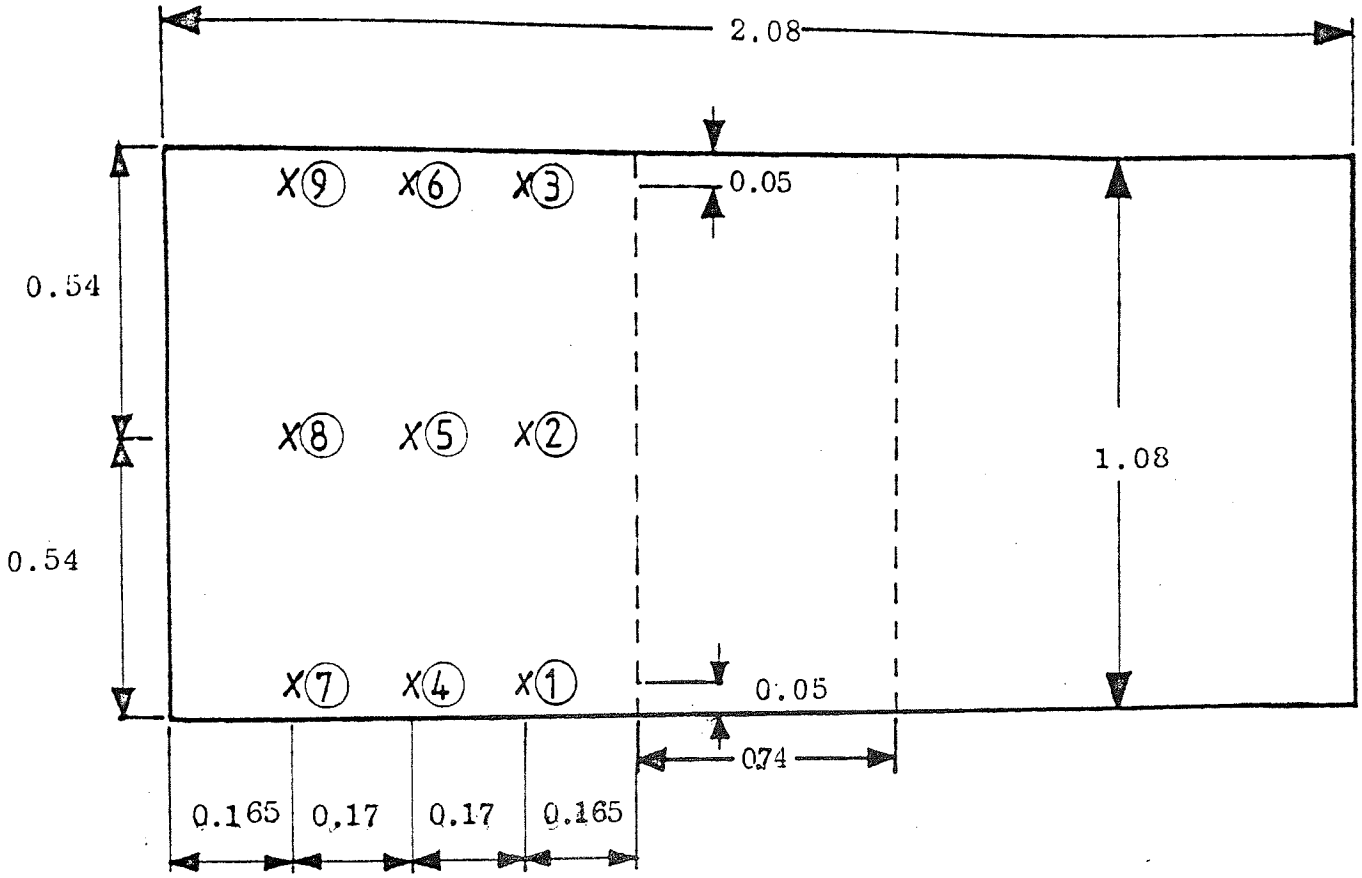

all dimensions in metres

Test Coil

Positions of the thermocouples fitted in the test coil

Figure 8.4

the annealing cycle. The test coil was "annealed" in different stacks having different number of coils and with different arrangements of coils of different sizes. These stacks are referred to in this thesis by the following notations:

Load L31 has 3 coils, the test coil at the bottom

Load L41 has 4 coils, the test coil at the bottom

Load L42 has 4 coils, the test coil number 2 from the bottom

Load L43 has 4 coils, the test coil number 3 from the bottom

Load L44 has 4 coils, the test coil at the top.

For all these loads, the minimum value of temperature measurements during the heating cycle, and the maximum temperature during the cooling cycle, lies at the centre of the coil laps as measured by thermocouple number 5. Since the mathematical model predicted the location of these limiting temperatures at about the same position in the coil, the computed values of the temperature at that point in the grid were compared with the measurements of thermocouple number 5. For comparison purposes, the measured and the predicted values of these temperature profiles were plotted on the same axes. See Figs. 8.5a to 8.5e.

As a further test of the model accuracy, times of the heating and cooling cycles calculated by the model were compared with their corresponding measured values. Also the rates of heating, in tons of steel per hour, were compared.

These comparisons were performed to test the reliability of the mathematical model for predicting the transient heat trnasfer in the furnace. The model was tested with the five arrangemnts of stacks of coils, so as to cover the widest range of stacking possibilities. The results are shown in Table 8.2.

8.2.1 Accuracy of the Model

From Table 8.2, the annealing time calculated by the mathematical model agrees with the measured value with 95% accuracy, if the results of Load L42 are not considered. For this load, the discrepancy was about 21%. Although for the other loads, the total annealing time agreed with the measured values reasonably well, the difference between the measured and the computed values for the heating and the cooling cycles, considered separately, was quite large.

For a stack with 3 coils, the predicted times for the heating, the cooling and the total annealing cycles were nearly equal to their corresponding measured values; and the difference in all cycles was less than 10%.

For the four-coil stacks, except the load L42 which has the test coil in the second position from the bottom of the stack, the difference between the measured and calculated values of the heating time was cancelled out by that of the cooling time. In the

case of Load L42, the model predicted longer times for both the heating and the cooling cycles, and hence longer annealing time than the measurements.

Table 8.2 also shows that for a stack of four coils, the difference between the computed and the measured cooling times increased as the test coil was moved from the bottom position to the top of the stack.

The profiles of the limiting temperature in the test coil, which were measured by thermocouple number 5, are shown in Fig. 8.5a to 8.5e. The limiting temperature is defined by the minimum temperature in the coil during the heating cycle and the maximum temperature during the cooling cycle.

The graphs in Fig. 8.5a show that the limiting temperature calculated by the model was always less than its value measured by the thermocouple for the whole annealing cycle. However, the difference between the two values was never greater than 20K, and the two values became closer to each other at the end of the heating cycle and the end of the cooling cycle.

Fig. 8.5b and 8.5e show that for four-coil stacks L41 and L44, the model predicted higher temperatures at location 5 than the measured values during the first half of the heating cycle; from thereon the predictions became less than the measurements until the end of the

heating cycle. During the cooling cycle, the computed values of the temperature were always higher than the measured values.

Fig. 8.5c shows that, for the first half of the heating cycle, the predicted and measured temperatures at location 5 of load L42 were almost similar. During the second half of the heating cycle, the predicted temperature became less than the measured temeperature. From the beginning of the cooling cycle onward, the computed temperature was considerably higher than the measured temperature. This is consistent with the results in Table 8.2, which show the difference in the cooling cycle as double the difference in the heating cycle for this load.

In the case of Load L43, the calculated values of the temperature at location 5 were higher than the measured values during all the heating cycle. During the cooling cycle, the measured temperature was higher than the predicted temperature. See Fig. 8.5d.

8.2.2 Location of Limiting Temperature

When the minimum temperature in the stack attains a value equal to the lower critical temperature of steel, the heating would be stopped, the cover furnace would be lifted off and the cooling cycle would start. The cooling cycle ends when the maximum temperature in the stack reaches a value below which the atmospheric

air does not oxidize the steel. The measurements of temperature in the coil indicated that the two limiting temperatures were located at the middle of the coil laps and measured by thermocouple number 5. The mathematical model predicted this location at the same position with a slight shift toward the hollow core of the coil.

The agreement between the model prediction and the thermocouple measurement of the location of the limiting temperature is an important test for the reliability of the model prediction. This is because the agreement in the location of the limiting temperature signifies the agreement in the prediction of temperature distribution in the coil.

The mathematical model was used with the five arrangements of coils, shown in section 8.2, to calculate the annealing cycle which is controlled by the limiting temperature in the whole stack, denoted by RUN 2, rather than the limiting temperature in the test coil only, whenever this was placed. The latter run was denoted by RUN 1. The results show that the limiting temperature in all these stacks would have been in the top coil whether it was the test coil or not. This was evident from the identical results of the two runs of load L44, which has the test coil at the top of the stack. See Table 8.3.

Table 8.3 also shows that the annealing cycle would be longer if the limiting temperature would have been in the top coil than any other position in the stack. The difference was very large for the case of the test coil being at the bottom, namely 81%. As the coil was moved from the bottom position upwards, the difference would become smaller until it disappeared altogether when the test coil was at the top. Table 8.3 also shows that the difference in the heating cycle would be 50% higher than the difference in the cooling cycle.

The above observations of the location of the limiting temperature in the top coil and the difference in the variation in the cooling and the heating cycles, could be explained by the fact that the top coil, although it receives a high radiative flux from the top of the cover via the top convector plate, it is the farthest coil from the burners' belt situated around the bottom coil.

8.3 Effect of Coil Opening

To investigate the effect of opening of the coil laps due to thermal expansion, the temperature distribution in the stacks, arranged in the order shown in section 8.2, was computed by the mathematical model considering the coils as solid hollow cylinders of steel. These coils will be called tight coils. This was compared with the results of the same loads treated as normal coils which may open

by thermal expansion of steel. These coils will be referred to as open coils. The results are presented in Table 8.4.

Table 8.4 shows that if the coils do not open by thermal expansion and behave as hollow solid cylinders, they would save about 30% of the total annealing time. This was valid for all the tested loads, whether they are of three or four coils.

The results show that the difference between the open and the tight coil would be mainly in the heating cycle where the tightness of the coils would save about 50% of the heating time. The difference in the cooling time was not so remarkable; it is only 3 to 9%. This phenomenon could be due to the contraction of the steel during cooling when the opening between the steel laps tends to close and return to its original tightness.

8.4 Stacking Arrangement

The Load L31 was composed of three coils of different sizes with the test coil being the largest one. The temperature distribution in this stack was calculated by the mathematical model with different arrangements of the coils to predict the optimal order of the coils in the stack. The following notations were used:

1 denotes the largest coil (test coil)

2 denotes the medium coil

3 denotes the smallest coil

b denotes the bottom position in the stack

m denotes the middle position in the stack

t denotes the top position in the stack

The results of these computations are shown in Table 8.5. This table shows that the order of the largest coil in the stacking arrangement has a significant affect on the time of the annealing cycle as well as on the fuel consumption. The results show that as the largest coil was moved from the bottom position to the top position in the stack, the annealing time increased from 59.5 to 128.5 hours. The effect of the position of the other two coils relative to that of the largest coil was not very serious. For example, when the largest coil was at the bottom of the stack, the interchange of the other two coils changed the total annealing time by only half an hour and the consumed fuel by less than 2%. On the other hand, the moving of the largest coil from the bottom to the top of the stack increased the cycle time from 60 to 127 hours, and used 14% more fuel. The results also show that this effect on the cooling cycle would be greater than on the heating cycle. The heating time was increased by about 60%, when the position of the largest coil was changed from the bottom to the top position of the stack, while the time of the cooling cycle was increase by 150%.

8.5 Effect of Dimensions of Convector Channels

The shape and the size of the channels in the convector plates have great effect on the rate of convective heat transfer between the gas flowing in the plates and the ends of the steel coils. To study this effect and to predict the optimum width-to-height ratio of the convector channels, the model was used to calculate the temperature distribution in the load L41 using different data on the width and the height of the channel entry at the outer periphery of the coils.

The following notation was used to represent the data on the channel dimensions:

W_1 is the conventional value of channel width

W_2 is 25% smaller than W_1

W_3 is 25% larger than W_1

H_1 is the conventional height of the channel

H_2 is 33% lower than H_1

H_3 is 33% higher than H_1

All the possible combinations of these data were used to predict the combination which produces the optimal convective transfer rate. The effect due to the change in the channel dimensions is expressed as a percentage of the results obtained by using the conventional dimensions as a datum, which is denoted in Table 8.6 by the Load H_1W_1.

The results in Table 8.6 show that the effect of changes in the channel height was more pronounced than the effect of changes in the width of the channel. Also, it

is noticed that the effect of changes in either dimension on fuel consumption was not considerable. 25% decrease in the channel width would not affect the heating time, but it would reduce the cooling cycle by about 3% and hence reduce the total annealing cycle by about 2%. This change would increase the pressure drop in the stack by 14%, but would not affect the consumed fuel. Also, an increase of 25% in the channel width would reduce the heating, the cooling and hence the annealing cycles by 3% each. The change in the width of the channel has no pronounced effect on fuel consumption in the furnace and negligible effect on the total pressure drop in the stack.

The decrease in the channel height by 33% would increase the heating time by 6% but would reduce the cooling time by 8% and thus reduce the total annealing time by 3%. This decrease in height would also increase the total pressure drop by 41% but would cause slight saving, of 1%, in fuel consumption. When the channel height was increased by 33%, both the heating and the cooling cycles would be reduced by 3% and 6% respectively. The reduction in the whole annealing cycle would then be 5%. The increase in height would not affect the amount of fuel consumed but would decrease the pressure drop in the stack by 19%.

In spite of reduction of both cycles caused by 33% increase in the channel height, Table 8.6 shows that the highest saving in the total annealing time (11%) would be achieved if the height is reduced by 33%. Similar savings of fuel and annealing time are indicated for either 25% increase in the channel width or 25% decrease. The maximum

temperature in the stack during cooling would be less if the channels were 25% wider with 25% fewer channels. For these optimal channel dimensions (33% decrease in height and 25% increase in width), the heating time would be increased by 6% only, but the cooling time would be reduced by 21% and thus the total annealing cycle would be reduced by 6%. These dimensional changes would produce the highest fuel saving, namely 2%. However, these changes would cause the highest increase in the total pressure drop, 64%. From these results, it is concluded that the optimum width-to-height ratio of the convective channels is 9.

8.6 Effect of Fan Capacity

The computer program of the annealing furnace was used to calculate the annealing cycle of Load L41 using different values for the volumetric capacity of the fan in the basement. The run using the present volumetric capacity of the fan was denoted by RUN 1. RUN 2 has a fan capacity 33% less than the present value and RUN 3 has 33% larger fan capacity. The results are shown in Table 8.7.

The results show that the bigger fan capacity would reduce the heating time by 11%, the cooling time by 8% and the total annealing cycle by 7%. On the other hand, a decrease of 33% in the fan capacity would produce 6% increase in the heating cycle, 13% increase in the cooling cycle, and 10% increase in the whole annealing cycle. The decrease in the fan capacity would result in 5% saving in fuel consumption and 2.2% decrease in the total heat given

to the stack. This decrease in capacity would reduce the total pressure drop by 57%. Increasing the fan capacity by 33% would increase the consumption of fuel by 4% but would also increase the useful heat given to the stack by 1.8%. It would also raise the total pressure in the stack by about 82%

The increase in the burned fuel associated with the higher fan capacity could be due to the increase of the total heat given to the steel coils. Another explanation could be attributed to the high firing rate at the beginning of the cycle where the gas temperature should be rapidly elevated. Also, the iterative procedure of estimating an initial temperature difference in the stack and an estimated temperature differential of the gas at the charge plate, may add some explanation of this increase in fuel.

8.7 Recycle of Furnace Gas

The mathematical model was used to investigate the effect of recycling the hot flue gases back to the firing zone in the furnace. Two different stacks, one with equally-sized coils and the other having coils of different dimensions, were used for the tests. Each of the two stacks was heated with and without recirculation of the furnace flue gases and the results are presented in Table 8.8.

8.7.1 General Observations

Table 8.8 shows the following:

(i) The heating time for the stacks of coils with either equal or different sizes would decrease if the flue gas is recycled. This saving in heating time would be about 26% if the coils have different sizes and 31% for equally-sized coils.

(ii) Whether the gas is recycled or not, the heating of coils having different dimensions would be faster than the heating of equally-sized coils; also the fuel consumption in therms per ton would be less.

(iii) Gas recirculation would increase the heating rate from 1.39 to 2.01 tons/h "44%" if the coils are equally-sized, and from 1.86 to 2.51 tons/h "35%" if the coils have different sizes. However, this would decrease the thermal efficiency by increasing the consumed fuel from 15.58 to 22.97 therms/ton "47%" for the case of equally-sized coils and from 14.92 to 19.30 therms/ton "30%" for the coils of different sizes.

(iv) The above observation shows that the recirculation of flue gases to the firing zone would improve the heating rate in terms of tons of steel per hour at the expense of the thermal efficiency of the furnace. The optimal operating conditions would be obtained by keeping the optimal balance between the thermal efficiency and the heating rate of the load. The latter depends on the stacking arrangement of the coils which has been discussed in detail in Section 8.4

8.8 Comparison of Coolers

The mathematical model was used to compare the performance of two types of cooler. A fluidized bed cooler whose thermal performance characteristics are shown in Fig. 8.6, was used and compared with the conventional shell and tube heat exchanger. The performance characteristics of the latter are shown in Fig. 8.7. A typical stack of steel coils with the dimensions shown in Table 8.9 was used for these tests.

The cooling cycle is defined, in these tests, by the time taken to cool the steel coils from an initial temperature of 900K everywhere in the coils until the maximum temperature in the stack is less than or equal to 450K.

8.8.1 Observations

(i) The fluidized bed cooler took 48 hours to finish the cooling cycle, while the shell and tube exchanger took 54 hours. See Table 8.10a and 8.10b.

(ii) The fluidized bed achieved a mean temperature in the stack equal to 450K in 45 hours, whereas it took the other cooler 51 hours to reach the same mean temperature.

(iii) When the mean temperature of the stack reached 450K, the maximum temperature in the bottom coil only was below 450K in the case of the fluidized bed. With the shell and tube cooler the maximum temperature in both the bottom and the second coils were under 450K at that stage.

(iv) When the mean temperature of the stack was 450K, the maximum temperatures in the four coils were higher in the case of the fluidized bed than the corresponding values with the shell and tube exchanger.

Observations (iii) and (iv) suggest that the shell and tube exchanger produces more uniform cooling of the stack up to this stage; but it is slower than the fluid bed cooler.

(v) Comparing the bottom lines of Table 8.10a and 8.10b, i.e. at the end of the cooling cycle the mean temperature of the stack produced by the fluidzed bed was cooler than that produced by the conventional cooler. The maximum temperatures in the two middle coils were almost the same for both coolers. The maximum temperature in the bottom coil was 5.3K cooler in the case of the fluidized bed than that of the shell and tube exchanger. This means that, for both coolers, the middle coils in the stack are subject to less temperature variation than those at the bottom and the top of the stack.

(vi) During the first five hours of cooling, the fluidized bed and the conventional exchanger produced identical values for the mean temperature in the stack. Fig. 8.8a shows that after the first five hours, the value obtained by the fluid bed, at any time interval, is cooler than that obtained by the shell and tube exchanger. The differential in the mean temperature increases with time along the cooling cycle.

(vii) For both types of cooler, the maximum heat removed from the stack ocurred at the beginning of the cycle. The cooling rate tends to decrease towards the end of the cycle. Fig. 8.8b shows that up to 45 hours, the amount of heat removed from the stack by the fluidized bed is larger than that removed by the shell and tube exchanger. The difference between the two values of heat removed is larger at the beginning of the cycle. After 45 hours, the values of heat removed by the two coolers are almost similar. This means that the fluidized bed extracts heat from the stack more quickly than the conventional cooler. However, towards the end of the cycle, the shell and tube exchanger catches up and even tends to overtake the rate of fluidized bed cooler.

(viii) The temperature of the gas entering the downcomer was lower in the case of the fluidized bed than the case of the shell and tube exchanger. This is valid at any time interval as shown in Fig. 8.8c.

(ix) From Fig. 8.8d, the temperature drop in the fluidized bed is greater than that in the conventional exchanger. The difference in the drop is larger at the beginning of the cycle, and diminishes with time up to the end of the cycle.

(x) The temperature of the gas leaving the fluid bed cooler and entering the stack is always lower than the temperature of the gas leaving the shell and tube exchanger. This is shown in Fig. 8.8e and seems to be consistent with observations (viii) and (ix).

(xi) The maximum temperatures in the coils are always located near the core for both cases of the fluidized bed and the shell and tube heat exchanger.

8.8.2 Comments

1. The above comparisons of the two types of cooler were based on an idealized initial state, whereby the coils were everywhere at 900K. In reality, at the end of the heating cycle there is a considerable temperature variation throughout the coils. The model was used to calculate the total cycle time with the two types of cooler. In these tests, the fluidized bed produced the same proportional decrease in the cooling cycle time, as with an idealized initial temperature. The probable explanation to these similar results is that at the beginning of the cooling cycle the temperature gradients in the coils tend to decrease before a significant amount of heat has been removed and the temperatures start to drop. See Fig. 8.9a and 8.9b where typical changes in the radial temperature profiles of the coils are shown. These graphs are plotted for the bottom coil at its half height.

2. The use of a fluidized bed as a cooler incorporates some problems of pressure drop and particle entrainment in the gas. It is possible that a shallow bed with a suitable diffuser plate would overcome

the high pressure problems. The pressure drop would also be reduced by passing part of the gas, rather than the whole gas flow, through the bed; but this would reduce the amount of heat removed from the load. The entrainment of the fluidized particles in the gas could be avoided by using a sieve plate at the exit of the bed.

Method	Cover temp. (K)	Typical H.T. Coefficients in Convector Plates			H.T. Coefficients 50% higher than typical values		
		Cycle time (h)	min. temp (K)	max. temp (K)	Cycle time (h)	min. temp (K)	max. temp (K)
ADI	900	83	901.0	903.6	79	901.4	904.3
	1000	77	901.7	916.2	68	900.5	913.4
	1050	82	900.4	964.0	72	901.8	957.1
Barakat	900	96	901.4	950.8	93	900.5	959.2
	1000	75	900.1	955.2	74	900.6	958.3
	1050	89	901.0	958.9	86	900.7	954.1

Table 8.1 - Results of the ADI and Barakat Predictions

Table 8.2 - Comparisons of Computed and Measured Results

Load	Weight (tons)	Type of data	Heating Time (h)	Cooling Time (h)	Total Annealing Time (h)
L31	65.21	measured	28.0	31.0	59.0
		computed	26.0	34.0	60.0
		diff. %	-7%	+9%	+2%
L41	73.07	measured	30.5	36.0	66.5
		computed	36.0	33.0	69.0
		diff. %	+18%	-8%	+4%
L42	70.80	measured	45.5	34.0	79.5
		computed	52.5	44.0	96.5
		diff. %	+15%	+29%	+21%
L43	75.33	measured	42.0	37.0	79.5
		computed	33.0	44.0	77.5
		diff. %	-21%	+20%	-3%
L44	77.23	measured	64.5	38.0	102.5
		computed	54.5	53.5	107.5
		diff. %	-16%	+40%	+5%

70

Table 8.3 - Comparisons of Different Limiting Temperatures in a Stack of Coils

Load	Weight (tons)	Type of Run	Heating Time (h)	Cooling Time (h)	Total Annealing Time (h)
L31	65.21	Run 1	26.0	34.0	60.0
		Run 2	34.5	64.0	98.5
		diff. %	33%	88%	64%
L41	73.07	Run 1	17.5	31.5	49.0
		Run 2	33.5	55.5	89.0
		diff. %	91%	76%	81%
L42	70.80	Run 1	24.0	40.0	64.0
		Run 2	42.0	60.5	102.0
		diff. %	75%	51%	59%
L43	75.33	Run 1	33.0	44.5	77.5
		Run 2	47.5	57.5	105.0
		diff. %	44%	29%	35%
L44	77.23	Run 1	54.0	53.5	107.5
		Run 2	54.0	53.5	107.5
		diff. %	0%	0%	0%

Table 8.4 - Comparison of Open and Tight Coils

Load	Heating Time (h)	Cooling Time (h)	Total Annealing Time (h)	Consumed Fuel (kg)
L31 open	48.5	31.5	80.0	1668
tight	26.0	34.0	60.0	1655
diff %	46%	9%	25%	1%
L41 open	36.0	33.0	69.0	1606
tight	17.5	31.5	49.0	1561
diff %	51%	5%	29%	3%
L42 open	52.5	44.0	96.5	2123
tight	24.0	40.0	64.0	1883
diff %	54%	9%	34%	11%
L43 open	56.0	53.5	109.5	2538
tight	33.0	44.5	77.5	2220
diff %	70%	17%	41%	14%

Table 8.5 - Results of Stacking Arrangements

Load			Heating Time (h)	Cooling Time (h)	Total Annealing Time (h)	Fuel Consumed (kg)
b	m	t				
1	2	3	26.0	34.0	60.0	1565
1	3	2	25.5	34.0	59.5	1591
2	1	3	31.5	54.0	85.5	1700
3	1	2	31.5	58.5	90.0	1709
2	3	1	41.0	85.5	127.0	1780
3	2	1	41.0	87.5	128.5	1740

Load Combination	Heating		Cooling		Annealing		Fuel		Pressure Drop	
	Time (h)	diff. %	Time (h)	diff. %	Time (h)	diff. %	(kg)	diff. %	mmwg.	diff. %
H_1W_1	17.5	-	31.5	-	49.0	-	1561	-	19.46	-
H_1W_2	17.5	0	30.5	-3%	48.0	-2%	1557	0	22.16	+14%
H_1W_3	17.0	-3%	30.5	-3%	47.5	-3%	1560	0	19.70	+1%
H_2W_1	18.5	+6%	29.0	-8%	47.5	-3%	1540	-1%	27.48	+41%
H_2W_2	18.5	+6%	25.0	-21%	43.5	-11%	1528	-2%	32.01	+64%
H_2W_3	18.5	+6%	25.0	-21%	43.5	-11%	1535	-2%	32.01	+64%
H_3W_1	17.0	-3%	29.5	-6%	46.5	-5%	1559	0	15.76	-19%
H_3W_2	17.0	-3%	32.5	+3%	49.5	+1%	1597	+2%	17.58	-10%
H_3W_3	17.0	-3%	32.5	+3%	49.5	+1%	1602	+3%	15.89	-18%

Table 8.6 - Sensitivity Study of Convector Channel Dimensions

Table 8.7 - Sensitivity Study of Fan Capacity

Cycle	RUN 1	RUN 2	RUN 3
Heating: time (h)	17.5	18.5	16.5
% change		+6%	-6 %
Cooling: time (h)	31.5	35.5	29.0
% change		+13%	-8%
Total Annealing time (h)	49.0	54.0	45.5
% change		+10%	-7%
Consumed Fuel kg	1561	1479	1621
% change		-5%	+4%
Total Heat into Stack kWh	12510	12230	12740
% change		-2.2%	+1.8%
Total Pressure Drop mm.w.g.	19.46	8.38	35.35
% change		-57%	+82%

		Equally-Sized Coils		Coils of Different Sizes	
	Weight (tons)	76.41		93.04	
	Dimensions (metres)	Diam.	Height	Diam.	Height
	Coil 1	1.83	1.07	2.13	1.22
	Coil 2	1.83	1.07	2.13	1.07
	Coil 3	1.83	1.07	1.83	0.91
	Coil 4	1.83	1.07	1.83	1.07
Gas Recirculation	Heating Time (h)	38		37	
	Rate (ton/h)	2.01		2.51	
	Eff. (therms/ton)	22.97		19.30	
No Gas Recirculation	Heating Time (h)	55		50	
	Rate (ton/h)	1.39		1.86	
	Eff. (therms/ton)	15.58		14.92	

Table 8.8 - Results of Gas Recirculation

Plate No.	Coil No.	Coil Dimensions (metres)			Coil Weight (tons)	No. of Channels	Height of Channel cm
		O.D.	I.D.	Height			
1						20	2.54
	1	2.13	0.69	1.22	30.70		
2						40	1.90
	2	2.13	0.71	1.07	26.86		
3						40	1.90
	3	1.83	0.67	0.92	16.37		
4						40	1.90
	4	1.83	0.69	1.07	19.10		
5						20	1.90
					93.03		

Table 8.9 - Dimensions of Stack used for Cooling Tests

TABLE 8.10a - Results of Fluidised Bed Cooler

Time (HOURS)	MAX. TEMPERATURE (K) IN: Coil 1	Coil 2	Coil 3	Coil 4	Mean Temp (K)	Temp to Cooler (K)	Temp Drop (K)	Fan Temp (K)	Heat Remove from Stack 10^{-1} CHU
1	899.8	899.8	899.7	899.8	891.4	725.8	172.6	553.2	2.05
2	898.7	898.7	897.8	898.6	880.5	667.5	143.3	524.2	4.34
3	896.4	896.6	894.4	896.2	869.7	636.9	128.6	508.3	4.23
4	892.9	893.2	889.4	892.4	858.7	619.7	120.6	499.2	4.24
5	887.8	888.2	882.8	887.4	847.5	608.1	115.2	492.9	4.22
6	881.1	881.7	874.4	881.1	836.3	599.3	111.2	488.1	4.21
7	872.7	874.0	864.5	873.2	824.9	591.8	107.8	484.0	4.19
8	862.8	865.4	853.3	863.7	813.5	585.1	104.9	480.3	4.17
9	851.3	855.9	841.2	852.6	801.9	578.9	102.1	475.8	4.15
10	838.5	845.4	828.2	840.2	790.2	573.0	99.5	473.5	4.13
11	825.3	833.9	814.8	826.8	778.4	567.2	97.0	470.2	4.11
12	811.4	821.9	801.1	812.6	766.6	561.5	94.5	467.0	4.08
13	797.0	809.2	787.3	797.9	754.7	555.8	92.1	463.7	4.05
14	782.3	796.2	773.6	782.9	742.7	550.1	89.7	460.5	4.00
15	767.4	782.9	759.9	778.0	730.8	544.4	87.3	457.2	3.96
16	752.5	769.4	746.5	753.2	718.8	538.7	84.9	453.8	3.90
17	737.6	755.9	733.3	738.6	706.9	532.9	82.5	450.4	3.84
18	722.9	742.4	720.5	724.4	695.1	527.1	80.1	447.0	3.77
19	708.3	729.1	707.8	710.4	683.4	521.3	77.8	443.6	3.69
20	694.1	715.9	795.3	696.9	671.8	515.5	75.4	440.1	3.61
21	680.2	702.8	683.1	683.7	660.3	509.6	73.1	436.6	3.53
22	666.5	690.1	671.2	670.9	649.0	503.8	70.8	433.0	3.44
23	653.3	677.7	659.5	658.4	637.8	498.0	68.5	429.5	3.35
24	640.3	665.5	648.1	646.3	626.9	492.2	66.3	426.0	3.26
25	627.8	653.5	636.9	634.6	616.2	486.5	64.1	422.5	3.17
26	615.6	641.7	625.9	623.2	605.6	480.9	61.9	418.9	3.08
27	603.7	630.1	615.2	612.2	595.3	475.3	59.2	416.1	2.99
28	592.2	618.8	604.7	601.5	585.3	470.2	57.3	412.9	2.89
29	581.1	607.7	594.5	591.1	575.4	464.9	55.4	409.5	2.80
30	570.3	596.9	584.5	581.0	565.8	459.6	53.5	406.2	2.72
31	559.9	586.3	574.8	571.3	556.5	454.4	51.6	402.8	2.63
32	549.8	576.0	565.3	561.8	547.3	449.2	49.8	399.5	2.55
33	540.1	565.9	556.0	552.6	538.4	444.2	48.0	396.1	2.46
34	530.7	556.1	547.0	543.8	529.8	439.2	46.3	392.9	2.38
35	521.5	546.6	538.2	535.0	521.3	434.3	44.6	389.7	2.31
36	512.7	537.3	529.6	526.6	513.1	429.5	43.0	386.5	2.23
37	504.2	528.3	521.3	518.4	505.2	424.8	41.4	383.4	2.16
38	496.0	519.5	513.2	510.5	497.4	420.2	39.9	380.3	2.08
39	488.0	571.0	505.3	502.8	489.9	415.7	38.4	377.3	2.01
40	480.3	502.7	497.6	495.3	482.6	411.3	37.0	374.3	1.94
41	472.9	494.7	490.2	488.1	475.5	407.1	35.6	371.4	1.88
42	465.7	486.9	482.9	481.1	468.6	402.9	34.3	368.6	1.81
43	458.8	479.4	475.9	474.2	461.9	398.8	33.0	365.8	1.75
44	452.1	472.1	469.0	467.6	455.5	394.9	31.8	363.0	1.69
45	445.7	465.0	462.4	461.2	449.2	391.0	30.6	360.4	1.63
46	439.5	458.2	455.9	455.0	443.1	387.2	29.5	357.7	1.57
47	433.5	451.6	449.7	448.9	437.2	383.6	28.4	355.2	1.52
48	427.7	445.2	443.6	443.0	431.5	380.0	27.3	352.7	1.46

TABLE 8.10b - Results of Shell and Tube Cooler

Time (HOURS)	MAX. TEMPERATURE (K) IN:				Mean Temp (K)	Temp to Cooler (K)	Temp Drop (K)	Fan Temp (K)	Heat Removed from Stack : 10^{-5} CHU
	Coil 1	Coil 2	Coil 3	Coil 4					
1	899.8	899.8	899.7	899.8	891.7	754.2	152.8	601.4	
2	898.8	898.8	898.0	898.7	881.7	702.4	129.5	572.8	4.00
3	896.7	896.8	895.0	896.4	871.7	673.5	117.1	556.4	3.90
4	893.5	893.7	890.5	893.2	861.6	665.6	110.0	546.5	3.90
5	888.9	888.2	884.5	888.9	851.4	644.8	105.2	539.6	3.89
6	882.8	883.6	877.0	883.1	841.1	635.9	101.6	534.3	3.88
7	875.4	877.3	868.1	875.9	830.7	628.3	98.5	529.8	3.86
8	866.6	869.9	858.1	867.1	820.2	621.6	95.8	525.7	3.84
9	856.6	861.6	847.2	856.9	809.7	615.3	93.4	521.9	3.82
10	845.9	852.2	835.6	845.5	799.0	609.3	91.0	518.3	3.81
11	834.2	842.1	832.5	833.2	788.3	603.5	88.8	514.8	3.78
12	827.1	831.3	811.1	820.0	777.5	597.8	86.6	511.3	3.76
13	809.4	820.0	798.6	806.4	766.7	592.1	84.4	507.8	3.73
14	796.4	808.3	786.1	792.6	755.8	586.5	82.2	504.2	3.70
15	783.0	796.3	773.6	778.7	744.9	580.8	80.1	500.7	3.66
16	769.5	784.1	761.4	765.0	734.0	575.1	78.0	497.1	3.61
17	755.9	77.1.8	749.4	751.5	723.2	569.4	75.9	493.5	3.56
18	742.4	759.6	737.5	738.1	712.4	563.6	73.7	489.9	3.50
19	729.3	747.3	725.9	725.1	701.7	557.9	71.6	486.2	3.42
20	716.4	735.3	714.4	712.4	691.0	552.1	69.6	482.5	3.37
21	703.7	723.3	703.1	700.0	680.5	546.3	67.5	478.8	3.30
22	691.3	711.5	692.0	688.0	670.2	540.5	65.5	475.1	3.22
23	679.1	699.9	681.1	676.3	659.9	534.8	63.4	471.4	3.15
24	667.2	688.4	670.4	665.0	649.8	429.1	61.5	467.6	3.07
25	655.6	677.2	660.0	654.0	639.9	523.4	59.5	463.9	2.99
26	644.3	66.1	649.7	643.3	630.2	517.8	56.9	460.8	2.91
27	633.3	655.3	639.7	632.9	620.6	512.6	55.2	457.4	2.83
28	622.6	644.8	629.9	622.9	611.3	507.3	53.5	453.9	2.75
29	612.2	634.5	620.3	613.1	602.1	502.0	51.7	450.3	2.67
30	602.1	624.4	610.9	603.6	593.2	496.7	50.0	446.7	2.59
31	592.3	614.6	601.7	594.4	584.4	491.4	48.8	443.1	2.52
32	582.7	604.9	592.8	585.5	575.8	486.3	46.7	439.6	2.44
33	573.5	595.5	584.0	576.8	567.5	481.3	45.1	436.0	2.37
34	564.5	586.3	575.5	568.3	559.3	476.1	43.6	432.6	2.30
35	555.8	577.3	567.1	570.1	551.3	471.2	42.0	429.2	2.23
36	547.3	568.5	559.0	552.2	543.5	466.4	40.6	425.8	2.16
37	539.1	559.9	551.0	544.4	535.9	461.6	39.1	422.5	2.10
38	531.2	551.6	543.2	537.9	528.5	457.0	37.8	419.2	2.03
39	523.5	543.4	535.7	529.6	521.3	452.4	36.4	416.0	1.97
40	516.0	535.5	528.3	522.5	514.3	448.0	35.1	412.8	1.91
41	508.7	527.8	521.1	515.6	507.5	443.6	33.9	409.7	1.85
42	501.7	520.3	514.1	508.9	500.9	439.4	32.7	406.7	1.79
43	494.9	513.0	507.3	502.3	494.4	435.2	31.5	403.7	1.73
44	488.3	505.9	500.6	469.0	488.1	431.1	30.4	400.8	1.68
45	482.0	499.1	494.2	489.8	482.0	427.1	29.3	397.9	1.62
46	475.8	492.4	487.9	483.8	476.1	423.3	28.2	395.1	1.57
47	469.8	485.9	481.8	478.0	470.3	419.5	27.2	392.3	1.52
48	464.0	479.6	475.8	472.4	464.7	415.8	26.2	389.6	1.47
49	485.4	473.5	470.1	466.9	459.3	412.2	25.2	387.0	1.42
50	453.0	467.6	464.5	461.5	454.0	408.7	24.3	384.4	1.38
51	447.8	416.9	459.0	456.3	448.9	405.3	23.4	381.9	1.33
52	442.7	456.3	453.8	451.3	443.9	402.0	22.6	379.4	1.29
53	437.8	450.9	448.6	446.4	439.1	398.7	21.7	377.0	1.24
54	433.0	445.7	443.7	441.6	434.4	395.6	20.9	374.7	1.20

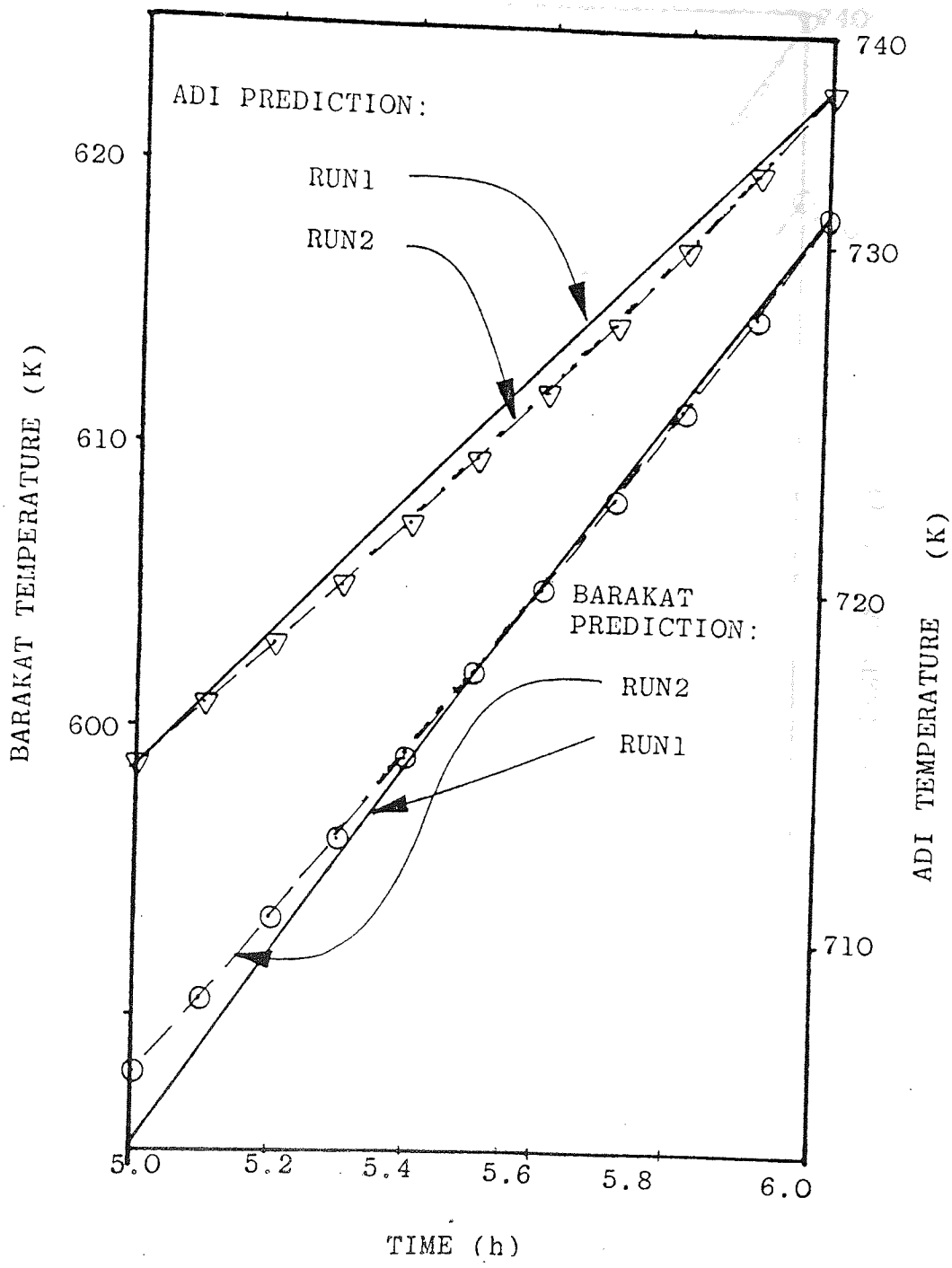

Figure 8.2a

TEMPERATURE OF THE MID-POINT OF THE OUTER PERIPHERY OF THE COIL

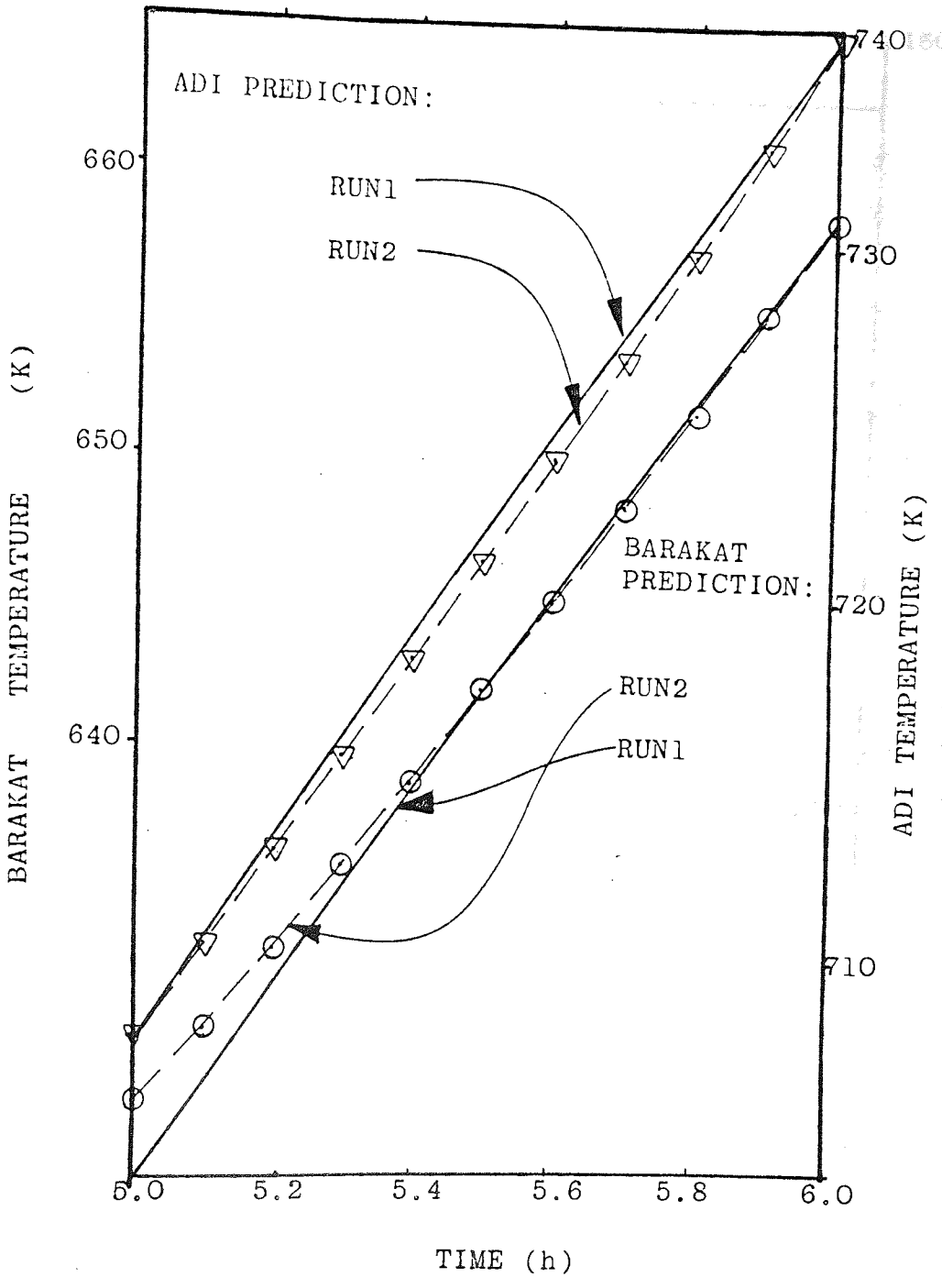

Figure 8.2b

TEMPERATURE OF THE BOTTOM POINT
IN THE OUTER PERIPHERY OF THE COIL

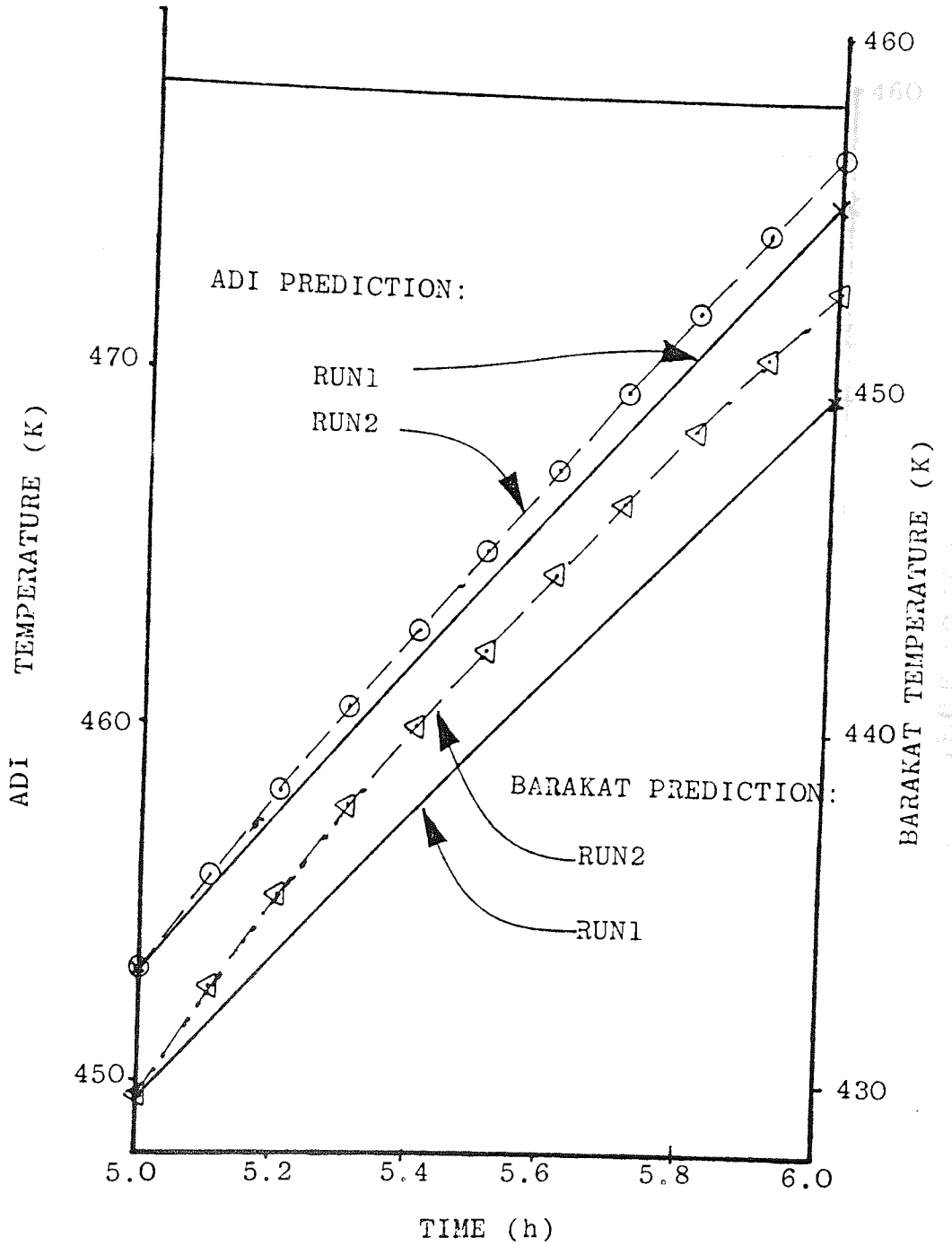

Figure 8.2c

TEMPERATURE OF THE MID-POINT
OF BOTTOM OF THE COIL

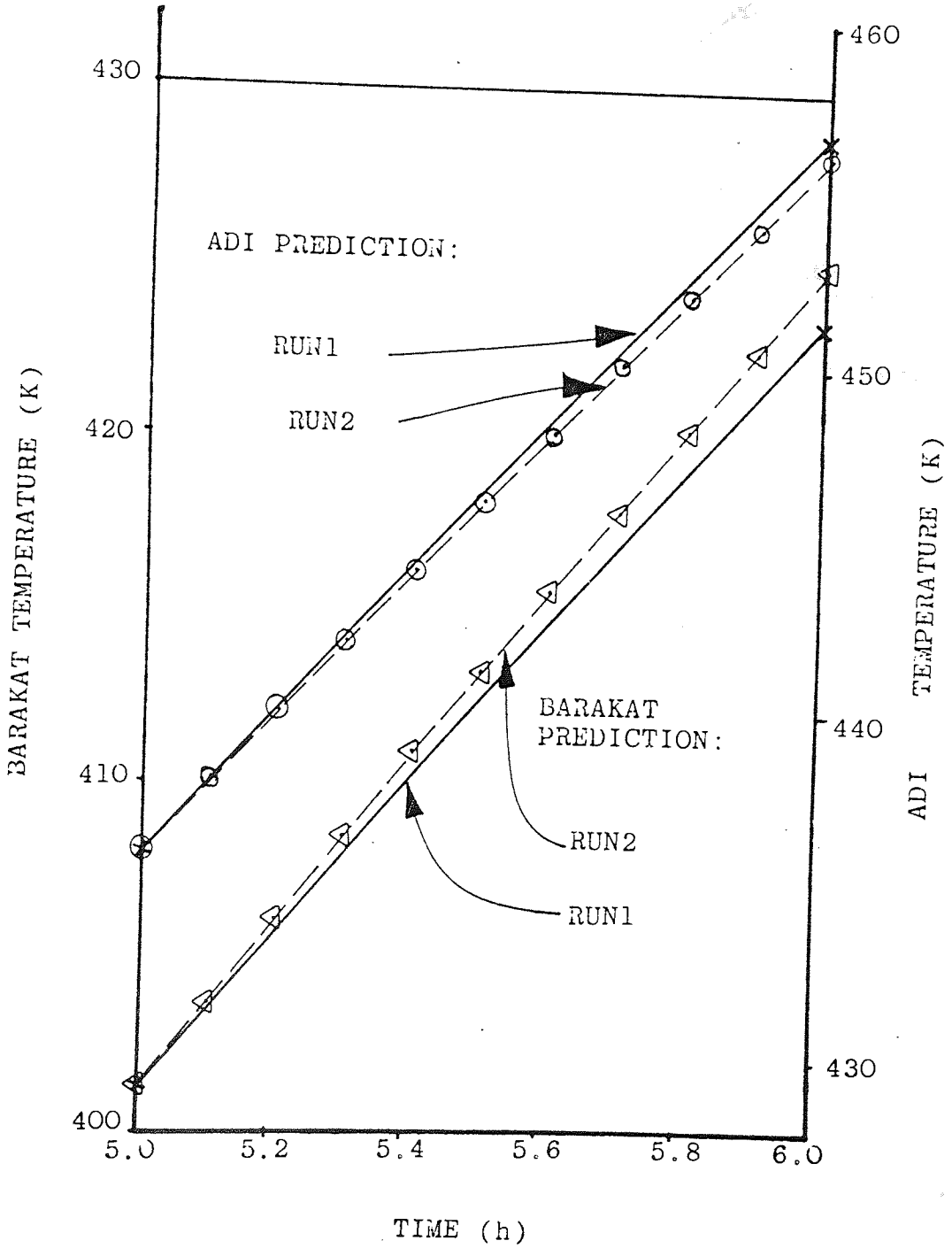

Figure 8.2d

TEMPERATURE OF THE CENTRE POINT OF THE COIL

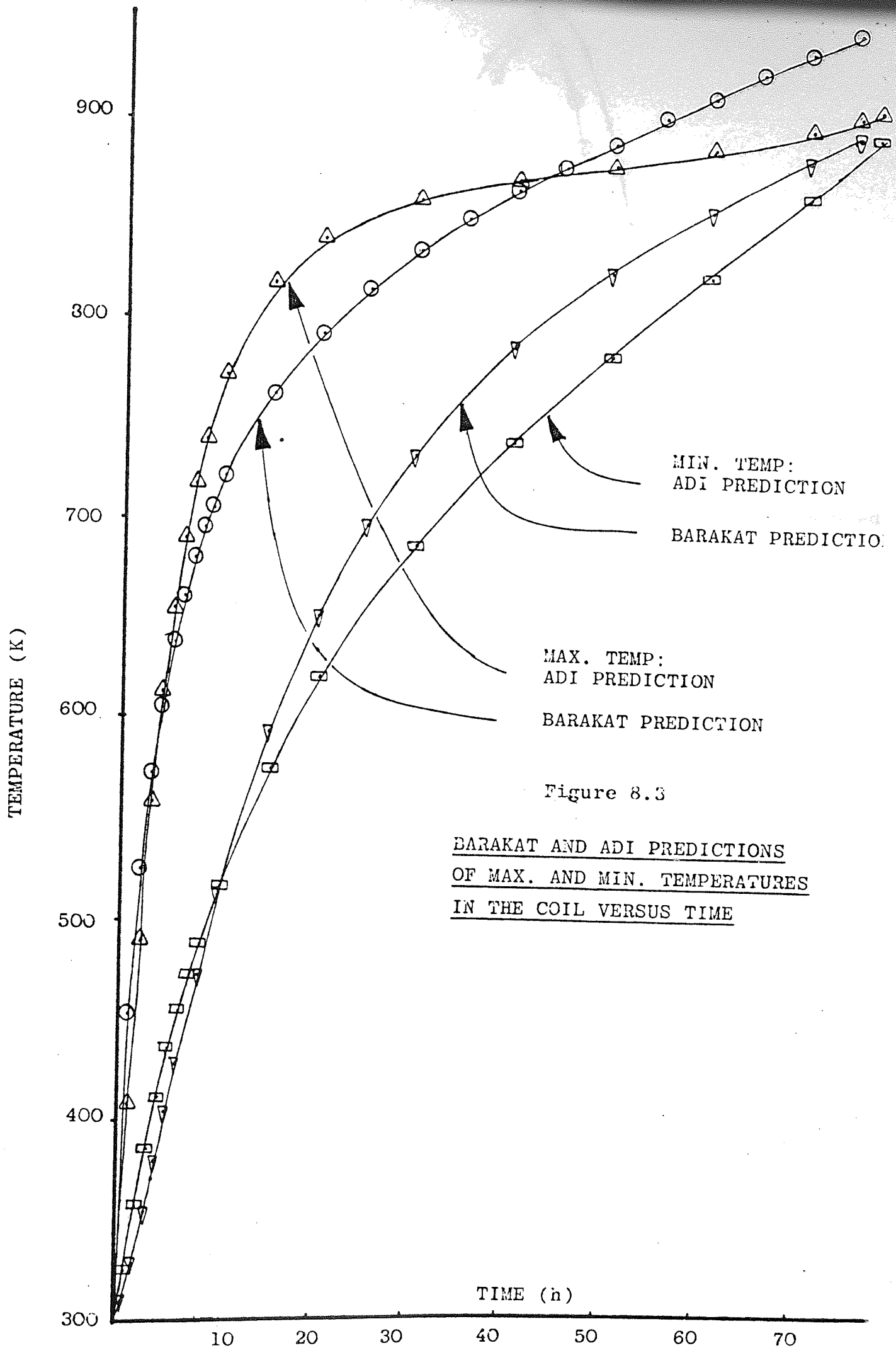

Figure 8.3

BARAKAT AND ADI PREDICTIONS OF MAX. AND MIN. TEMPERATURES IN THE COIL VERSUS TIME

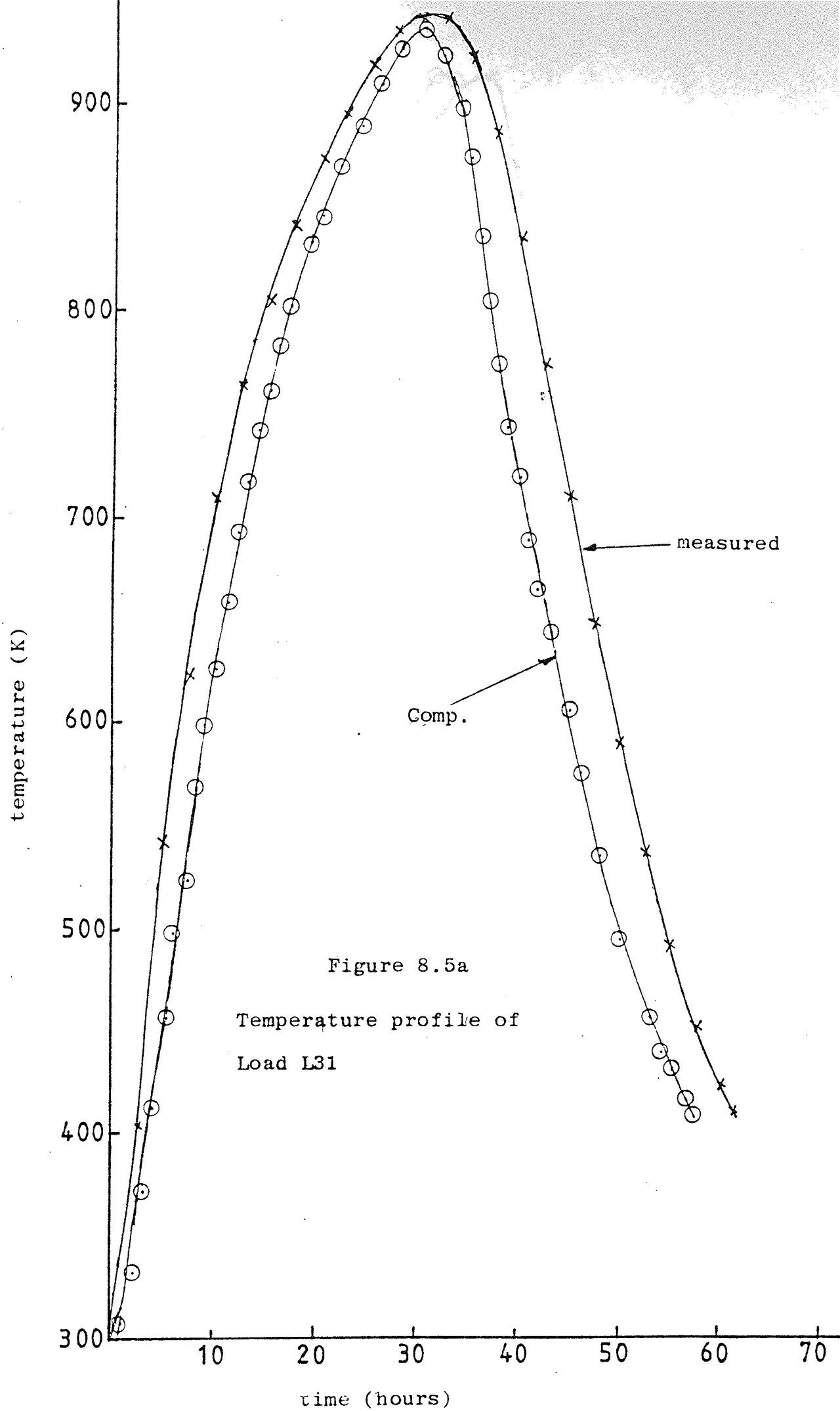

Figure 8.5a

Temperature profile of

Load L31

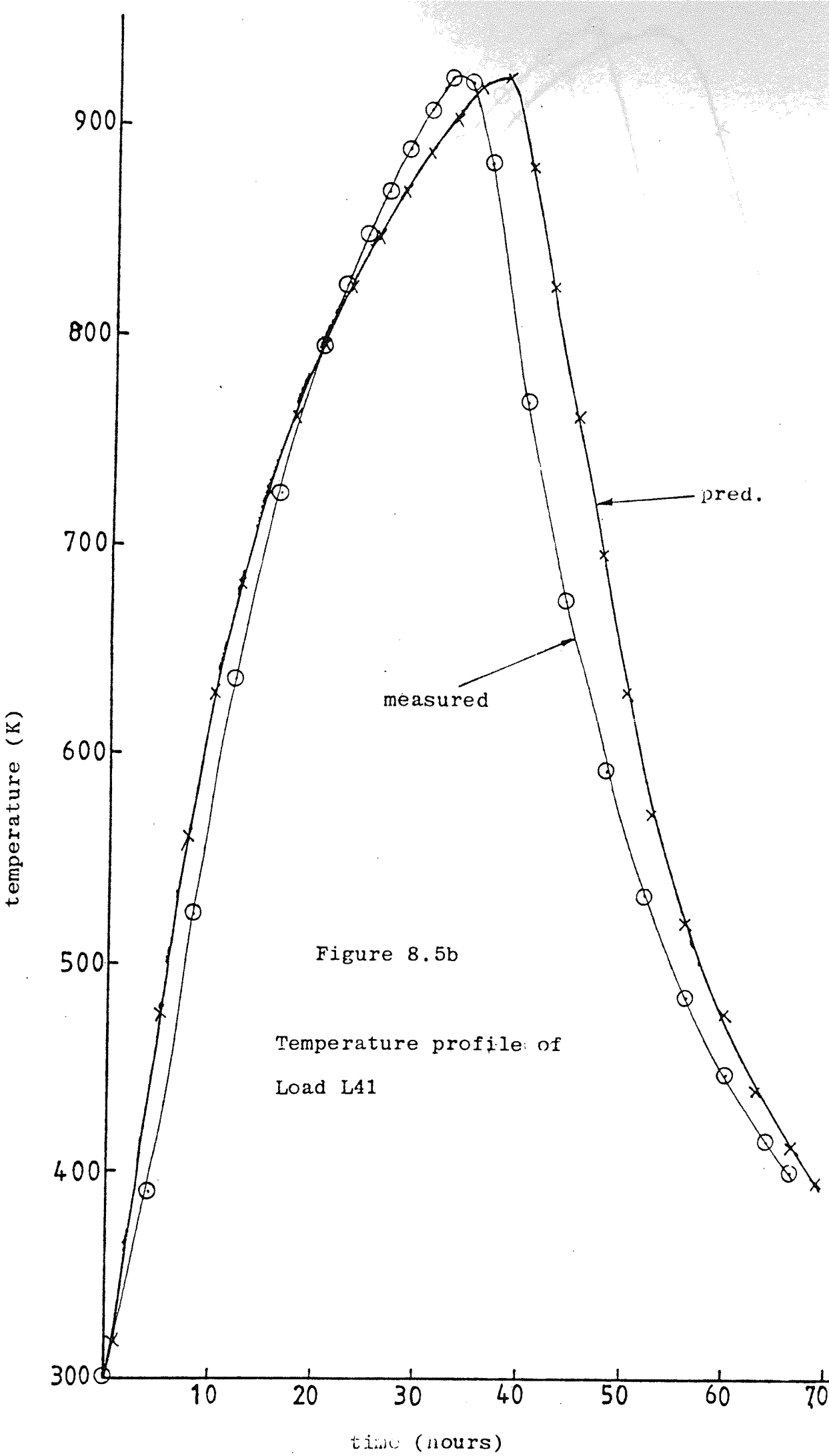

Figure 8.5b

Temperature profile of

Load L41

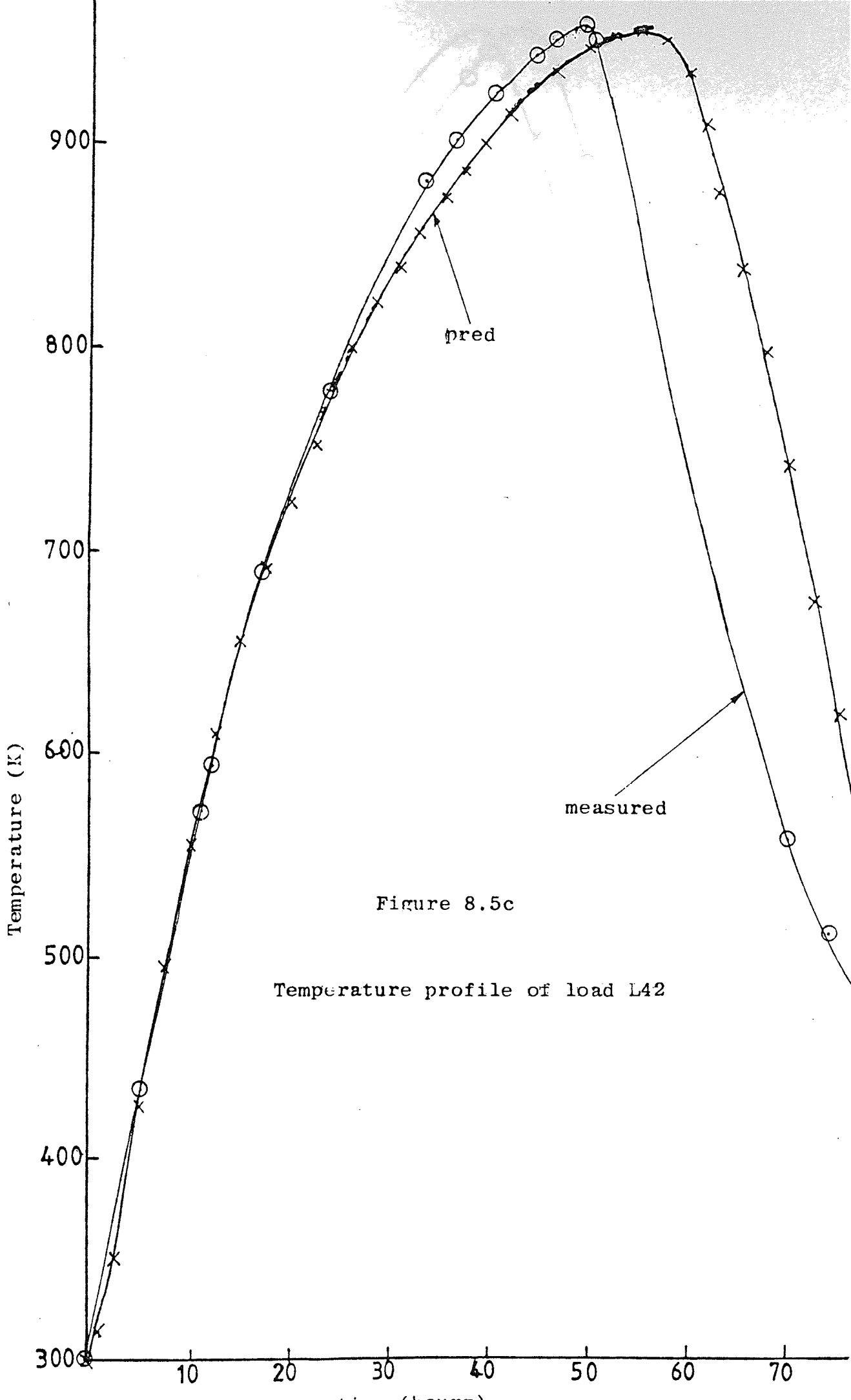

Figure 8.5c

Temperature profile of load L42

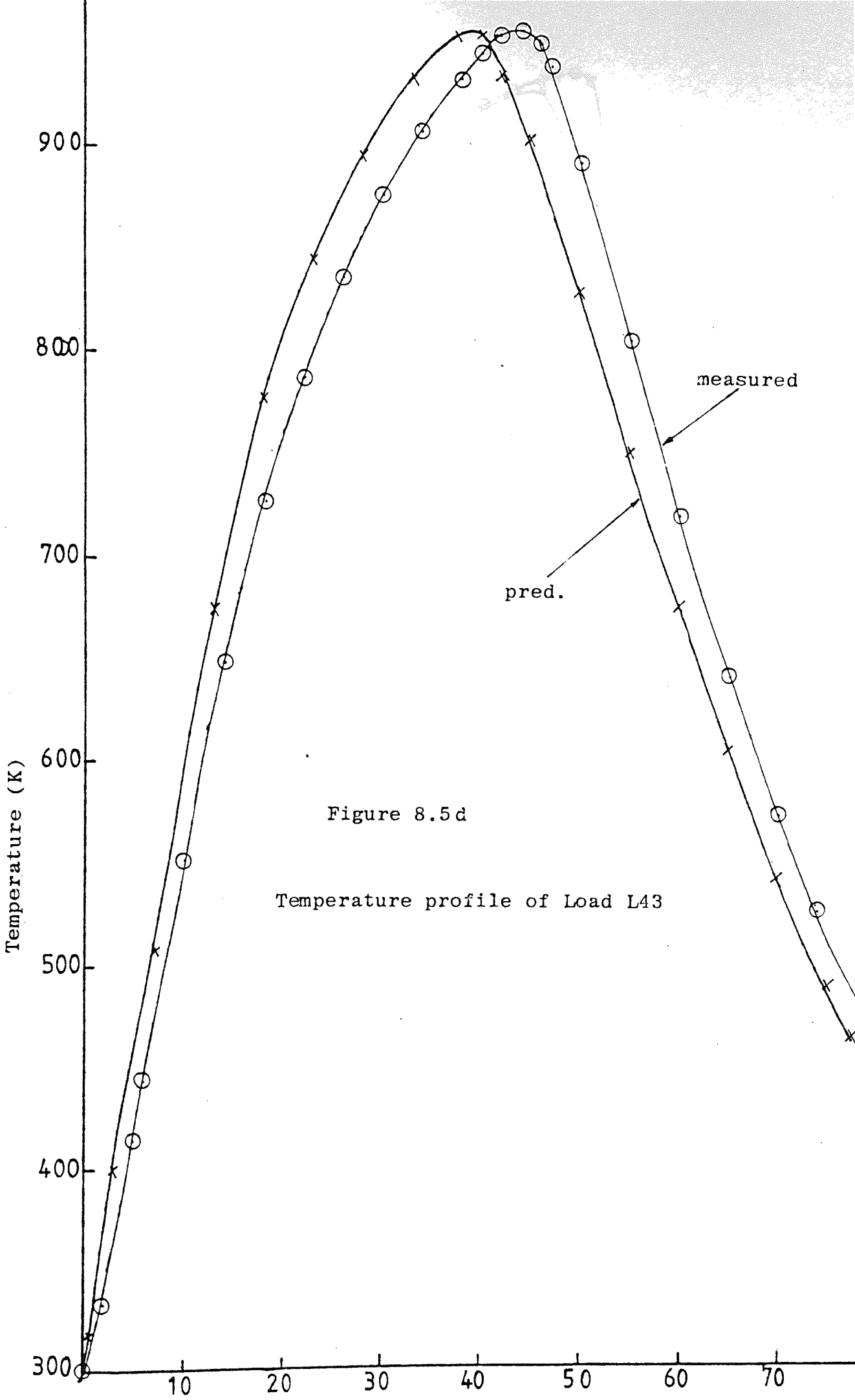

Figure 8.5d

Temperature profile of Load L43

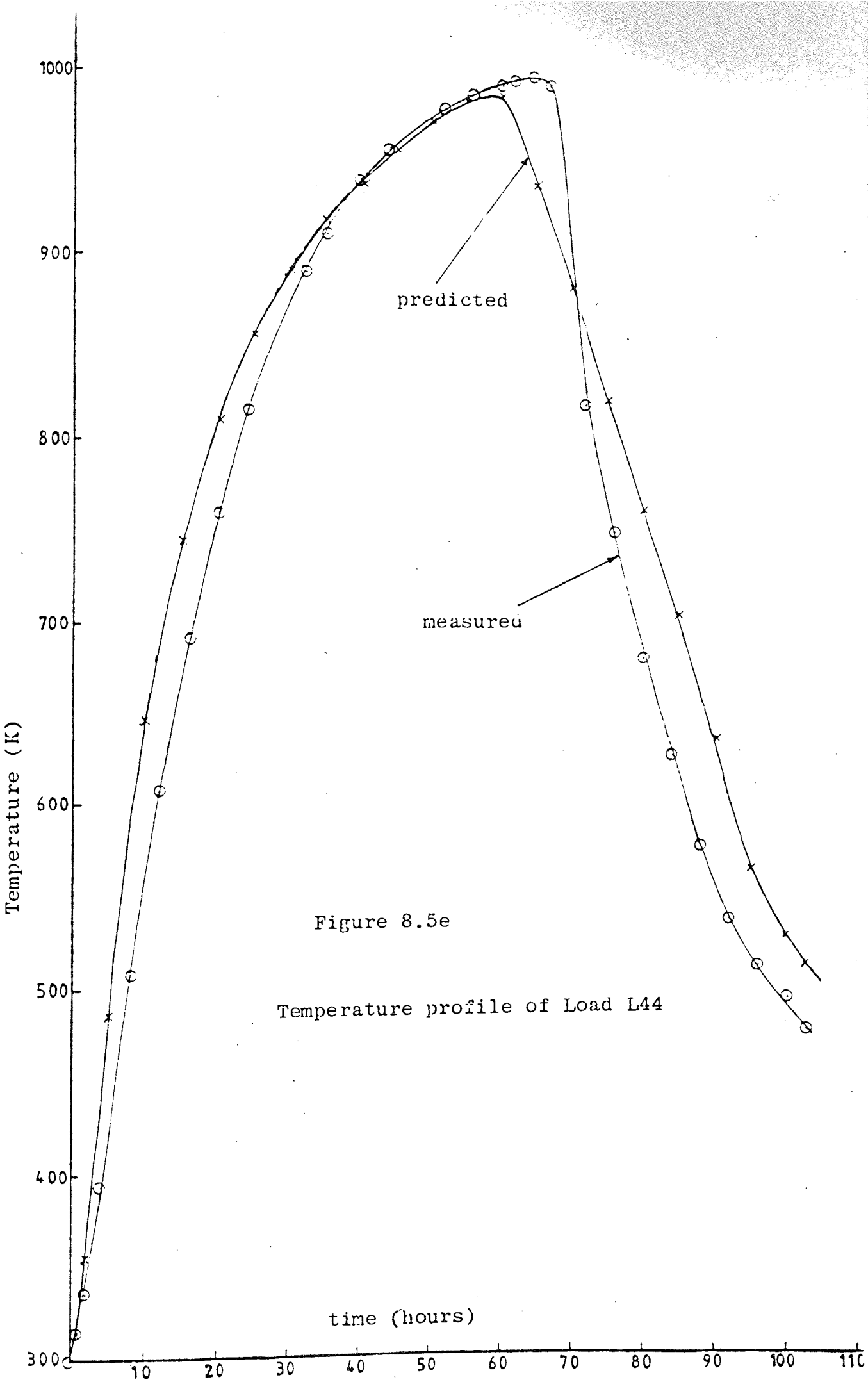

Figure 8.5e

Temperature profile of Load L44

Figure 8.6

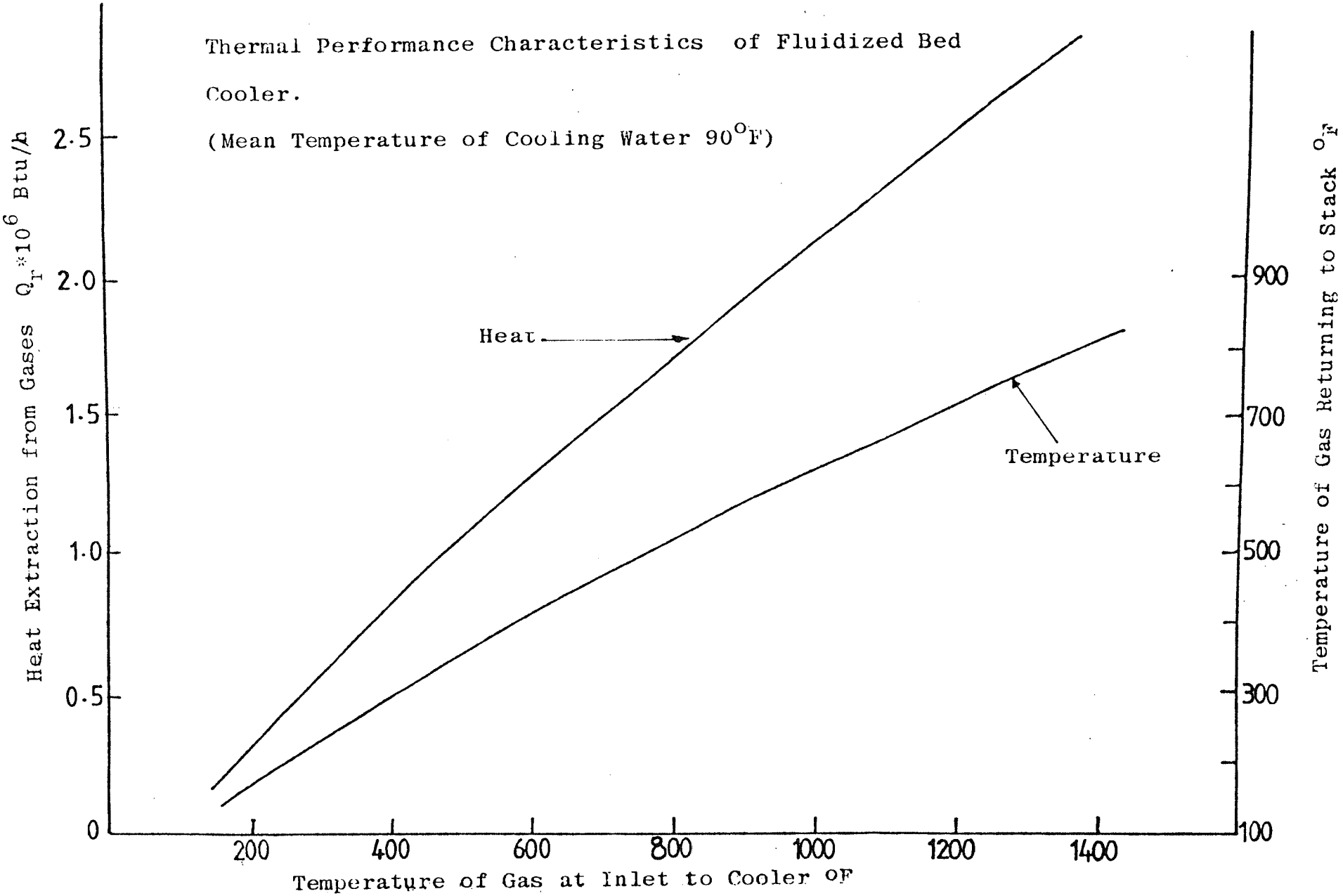
Thermal Performance Characteristics of Fluidized Bed Cooler.
(Mean Temperature of Cooling Water 90°F)
Heat
Temperature
Heat Extraction from Gases Q_T *10^6 Btu/h
Temperature of Gas Returning to Stack °F
Temperature of Gas at Inlet to Cooler °F
0
0.5
1.0
1.5
2.0
2.5
100
300
500
700
900
200
400
600
800
1000
1200
1400

Figure 8.7

Thermal Performance Characteristic of Shell and Tube Cooler

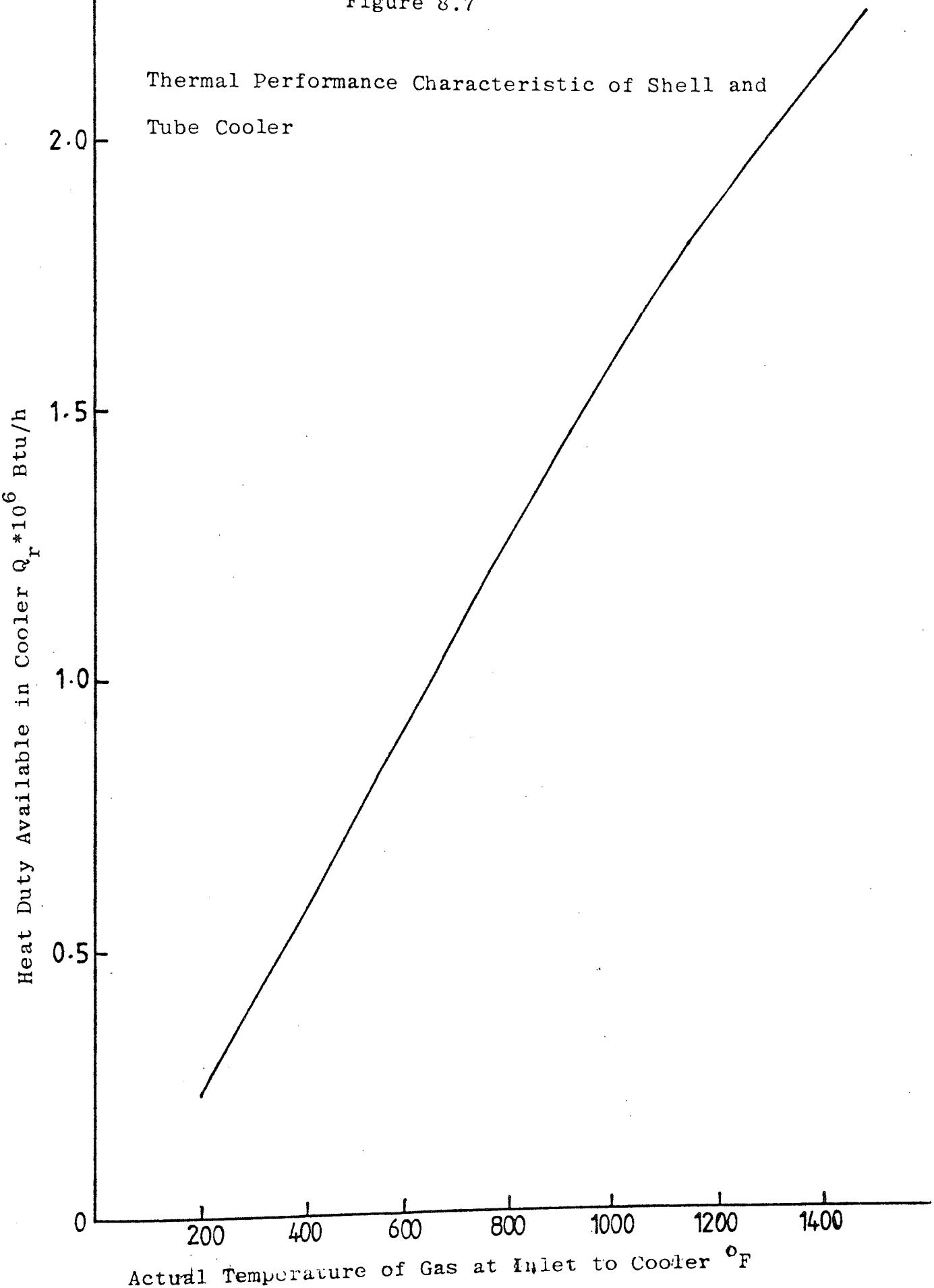

Figure 8.8a

Mean Temperature of the Stack Versus Time

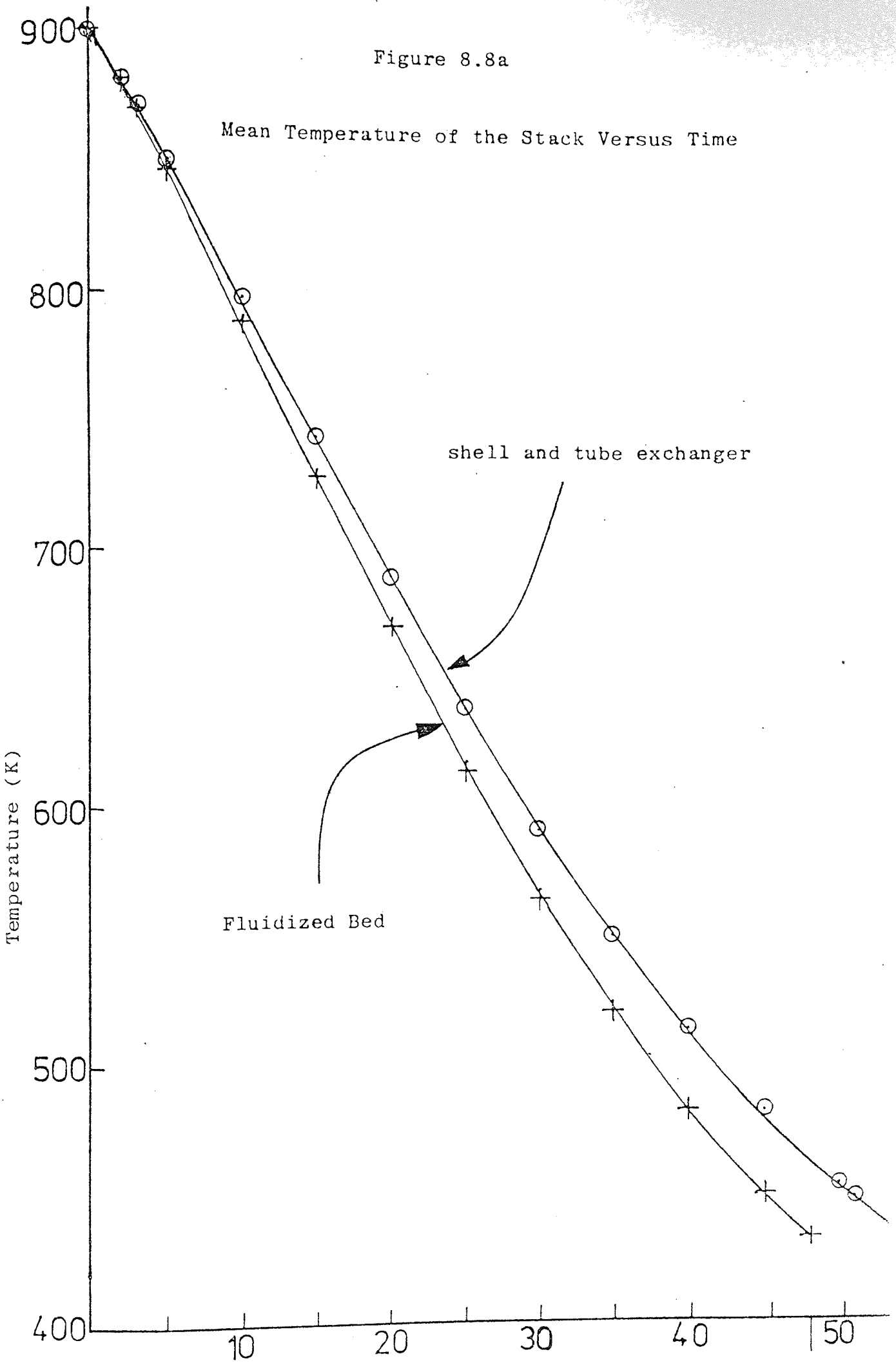

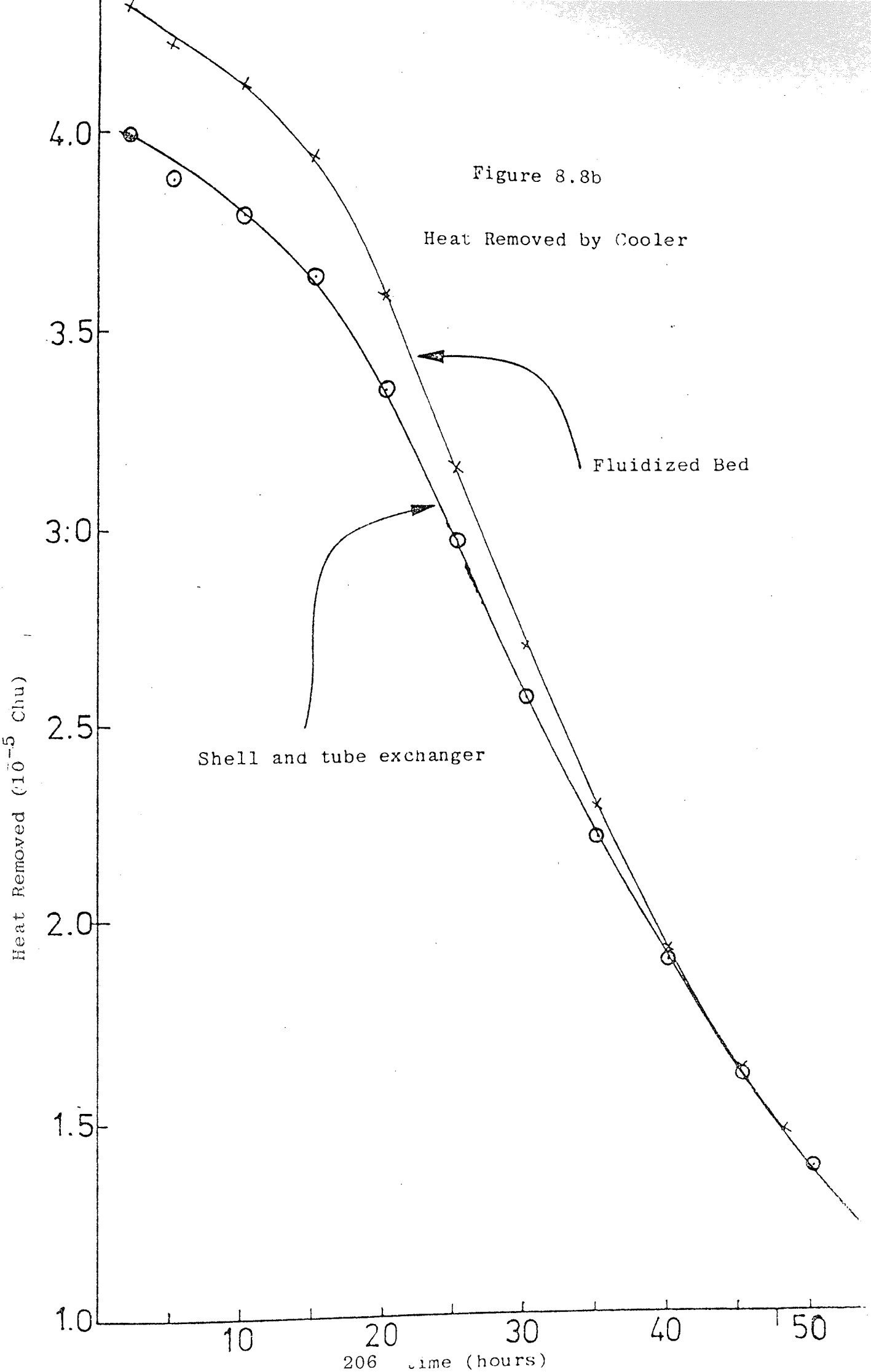
Figure 8.8b
Heat Removed by Cooler
Fluidized Bed
Shell and tube exchanger
Heat Removed (10^{-5} Chu)
4.0
3.5
3.0
2.5
2.0
1.5
1.0
10
20
30
40
50
Time (hours)

Figure 8.8c

The Temperature of Gas Entering the Cooler

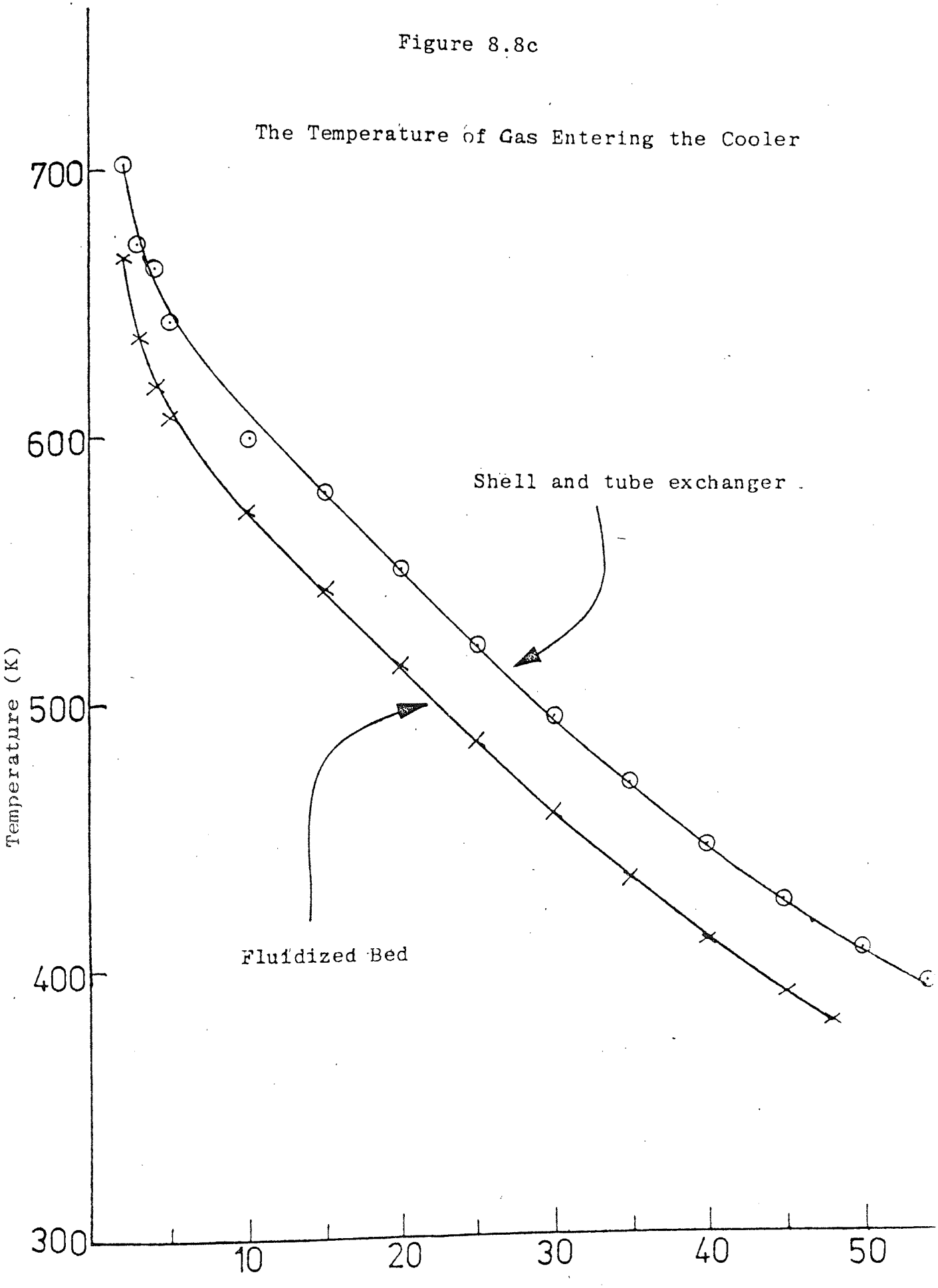

Figure 8.8d

The Temperature Drop in the Cooler

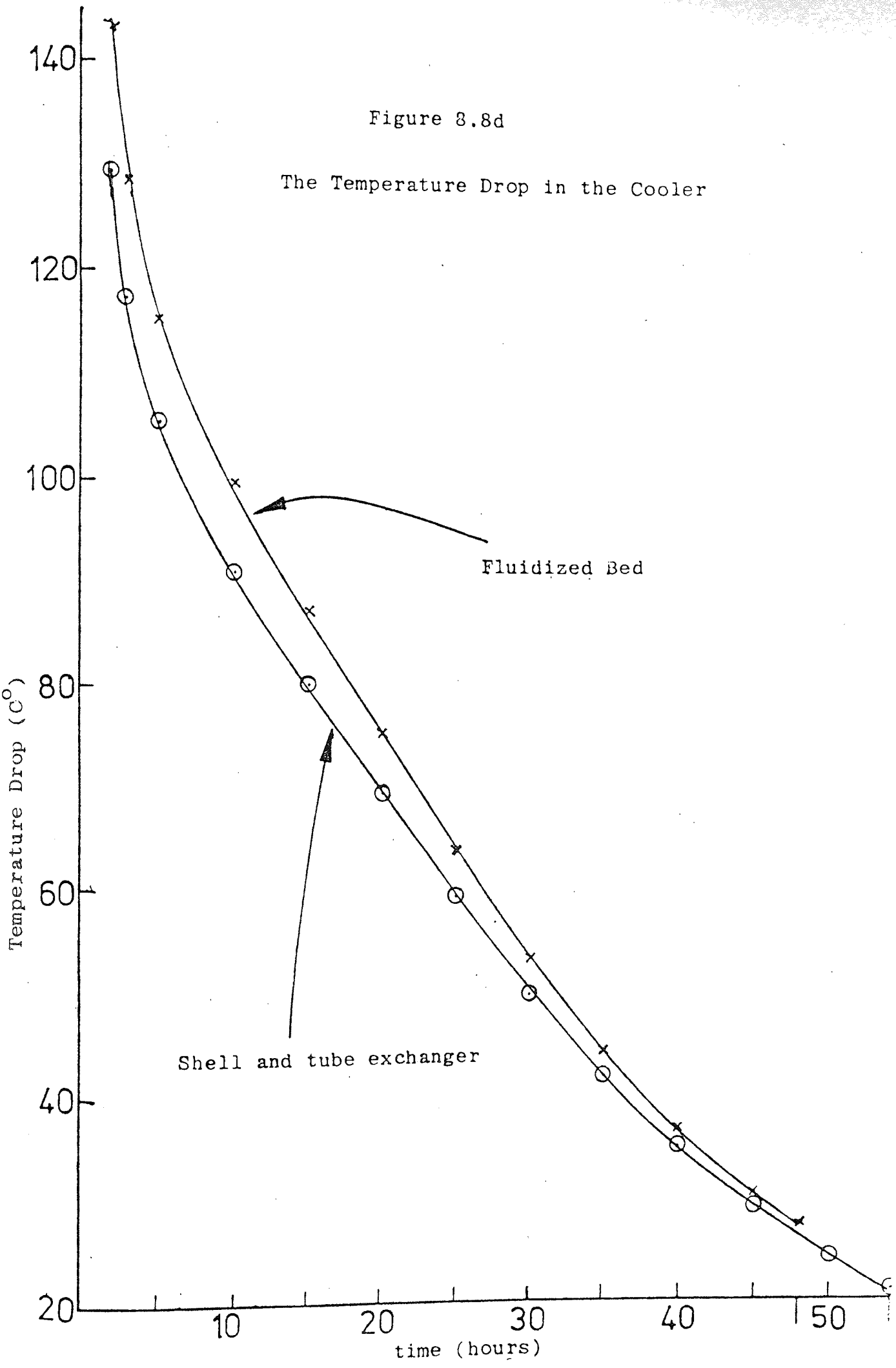

Figure 8.8e

The Temperature of the Cold Gas Leaving the Cooler versus Time

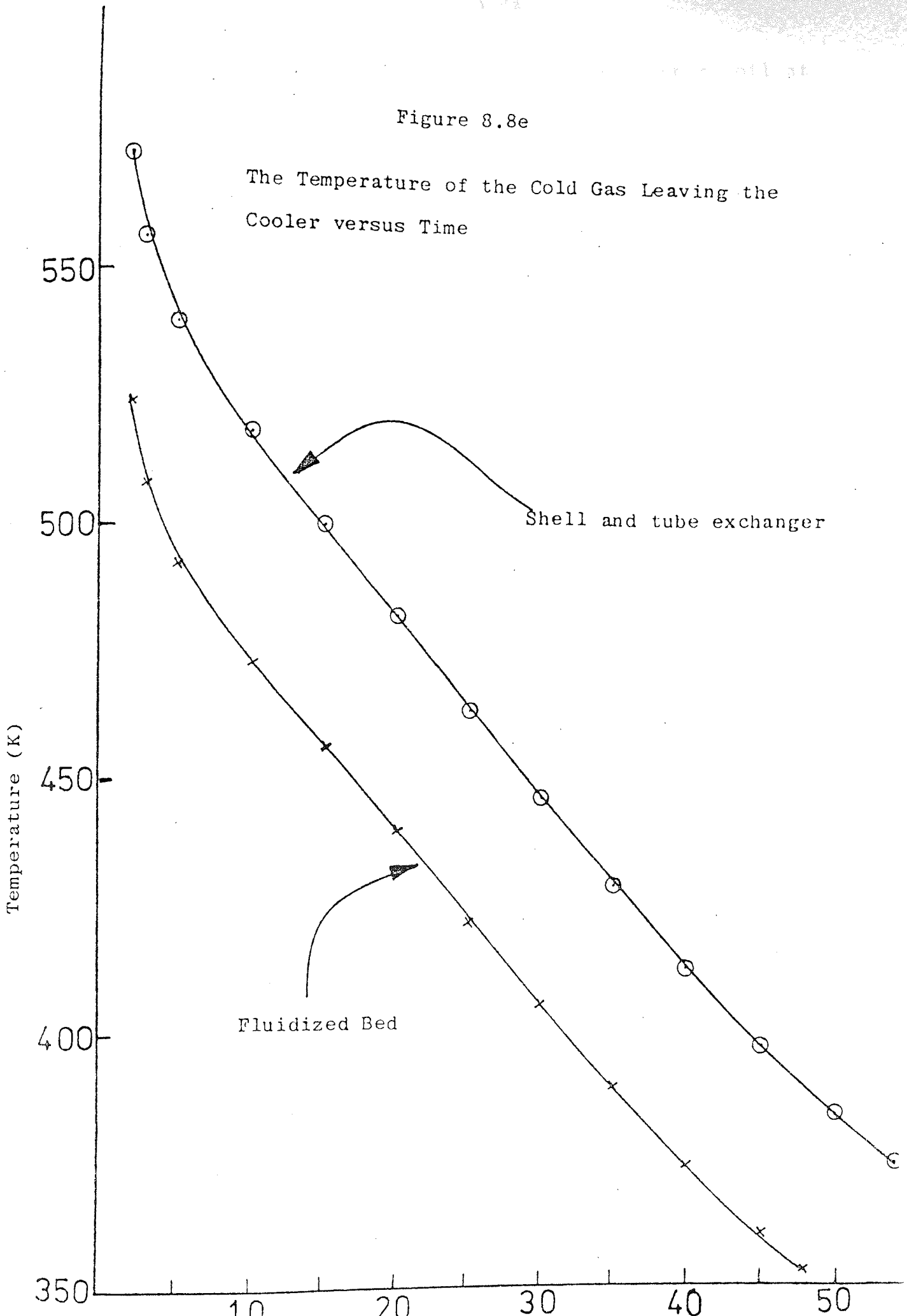

Figure 8.9a

Radial Temperature Profiles in Bottom Coil at Early Cooling Stages

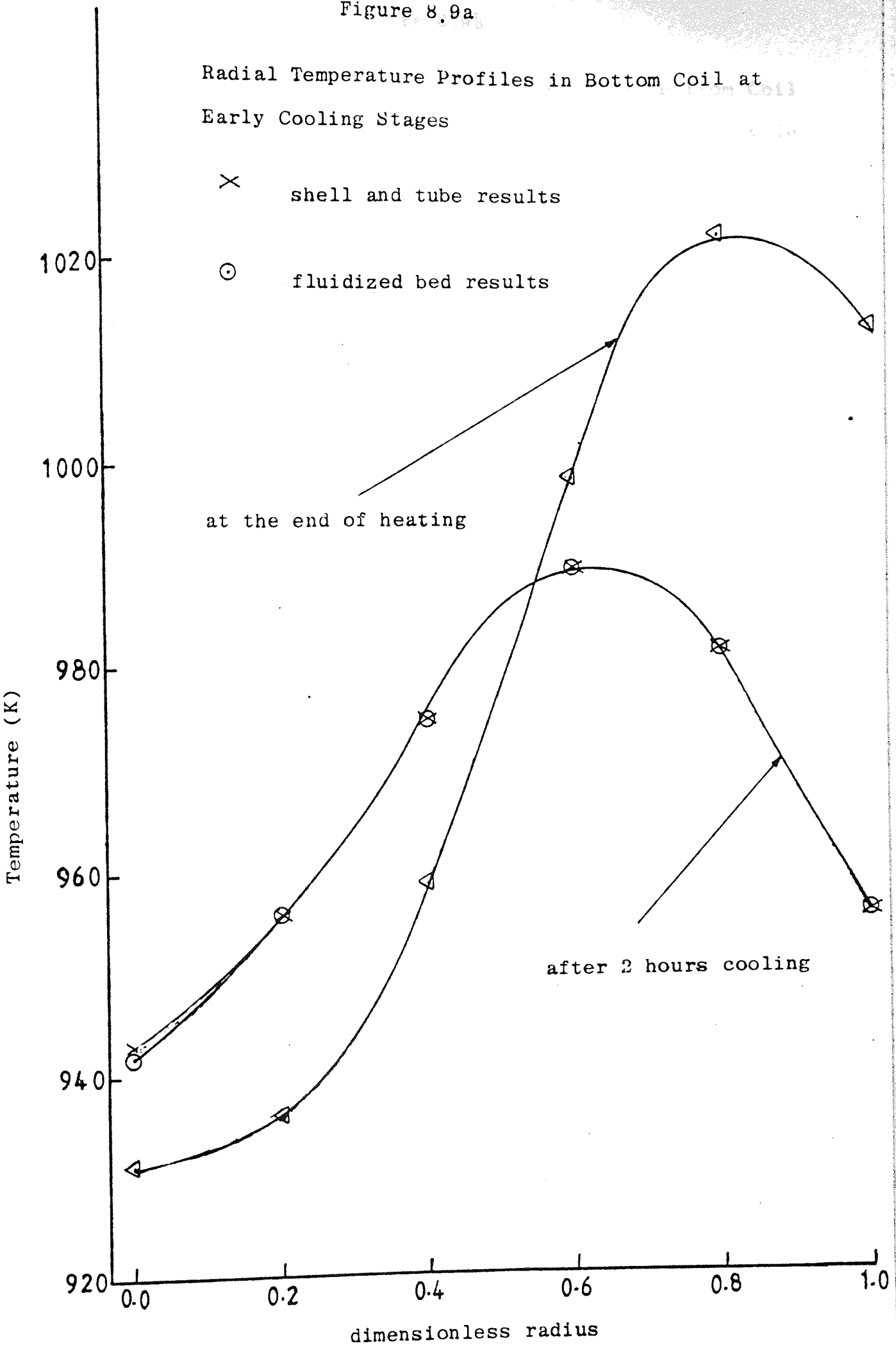

Figure 8.9b

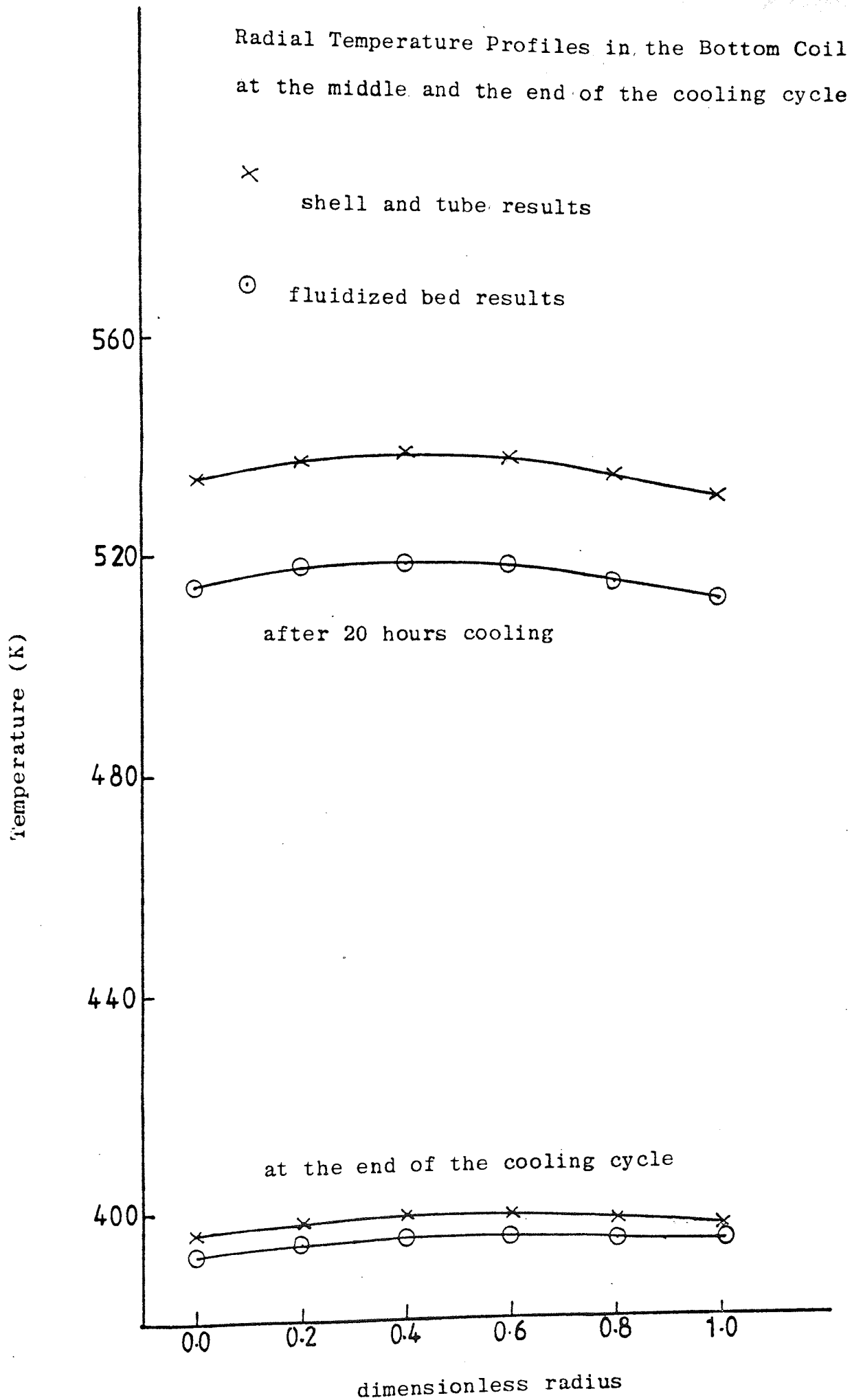
Radial Temperature Profiles in the Bottom Coil
at the middle and the end of the cooling cycle
shell and tube results
fluidized bed results
560
520
480
440
400
Temperature (K)
after 20 hours cooling
at the end of the cooling cycle
0.0
0.2
0.4
0.6
0.8
1.0
dimensionless radius

CHAPTER NINE

CONCLUSIONS AND COMMENTS

CONCLUSIONS AND COMMENTS

9.1 Conclusions

The results of the investigation of the performance of a batch annealing furnace, obtained by using mathematical modelling are presented and discussed in Chapter 8. The general conclusions about the effects of the investigated design factors and operating parameters are as follows:

(a) Location of Limiting Temperature. The results in Chapter 8.2 show that the model represents the process of heat transfer in the furnace fairly well. This model predicted the location of the limiting temperature at the centre of the coil laps with a slight shift towards the hollow core of the coils. The overall limiting temperature in the stack would be the limiting temperature of the top coil.

(b) Coil Opening. The thermal expansion of the steel sheets, forming the coil, may cause the coil laps to open and hence reduce the effective thermal conductivity in the radial direction. This would effectively prolong the annealing cycle by about 30% from that of a situation in which the coils behave like hollow solid cylinders. This effect could be eliminated by increasing the winding tension in the coils and/or heating from within the central core of the stack.

(c) Stacking Arrangement. For any stack of coils, there is an optimal stacking arrangement of coils. It is found that, the largest coil should be placed in the bottom position of the stack. The positions of the remaining coils have less effect on the heating and cooling rates in the furnace. This is because the burner belt is situated around the bottom coil.

(d) Optimal Convective Heat Transfer Rate. Sensitivity studies of the effects of the dimensions of the convector channels indicate that the height of the channel has a significant effect on the rate of convective transfer between the inert gas in the plates and the ends of the coils. The effect of the channel width is not so pronounced. This may be due to the fact that the hydraulic mean diameter approximates to twice the channel height if the width-to-height ratio is comparatively large. An optimal ratio of width-to-height has been predicted as 9.

The rate of convective heat transfer is also dependent on the fan capacity. The investigation of this effect shows that a bigger fan capacity would produce faster heating and cooling rates but would increase the use of fuel. In practice, the optimal fan capacity could be obtained by an optimal balance between the annealing rate and the consumption of fuel.

(e) Recycle of Flue Gas. The recycle of hot flue gases to the firing zone of the furnace has been proven to make the thermal efficiency 'therms per ton of steel' worse. However, the gas recycle would reduce the heating rate expressed in terms of tons of steel per hour. An optimal recycle ratio could be obtained by keeping an optimal balance between heating rate and thermal efficiency.

(f) Cooling. The comparison of a fluidized bed cooler with the conventional shell and tube exchanger showed that the former would produce faster cooling than the latter. However, the fluidized bed is accompanied by practical problems of high pressure drop and possible entrainment of bed particles in the flowing gas. Passing part of the gas, instead of the total flow, through the bed and using a shallow bed may overcome the first problem. For the other problem, the use of a sieve plate at the gas exit from the bed would be a reasonable solution.

9.2 Comments

As mentioned in Chapter 1, mathematical models are only reliable if their validation is confirmed by testing them in practical situations. In this work, industrial measurements have been used to confirm the reliability of the model. Although a fair agreement has been obtained, the conclusions drawn by using this model would need to be confirmed by practical industrial tests.

Implementation of the optimal design factors and better operating conditions, which have been demonstrated by means of the mathematical model, may be constrained in practice. For example, the optimal stacking arrangement is limited by the size of coils available for annealing. Another constraint is the availability of suitable lifting cranes. In the case of the cooler and the fan, the change of the present equipment may cause a space problem in the base. For the optimal channels of convector plates, all the existing plates would need to be scrapped. Stacks containing a mixture of new and old plates could produce unexpected flow distributions. Reversing the direction of flow of the inert gas in the stack would enhance heating from the central core. The furnace and cover would need to be completely redesigned if the furnace is required to be fired axially up a central duct within the hollow core of the stack.

Since the objective of any industrial investment is making profit, the cost factor will control any process development. This work has been confined to technical aspects only and no monetary analysis has been investigated. Nonetheless, the above conclusions are worthy of some investment to test them on existing furnaces.

9.3 Suggestions for Further Work

(a) Although the mathematical model has been verified with some industrial measurements, the optimal design factors and operating parameters have to be tested

experimentally. This would need to be done on a full-scale furnace, by fabricating test convector plates, installing a fluidized bed and a bigger capacity recirculating fan.

(b) Experimental simulation of convective heat transfer in the channels of the plates is another field which could be investigated. The simulation would verify the predicted effects of the channel dimensions and could be used to investigate the optimal shape of the channel.

(c) The mathematical model of effective thermal conductivity in the radial direction of the coil could be further developed to include a relationship between the coil opening and the residual tension in the coil. From such a relationship, the initial tension required to prevent the laps separating during heating could be predicted.

A P P E N D I C E S

A Correlations of physical properties of steel with temperature

B Correlations of physical and transport properties of inert gas with temperature

C The flowsheets of the Computer Program for the Annealing Furnace

D The listing of the Computer Program for the Annealing Furnace

APPENDIX A.1

Composition of Steel

The composition of the steel used in this work is given in table 248 by Spiers[24] "Technical Data on Fuel", 1961. This composition is as follows:

Iron	98.96%
Carbon	0.23%
Silicon	0.11%
Manganese	0.63%
Nickel	0.07%

Tabulated data on the physical properties of steel and gases at different temperatures were obtained from the literature. From these data, the physical properties were correlated as polynomials of absolute temperature by using the least square technique.

APPENDIX A.2

Thermal Conductivity of Steel

The data on the thermal conductivity of steel K_s was taken from Spiers[24], table 252 as the following:

Temp K	Reported Cond. K_s $\frac{cal}{cmsK}$	Reported Cond. K_s*10^2 $\frac{kW}{mK}$	Correlated Cond. K_s*10^2 $\frac{kW}{mK}$	
273	0.124	5.192	5.188	plot 1
373	0.122	5.108	5.117	
473	0.117	4.899	4.893	
573	0.110	4.605	4.594	
673	0.101	4.271	4.268	
773	0.094	3.936	3.931	
873	0.085	3.559	3.572	
973	0.076	3.182	3.150	
1073	0.062	2.596	2.592	
1173	0.063	2.638	2.642	plot 2
1273	0.066	2.763	2.751	
1373	0.068	2.847	2.860	
1473	0.071	2.973	2.969	

Plot 1 represents the following polynomical

$$K_2*100 = 3.836 + 11.52*(\frac{T}{1000}) - 0.314*(\frac{T}{1000})^2 + 0.301*(\frac{T}{1000})^3 - 0.11*(\frac{T}{1000})^4 \qquad (1)$$

for $T < 1080K$

Plot 2 represents the following straight line equation for $T \geq 1080K$:

$$K_s*100 = 1.365 + 1.089*(\frac{T}{1000})$$

Figure A2

Thermal Conductivity of Steel

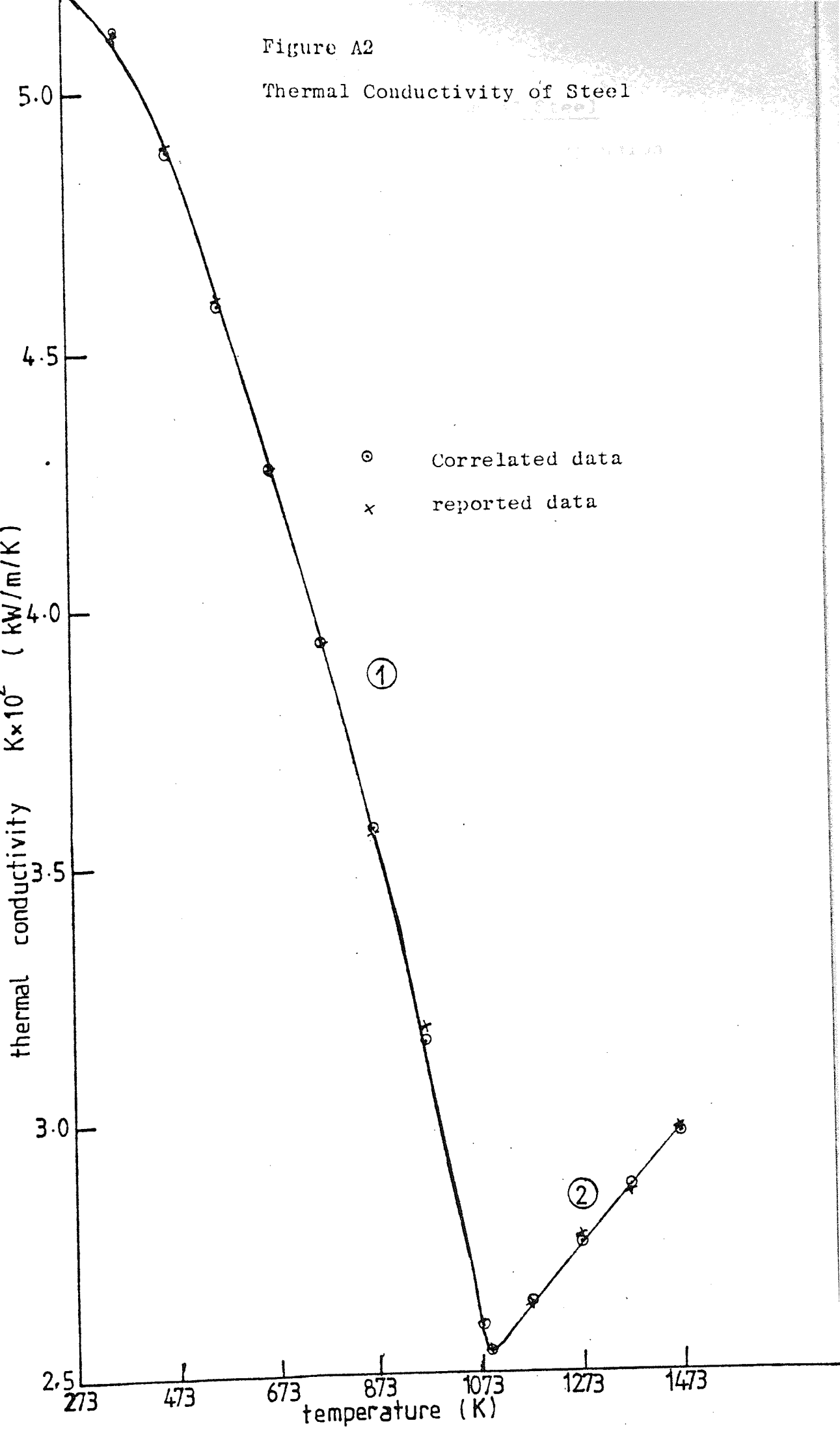

APPENDIX A.3

Coefficient of Linear Thermal Expansion of Steel

Spiers[24] in table (250) gave the linear expansion as follows:

Temp. K Change ΔTC^{o}	Reported Coeff. $\lambda*10^{6}\ {}^{o}C^{-1}$	Correlated Coeff. $\lambda*10^{6}\ K^{-1}$	
100	12.18	12.18	plot 1
200	12.66	12.63	
300	13.08	13.07	
400	13.47	13.51	
500	13.92	13.96	
600	14.41	14.40	
700	14.88	14.88	plot 2
800	12.64	12.65	
900	12.41	12.41	
1000	13.37	13.37	plot 3
1100	14.32	14.32	
1200	15.27	15.27	

These data are correlated by three functions as follows:

For the temperature T < 975K, the following straight line equation represents the coefficient

$$\lambda*10^{6} = 10.52 + 4.443*(\frac{T}{1000}) \qquad (1)$$

The coefficient of linear expansion is given by the following polynomial in the temperature range of

$975K \leq T < 1173K$

$$\lambda*10^6 = 65.41 - 41.41*(\frac{T}{1000}) - 22.22*(\frac{T}{1000})^2$$

$$-10.06*(\frac{T}{1000})^3 + 22.39*(\frac{T}{1000})^4 \qquad (2)$$

and $\lambda*10^6 = 1.234 + 9.53*(\frac{T}{1000})$ (3)

for $T \geq 1173$

Figure A3

Coefficient of themral linear expansion of steel

⊙ correlated data

× reported data

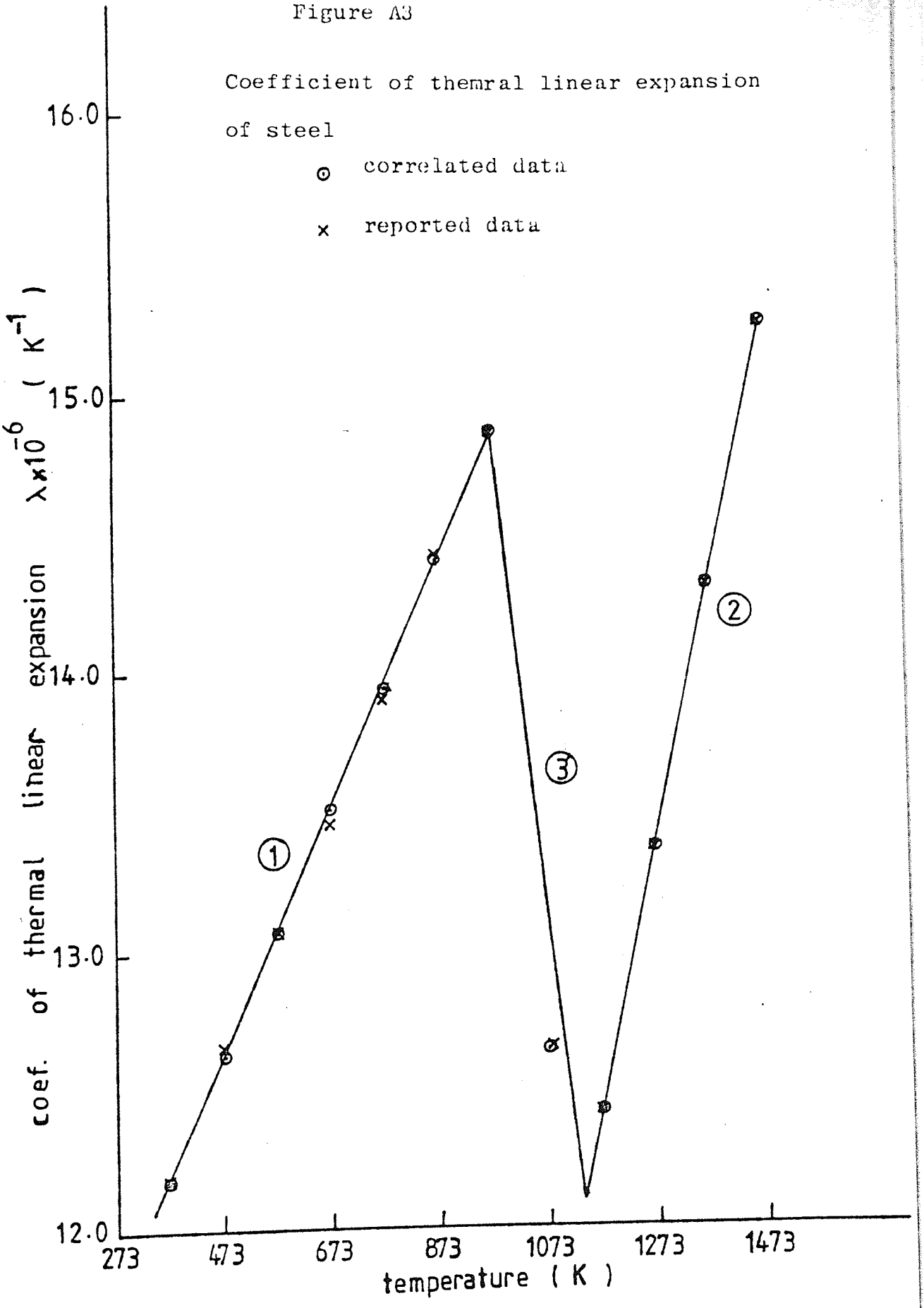

APPENDIX A.4

Volumetric Thermal Capacity of Steel

This is the heat capacity per unit volume calculated as $C = C_p \rho$ where ρ and C_p are the density and specific heat of steel. The density of the steel changes with temperature because of the expansion of steel. Therefore, this density is calculated from the thermal coefficient of linear expansion λ and the temperature change ΔT as follows:

$$\rho = \frac{\rho_o}{(1+\lambda * \Delta T)^3}$$

where ρ_o is the density of steel at 20^oC and $\rho_o = 7873.3\ kg/m^3$.

Temp. K	$\lambda*10^6$ K^{-1}	ρ kg/m^3	C_p*10^4 kWh/kg/K	Reported Cap. C $\frac{kWh}{m^3K}$	Correl. Cap. C $\frac{kWh}{m^3K}$
273	-	7873.5	1.279	1.007	1.012
373	12.18	7844.8	1.312	1.077	1.062
473	12.66	7814.0	1.465	1.145	1.150
573	13.08	7781.5	1.510	1.222	1.238
673	13.47	7747.6	1.710	1.325	1.322
773	13.92	7711.4	1.907	1.471	1.441
873	14.41	7672.8	2.140	1.642	1.669
973	14.88	7632.5	2.191	2.130	2.122
1073	12.64	7639.4	2.605	1.990	1.868
1173	12.41	7615.5	1.849	1.408	1.583
1273	13.37	7566.0	1.814	1.373	1.297
1373	14.37	7511.6	1.826	1.372	1.380
1473	15.27	7456.1	1.812	1.396	1.392

The above data were correlated by three polynomicals as follows:

$$C = 1.857 - 8.141*(\frac{T}{1000}) + 26.64*(\frac{T}{1000})^2 - 34.29*(\frac{T}{1000})^3 + 16.24*(\frac{T}{1000})^4 \quad (1)$$

for $T < 970K$

$$C = 4.929 - 2.853*(\frac{T}{1000}) \quad (2)$$

for $970K \leq T \leq 1250K$

$$C = 1.222 + 0.115*(\frac{T}{1000}) \quad (3)$$

for $T > 1250K$

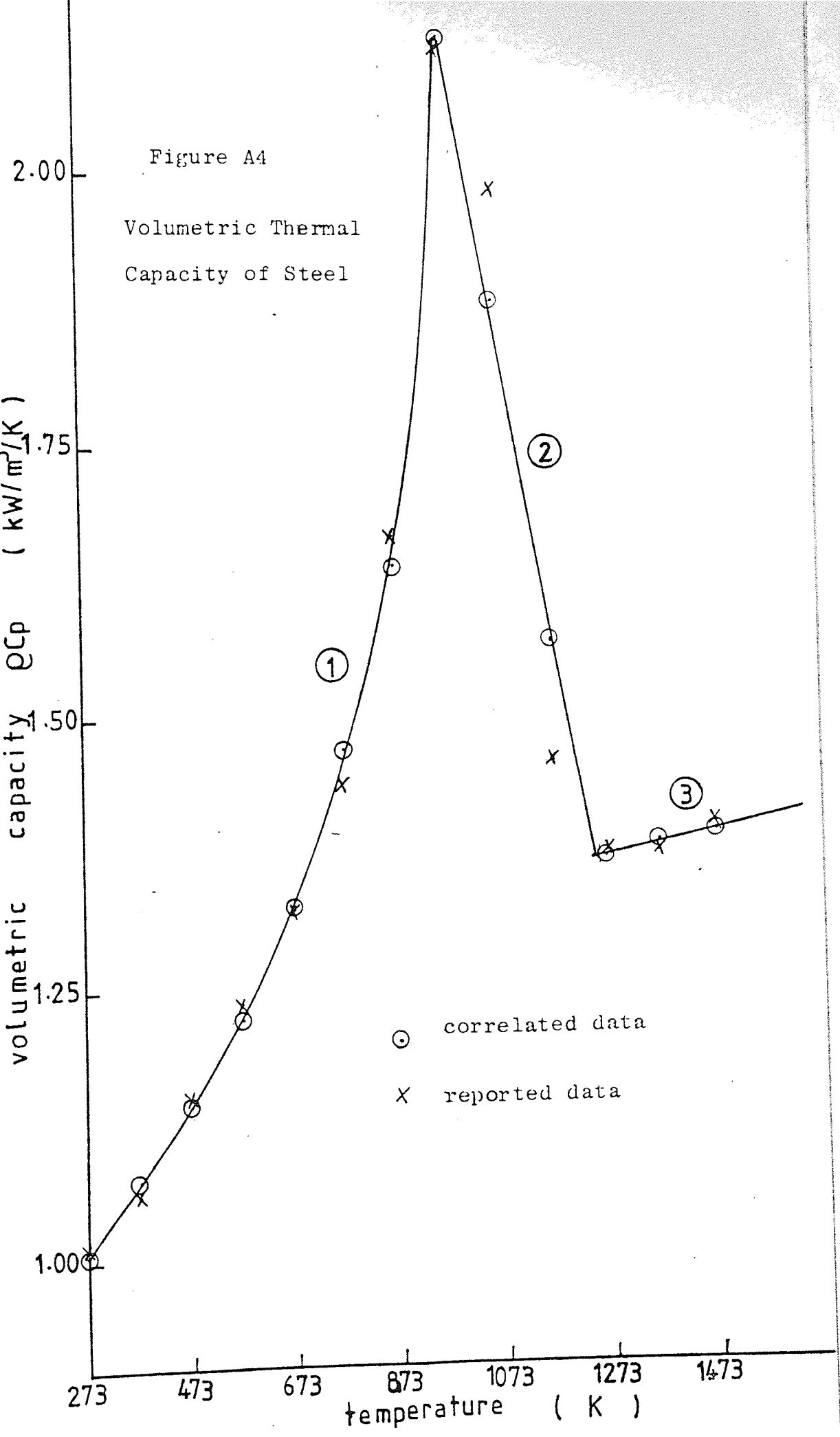

Figure A4

Volumetric Thermal Capacity of Steel

APPENDIX A.5

Volumetric Enthalpy of Steel

This is the enthalpy of a unit volume of steel at temperature T with the enthalpy at 273K as a datum. This is calculated by the integral $H = \int_{273}^{T} C(T)dT$ where C(T) is the volumetric thermal capacity at temperature T given in Appendix (A.4).

Temp. K	Reported Enthalpy H*100kWh/m^3	Correlated Enthalpy H*100kWh/m^3	
273	—	—	
373	126.8	126.0	
473	286.6	263.2	
573	425.3	421.1	plot 1
673	616.8	612.2	
773	862.2	849.9	
873	1158.5	1148.8	
973	1791.6	1783.0	
1073	1860.3	1844.7	plot 2
1173	1376.7	1365.9	
1273	1472.9	1445.6	
[illegible]	[illegible]	1597.9	plot 3
1473	1781.4	1760.1	

The above table was correlated in the following functions of temperature

$$H_v = -385 + 1642*(\frac{T}{1000}) - 1230*(\frac{T}{1000})^2 + 1186*(\frac{T}{1000})^3 + 429*(\frac{T}{1000})^4 \quad \text{where} \quad T \leq 900K \qquad (1)$$

$$H_v = -9021 + 12004*(\frac{T}{1000}) + 1350(\frac{T}{1000})^2 + 3019*(\frac{T}{1000})^3 - 5506*(\frac{T}{1000})^4 \qquad (2)$$

for the temperature range of $900K < T \leq 1237K$.

$$H_v = -493 + 1.523*T \quad \text{for} \quad T > 1273K. \qquad (3)$$

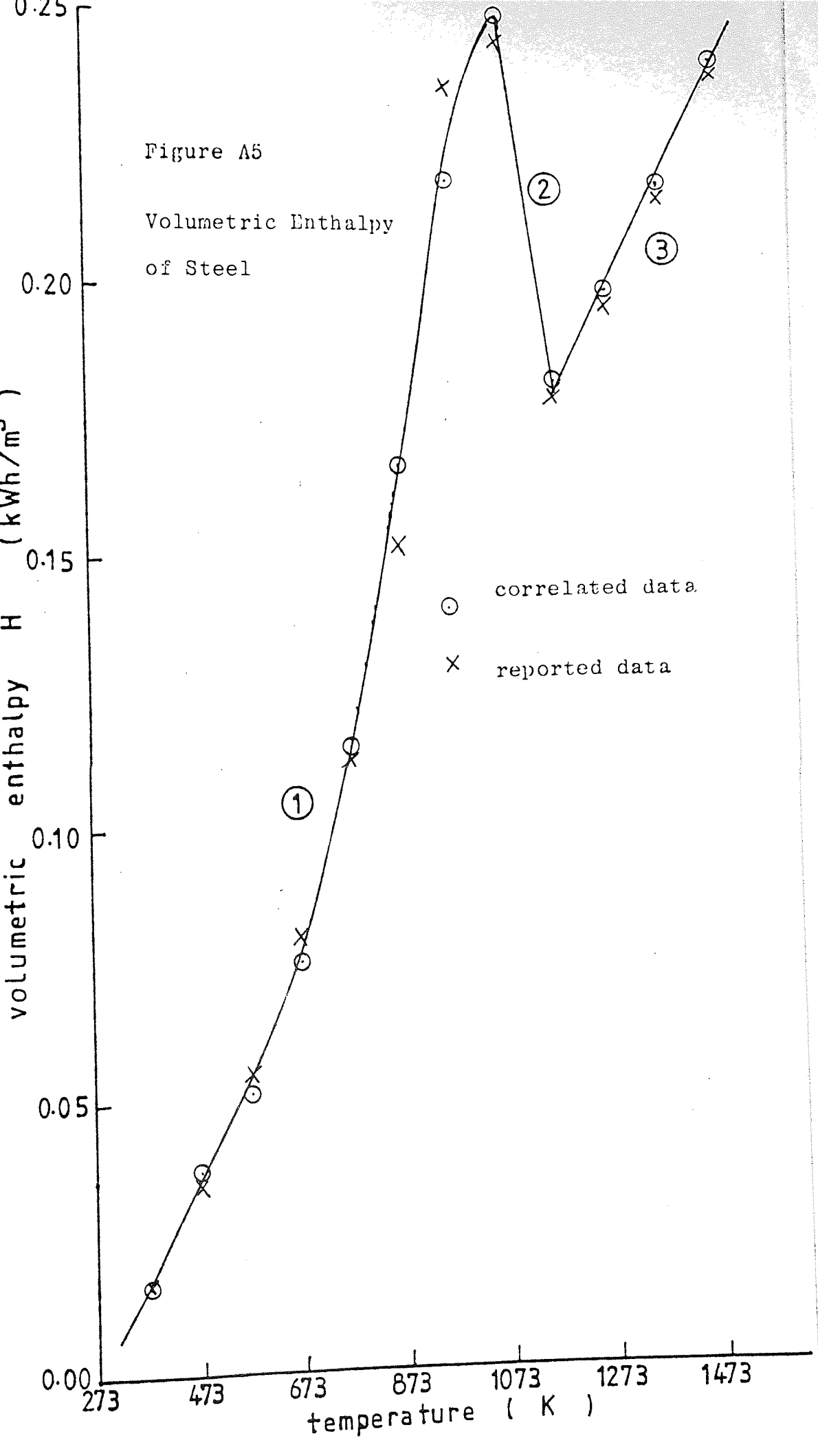

Figure A5

Volumetric Enthalpy of Steel

APPENDIX B.1

Thermal Conductivity of Nitrogen

The following data of thermal conductivity of nitrogen K_g was calculated from the data given in table 3.285 by Perry[30]

Temp. K	Reported Cond. K_g*10^5 (kW/m/K)	Correlated Cond. K_g*10^5 (kW/m/K)
273	2.282	2.369
373	2.918	2.929
473	3.483	3.490
573	4.066	4.051
673	4.647	4.611
773	5.221	5.172
873	5.782	5.732
973	6.348	6.293
1073	6.879	6.854
1173	7.385	7.414
1273	7.879	7.975

The above data was fitted by the following straight line equation:

$$K_g = 8.384*10^{-6} + 5.606*10^{-8}*T$$

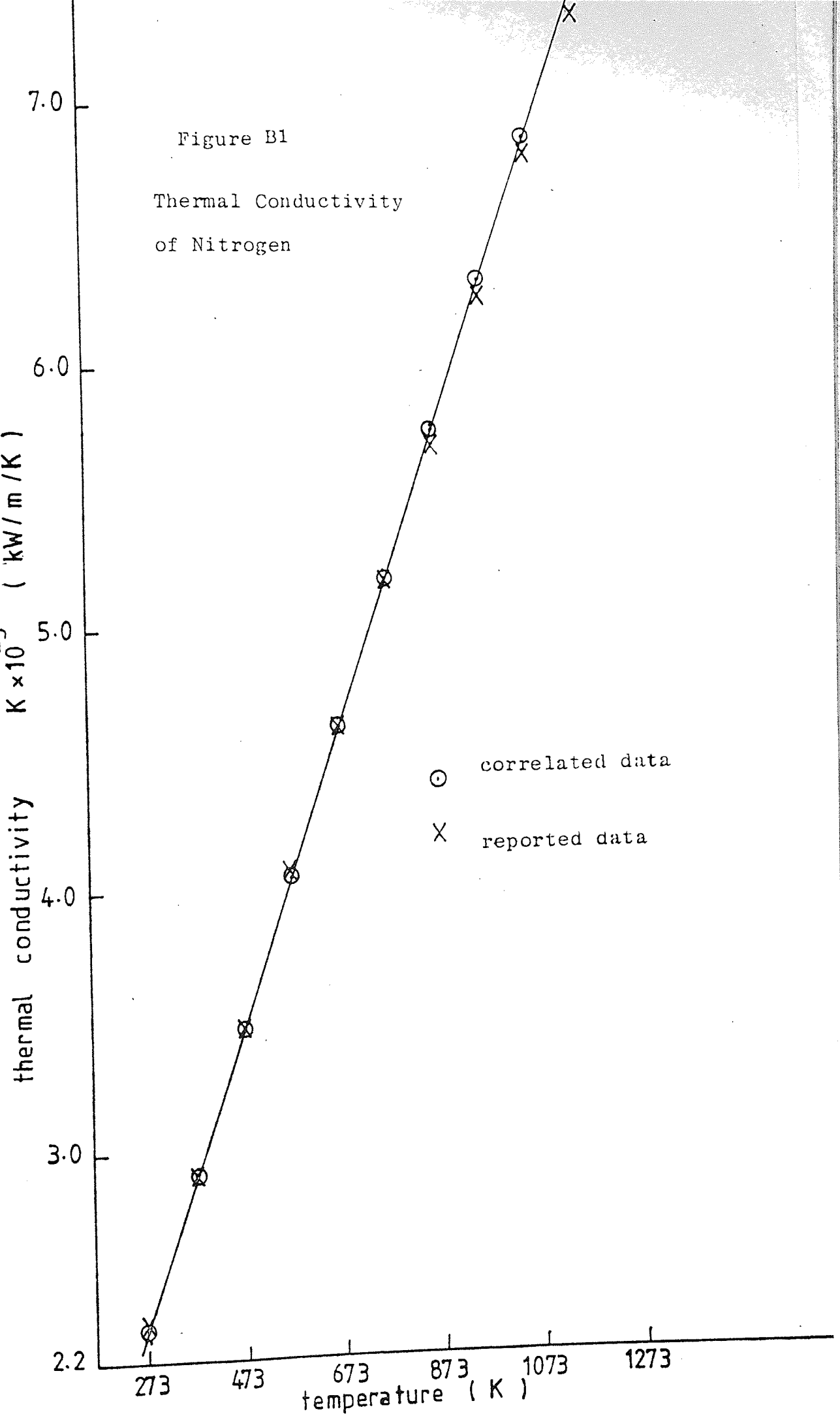

Figure B1

Thermal Conductivity

of Nitrogen

APPENDIX B.2

Specific Heat of Nitrogen

Spiers listed the mean specific heat of gases at constant pressure between $0^{o}C$ and $T^{o}C$ in table 174. The specific heat of nitrogen is tabulated below and converted to kWh/Kg/K.

Temp. K	C_{p_g} kcal/kg/k	Reported $C_{p_g} * 10^4$ kWh/kg/k	Corr. $C_{p_g} * 10^4$ kWh/kg/K
273	0.248	2.884	2.883
373	0.248	2.884	2.885
473	0.249	2.896	2.894
573	0.250	2.908	2.909
673	0.252	2.931	2.929
773	0.254	2.954	2.952
873	0.256	2.977	2.977
973	0.258	3.001	3.004
1073	0.261	3.035	3.034
1173	0.264	3.070	3.064
1273	0.266	3.094	3.095

From above, the specific heat was fitted as follows

$$C_{p_g} = 2.93*10^{-4} - 3.401*10^{-8}*T + 7.223*10^{-11}*T^2 - 3.794*10^{-4}*T^3 + 8.051*10^{-18}*T^4$$

Figure B2

Specific Heat of Nitrogen

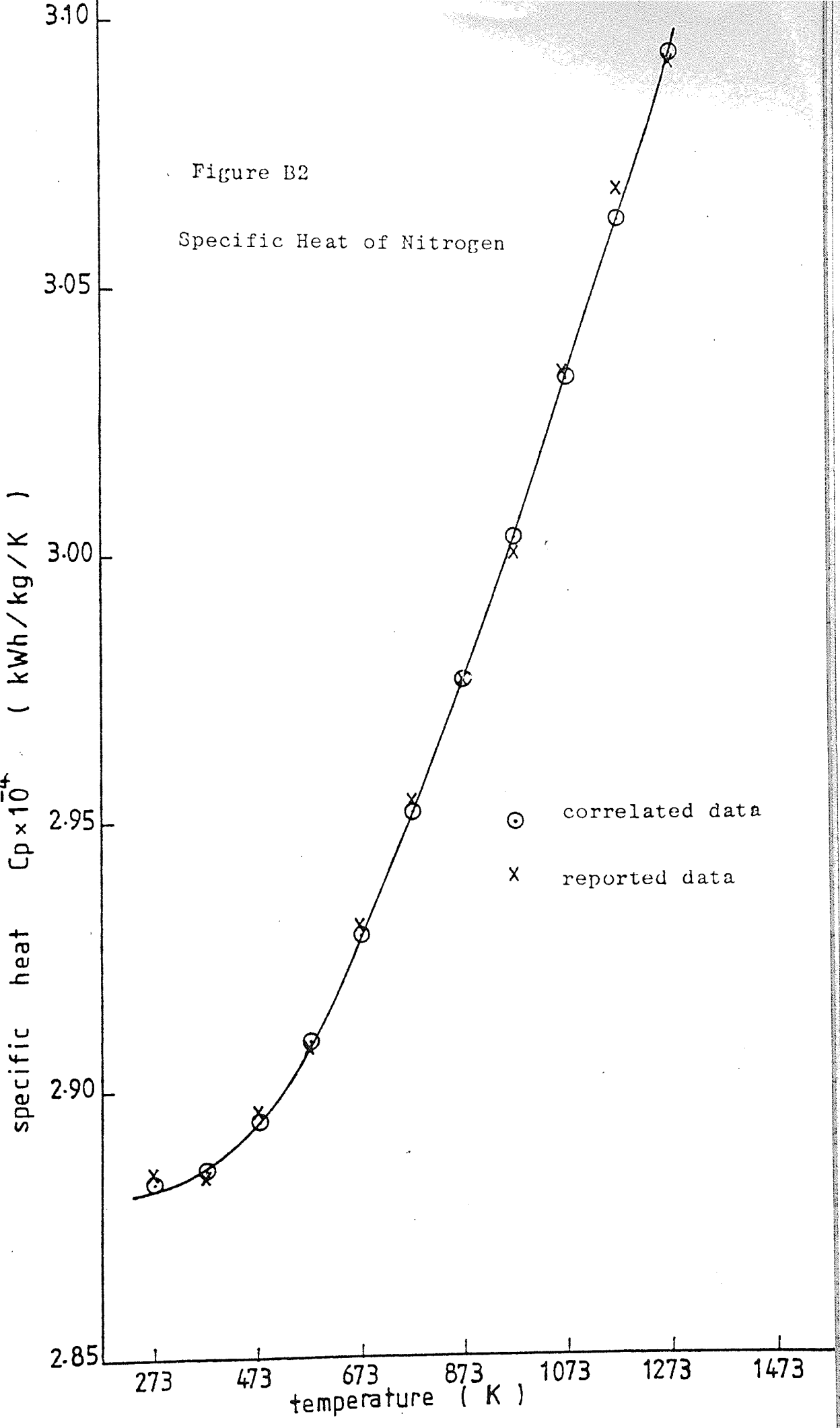

APPENDIX B.3

Thermal Enthalpy of Nitrogen

The enthalpy of gases above $0^{o}C$ is listed against temperature by Spiers in table 176. The enthalpy of nitrogen is shown below.

Temp. K	H_g kCal/kg	Reported Enth. H_g kWh/kg	Corr. Enth. H_g kWh/kg
273	—	—	—
373	24.8	0.0288	0.0253
473	49.8	0.0582	0.0571
573	75.0	0.0879	0.0889
673	100.7	0.1185	0.1207
773	127.0	0.1496	0.1526
873	153.6	0.1812	0.1844
973	180.8	0.2133	0.2162
1073	208.9	0.2469	0.2480
1173	237.2	0.2814	0.2798
1273	266.1	0.3151	0.3117

This enthalpy was expressed by a straight line equation

$$H_g = -9.34*10^{-2} + 3.182*10^{-4}*T$$

Figure B3

Thermal Enthalpy of Nitrogen

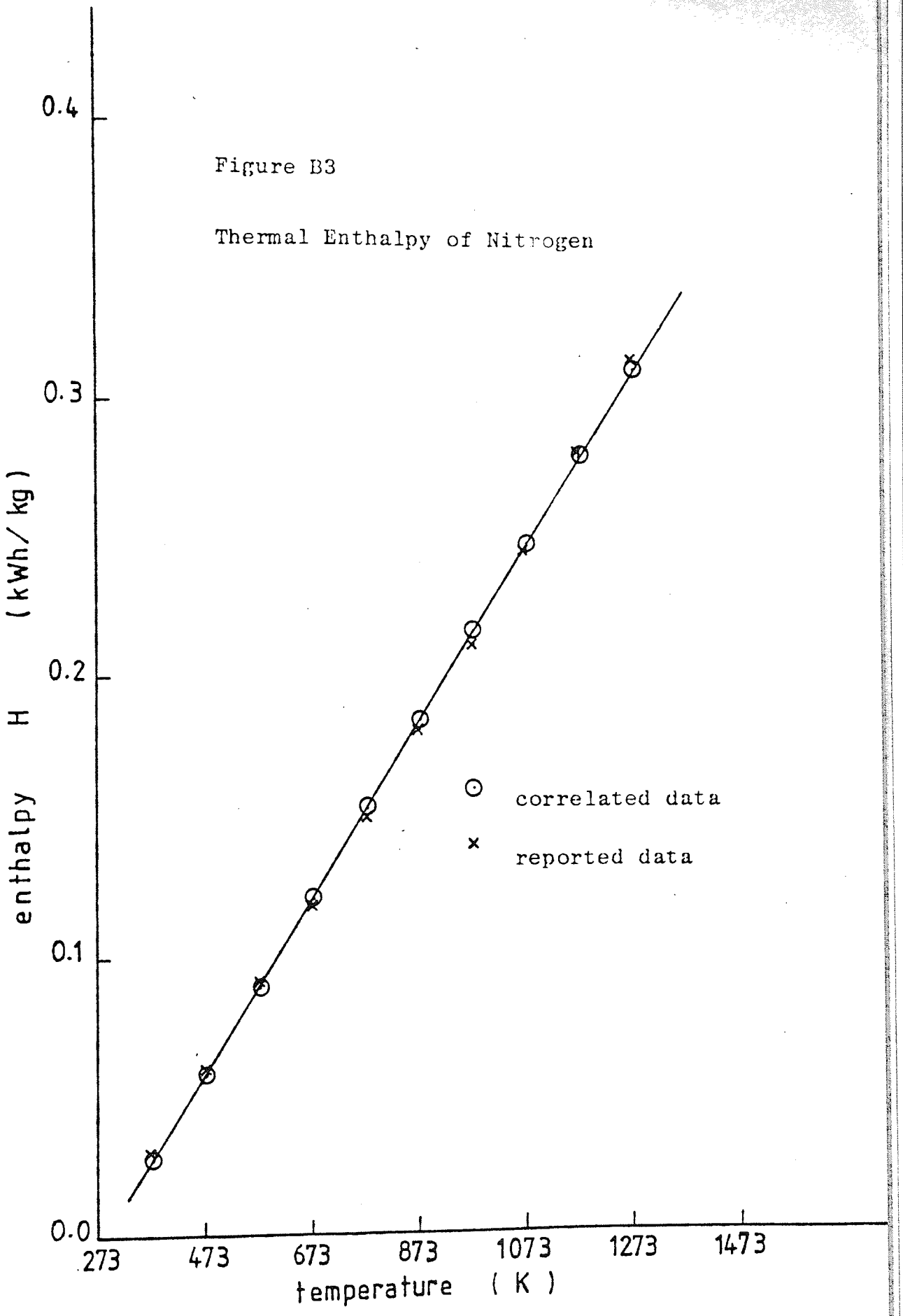

APPENDIX B.4

Functions of Physical Properties of Nitrogen

The thermal conductivity and the specific heat of nitrogen are shown in Appendices B.1 and B.2. The dynamic viscosity of nitrogen is taken from table 148 by Spiers' 'Technical Data on Fuel'. These properties are tabulated as follows:

APPENDIX B.4

Functions of Physical Properties of Nitrogen

Temp. K	$\mu_g * 10^6$ g/cm/s	$\mu_g * 10^2$ kg/m/h	$FY*10^4 = C_{p_g}^{.4} K_g^{.6} / \mu_g^{.4}$		$FA*10^4 = C_{p_g}^{1/3} K_g^{2/3} \mu_g^{1/3}$	
			Reported	Correlated	Reported	Correlated
273	166	5.98	1.942	1.944	1.359	1.357
373	209	7.52	2.054	2.047	1.484	1.474
473	247	8.89	2.140	2.143	1.581	1.581
573	282	10.15	2.230	2.234	1.679	1.680
673	313	11.27	2.325	2.324	1.778	1.774
773	342	12.31	2.414	2.412	1.870	1.865
873	368	13.25	2.500	2.498	1.958	1.954
973	393	14.15	2.583	2.581	2.045	2.040
1073	417	15.01	2.660	2.660	2.123	2.122
1173	440	15.84	2.729	2.731	2.195	2.195
1273	461	16.60	2.793	2.790	2.262	2.258

The first term FY was correlated as follows:

$$FY*10^4 = 1.595 + 1.55*(T/1000) - 1.276*(T/1000)^2 + 1.133*(T/1000)^3 - 0.399*(T/1000)^4$$

The second term FA was fitted by the following polynomial

$$FA*10^4 = 0.941 + 1.895*(T/1000) - 1.692*(T/1000)^2 + 1.36*(T/1000)^3 - 0.441*(T/1000)^4$$

Figure B4

Functions of Physical Properties of Nitrogen

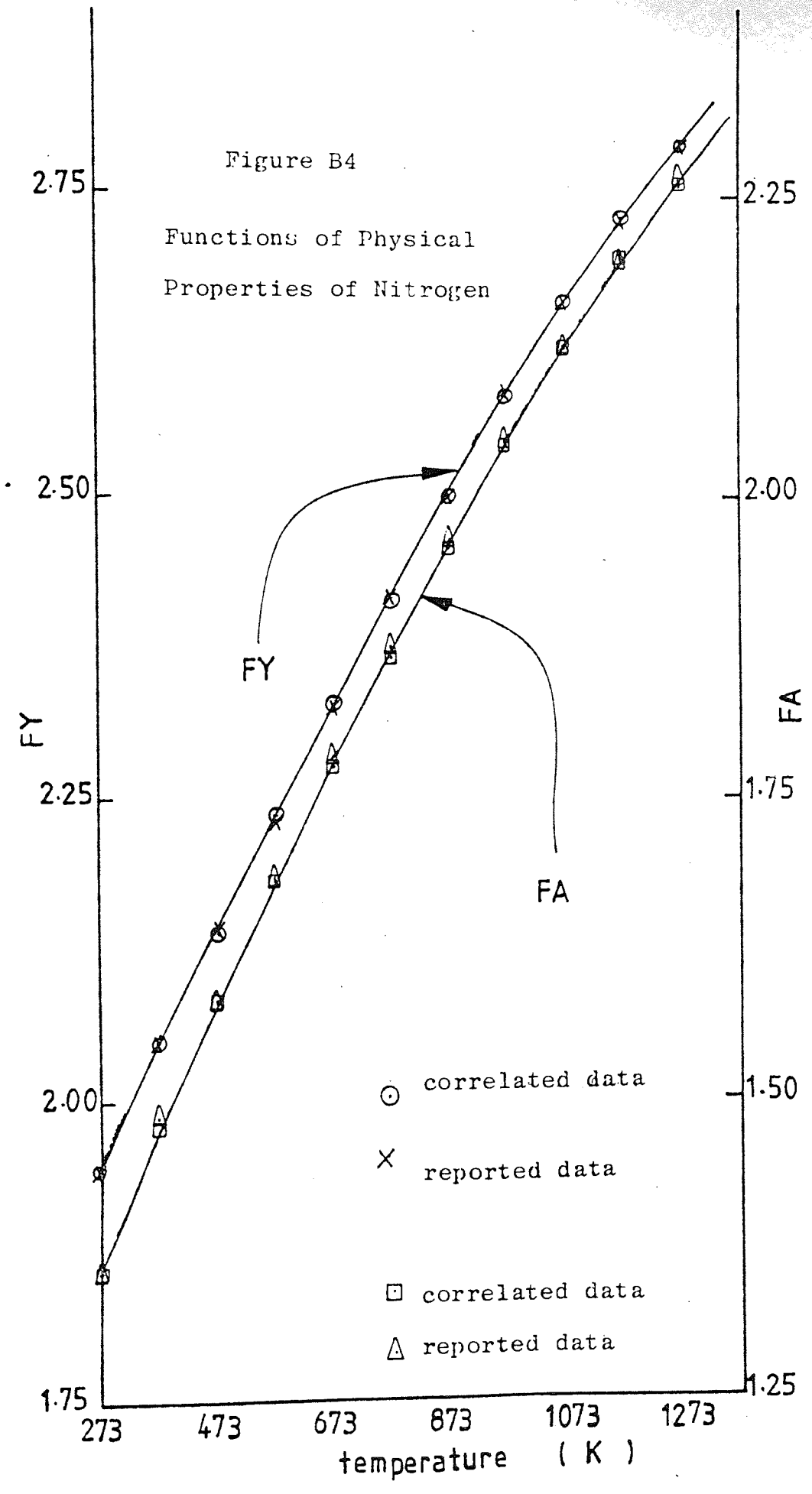

APPENDIX C

The Flow Sheets of the Computer Program for Calculating Transient Heat Transfer in the Annealing Furnace.

Main Program

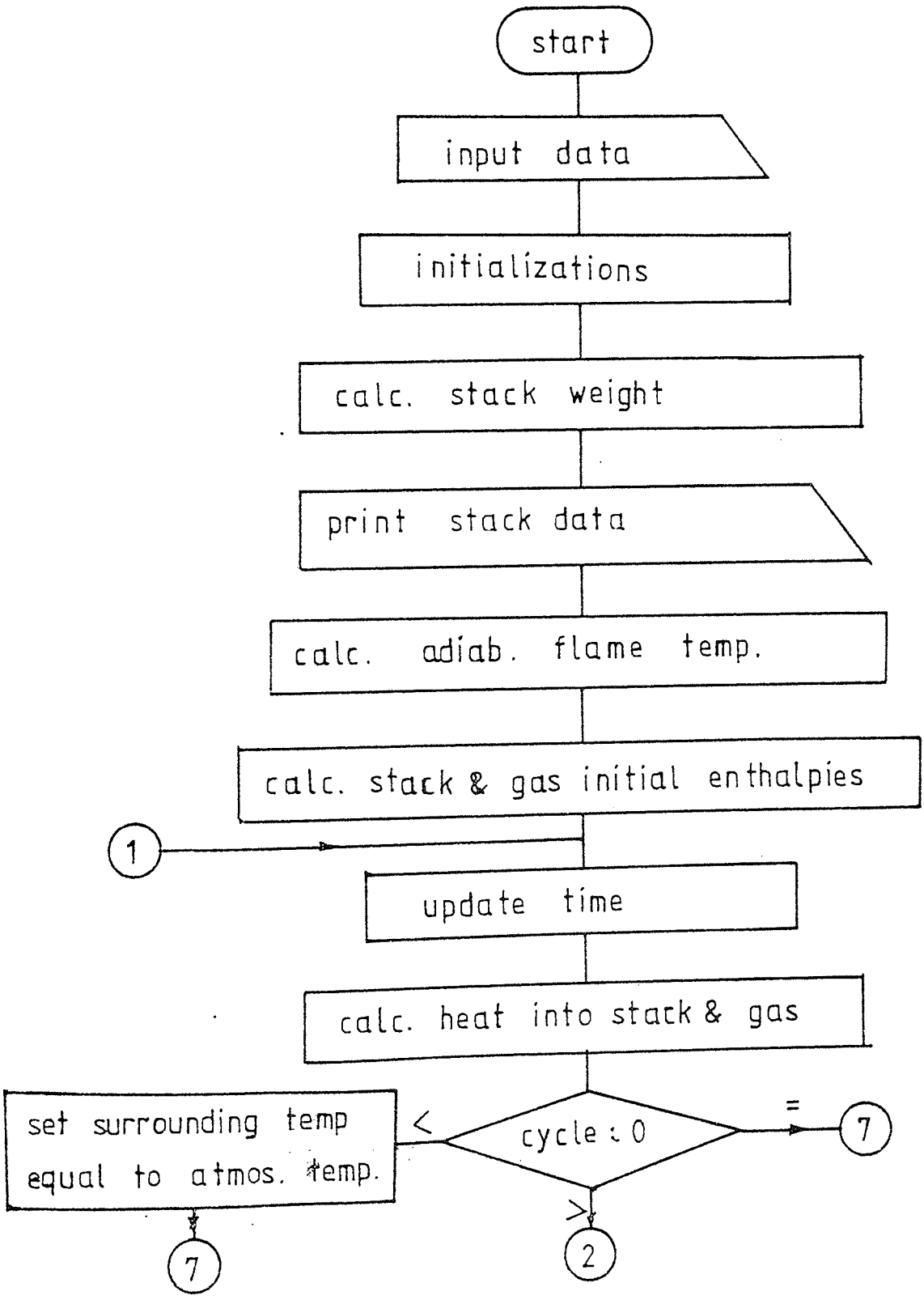

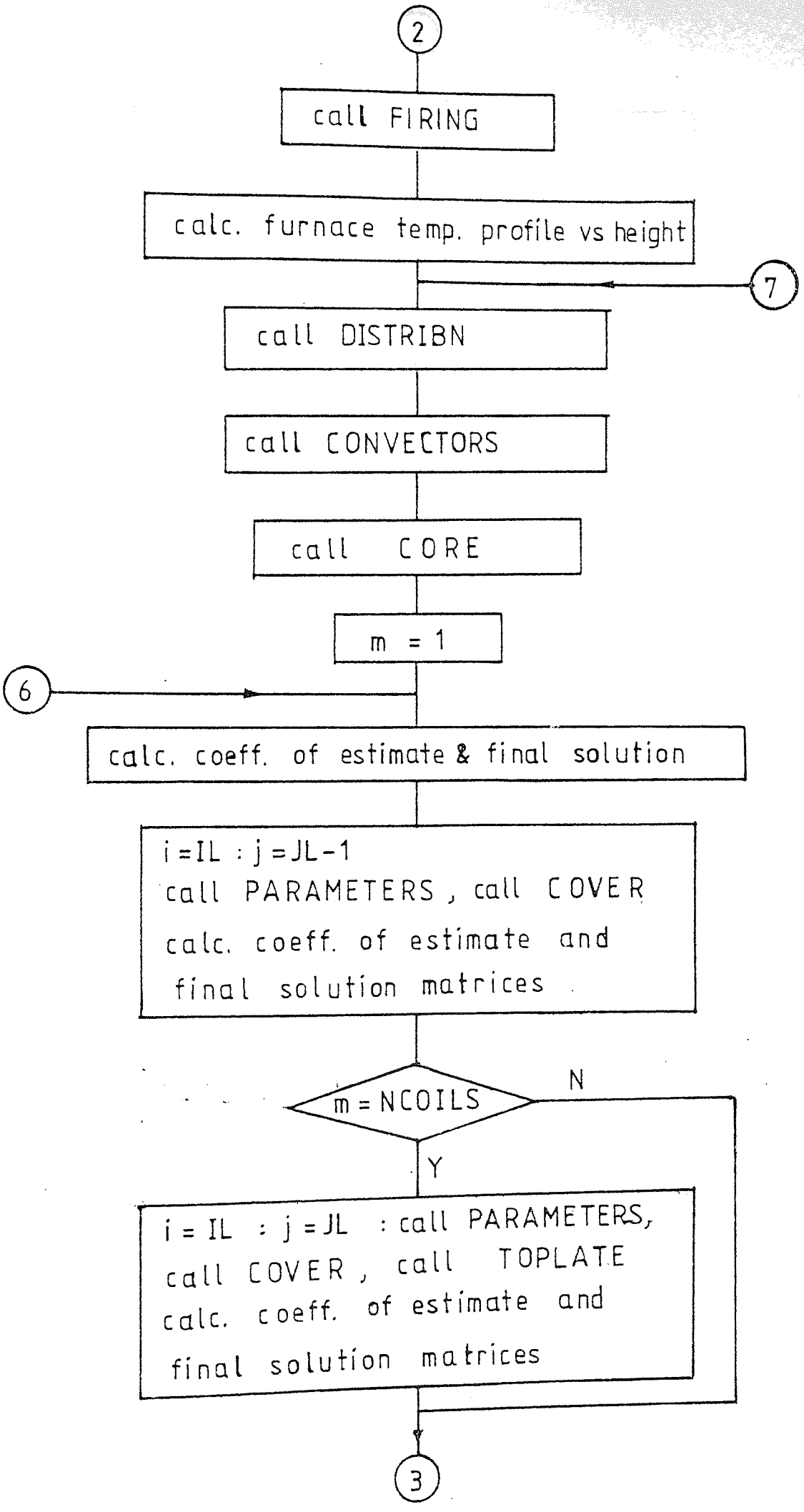
2
call FIRING
calc. furnace temp. profile vs height
7
call DISTRIBN
call CONVECTORS
call CORE
m = 1
6
calc. coeff. of estimate & final solution
i=IL : j=JL-1
call PARAMETERS , call COVER
calc. coeff. of estimate and
final solution matrices
m = NCOILS
N
Y
i = IL : j = JL : call PARAMETERS,
call COVER , call TOPLATE
calc. coeff. of estimate and
final solution matrices
3

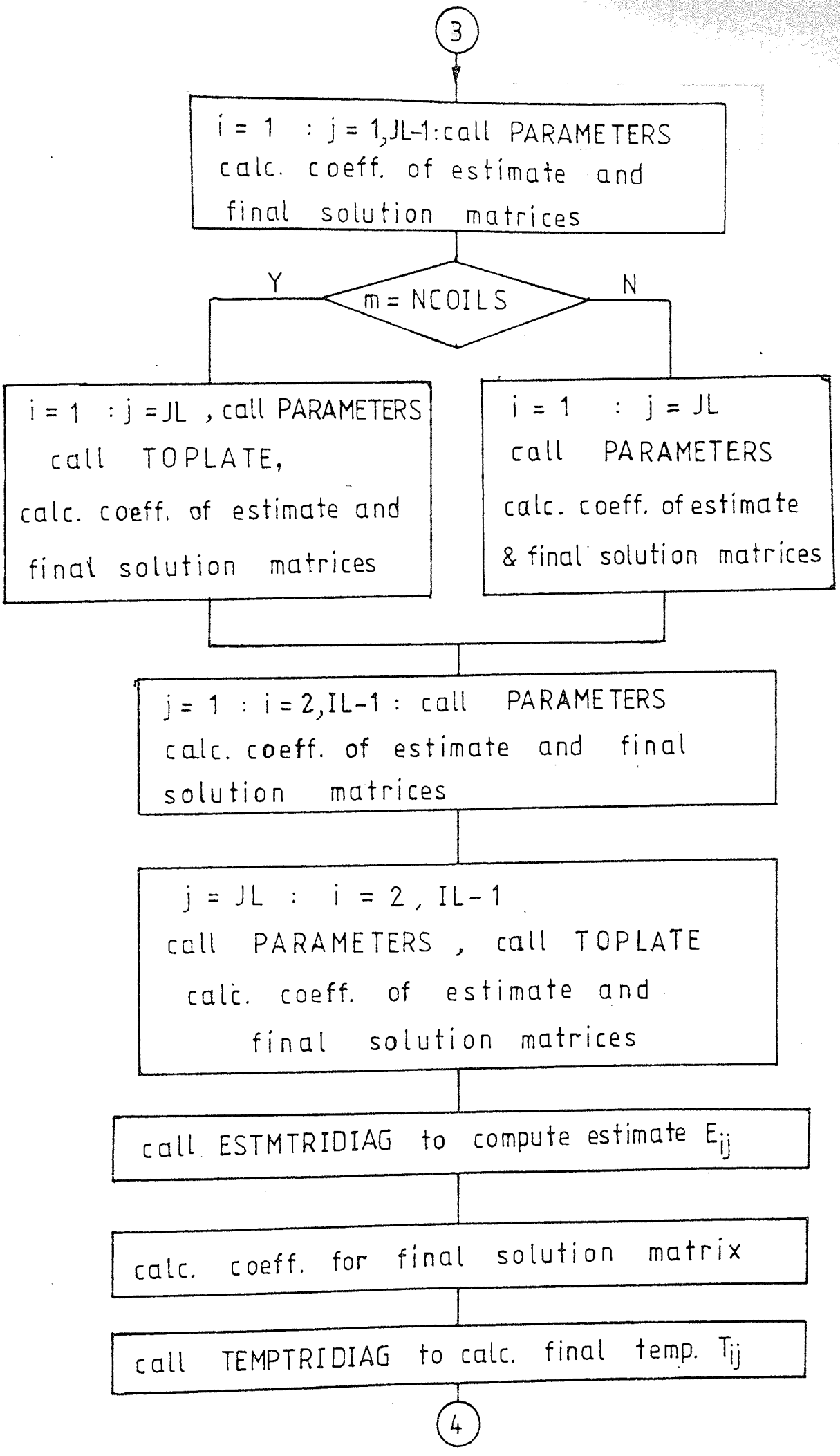
3
i = 1 : j = 1,JL-1:call PARAMETERS
calc. coeff. of estimate and
final solution matrices
Y
m = NCOILS
N
i = 1 : j = JL , call PARAMETERS
call TOPLATE,
calc. coeff. of estimate and
final solution matrices
i = 1 : j = JL
call PARAMETERS
calc. coeff. of estimate
& final solution matrices
j = 1 : i = 2,IL-1 : call PARAMETERS
calc. coeff. of estimate and final
solution matrices
j = JL : i = 2 , IL-1
call PARAMETERS , call TOPLATE
calc. coeff. of estimate and
final solution matrices
call ESTMTRIDIAG to compute estimate E_{ij}
calc. coeff. for final solution matrix
call TEMPTRIDIAG to calc. final temp. T_{ij}
4

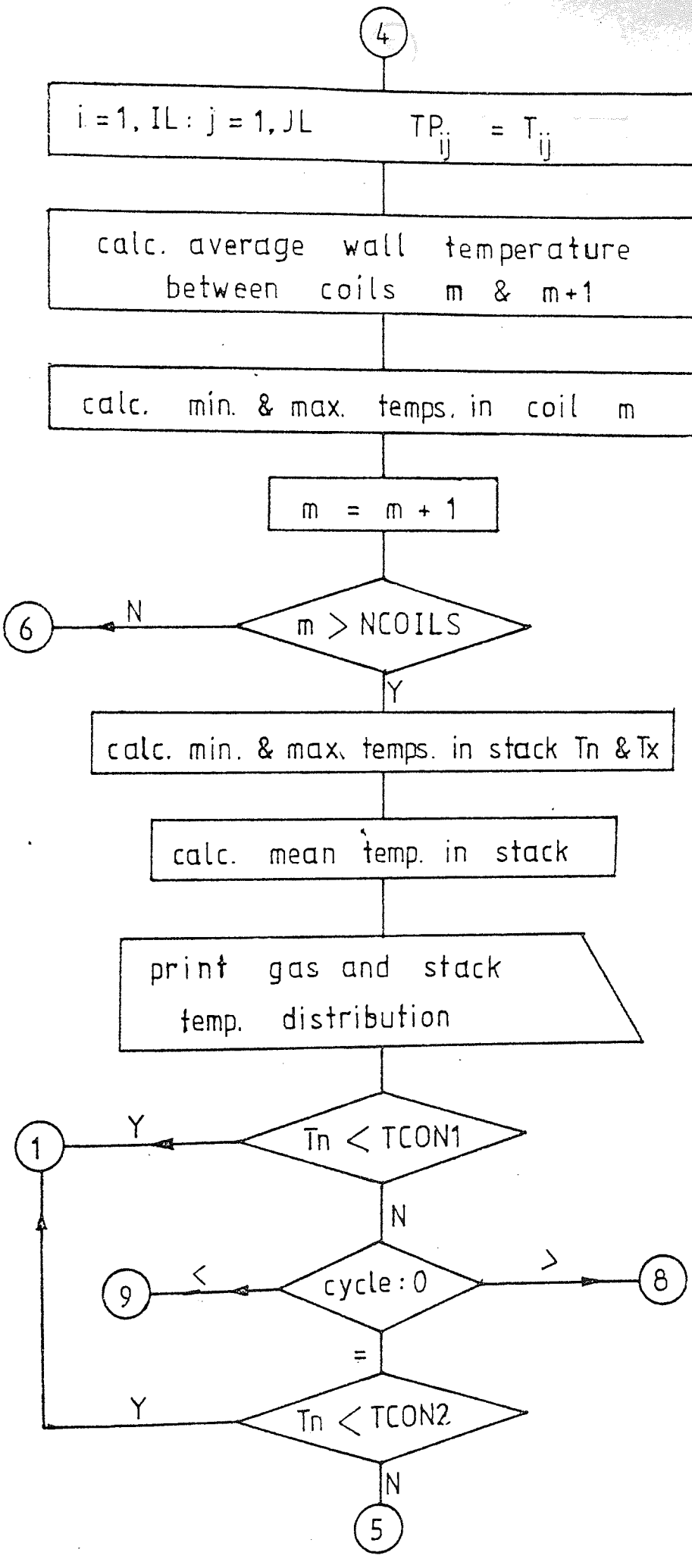
4
i = 1, IL : j = 1, JL
TP_ij = T_ij
calc. average wall temperature between coils m & m+1
calc. min. & max. temps. in coil m
m = m + 1
m > NCOILS
N
6
Y
calc. min. & max. temps. in stack Tn & Tx
calc. mean temp. in stack
print gas and stack temp. distribution
Tn < TCON1
Y
1
N
cycle : 0
<
9
>
8
=
Tn < TCON2
Y
N
5

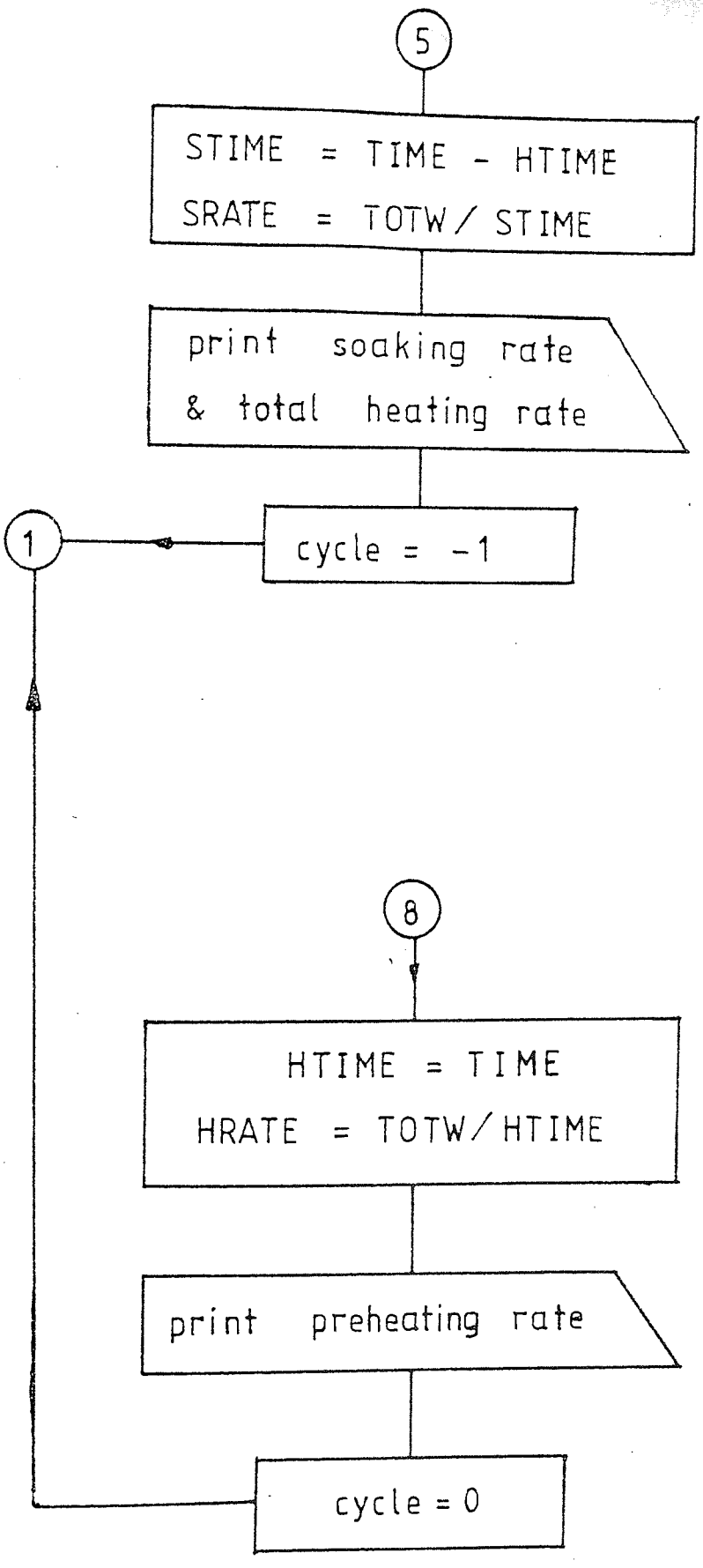
5
STIME = TIME - HTIME
SRATE = TOTW / STIME
print soaking rate
& total heating rate
1
cycle = -1
8
HTIME = TIME
HRATE = TOTW / HTIME
print preheating rate
cycle = 0

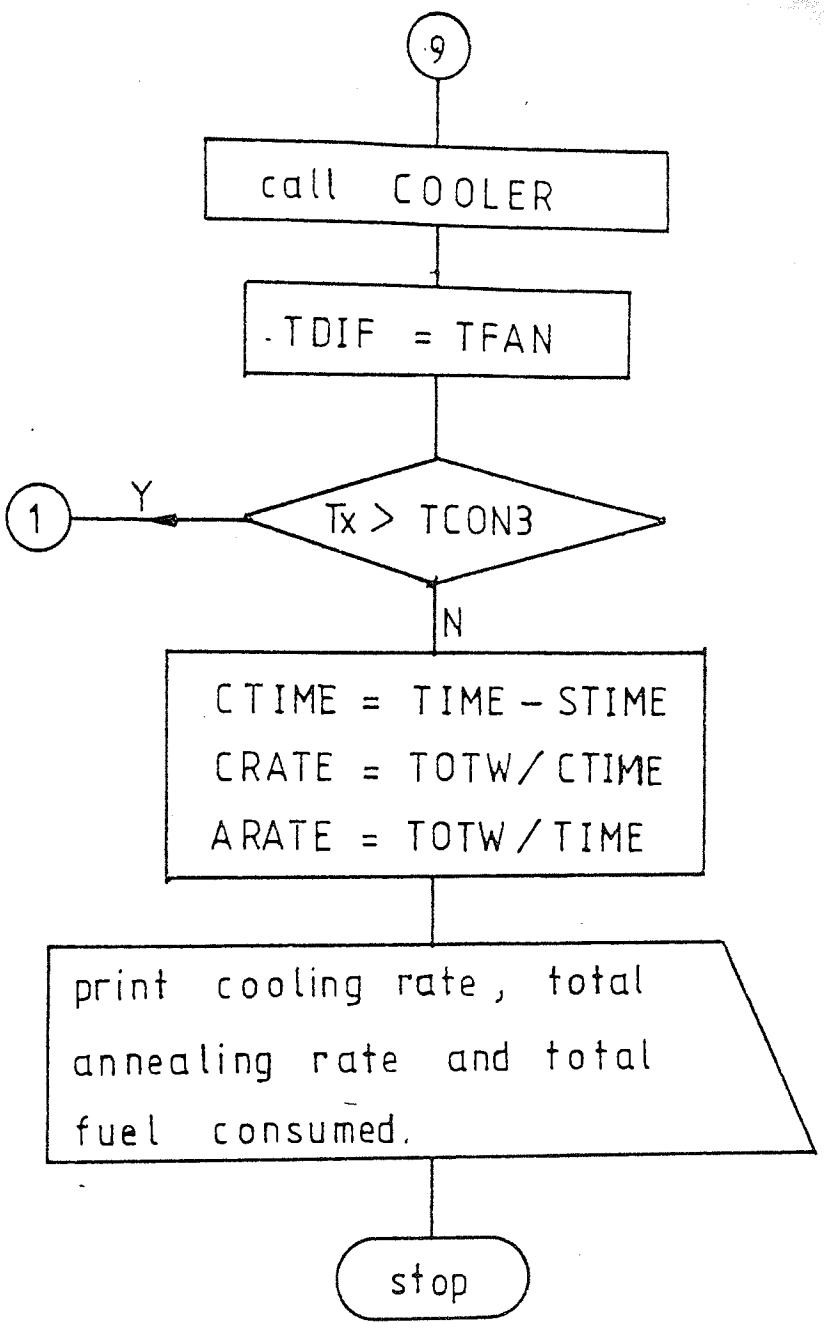
9
call COOLER
TDIF = TFAN
1
Y
Tx > TCON3
N
CTIME = TIME - STIME
CRATE = TOTW / CTIME
ARATE = TOTW / TIME
print cooling rate, total annealing rate and total fuel consumed.
stop

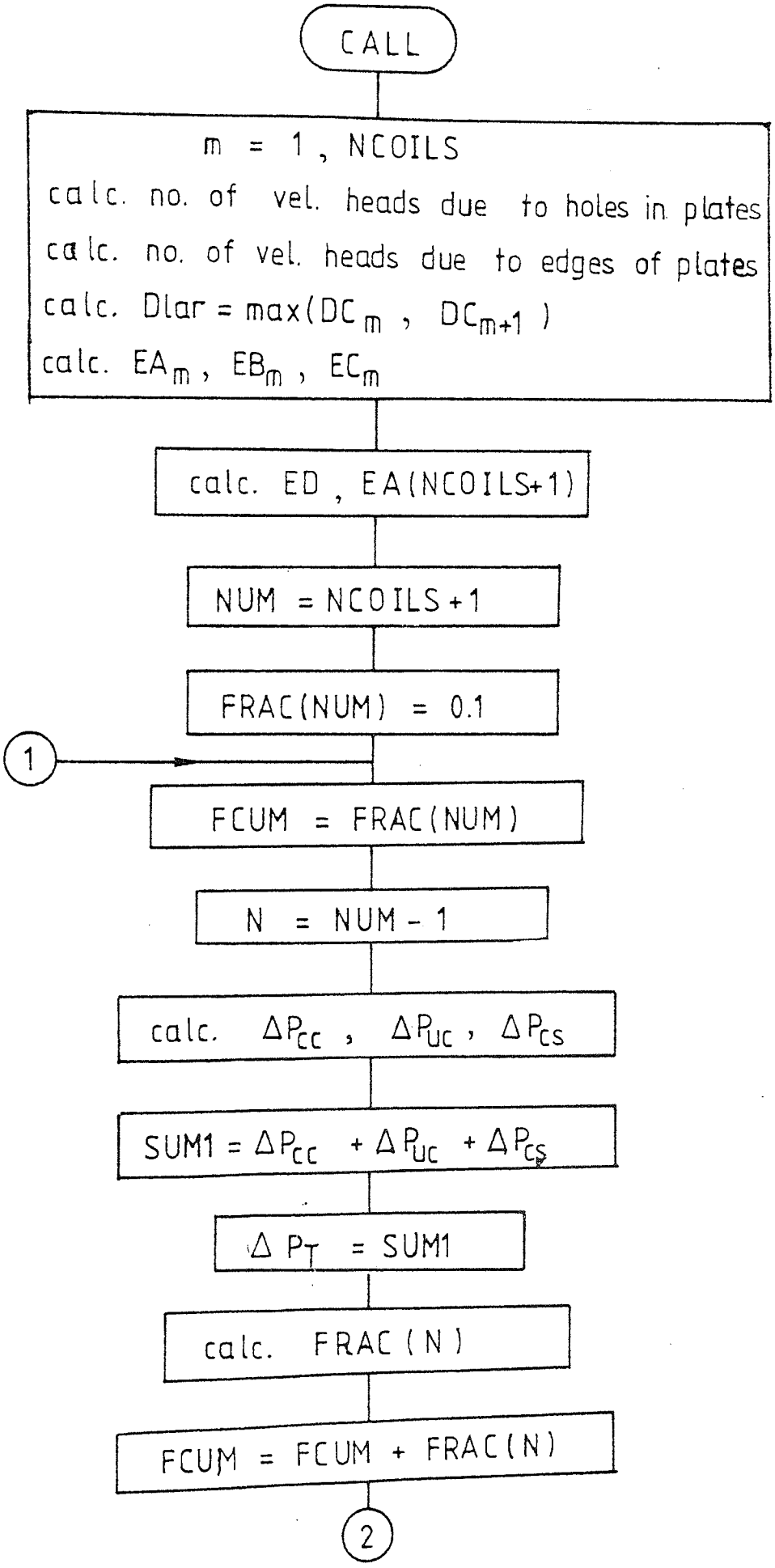
CALL
m = 1 , NCOILS
calc. no. of vel. heads due to holes in plates
calc. no. of vel. heads due to edges of plates
calc. Dlar = max(DC m , DC m+1)
calc. EA m , EB m , EC m
calc. ED , EA(NCOILS+1)
NUM = NCOILS+1
FRAC(NUM) = 0.1
1
FCUM = FRAC(NUM)
N = NUM - 1
calc. ΔP CC , ΔP UC , ΔP CS
SUM1 = ΔP CC + ΔP UC + ΔP CS
Δ P T = SUM1
calc. FRAC(N)
FCUM = FCUM + FRAC(N)
2

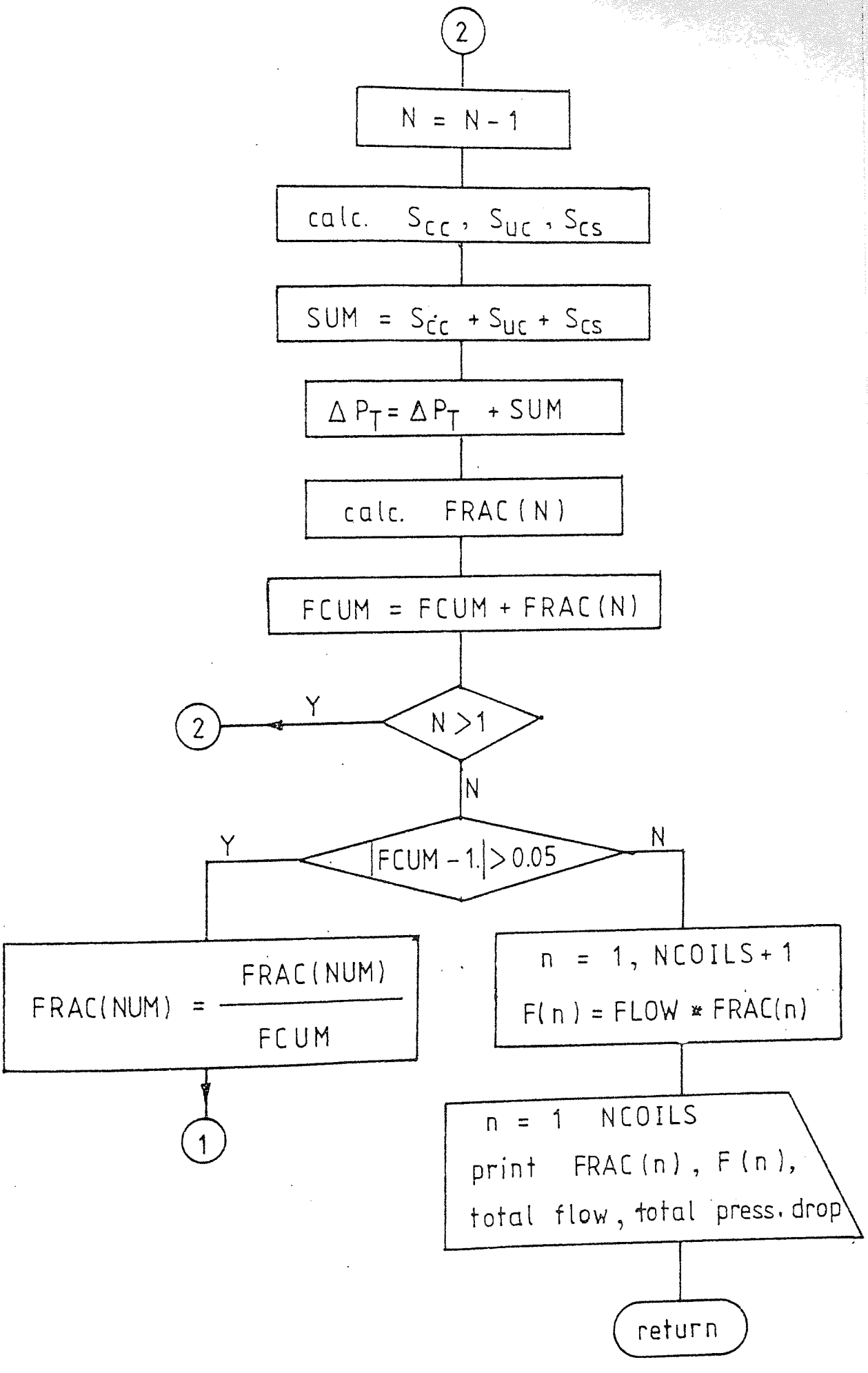
2
N = N - 1
calc. S_{cc}, S_{uc}, S_{cs}
SUM = S_{cc} + S_{uc} + S_{cs}
$\Delta P_T = \Delta P_T$ + SUM
calc. FRAC(N)
FCUM = FCUM + FRAC(N)
N > 1
Y
2
N
|FCUM - 1.| > 0.05
Y
N
FRAC(NUM) = FRAC(NUM) / FCUM
1
n = 1, NCOILS + 1
F(n) = FLOW * FRAC(n)
n = 1 NCOILS
print FRAC(n), F(n),
total flow, total press. drop
return

Subroutine CONVECTORS

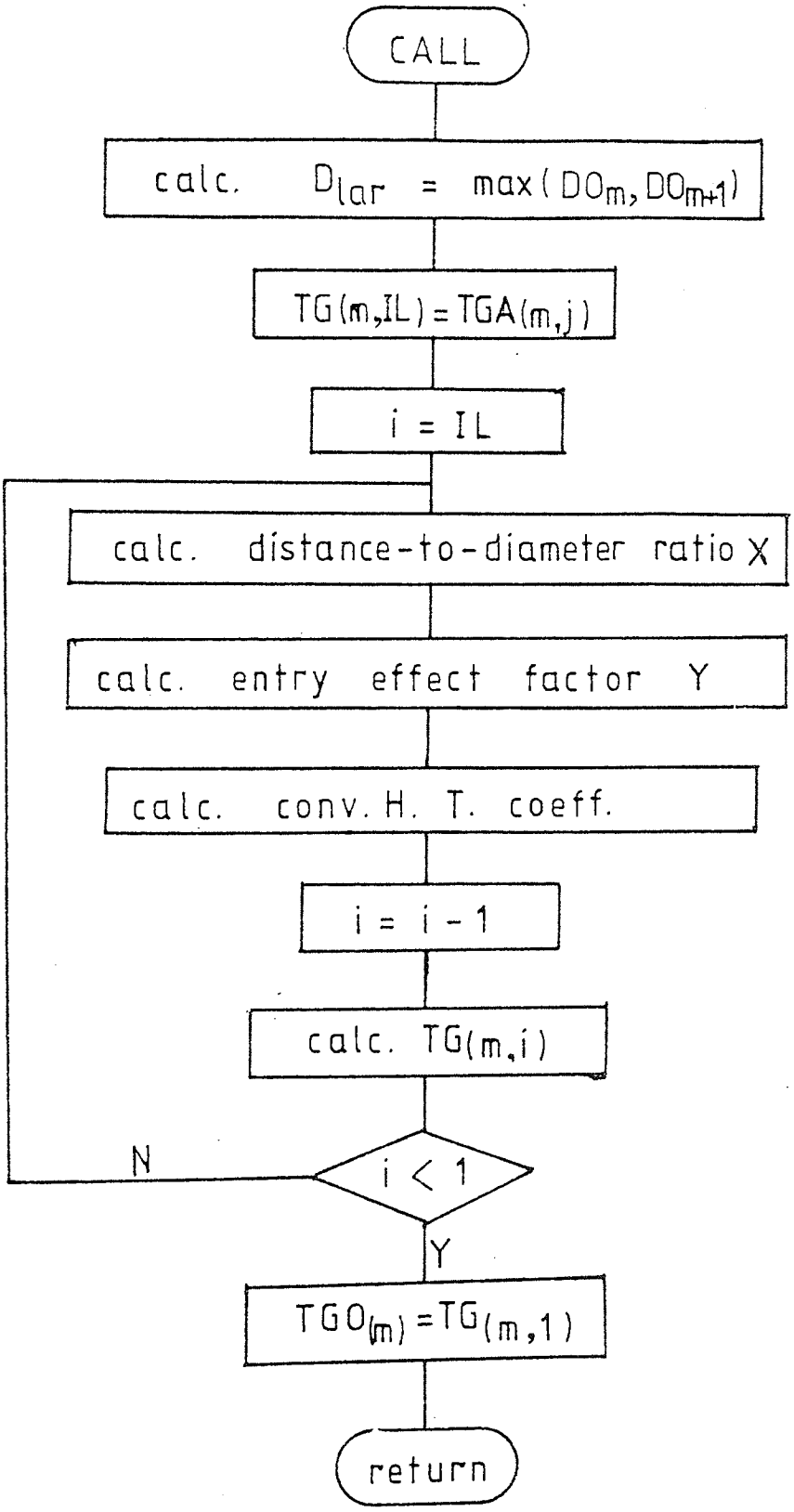

Subroutine FIRING

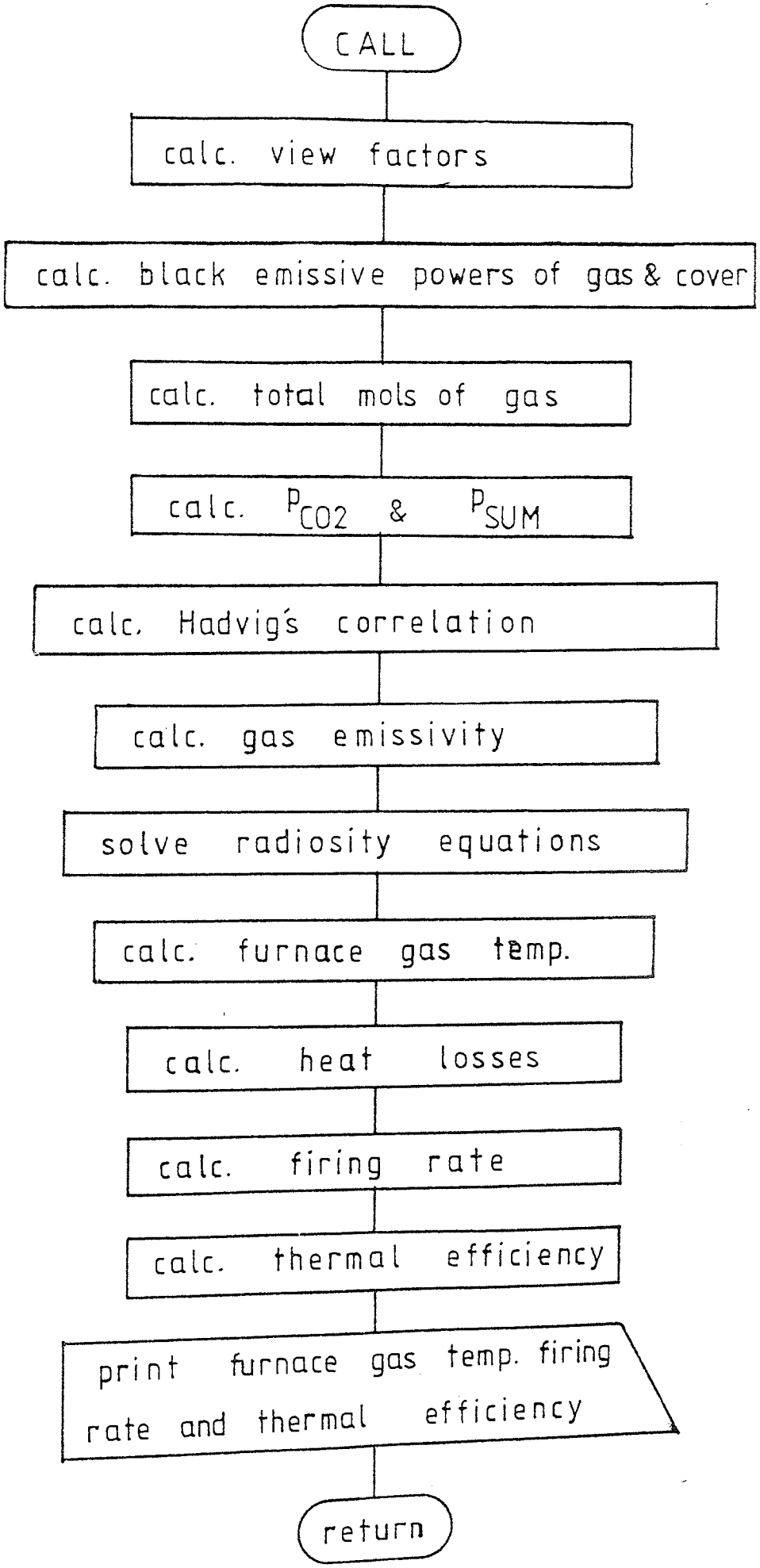

Subroutine COVER

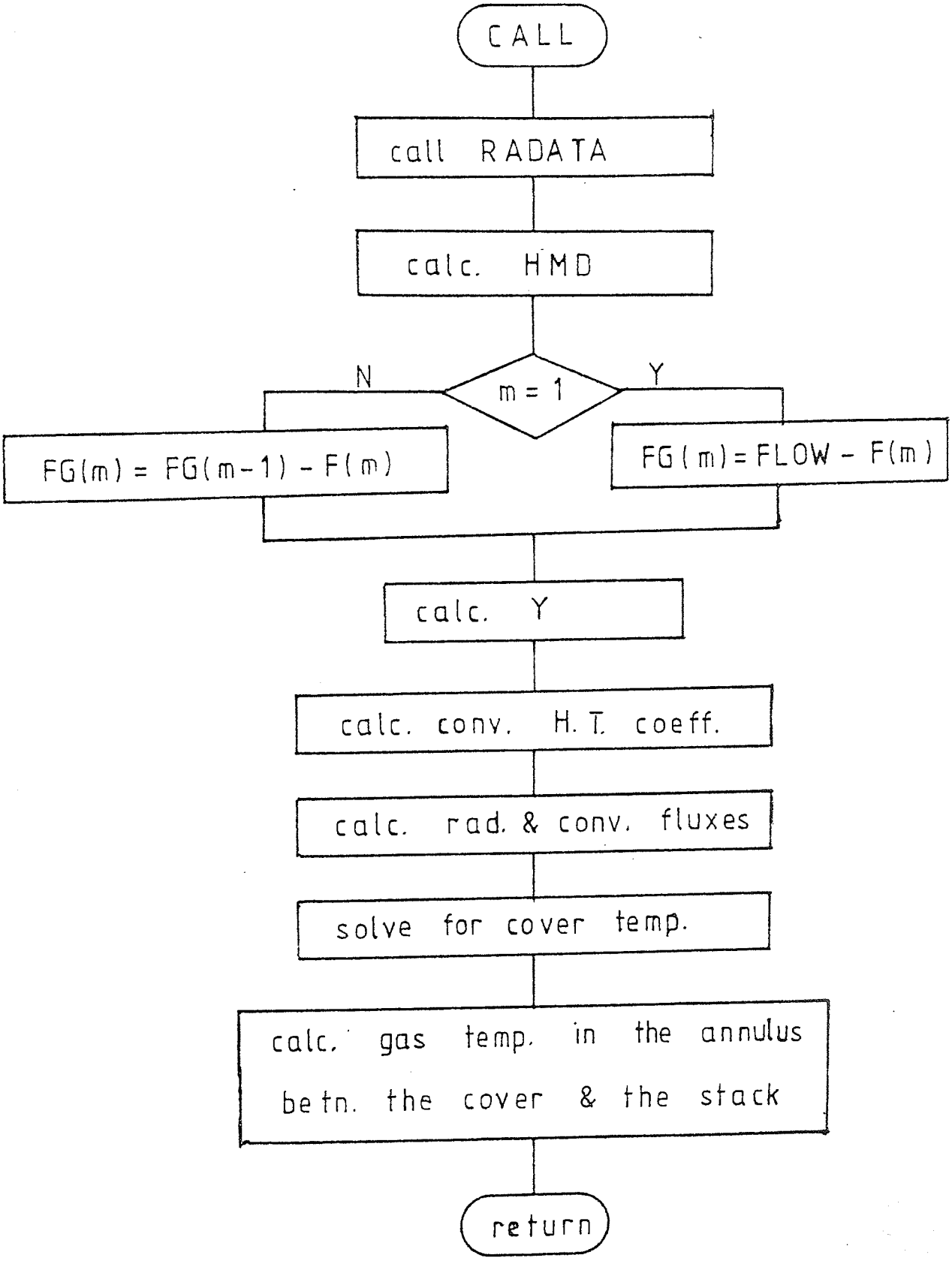

Subroutine CORE

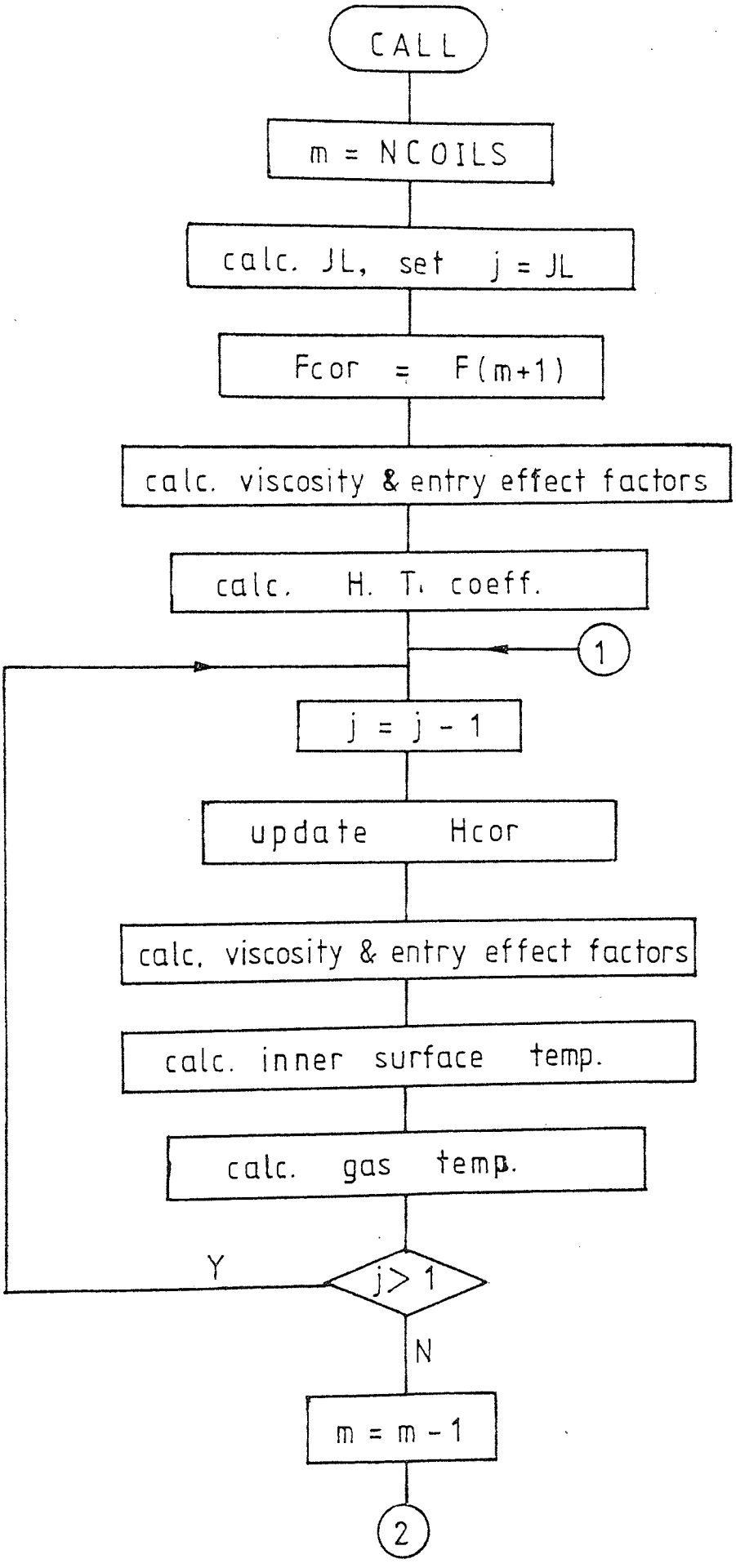

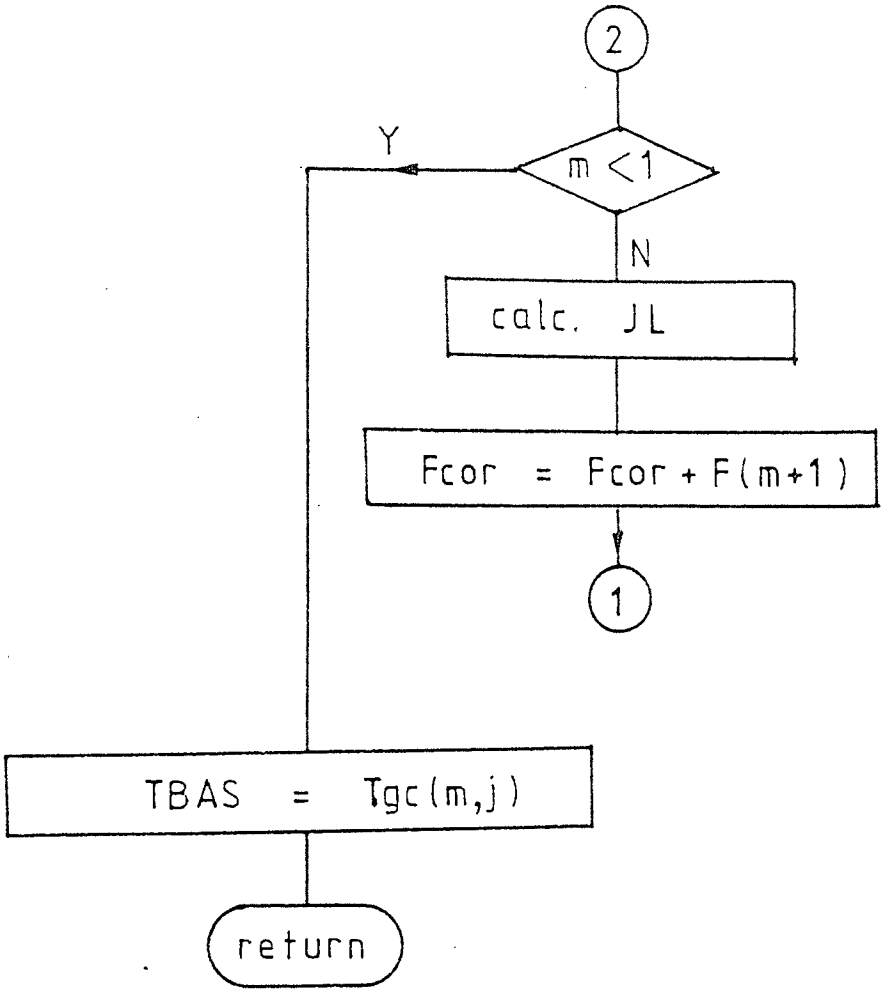
2
Y
m <1
N
calc. JL
Fcor = Fcor + F(m+1)
1
TBAS = Tgc(m,j)
return

APPENDIX D

The Computer Program for the Annealing Furnace

```
      DOCUMENT     FURN


            MASTER ANNEALING
      C   ***************************************************************
      C   *  THIS PROGRAM SIMULATES THE ANNEALING CYCLE IN A LIFT-OFF *
      C   *  FURNACE. THE STEEL IS LOADED IN FORM OF COILS STACKED ON *
      C   *  EACH OTHER WITH CONVECTOR PLATES BETWEEN THEM AND CHARGE *
      C   *  AND TOP PLATES AT BOTTOM AND TOP OF THE STACK            *
      C   *  RESPECTIVELY.                                            *
      C   ***************************************************************
      C
      C     N O T A T I O N :
      C     ==================
      C
      C    ****  SUBSCRIPTS:
      C    ----------------
      C    M           SUBSCRIPT FOR COIL
      C    I           SUBSCRIPT FOR RADIAL POSITION IN COIL(M)
      C    J           SUBSCRIPT FOR AXIAL POSITION IN COIL(M)
      C    K           SUBSCRIPT FOR TIME INTERVAL
      C
      C    ****  DIMENSIONS IN METRES:
      C    ---------------------------
      C    DC(M)       OUTER DIAM OF COIL(M)
      C    DCOR(M)     INNER DIAM OF COIL(M)
      C    H(M)        TOTAL HEIGHT OF COIL(M)
      C    DCOV        DIAM OF INNER COVER
      C    HCOV        HEIGHT OF INNER COVER
      C    DPLAT       DAIM OF CONVECTOR PLATE
      C    DHOL        DIAM OF THE HOLE IN THE CENTRE OF THE PLATE
      C    DREF        DIAM OF REFRACTORY WALL
      C    DCAS        DIAM OF OUTER CASING OF FURNACE
      C    HSTACK      MAX. STACKING HEIGHT
      C    HFUR        HEIGHT OF PORTABLE FURNACE COVER
      C    DR(M)       SIZE OF RADIAL SPACE INCREMENT IN COIL(M)
      C    DZ(M)       SIZE OF AXIAL SPACE INCREMENT IN COIL(M)
      C    NC(M)       NUMBER OF CHANNELS IN CONVECTOR PLATE(M)
      C    B1(M)       HEIGHT OF CONVECTIVE CHANNEL IN PLATE(M)
      C    WO          OUTER WIDTH OF CONVECTIVE CHANNEL
      C    WI          INNER WIDTH OF CONVECTIVE CHANNEL
      C    VLEN        RADIAL LENGTH OF CONVECTIVE CHANNEL
```

```
C
C     ****  OTHER NOTATIONS:
C     ---------------------
C     CFAN        FAN CAPACITY IN M**3/H
C     E1          EMISSIVITY OF STEEL
C     E2          EMISSIVITY OF INNER SURFACE OF COVER
C     NCOILS      NUMBER OF COILS IN STACK
C     DT          LENGTH OF TIME INTERVAL IN HOURS
C     TO          INITIAL TEMPERATURE OF STACK AND GAS
C     EXAIR       AIR FED PER KG STOICHIOMETRIC AIR
C     RCOEF       HEAT TRANSFER COEFFICIENT OF REFRACTORY WALL
C     TFLU        TEMPERATURE OF FLUE GASES LEAVING THE FURNACE
C     NTIGHT      FLAG FOR CORRECTION OF RADIAL CONDUCTIVITY
C                 1   FOR TIGHT COIL
C                 0   FOR COIL THAT OPENS BY HEAT
C     CYCLE       FLAG INDICATING ANNEALING CYCLES
C                 1    FOR HEATING CYCLE
C                 0    FOR SOAKING CYCLE
C                 -1    FOR COOLING CYCLE
C     NTYPE       FLAG FOR TYPE OF HEAT EXCHANGER USED AS COOLER
C                 1    FOR SHELL AND TUBE HEAT EXCHANGER
C                 0    FOR FLUIDIZED BED COOLER
C     NCONT       FLAG INDICATING  POSITION OF TEST COIL IN STACK
C                 0     INDICATES  THERE IS NO SPECIFIC TEST COIL
C     TCON1       MIN. TEMP AT THE END OF HEATING CYCLE
C     TCON2       MIN. TEMP AT THE END OF SOAKING CYCLE
C     TCON3       MAX. TEMP AT THE END OF COOLING CYCLE
C
      DIMENSION NC(5),DC(5),DCOR(5),H(5),DR(5),DZ(5)
      DIMENSION F(5),B1(5),WGT(5)
      DIMENSION BHTC(5,8),THTC(5,8),HTCOR(5,9),QCL0(5),QCL1(5)
     1,QS(5,9)
      DIMENSION TGB(5,8),TGT(5,8),TGP(5,9),TGA(5,9),TGC(5,9),
     1TGO(5),TGI(5),TCOV(5,9),TF(40),TFRN(5,9)
      DIMENSION TMIN(5),IMIN(5),JMIN(5),TMAX(5),IMAX(5),JMAX(5)
      DIMENSION U1(8,9),U2(8,9),U3(8,9),U4(8,9)
      DIMENSION V1(8,9),V2(8,9),V3(8,9),V4(8,9)
      DIMENSION TW(5,8),TP(5,8,9),T(5,8,9),ES(5,8,9)
      INTEGER CYCLE
C     ------------------------------------------------------------
C     * THE DIMENSIONS OF THE COVER,THE FURNACE AND THE COILS    *
C     * ARE READ FORM A SEPERATE DATA FILE. THE DIMENSIONS OF    *
C     * THE CONVECTIVE CHANNELS AND THE EMISSIVITY OF METAL      *
C     * AS WELL AS CONTROL TEMPERATURES AND TEMPERATURE OF       *
C     * THE FURNACE GAS ARE READ FROM THE SAME DATA FILE.        *
C     ------------------------------------------------------------
      READ(1,1001) NCOILS,KP0,DT,T0,EXAIR,RCOEF
      READ(1,1002) DCOV,DHOL,DPLAT,DREF,DCAS,HCOV,HFUR,HSTACK
     1,CFAN
      IF (NCOILS .EQ. 3) GOTO 1
      READ(1,1003) (DC(M),H(M),DCOR(M),DR(M),DZ(M),M=1,NCOILS)
      READ(1,1004) (NC(M),B1(M),M=1,NCOILS+1)
      GOTO 6
    1 READ(1,1103) (DC(M),H(M),DCOR(M),DR(M),DZ(M),M=1,NCOILS)
      READ(1,1104) (NC(M),B1(M),M=1,NCOILS+1)
    6 READ(1,1005) NTIGHT,NTYPE,DCLR,VLEN,E1,E2,WI,WO,TTCOV
     1,TFLU
      READ(1,1006) NCONT,TCON1,TCON2,TCON3
```

```
C   INITIALIZE THE VARIABLES AND ARRAYS
      K=0
      NSOAK=0
      NCOOL=0
      KPR=KP0
      CYCLE=1
      TIME=0.0
      DO 2 M=1,NCOILS+1
      TGI(M)=600.
    2 CONTINUE
      DO 10 M=1,NCOILS
      II=IFIX((DC(M)-DCOR(M))/(2.*DR(M))+0.1)+1
      JJ=IFIX(H(M)/DZ(M)+0.1)+1
      TGO(M)=500.
      IF (M .GT. 1) GOTO 21
      IL=II
      JL=JJ
      GOTO 23
   21 IF (IL .GT. II) GOTO 22
      IL=II
   22 IF (JL .GT. JJ) GOTO 23
      JL=JJ
   23 DO 10 I=1,IL
      DO 10 J=1,JL
      TP(M,I,J)=T0
      ES(M,I,J)=T0
      TGA(M,J)=TGI(M)
      TGP(M,J)=TGI(M)
      TGC(M,J)=500.
      TW(M,I)=T0
      IF (M .EQ. NCOILS) TW(NCOILS+1,I)=T0
   10 CONTINUE
      TGO(NCOILS+1)=500.
      TBAS=600.
      TDIF=600.
      TFAN=600.
C   PRINT THE STACK DATA
      DO 5 M=1,NCOILS
      IL=IFIX((DC(M)-DCOR(M))/(2.*DR(M))+0.1)+1
      JL=IFIX(H(M)/DZ(M)+0.1)+1
      VCOIL=0.7854*H(M)*(DC(M)**2-DCOR(M)**2)
      WGT(M)=7.9*VCOIL
      VOL=VOL+VCOIL
      TOTW=TOTW+WGT(M)
      HH=HH+H(M)
    5 CONTINUE
      HPLATS=B1(1)+0.01
      DO 4 M=2,NCOILS
    4 HPLATS=HPLATS+2.*B1(M)+0.01
      HPLATS=HPLATS+B1(NCOILS+1)+0.01
      WRITE(2,2001)
      DO 3 M=1,NCOILS
      WRITE(2,2002) M,NC(M),B1(M)
      WRITE(2,2003) M,DC(M),DCOR(M),H(M),WGT(M)
    3 CONTINUE
      M=NCOILS+1
      WRITE(2,2002) M,NC(M),B1(M)
      WRITE(2,2004) TOTW
```

```
C   COMPUTE THE ADIABATIC FLAME TEMPERATURE
        FHEAT=14.544+1.425*EXAIR
        FMIX=1.+17.05*EXAIR
        TADB=2000.
  123   FFN=2.971E-4*TADB+2.303E-8*TADB**2+1.721E-11*TADB**3-5
       1.82E-15*TADB**4-FHEAT/FMIX
        FFD=2.971E-4+4.605E-8*TADB+5.164E-11*TADB**2-2.328E-14
       1*TADB**3
        TADB=TADB-FFN/FFD
        IF (ABS(FFN/FFD) .GT. 2.) GOTO 123
        PERCNT=(EXAIR-1.)*100.
        WRITE(2,2005) PERCNT,TADB
        WRITE(2,2007)
C   COMPUTE THE INITIAL GAS AND STACK ENTHALPIES
        CALL STEELVENT(TO,FVO)
        QSO=VOL*FVO
        CALL GASENTH(TO,FE)
        FLOW=2.048E4*CFAN/TO
        QGO=FLOW*FE
        CALL STEELVENT(TO+10.,FV1)
        QS1=VOL*FV1
        QPLO=QSO*HPLATS/HH
        QPL1=QS1*HPLATS/HH
        DO 13 M=1,NCOILS
        VV=0.7854*(DC(M)**2-DCOR(M)**2)*H(M)
        QCLO(M)=VV*FVO+QPLO/FLOAT(NCOILS)
        QCL1(M)=VV*FV1+QPL1/FLOAT(NCOILS)
        JL=IFIX(H(M)/DZ(M)+0.01)+1
        DO 13 J=1,JL
        QS(M,J)=(QCL1(M)-QCLO(M))/FLOAT(JL)
    13  CONTINUE
        QSS=QCL1(1)-QCLO(1)
        CALL GASENTH(TO+50.,FE)
        FLOW=2.048E4*CFAN/(TO+50.)
        QG1=FLOW*FE
        K=K+1
        DO 117 M=1,NCOILS
  117   QCLO(M)=QCL1(M)
        QPLO=QPL1
        TCC=850.
        GOTO 8
C   START A NEW TIME INTERVAL
    15  K=K+1
        DTGA=80.
        IF ((TIME .GE. 25.).AND.(CYCLE .GT. 0)) DTGA=DTGA+3.
        IF ((CYCLE .LT. 0).AND.(NK .LE. 1)) DTGA=-80.
        IF (NK .GE. 10) DTGA=DTGA-5.
        TCC=TCOV(1,3)
```

```
C   CALCULATE THE CURRENT ENTHALPIES OF STACK AND GAS
      QS1=0.
      DO 12 M=1,NCOILS
      IL=IFIX((DC(M)-DCOR(M))/(2.*DR(M))+0.1)+1
      JL=IFIX(H(M)/DZ(M)+0.1)+1
      QCL1(M)=0.0
      DO 11 I=1,IL-1
      DO 11 J=1,JL-1
      R=DCOR(M)/2.+FLOAT(I-1)*DR(M)
      V=3.1416*DZ(M)*DR(M)*(2.*R+DR(M))
      TT=(TP(M,I,J)+TP(M,I,J+1)+TP(M,I+1,J)+TP(M,I+1,J+1))/4.
      CALL STEELVENT(TT,FV)
   11 QCL1(M)=QCL1(M)+V*FV
      QS1=QS1+QCL1(M)
   12 CONTINUE
      QPL1=QS1*HPLATS/HH
      QS1=QS1+QPL1
      QCL1(1)=QCL1(1)+QPL1/FLOAT(NCOILS)
      QSS=QCL1(1)-QCL0(1)
      CALL GASENTH(TBAS,FE)
      FLOW=2.048E4*CFAN/TBAS
      QG1=FLOW*FE
    8 QSTAK=QS1-QS0
      QGAS=QG1-QG0
      WRITE(2,2006) QSTAK,QGAS
      QSS=QSS/DT
      QSTAK=QSTAK/DT
      QGAS=QGAS/DT
C   CALCULATE THE FURNACE TEMP. NEAR THE BOTTOM COIL
      IF (CYCLE .LE. 0) GOTO 133
      CALL FIRING(QSTAK,QGAS,DREF,DCAS,DCOV,RCOEF,TFLU,TADB,
     1TCC,HFUR,FRATE,E2,EXAIR,TMAXX,TFR,FHEAT)
      FUEL=FUEL+FRATE*DT
      WRITE(2,2016) FUEL
```

```
C   COMPUTE PROFILE OF FURNACE TEMP. WITH FURNACE HEIGHT
      JL=IFIX(H(1)/DZ(1)+0.1)+1
      DO 7 J=1,JL
    7 TFRN(1,J)=TFR
      JLT=1
      DO 9 M=2,NCOILS
      JL=IFIX(H(M)/DZ(M)+0.1)
    9 JLT=JLT+JL
      CDIF=(TFR-TFLU)/FLOAT(JLT)
      TF(1)=TFR
      DO 16 J1=2,JLT
   16 TF(J1)=TF(J1-1)-CDIF
      JT=0
      DO 18 M=2,NCOILS
      JL=IFIX(H(M)/DZ(M)+0.1)+1
      DO 17 J=1,JL
      JT=JT+1
   17 TFRN(M,J)=TF(JT)
   18 JT=JT-1
      GOTO 33
C   DURING COOLING SET FURNACE TEMP. EQUAL ATMOS. TEMP.
  133 DO 28 M=1,NCOILS
      JL=IFIX(H(M)/DZ(M)+0.1)+1
      DO 28 J=1,JL
      TFRN(M,J)=T0
   28 CONTINUE
C   COMPUTE THE FLOW DISTRIBUTION IN THE CONVECTOR PLATES
   33 CALL DISTRIBN(NCOILS,H,VLEN,DC,DCOV,DHOL,DCLR,DCOR,DPLAT
     1,HSTACK,CFAN,TGC,TGI,TFAN,TDIF,NC,B1,WO,WI,FLOW,F)
C   COMPUTE  PROFILE OF GAS TEMP. AND H.T.COEFF. IN CONV PLATES
      DO 115 M=1,NCOILS
      IL=IFIX((DC(M)-DCOR(M))/(2.*DR(M))+.1)+1
      JL=IFIX(H(M)/DZ(M)+.1)+1
      IF (M .GT. 1) GOTO 37
      JV=1
      CALL CONVECTORS(NCOILS,IL,JL,M,JV,DC,DCOR(M),DR(M),TW,F(M)
     1,BHTC,NC(M),B1(M),WO,WI,VLEN,TGB,TGA,TGO(M))
      JV=JL
      CALL CONVECTORS(NCOILS,IL,JL,M,JV,DC,DCOR(M),DR(M),TW
     1,F(M+1),THTC,NC(M+1),B1(M+1),WO,WI,VLEN,TGT,TGA,TGO(M+1))
      GOTO 115
   37 DO 39 I=1,IL
      TGB(M,I)=TGT(M-1,I)
      BHTC(M,I)=THTC(M-1,I)
   39 CONTINUE
      JV=JL
      CALL CONVECTORS(NCOILS,IL,JL,M,JV,DC,DCOR(M),DR(M),TW
     1,F(M+1),THTC,NC(M+1),B1(M+1),WO,WI,VLEN,TGT,TGA,TGO(M+1))
  115 CONTINUE
```

```
C   COMPUTE PROFILE OF GAS TEMP. AND H.T.COEF IN  CORE OF STACK
      CALL CORE(NCOILS,H,F,B1,DCOR,DHOL,DZ,TP,TGO,TGC,TBAS,
     1HTCOR)
      IF (CYCLE .LT. 0) GOTO 14
      TDIF=TBAS+DTGA
      TFAN=TBAS
C
C   CALCULATE THE TEMP. DISTRIBUTION COIL BY COIL
   14 DO 120 M=1,NCOILS
      IL=IFIX((DC(M)-DCOR(M))/(2.*DR(M))+0.1)+1
      JL=IFIX(H(M)/DZ(M)+0.1)+1
      ACOIL=3.1416*DC(M)*DZ(M)
      DO 20 I=2,IL-1
      R=DCOR(M)/2.+FLOAT(I-1)*DR(M)
      DO 20 J=2,JL-1
      CALL PARAMETERS(NTIGHT,M,IL,I,J,DCOR(M),DR(M),DZ(M),DT,
     1TP,ALPH1,ALPH2,ALPH3,FF,FC)
C   CALCULATE THE COEFFICIENTS FOR ESTIMATE AND TEMPERATURE
      U1(I,J)=-ALPH1/2.
      U2(I,J)=1.+ALPH1
      U3(I,J)=-ALPH1/2.
      U4(I,J)=ALPH1/2.*(TP(M,I,J+1)+TP(M,I,J-1))+(ALPH2+ALPH3)
     1*TP(M,I+1,J)+(ALPH2-ALPH3)*TP(M,I-1,J)+(1.-ALPH1-2.
     2*ALPH2)*TP(M,I,J)
      V1(I,J)=(ALPH3-ALPH2)/2.
      V2(I,J)=1.+ALPH2
      V3(I,J)=-(ALPH2+ALPH3)/2.
      V4(I,J)=-(ALPH2+ALPH3)/2.*TP(M,I+1,J)+ALPH2*TP(M,I,J)+
     1(ALPH3-ALPH2)/2.*TP(M,I-1,J)
   20 CONTINUE
```

```
C   CALCULATE THE COEFFICIENTS FOR THE BOUNDARY CONDITIONS
C   THE OUTER PERIPHERY OF THE COIL
      I=IL
      J=1
      CALL PARAMETERS(NTIGHT,M,IL,I,J,DCOR(M),DR(M),DZ(M),DT,
     1TP,ALPH1,ALPH2,ALPH3,FF,FC)
      CALL COVER(IL,JL,M,J,DR(M),DZ(M),E1,E2,DC,DCOV,DREF,FLOW
     1,FRATE,TDIF,TGA,TFRN(M,J),TP,H,F,EQ,B1,EXAIR,TCOV,K,
     2QOUT,CYCLE)
      TERM=2.*DZ(M)*BHTC(M,I)/FC
      PHI=2.*DR(M)/(FF*FC)
      EQ=EQ*PHI
      QOUT=QOUT*PHI
      QS(M,J)=ACOIL*QOUT
      U1(I,J)=0.
      U2(I,J)=1.+ALPH1/2.*(2.+TERM)
      U3(I,J)=-ALPH1
      U4(I,J)=(1.-ALPH1/2.*(2.+TERM)-2.*ALPH2-(ALPH2+ALPH3)*
     1EQ)*TP(M,I,J)+2.*ALPH2*TP(M,I-1,J)+ALPH1*TP(M,I,J+1)
     2+ALPH1*TERM*TGB(M,I)+(ALPH2+ALPH3)*QOUT
      V1(I,J)=-ALPH2
      V2(I,J)=1.+ALPH2+(ALPH2+ALPH3)/2.*EQ
      V3(I,J)=0.
      V4(I,J)=(ALPH2+(ALPH2+ALPH3)/2.*EQ)*TP(M,I,J)-ALPH2*TP
     1(M,I-1,J)
      DO 30 J=2,JL-1
      CALL PARAMETERS(NTIGHT,M,IL,I,J,DCOR(M),DR(M),DZ(M),DT,
     1TP,ALPH1,ALPH2,ALPH3,FF,FC)
      CALL COVER(IL,JL,M,J,DR(M),DZ(M),E1,E2,DC,DCOV,DREF,FLOW
     1,FRATE,TDIF,TGA,TFRN(M,J),TP,H,F,EQ,B1,EXAIR,TCOV,K,
     2QOUT,CYCLE)
      PHI=2.*DR(M)/(FF*FC)
      EQ=EQ*PHI
      QOUT=QOUT*PHI
      QS(M,J)=ACOIL*QOUT
      U1(I,J)=-ALPH1/2.
      U2(I,J)=1.+ALPH1
      U3(I,J)=-ALPH1/2.
      U4(I,J)=(1.-ALPH1-2.*ALPH2-(ALPH2+ALPH3)*EQ)*TP(M,I,J)
     1+2.*ALPH2*TP(M,I-1,J)+ALPH1/2.*(TP(M,I,J+1)+TP(M,I,J-1)
     2)+(ALPH2+ALPH3)*QOUT
      V1(I,J)=-ALPH2
      V2(I,J)=1.+ALPH2+(ALPH2+ALPH3)/2.*EQ
      V3(I,J)=0.
      V4(I,J)=(ALPH2+(ALPH2+ALPH3)/2.*EQ)*TP(M,I,J)-ALPH2*TP
     1(M,I-1,J)
   30 CONTINUE
```

```
      J=JL
      CALL PARAMETERS(NTIGHT,M,IL,I,J,DCOR(M),DR(M),DZ(M),DT,
     1TP,ALPH1,ALPH2,ALPH3,FF,FC)
      CALL COVER(IL,JL,M,J,DR(M),DZ(M),E1,E2,DC,DCOV,DREF,FLOW
     1,FRATE,TDIF,TGA,TFRN(M,J),TP,H,F,EQ,B1,EXAIR,TCOV,K,
     2QOUT,CYCLE)
      IF (M .EQ. NCOILS) GOTO 32
      TERM=2.*DZ(M)*THTC(M,I)/FC
      PHI=2.*DR(M)/(FF*FC)
      EQ=EQ*PHI
      QOUT=QOUT*PHI
      QS(M,J)=ACOIL*QOUT
      IF (M .EQ. 2) TCC=TCOV(M,J)
      GOTO 36
   32 CALL TOPLATE(NCOILS,IL,JL,DC,DCOR(M),DCOV,DPLAT,DR(M),H
     1,HCOV,TP,TTCOV,E1,E2,TFLU,QF,B1,HH,I,CYCLE)
      QTOP=2.*QF*DZ(M)/FC
   36 U1(I,J)=-ALPH1
      U2(I,J)=1.+ALPH1/2.*(2.+TERM)
      U3(I,J)=0.
      IF (M .EQ. NCOILS) GOTO 51
      U4(I,J)=(1.-ALPH1/2.*(2.+TERM)-2.*ALPH2-(ALPH2+ALPH3)
     1*EQ)*TP(M,I,J)+2.*ALPH2*TP(M,I-1,J)+ALPH1*TP(M,I,J-1)
     2+ALPH1*TERM*TGT(M,I)+(ALPH2+ALPH3)*QOUT
      GOTO 52
   51 U2(I,J)=1.+ALPH1
      U4(I,J)=(1.-ALPH1-2.*ALPH2-(ALPH2+ALPH3)*EQ)*TP(M,I,J)
     1+ALPH1*TP(M,I,J-1)+2.*ALPH2*TP(M,I-1,J)+ALPH1*QTOP
     2+(ALPH2+ALPH3)*QOUT
   52 V1(I,J)=-ALPH2
      V2(I,J)=1.+ALPH2+(ALPH2+ALPH3)/2.*EQ
      V3(I,J)=0.
      V4(I,J)=(ALPH2+(ALPH2+ALPH3)/2.*EQ)*TP(M,I,J)-ALPH2
     1*TP(M,I-1,J)
C   THE INNER BOUNDARY OF THE COIL
      I=1
      J=1
      CALL PARAMETERS(NTIGHT,M,IL,I,J,DCOR(M),DR(M),DZ(M),DT,
     1TP,ALPH1,ALPH2,ALPH3,FF,FC)
      BETA=2.*DR(M)*HTCOR(M,J)/(FF*FC)
      TERM=2.*DZ(M)*BHTC(M,I)/FC
      U1(I,J)=0.
      U2(I,J)=1.+ALPH1/2.*(2.+TERM)
      U3(I,J)=-ALPH1
      U4(I,J)=(1.-ALPH1/2.*(2.+TERM)-2.*ALPH2-(ALPH2-ALPH3)
     1*BETA)*TP(M,I,J)+ALPH1*TP(M,I,J+1)+2.*ALPH2*TP(M,I+1,J)
     2+ALPH1*TERM*TGB(M,I)+(ALPH2-ALPH3)*BETA*TGC(M,J)
      V1(I,J)=0.
      V2(I,J)=1.+ALPH2+(ALPH2-ALPH3)/2.*BETA
      V3(I,J)=-ALPH2
      V4(I,J)=(ALPH2+(ALPH2-ALPH3)/2.*BETA)*TP(M,I,J)-ALPH2
     1*TP(M,I+1,J)
```

```
      DO 25 J=2,JL-1
      CALL PARAMETERS(NTIGHT,M,IL,I,J,DCOR(M),DR(M),DZ(M),DT,
     1TP,ALPH1,ALPH2,ALPH3,FF,FC)
      BETA=2.*DR(M)*HTCOR(M,J)/(FF*FC)
      U1(I,J)=-ALPH1/2.
      U2(I,J)=1.+ALPH1
      U3(I,J)=-ALPH1/2.
      U4(I,J)=(1.-ALPH1-2.*ALPH2-(ALPH2-ALPH3)*BETA)*TP(M,I
     1,J)+ALPH1/2.*(TP(M,I,J+1)+TP(M,I,J-1))+2.*ALPH2*TP(M,
     2I+1,J)+(ALPH2-ALPH3)*BETA*TGC(M,J)
      V1(I,J)=0.
      V2(I,J)=1.+ALPH2+(ALPH2-ALPH3)/2.*BETA
      V3(I,J)=-ALPH2
      V4(I,J)=(ALPH2+(ALPH2-ALPH3)/2.*BETA)*TP(M,I,J)-ALPH2
     1*TP(M,I+1,J)
   25 CONTINUE
      J=JL
      CALL PARAMETERS(NTIGHT,M,IL,I,J,DCOR(M),DR(M),DZ(M),DT,
     1TP,ALPH1,ALPH2,ALPH3,FF,FC)
      IF (M .EQ. NCOILS) GOTO 26
      BETA=2.*DR(M)*HTCOR(M,J)/(FF*FC)
      TERM=2.*DZ(M)*THTC(M,I)/FC
      GOTO 29
   26 CALL TOPLATE(NCOILS,IL,JL,DC,DCOR(M),DCOV,DPLAT,DR(M),H
     1,HCOV,TP,TTCOV,E1,E2,TFLU,QF,B1,HH,I,CYCLE)
      QTOP=2.*QF*DZ(M)/FC
   29 U1(I,J)=-ALPH1
      U2(I,J)=1.+ALPH1/2.*(2.+TERM)
      U3(I,J)=0.
      IF (M .EQ. NCOILS) GOTO 61
      U4(I,J)=(1.-ALPH1/2.*(2.+TERM)-2.*ALPH2-(ALPH2-ALPH3)
     1*BETA)*TP(M,I,J)+2.*ALPH2*TP(M,I+1,J)+ALPH1*TERM*TGT
     2(M,I)+(ALPH2-ALPH3)*BETA*TGC(M,J)+ALPH1*TP(M,I,J-1)
      GOTO 62
   61 U2(I,J)=1.+ALPH1
      U4(I,J)=(1.-ALPH1-2.*ALPH2-(ALPH2-ALPH3)*BETA)*TP(M,I
     1,J)+ALPH1*TP(M,I,J-1)+2.*ALPH2*TP(M,I+1,J)+ALPH1*QTOP
     2+(ALPH2-ALPH3)*BETA*TGC(M,J)
   62 V1(I,J)=0.
      V2(I,J)=1.+ALPH2+(ALPH2-ALPH3)/2.*BETA
      V3(I,J)=-ALPH2
      V4(I,J)=(ALPH2+(ALPH2-ALPH3)/2.*BETA)*TP(M,I,J)-ALPH2
     1*TP(M,I+1,J)
```

```
C   THE BOTTOM BOUNDARY OF THE COIL
      J=1
      DO 35 I=2,IL-1
      CALL PARAMETERS(NTIGHT,M,IL,I,J,DCOR(M),DR(M),DZ(M),DT,
     1TP,ALPH1,ALPH2,ALPH3,FF,FC)
      TERM=2.*DZ(M)*BHTC(M,I)/FC
      U1(I,J)=0.
      U2(I,J)=1.+ALPH1/2.*(2.+TERM)
      U3(I,J)=-ALPH1
      U4(I,J)=(1.-ALPH1/2.*(2.+TERM)-2.*ALPH2)*TP(M,I,J)+ALP
     1H1*TP(M,I,J+1)+(ALPH2+ALPH3)*TP(M,I+1,J)+(ALPH2-ALPH3)
     2*TP(M,I-1,J)+ALPH1*TERM*TGB(M,I)
      V1(I,J)=(ALPH3-ALPH2)/2.
      V2(I,J)=1.+ALPH2
      V3(I,J)=-(ALPH2+ALPH3)/2.
      V4(I,J)=ALPH2*TP(M,I,J)-(ALPH2+ALPH3)/2.*TP(M,I+1,J)+
     1(ALPH3-ALPH2)/2.*TP(M,I-1,J)
   35 CONTINUE
C   THE TOP BOUNDARY OF THE COIL
      J=JL
      DO 40 I=2,IL-1
      CALL PARAMETERS(NTIGHT,M,IL,I,J,DCOR(M),DR(M),DZ(M),DT,
     1TP,ALPH1,ALPH2,ALPH3,FF,FC)
      IF (M .EQ. NCOILS) GOTO 43
      TERM=2.*DZ(M)*THTC(M,I)/FC
      GOTO 44
   43 CALL TOPLATE(NCOILS,IL,JL,DC,DCOR(M),DCOV,DPLAT,DR(M),H
     1,HCOV,TP,TTCOV,E1,E2,TFLU,QF,B1,HH,I,CYCLE)
      QTOP=2.*QF*DZ(M)/FC
   44 U1(I,J)=-ALPH1
      U2(I,J)=1.+ALPH1/2.*(2.+TERM)
      U3(I,J)=0.
      IF (M .EQ. NCOILS) GOTO 71
      U4(I,J)=(1.-ALPH1/2.*(2.+TERM)-2.*ALPH2)*TP(M,I,J)+ALP
     1H1*TP(M,I,J-1)+(ALPH2+ALPH3)*TP(M,I+1,J)+(ALPH2-ALPH3)
     2*TP(M,I-1,J)+ALPH1*TERM*TGT(M,I)
      GOTO 72
   71 U2(I,J)=1.+ALPH1
      U4(I,J)=(1.-ALPH1-2.*ALPH2)*TP(M,I,J)+ALPH1*TP(M,I,J-1)
     1+(ALPH2+ALPH3)*TP(M,I+1,J)+(ALPH2-ALPH3)*TP(M,I-1,J)
     2+ALPH1*QTOP
   72 V1(I,J)=(ALPH3-ALPH2)/2.
      V2(I,J)=1.+ALPH2
      V3(I,J)=-(ALPH2+ALPH3)/2.
      V4(I,J)=ALPH2*TP(M,I,J)-(ALPH2+ALPH3)/2.*TP(M,I+1,J)+
     1(ALPH3-ALPH2)/2.*TP(M,I-1,J)
   40 CONTINUE
C  USE ADI TO SOLVE FOR THE ESTIMATE OF TEMPERATURE
      CALL ESTMTRIDIAG(M,IL,JL,U1,U2,U3,U4,ES)
      DO 50 I=1,IL
      DO 50 J=1,JL
      V4(I,J)=V4(I,J)+ES(M,I,J)
   50 CONTINUE
```

```
C  USE ADI TO SOLVE FOR THE GRID TEMPERATURE
      CALL TEMPTRIDIAG(M,IL,JL,V1,V2,V3,V4,T)
      DO 100 I=1,IL
      DO 100 J=1,JL
      TP(M,I,J)=T(M,I,J)
C  COMPUTE THE AVERAGE WALL TEMPERATURE BETWEEN COILS
      IF ((J .NE. 1).OR.(J .NE. JL)) GOTO 100
      IF (M .GT.1) GOTO 86
      IF (J .EQ. 1) TW(M,I)=TP(M,I,J)
      IF (J .EQ. JL) ST=TP(M,I,J)
      GOTO 100
   86 IF (M .LT. NCOILS) GOTO 87
      IF (J .EQ. 1) TW(M,I)=(ST+TP(M,I,J))/2.
      IF (J .EQ. JL) TW(M+1,I)=TP(M,I,J)
      GOTO 100
   87 IF (J .EQ. 1) TW(M,I)=(ST+TP(M,I,J))/2.
      IF (J .EQ. JL) ST=TP(M,I,J)
  100 CONTINUE
C  COMPUTE THE LIMITING TEMPERATURES IN COILS
C  LL IS A FLAG: LL=0 FOR MIN. TEMP. & LL=1 FOR MAX. TEMP.
      LL=0
      CALL TLIMIT(M,LL,IL,JL,IMIN(M),JMIN(M),T,TMIN(M))
      LL=1
      CALL TLIMIT(M,LL,IL,JL,IMAX(M),JMAX(M),T,TMAX(M))
      IF (M .EQ. NCOILS) TCOV(M,JL)=TTCOV
      IF (M .EQ. 1) TGI(M)=TGA(M,1)+DTGA
      IF (M .NE. 1)TGI(M)=(TGA(M-1,JL)+TGA(M,1))/2.+DTGA
  120 CONTINUE
      TGI(NCOILS+1)=TGA(NCOILS,JL)+DTGA
C  COMPUTE THE MAX TEMP IN THE STACK
      TMAXX=TMAX(1)
      DO 127 M=2,NCOILS
      IF (TMAXX .GE. TMAX(M)) GOTO 127
      TMAXX=TMAX(M)
  127 CONTINUE
C  COMPUTE THE MIN TEMP IN THE STACK
      TMINM=TMIN(1)
      DO 135 M=2,NCOILS
      IF (TMINM .LE. TMIN(M)) GOTO 135
      TMINM=TMIN(M)
  135 CONTINUE
C  OUTPUT THE CURRENT RESULTS
      TIME=TIME+DT
      WRITE(2,2008) DT
      WRITE(2,2010) TIME
      IF (ABS(TMINM) .LT. TCON1) GOTO 128
      NS=NS+1
      IF (NS .EQ. 1) GOTO 130
      IF (ABS(TMINM) .GE. TCON2) GOTO 130
      IF (ABS(TMAXX) .LE. TCON3) GOTO 130
  128 IF (TIME .LE. 1.0) GOTO 130
      IF (K .EQ. KPR) GOTO 129
      GOTO 134
  129 KPR=KPR+KP0
  130 M=NCOILS
```

```
      IL=IFIX((DC(M)-DCOR(M))/(2.*DR(M))+0.1)+1
      WRITE(2,2021)
      MN=M+1
      WRITE(2,2011) MN,(TGT(M,I),I=1,IL)
  108 WRITE(2,2012) M
      J=IFIX(H(M)/DZ(M)+0.1)+1
      IL=IFIX((DC(M)-DCOR(M))/(2.*DR(M))+0.1)+1
  110 WRITE(2,2014) J,TGC(M,J),(T(M,I,J),I=1,IL),TGA(M,J),
     1TCOV(M,J),TFRN(M,J)
      J=J-1
      IF (J .GT. 0) GOTO 110
      WRITE(2,2013) TMIN(M),IMIN(M),JMIN(M)
      WRITE(2,2015) TMAX(M),IMAX(M),JMAX(M)
      WRITE(2,2011) M,(TGB(M,I),I=1,IL)
      M=M-1
      IF (M .GT. 0) GOTO 108
  134 CALL TMEAN(NCOILS,T,DC,DCOR,DR,DZ,H,TM)
      DO 132 M=1,NCOILS
      QCLO(M)=QCL1(M)
  132 CONTINUE
      WRITE(2,2017) TMINM,TMAXX
      WRITE(2,2018) TM
      WRITE(2,2020)
  145 QPLO=QPL1
      QSO=QS1
      QGO=QG1
      IF (NSOAK .GT. 0) GOTO 147
      IF (NCONT .EQ. 0) GOTO 146
      TMINM=TMIN(NCONT)
  146 IF (ABS(TMINM) .LT. TCON1) GOTO 15
      IF (NSOAK .GT. 0) GOTO 147
      HTIME=TIME
      HRATE=TOTW/HTIME
      WRITE(2,2026) HRATE
      NSOAK=K
      CYCLE=0
      WRITE(2,2009)
  147 IF (NCOOL .GT. 0) GOTO 149
      IF (NCONT .EQ. 0) GOTO 148
      TMINM=TMIN(NCONT)
  148 IF (ABS(TMINM) .LT. TCON2) GOTO 15
      IF (NCOOL .GT. 0) GOTO 149
      STIME=TIME-HTIME
      SRATE=TOTW/STIME
      WRITE(2,2028) SRATE
      HCRATE=TOTW/TIME
      WRITE(2,2030) HCRATE
      NK=NK+1
      NCOOL=K
      CYCLE=-1
      WRITE(2,2019)
  149 CALL COOLER(NTYPE,CFAN,TBAS,TFAN)
      TDIF=TFAN
      NK=NK+1
      IF (NCONT .EQ. 0) GOTO 150
      TMAXX=TMAX(NCONT)
```

```
  150 IF (ABS(TMAXX) .GT. TCON3) GOTO 15
      CTIME=TIME-STIME-HTIME
      CRATE=TOTW/CTIME
      TRATE=TOTW/TIME
      WRITE(2,2032) CRATE
      WRITE(2,2034) TRATE
      WRITE(2,2036) FUEL
      STOP
 1001 FORMAT(2I5,4F10.0)
 1002 FORMAT(5F10.0,/4F10.0)
 1003 FORMAT(5F10.0,/5F10.0,/5F10.0,/5F10.0)
 1103 FORMAT(5F10.0,/5F10.0,/5F10.0)
 1004 FORMAT(I5,F10.0,/I5,F10.0,/I5,F10.0,/I5,F10.0,/I5,F10.0)
 1104 FORMAT(I5,F10.0,/I5,F10.0,/I5,F10.0,/I5,F10.0)
 1005 FORMAT(2I5,8F8.0)
 1006 FORMAT(I5,6F10.0)
 2001 FORMAT(//27X,' STACK   DATA ',/27X,' ============',//20X,
     1' ALL DIMENSIONS IN METERS',//' NO.',3X,' O.D.',4X,' I.D.'
     2,4X,' HT.',3X,' WT.(TON)',3X,'VANES',3X,' V. HT.')
 2002 FORMAT(I3,39X,I6,3X,F7.3)
 2003 FORMAT(I3,2(2X,F7.2),F8.2,3X,F7.3)
 2004 FORMAT(33X,6('-'),/33X,F6.3,/33X,6('='))
 2005 FORMAT(/' THE EXCESS AIR =',F5.2,' %',/' THE ADIAB ',
     1' FLAME TEMP =',F7.0)
 2006 FORMAT(//' HEAT INTO STACK=',E10.4,'  (KWH)',/
     1' HEAT INTO GAS  =',E10.4,'  (KWH)')
 2007 FORMAT(///10X,'  START HEATING NOW',/12X,17('='))
 2008 FORMAT(/'  TIME INTERVAL=',F5.2,' H.')
 2009 FORMAT(///10X,'  START SOAKING NOW',/12X,17('='))
 2010 FORMAT(/' TIME ELAPSED =',F6.2,' H.')
 2011 FORMAT(/' GAS TEMP IN PL(',I1,')',6F6.0,/)
 2012 FORMAT('  COIL NO.(',I2,'):')
 2013 FORMAT(/10X,' MIN TEMP IN COIL =',F6.0,3X,' LOCATED AT I='
     1,I1,' & J=',I1)
 2014 FORMAT(/,2X,' J=',I2,F8.0,3X,6F6.0,F7.0,F6.0,F8.0)
 2015 FORMAT(/10X,' MAX TEMP IN COIL =',F6.0,3X,' LOCATED AT I='
     1,I1,' & J=',I1)
 2016 FORMAT(/5X,' TOTAL FUEL BURNED SO FAR =',F6.1,'  (KG)')
 2017 FORMAT(/5X,' MIN TEMP IN STACK =',F7.0,3X,
     1' AND    MAX TEMP IN STACK =',F7.0)
 2018 FORMAT(/25X,' THE MEAN TEMP. OF STACK =',F7.0)
 2019 FORMAT(///10X,'  START COOLING NOW',/12X,17('='))
 2020 FORMAT(/23X,35('*'))
 2021 FORMAT(/9X,' TGC',6X,' I=1',2X,' I=2',2X,' I=3',
     12X,' I=4',2X,' I=5',2X,' I=6',3X,' TGA',2X,' TCOV'
     2,2X,' TFUR')
 2026 FORMAT(/10X,' THE HEATING OUTPUT =',E10.3,' (TON/H.)')
 2028 FORMAT(/10X,' THE SOAKING OUTPUT =',E10.3,' (TON/H.)')
 2030 FORMAT(/10X,' THE OVERALL HEATING OUTPUT =',E10.3,
     1' (TON/H.)')
 2032 FORMAT(/10X,' THE COOLING OUTPUT =',E10.3,' (TON/H.)')
 2034 FORMAT(/10X,' THE OVERALL ANNEALING OUTPUT =',E10.3,
     1' (TON/H.)')
 2036 FORMAT(/10X,' THE TOTAL FUEL BURNED =',F8.1,'  (KG)')
      END
```

```
C
C   ****************************************************************
C   *  SUBROUTINE OF GUASS ELIMINATION TO SOLVE THE MATRIX OF      *
C   *  THE FIRST ESTIMATE OF TEMPERATURE PROFILE IN THE COIL       *
C   ****************************************************************
      SUBROUTINE ESTMTRIDIAG(M,IL,JL,U1,U2,U3,U4,ES)
      DIMENSION U1(8,9),U2(8,9),U3(8,9),U4(8,9),ES(5,8,9)
      DIMENSION A(9),B(9),C(9),D(9),X(9),BETA(9),DELT(9)
      DO 50 I=1,IL
      DO 10 J=1,JL
      A(J)=U1(I,J)
      B(J)=U2(I,J)
      C(J)=U3(I,J)
      D(J)=U4(I,J)
   10 CONTINUE
      BETA(1)=B(1)
      DELT(1)=D(1)
      DO 20 J=2,JL
      BETA(J)=B(J)-A(J)*C(J-1)/BETA(J-1)
      DELT(J)=D(J)-A(J)*DELT(J-1)/BETA(J-1)
   20 CONTINUE
      J=JL
      X(J)=DELT(J)/BETA(J)
   30 J=J-1
      X(J)=(DELT(J)-C(J)*X(J+1))/BETA(J)
      IF (J .GT. 1) GOTO 30
      DO 40 J=1,JL
      ES(M,I,J)=X(J)
   40 CONTINUE
   50 CONTINUE
      RETURN
      END
C
C   ****************************************************************
C   *  SUBROUTINE OF GUASS ELIMINATION TO SOLVE THE MATRIX OF      *
C   *  THH FINAL SOLUTION OF TEMPERATURE PROFILE IN THE COIL       *
C   ****************************************************************
      SUBROUTINE TEMPTRIDIAG(M,IL,JL,V1,V2,V3,V4,T)
      DIMENSION V1(8,9),V2(8,9),V3(8,9),V4(8,9),T(5,8,9)
      DIMENSION A(8),B(8),C(8),D(8),X(8),BETA(8),DELT(8)
      DO 50 J=1,JL
      DO 10 I=1,IL
      A(I)=V1(I,J)
      B(I)=V2(I,J)
      C(I)=V3(I,J)
      D(I)=V4(I,J)
   10 CONTINUE
      BETA(1)=B(1)
      DELT(1)=D(1)
      DO 20 I=2,IL
      BETA(I)=B(I)-A(I)*C(I-1)/BETA(I-1)
      DELT(I)=D(I)-A(I)*DELT(I-1)/BETA(I-1)
   20 CONTINUE
```

```
      I=IL
      X(I)=DELT(I)/BETA(I)
   30 I=I-1
      X(I)=(DELT(I)-C(I)*X(I+1))/BETA(I)
      IF (I .GT. 1) GOTO 30
      DO 40 I=1,IL
      T(M,I,J)=X(I)
   40 CONTINUE
   50 CONTINUE
      RETURN
      END
C
C  ****************************************************************
C  *  SUBPROGRAM TO CALCULATE THE COEFFICIENTS OF THE MATRIX      *
C  *  OF THE PARTIAL DIFFERENTIAL EQUATION. THIS CALLS THE        *
C  *  SUBROUTINES OF CONDUCTIVITY AND THERMAL CAPACITY OF         *
C  *  STEEL AS WELL AS THOSE OF GAS CONDUCTIVITY AND              *
C  *  CORRECTION FOR RADIAL CONDUCTIVITY                          *
C  ****************************************************************
      SUBROUTINE PARAMETERS(N,M,IL,I,J,DCOR,DR,DZ,DT,TP,A1,
     1A2,A3,FF,FC)
      DIMENSION TP(5,6,9)
      R=DCOR/2.+FLOAT(I-1)*DR
      CALL STEELCOND(TP(M,I,J),FC)
      CALL STEELCAP(TP(M,I,J),FP,FR)
      IF (N .EQ. 1) GOTO 15
      CALL STEELINEXP(TP(M,I,J),FL)
      CALL GASCOND(TP(M,I,J),FU)
      C1=FL*FC/FU
      IF (I .EQ. 1) GOTO 5
      IF (TP(M,I-1,J) .GE.TP(M,I+1,J)) GOTO 15
      CALL RADCOND(TP(M,I-1,J),TP(M,I,J),TP(M,I+1,J),R,DR,
     1C1,FF,FD)
      GOTO 20
    5 IF (TP(M,I,J) .GE. TP(M,I+1,J)) GOTO 15
      CALL RADCOND(TP(M,I,J),TP(M,I,J),TP(M,I+1,J),R,DR,C1,
     1FF,FD)
      GOTO 20
   15 FF=1.
      FD=0.
   20 ZZ=FC/(FP+FR*TP(M,I,J))
      A1=ZZ*DT/DZ**2
      A2=ZZ*DT*FF/DR**2
      A3=ZZ*DT*(FF/R+FD)/(2.*DR)
      RETURN
      END
```

```
C   ***************************************************************
C   *   THIS SUBPROGRAM SOLVES THE HEAT BALANCE EQUATION OVER     *
C   *   THE COOLER TO COMPUTE THE TEMPERATURE OF THE INERT GAS    *
C   *   LEAVING THE COOLER AND ENTERING THE STACK                 *
C   ***************************************************************
      SUBROUTINE COOLER(N,RATE,TH,TC)
      A=2.93E-4
      B=-3.40E-8
      C=7.22E-11
      D=-3.79E-14
      E=8.05E-18
      TC=500.
      U=20483.4*RATE
      IF (N .EQ. 1) GOTO 10
      Q=-567.09+2.167*TH-1.182E-3*TH**2+4.07E-7*TH**3
      GOTO 20
   10 Q=0.938*TH-278.641
   20 FN=U*(A/TC+B+C*TC+D*TC**2+E*TC**3)*(TH-TC)-Q
      FD=U*(TH*(-A/TC**2+C+2.*D*TC+3.*E*TC**2)-B-2.*C*TC-3.
     1*D*TC**2-4.*E*TC**3)
      TC=TC-FN/FD
      IF (ABS(FN/FD) .GT. 1.) GOTO 20
      RETURN
      END
C
C   ***************************************************************
C   *   THIS IS THE CORRELATION OF THE THERMAL CONDUCTIVITY OF    *
C   *   STEEL WITH TEMPERATURE                                    *
C   ***************************************************************
      SUBROUTINE STEELCOND(T,FC)
      IF (T .GE. 1080.) GOTO 10
      FC=3.836E-2+1.152E-4*T-3.140E-7*T**2+3.007E-10*T**3-1
     1.1E-13*T**4
      GOTO 20
   10 FC=0.01365+1.089E-5*T
   20 RETURN
      END
C
C   ***************************************************************
C   *   THIS THE CORRELATION OF THE VOLUMETRIC THERMAL CAPACITY   *
C   *   OF STEEL AS A FUNCTION OF TEMPERATURE                     *
C   ***************************************************************
      SUBROUTINE STEELCAP(T,FP,FR)
      FP=0.6352+2.1455E-3*T-3.8131E-6*T**2+3.1345E-9*T**3
      FR=2.1455E-3-7.6262E-6*T+9.4035E-9*T**2
      RETURN
      END
```

```
C
C   ***************************************************************
C   *  THIS IS THE VOLUMETRIC ENTHALPY OF STEEL CORRELATED AS     *
C   *  A FUNCTION OF TEMPERATURE                                  *
C   ***************************************************************
      SUBROUTINE STEELVENT(T,FV)
      IF (T .LE. 900.) GOTO 10
      IF (T .GT. 1273.) GOTO 20
      FV=-9021.+12.004*T+1.35E-3*T**2+3.019E-6*T**3-5.506E-9
     1*T**4
      GOTO 30
   10 FV=-385.2+1.642*T-1.23E-3*T**2+1.186E-6*T**3+4.285E-10
     1*T**4
      GOTO 30
   20 FV=-492.5+1.5225*T
   30 RETURN
      END
C
C   ***************************************************************
C   *  THIS IS THE FUNCTION OF THE THERMAL LINEAR EXPANSION       *
C   *  OF STEEL WITH THE TEMPERATURE                              *
C   ***************************************************************
      SUBROUTINE STEELINEXP(T,FL)
      IF (T .LT. 975.) GOTO 10
      IF (T .GE. 1173.) GOTO 20
      FL=6.541E-5-4.141E-8*T-2.222E-11*T**2-1.006E-14*T**3+
     12.239E-17*T**4
      GOTO 30
   10 FL=1.052E-5+4.443E-9*T
      GOTO 30
   20 FL=1.234E-6+9.53E-9*T
   30 RETURN
      END
C
C   ***************************************************************
C   *  THIS IS THE SUBROUTINE FOR THE CALCULATION OF THE          *
C   *  CORRECTION FACTOR OF THE THERMAL CONDUCTIVITY IN           *
C   *  THE RADIAL DIRECTION                                       *
C   ***************************************************************
      SUBROUTINE RADCOND(T1,T2,T3,R,DR,C1,FF,FD)
      FF=1./(1.+C1*R*(T3-T1)/(2.*DR))
      FD=-C1*((T3-T1)/(2.*DR)+R*(T3-2.*T2+T1)/DR**2)/(1.+C1
     1*R*(T3-T1)/(2.*DR))**2
      RETURN
      END
C
C   ***************************************************************
C   *  THIS IS A FUNCTION OF THE PHYSICAL PROPERTIES OF THE       *
C   *  GAS IN TERMS OF TMPERATURE EXPRESSED AS FOLLOWS            *
C   *  CP**(.4)*K**(.6)/MEW**(.4)                                 *
C   ***************************************************************
      SUBROUTINE GASPROP(T,FY)
      FY=1.595E-4+1.55E-7*T-1.276E-10*T**2+1.133E-13*T**3-
     13.988E-17*T**4
      RETURN
      END
```

```
C
C   ***************************************************************
C   * THIS IS A FUNCTION OF THE PHYSICAL PROPERTIES OF THE        *
C   *  GAS IN TERMS OF TEMPERATURE EXPRESSED AS FOLLOWS           *
C   *  CP**(1/3)*K**(2/3)/MEW**(1/3)                              *
C   ***************************************************************
      SUBROUTINE GASPROPY(T,FA)
      FA=9.406E-5+1.895E-7*T-1.692E-10*T**2+1.36E-13*T**3-
     14.412E-17*T**4
      RETURN
      END
C
C   ***************************************************************
C   *  THIS CALCULATES THE SPECIFIC HEAT OF THE INERT GAS         *
C   *  AS FUNCTION OF TEMPERATURE                                 *
C   ***************************************************************
      SUBROUTINE GASPHEAT(T,FS)
      FS=2.93E-4-3.4014E-8*T+7.223E-11*T**2-3.794E-14*T**3+
     18.U5E-18*T**4
      RETURN
      END
C
C   ***************************************************************
C   *  THIS IS THE RELATIONSHIP OF THE ENTHALPY OF THE INERT      *
C   *  GAS WITH TEMPERATURE                                       *
C   ***************************************************************
      SUBROUTINE GASENTH(T,FE)
      FE=-9.34E-2+3.182E-4*T
      RETURN
      END
C
C   ***************************************************************
C   *  THIS IS THE THERMAL CONDUCTIVITY OF THE INERT GAS AS       *
C   *  A FUNCTION OF TEMPERATURE                                  *
C   ***************************************************************
      SUBROUTINE GASCOND(T,FU)
      FU=8.384E-6+5.606E-8*T
      RETURN
      END
C
C   ***************************************************************
C   *  THIS IS THE SPECIFIC HEAT OF THE COMBUSTION PRODUCTS       *
C   *  CALCULATED AS A FUNCTION OF TEMPERATURE                    *
C   ***************************************************************
      SUBROUTINE SPHCOMPROD(T,FO)
      FO=2.972E-4+2.303E-8*T+1.721E-11*T**2-5.819E-15*T**3
      RETURN
      END
```

```
C
C   ***********************************************************
C   *  THIS SUBPROGRAM CALCULATES THE FLOW DISTRIBUTION OF    *
C   *  NITROGEN BETWEEN THE CONVECTOR PLATES AND THE TOTAL    *
C   *  PRESSURE DROP IN THE STACK.                            *
C   ***********************************************************
      SUBROUTINE DISTRIBN(NCOILS,H,VLEN,DC,DCOV,DHOL,DCLR,
     1DCOR,DPLAT,HSTACK,CFAN,TGC,TGI,TFAN,TDIF,NC,B,WO,WI
     2,FLOW,F)
      DIMENSION NC(5),H(5),FRAC(5),F(5),TGI(5),EA(5),EB(5),
     1EC(5),DCOR(5),DC(5),TGC(5,9),B(5)
      SORF=((DCOR(NCOILS)/DHOL)**4-1.)*(1.-(DHOL/DCOR(NCOILS))
     1**2)/.36
      DO 10 M=1,NCOILS
      SCOV=(((DCOV-DC(M))/(DCOV-DPLAT))**4-1.)*(1.-((DCOV-
     1DPLAT)/(DCOV-DC(M)))**2)
      Y=(CFAN/DCOR(M)**2)**2
      IF ((M .EQ. 1).OR.(M .EQ. NCOILS)) GOTO 5
      IF (DC(M) .GT. DC(M+1)) GOTO 5
      DLAR=DC(M+1)
      GOTO 8
    5 DLAR=DC(M)
      IF (M .GT. 1) GOTO 7
      AL=(DLAR-DCOR(M))/2.
      GOTO 8
    7 AL=VLEN*(DLAR-DCOR(M))/(DPLAT-DCLR)
    8 EA(M)=1.864E-9*(CFAN/(NC(M)*B(M)*WO))**2*(1.+.01*AL/
     1WI*(1.+WO/WI+2.*WO/B(M)))
      EB(M)=6.043E-9*SCOV*(CFAN/(DCOV**2-DC(M)**2))**2
      EC(M)=2.417E-8*H(M)/DCOR(M)*Y
   10 CONTINUE
      ED=6.043E-9*SORF*Y
      NUM=NCOILS+1
      EA(NUM)=1.864E-9*(CFAN/(NC(NUM)*B(NUM)*WO))**2*(1.+.01
     1*AL/WI*(1.+WO/WI+2.*WO/B(NUM)))
      WRITE(2,101)
      FRAC(NUM)=.1
   15 FCUM=FRAC(NUM)
      N=NUM-1
      TI=(TGC(N,1)+TGC(N+1,1))/2.
      PDCC=EA(N+1)*TGI(N+1)
      PDUC=EB(N-1)*TDIF
      PDCS=EC(N)*TI
      SUM1=PDCC+PDUC+PDCS
      FRAC(N)=FRAC(N+1)*SQRT(SUM1/(EA(N)*TGI(N)))
      FCUM=FCUM+FRAC(N)
      PDSTAK=SUM1
   20 N=N-1
      SCC=EA(N+1)*TGI(N+1)*FRAC(N+1)**2
      IF (N .EQ. 1) GOTO 21
      SUC=EB(N-1)*TDIF*FCUM**2
      GOTO 22
```

```
   21 SUC=EB(1)*TDIF*FCUM**2
   22 SCS=(EC(N)*FCUM**2+ED*(FCUM-FRAC(N+1))**2)*TI
      SUM=SCC+SUC+SCS
      FRAC(N)=SQRT(SUM/(EA(N)*TGI(N)))
      PDSTAK=PDSTAK+SUM
      FCUM=FCUM+FRAC(N)
      IF (N .GT. 1) GOTO 20
      IF (ABS(FCUM-1.) .LE. .005) GOTO 25
      FRAC(NUM)=FRAC(NUM)/FCUM
      GOTO 15
   25 TOTF=0.
      DO 100 N=1,NCOILS+1
      F(N)=FLOW*FRAC(N)
      TOTF=TOTF+F(N)
      WRITE(2,102) N,F(N),FRAC(N)
  100 CONTINUE
      WRITE(2,104) TOTF
      WRITE(2,103) PDSTAK
  101 FORMAT(/' THE FLOW DISTRIBUTION IN CONVECTOR PLATES:'
     1,//' NO.',4X,' FLOW(KG/H)',6X,' FRACTN.')
  102 FORMAT(5(I3,4X,F11.2,8X,F7.4))
  103 FORMAT(//' TOTAL PRESSURE DROP IN THE STACK=',F7.4,
     1'  (MM.W.G.)')
  104 FORMAT(9X,9('-'),/10X,F8.2)
      RETURN
      END
C
C  ************************************************************
C  *  THIS IS THE COMPUTATION OF THE PROFILE OF THE HEAT       *
C  *  TRANSFER COEFFICIENTS AND THE GAS TEMPERATURE           *
C  *  DISTRIBUTION IN THE CONVECTIVE CHANNELS OF THE          *
C  *  CONVECTOR PLATES. THIS CALCULATION IS BASED ON THE      *
C  *  FLOW DISTRIBUTION OF THE INERT GAS BETWEEN PLATES       *
C  ************************************************************
      SUBROUTINE CONVECTORS(NCOILS,IL,JL,M,J,DC,DCOR,DR,TW,F,
     1CHTC,NC,B,WO,WI,VLEN,TG,TGA,TGO)
      DIMENSION DC(5),TG(5,8),TGA(5,9),TW(5,8),CHTC(5,8)
      IF ((M .EQ. 1).AND.(J .EQ. 1)) GOTO 5
      IF ((M .EQ. NCOILS).AND.(J .EQ. JL)) GOTO 5
      IF (M .LT. NCOILS) GOTO 3
      IF (M .EQ. NCOILS) GOTO 4
      GOTO 7
    3 IF (DC(M) .GT. DC(M+1)) GOTO 5
      DLAR=DC(M+1)
      IF (J .EQ. JL) TG(M,IL)=(TGA(M,JL)+TGA(M+1,1))/2.
      GOTO 8
    4 IF (DC(M) .GT. DC(M-1)) GOTO 5
      DLAR=DC(M-1)
      GOTO 8
    7 DLAR=DC(NCOILS)
      GOTO 8
    5 DLAR=DC(M)
      TG(M,IL)=TGA(M,J)
    8 AL=(DLAR-DCOR)/2.
      IF (J .EQ. 1) GOTO 9
```

```
      DO 17 I=1,IL
   17 TW(M,I)=TW(M+1,I)
    9 U=VLEN/(2.*(WO-WI))
      I=IL
   10 Z=FLOAT(I-1)*DR
      W=WI+(WO-WI)*Z/AL
      X=U*(ALOG(WO/W)+(WO-W)/B)
      IF ((X .GT. .4).AND.(X .LT. 24.)) GOTO 15
      Y=0.25
      GOTO 20
   15 Y=0.418+0.204*ALOG(X)
   20 CALL GASPROP(TG(M,I),FY)
      D1=.023*FY*(F/FLOAT(NC))**(.8)
      CHTC(M,I)=D1*(W+B)**(.2)/(Y*W*B)
      CALL GASPHEAT(TG(M,I),FS)
      RR=DCOR/2.+Z
      TERM=3.1416*(2.*RR-DR)*DR*CHTC(M,I)
      IF ((M .EQ. 1).AND.(J .EQ. 1)) TERM=TERM/2.
      DEN=F*FS+TERM/2.
      I=I-1
      IF (I .LT. 1) GOTO 30
      TG(M,I)=((F*FS-TERM/2.)*TG(M,I+1)+TERM*TW(M,I))/DEN
      IF (I .GE. 1) GOTO 10
   30 TGO=TG(M,1)
      RETURN
      END
C
C  ***************************************************************
C  *  THIS SUBROUTINE CALCULATES THE TEMPERATURE OF THE          *
C  *  FURNACE GAS BASED ON THE COMBUSTION ADIABATIC FLAME        *
C  *  TEMPERATURE. IT ALSO CALCULATES THE RATE OF FUEL           *
C  *  FIRING IN THE FURNACE TOGETHER WITH THE THERMAL            *
C  *  EFFICIENCY OF THE FURNACE.                                 *
C  ***************************************************************
      SUBROUTINE FIRING(QSTAK,QGAS,DREF,DCAS,DCOV,RCOEF,TFLU
     1,TADB,TCC,HFUR,FRATE,E1,EXAIR,TCONT,TFR,FHEAT)
      SIG=56.71E-12
      IF (TCONT .GT. 1000.) GOTO 10
      F21=DCOV/DREF
      F23=1.-F21
      F31=F21
      F33=F23
      EP1=SIG*TCC**4
      EPG=SIG*TADB**4
      TOTMOL=10.879+9.868*(EXAIR-1.)
      PCO2=1.017/TOTMOL
      PSUM=2.978*PCO2
      PR=0.875*PSUM*(DREF-DCOV)
      F=.02668+1.236*PR-5.676*PR**2+17.46*PR**3-30.31*PR**4
     1+26.71*PR**5-9.291*PR**6
      EG=(2.7-TADB/1000.)*F
```

```
      A1=1.
      A3=-(1.-E1)*(1.-EG)
      A5=E1*EP1+EG*(1.-E1)*EPG
      B1=-(1.-EG)*F31
      B3=1.-(1.-EG)*F33
      B5=EG*EPG
      W3=(A5*B1-A1*B5)/(A3*B1-A1*B3)
      W1=A5-A3*W3
      W2=EG*EPG+(1.-EG)*(W1*F21+W3*F23)
      TFR=(W2/SIG)**(0.25)
   10 CALL SPHCOMPROD(TFLU,CP)
      AA=(1.+17.05*EXAIR)*CP*TFLU
      TOPLOS=.7854*DREF**2*RCOEF*(TFLU-350.)
      BB=3.1416*DCAS*RCOEF
      SIDLOS=BB*HFUR*((TFR+TFLU)/2.-350.)
      FRATE=(QSTAK+QGAS+TOPLOS+SIDLOS)/(FHEAT-AA)
      WRITE(2,102) TFR
  102 FORMAT(/15X,' TFUR =',F8.0)
      EFF=QSTAK/(FRATE*FHEAT)
      WRITE(2,101) FRATE,EFF
  101 FORMAT(/15X,' THE FIRING RATE =',E10.4,' KG/H',/15X,
     1' THERM. EFF.=',F6.2,' %')
      RETURN
      END
C
C   ***************************************************************
C   *   THIS PROGRAM CALCULATES THE TEMPERATURE DISTRIBUTION *
C   *   AND THE PROFILE OF HEAT TRANSFER COEFFICIENTS IN THE *
C   *   CORE OF THE STACK.                                    *
C   ***************************************************************
      SUBROUTINE CORE(NCOILS,H,F,B,DCOR,DHOL,DZ,TP,TGO,TGC
     1,TBAS,HTCOR)
      DIMENSION F(5),H(5),B(5),TGO(5),TGC(5,9),TP(5,8,9),
     1DCOR(5),DZ(5),HTCOR(5,9)
      M=NCOILS
      J=IFIX(H(M)/DZ(M)+.1)+1
      JL=J
      FCOR=F(M+1)
      TGC(M,J)=TGO(M+1)
      Y=0.25
      IF (TGC(M,J) .LT. TP(M,1,J)) GOTO 8
      Z=1.
      GOTO 9
    8 Z=(TGC(M,J)/TP(M,1,J))**(.49)
    9 CALL GASPROP(TGC(M,J),FY)
      HTCOR(M,J)=0.0279*Z*FY*FCOR**(.8)/(Y*DCOR(M)**(1.8))
      PTH=.01
      HCOR=PTH+B(M+1)
    5 J=J-1
      HCOR=HCOR+DZ(M)
      X=HCOR/DCOR(M)
      IF (X .GE. .4) GOTO 10
      Y=.25
      GOTO 13
```

```
   10 Y=.418+.204*ALOG(X)
   13 IF (TGC(M,J+1) .LT. TP(M,1,J+1)) GOTO 15
      Z=1.
      GOTO 18
   15 Z=(TGC(M,J+1)/TP(M,1,J+1))**(.49)
   18 CALL GASPROP(TGC(M,J+1),FY)
      CALL GASPHEAT(TGC(M,J+1),FS)
      HTCOR(M,J)=.0279*Z*FY*FCOR**(.8)/(Y*DCOR(M)**(1.8))
      TW=(TP(M,1,J)+TP(M,1,J+1))/2.
      TERM=3.1416*DZ(M)*DCOR(M)*HTCOR(M,J)
      DEN=FCOR*FS+TERM/2.
      TGC(M,J)=((FCOR*FS-TERM/2.)*TGC(M,J+1)+TERM*TW)/DEN
      IF (J .GT. 1) GOTO 5
      HCOR=HCOR+PTH+2.*B(M+1)
      IF (M .EQ. 1) TBAS=TGC(M,J)
      TTEM=TGC(M,J)
      FTEM=FCOR
      M=M-1
      IF (M .LT. 1) GOTO 20
      J=IFIX(H(M)/DZ(M)+.1)+1
      JL=J
      FCOR=FCOR+F(M+1)
      TGC(M,J)=(FTEM*TTEM+F(M+1)*TGO(M+1))/FCOR
      HCOR=HCOR+PTH+B(M+1)
      X=HCOR/DCOR(M)
      IF (X .GE. .4) GOTO 35
      Y=.25
      GOTO 40
   35 Y=.418+.204*ALOG(X)
   40 IF (TGC(M,J) .LT. TP(M,1,J)) GOTO 48
      Z=1.
      GOTO 49
   48 Z=(TGC(M,J)/TP(M,1,J))**(.49)
   49 CALL GASPROP(TGC(M,J),FY)
      HTCOR(M,J)=0.0279*Z*FY*FCOR**(.8)/(Y*DCOR(M)**(1.8))
      GOTO 5
   20 RETURN
      END
C
C  ***************************************************************
C  *  THIS SUBROUTINE SOLVES THE RADIATIVE AND CONVECTIVE        *
C  *  HEAT TRANSFER AT THE TOP CONVECTOR PLATE AND COMPUTES      *
C  *  THE HEAT FLUX TO THE TOP COIL IN THE STACK.                *
C  ***************************************************************
      SUBROUTINE TOPLATE(NCOILS,IL,JL,DC,DCOR,DCOV,DPLAT,DR
     1,H,HCOV,TP,TTCOV,E1,E2,TFLU,FLUX,B1,HH,I,CYCLE)
      DIMENSION DC(5),B1(5),H(5),TP(5,8,9)
      IF (CYCLE .LT. 0) TFLU=300.
      PTH=.01
      THIK=B1(1)+PTH
      M=NCOILS
      DO 10 N=2,M
      THIK=THIK+2.*B1(N)+PTH
   10 CONTINUE
```

```
      THIK=THIK+PTH+B1(NCOILS+1)
      DISH=.25
      HSS=HCOV-HH-THIK
      A=DCOV**2+4.*DCOV*HSS+4.*DISH**2
      B=DC(M)**2-DCOR**2
      SUM=0.
      RAD=DCOR/2.
      DO 20 II=1,IL-1
      TEMP=(TP(M,II,JL)+TP(M,II+1,JL))/2.
      C=2.*RAD*DR+DR**2
      SUM=SUM+C*TEMP**4
      RAD=RAD+DR
   20 CONTINUE
      TTOP=(4.*SUM/B)**(.25)
   30 T=(TTOP+TTCOV)/2.
      TATM=TFLU
      CALL GASPROPY(T,FA)
      A1=5.671E-11*E1*E2*A/(E2*A+E1*(1.-E2)*B)
      A2=120.16*DPLAT**2*FA/(T*B)
      A3=224.29*A*FA/(T*B)
      A4=7.372E-11*E2*A/B
      IF(CYCLE .LT. 0) GOTO 35
      F1=A1*(TTCOV**4-TTOP**4)+A2*(TTCOV-TTOP)**(4./3.)
      F2=A3*(TATM-TTCOV)**(4./3.)+A4*(TATM**4-TTCOV**4)
      E=F2-F1
      DE=-4.*(A1+A4)*TTCOV**3-4./3.*(A2*(TTCOV-TTOP)**
     1(1./3.)+A3*(TATM-TTCOV)**(1./3.))
      GOTO 50
   35 IF (TTCOV .GT. TTOP) GOTO 40
      F1=A1*(TTOP**4-TTCOV**4)+A2*(TTOP-TTCOV)**(4./3.)
      F2=A3*(TTCOV-TATM)**(4./3.)+A4*(TTCOV**4-TATM**4)
      E=F2-F1
      DE=4.*(A1+A4)*TTCOV**3+4./3.*(A2*(TTOP-TTCOV)**
     1(1./3.)+A3*(TTCOV-TATM)**(1./3.))
      GOTO 50
   40 F1=A1*(TTCOV**4-TTOP**4)+A2*(TTCOV-TTOP)**(4./3.)
      F1=-F1
      F2=A3*(TTCOV-TATM)**(4./3.)+A4*(TTCOV**4-TATM**4)
      E=F2-F1
      DE=4.*(A1+A4)*TTCOV**3+4./3.*(A2*(TTCOV-TTOP)**
     1(1./3.)+A3*(TTCOV-TATM)**(1./3.))
   50 TTCOV=TTCOV-E/DE
      IF (ABS(E/DE) .GT. 1.) GOTO 30
      IF (TTCOV .GT. TP(M,I,JL)) GOTO 60
      FLUX=-A1*(TP(M,I,JL)**4-TTCOV**4)-A2*(TP(M,I,JL)-
     1TTCOV)**(4./3.)
      GOTO 70
   60 FLUX=A1*(TTCOV**4-TP(M,I,JL)**4)+A2*(TTCOV-TP(M,I
     1,JL))**(4./3.)
   70 RETURN
      END
```

```
C
C   ***************************************************************
C   *   THIS SUBPROGRAM SOLVES THE ENERGY BALANCE BETWEEN         *
C   *   THE OUTER PERIPHERY OF THE COIL,THE INNER COVER,THE       *
C   *   INERT GAS AND THE COMBUSTION PRODUCTS OR THE              *
C   *   AMBIENT ATMOSPHERE. FORM THIS HEAT BALANCE THE            *
C   *   TEMPERATURE OF THE COVER AT THE AXIAL LOCATION IS         *
C   *   CALCULATED. IT ALSO CALCULATES THE TEMPERATURE            *
C   *   PROFILE OF THE NITROGEN IN THE ANNULUS BETWEEN THE        *
C   *   COVER AND THE STACK.                                      *
C   ***************************************************************
      SUBROUTINE COVER(IL,JL,M,J,DR,DZ,E1,E2,DC,DCOV,DREF,
     1FLOW,FRATE,TDIF,TGA,TFURN,TP,H,F,EQ,B1,EXAIR,TCOV,K,
     1QOUT,CYCLE)
      DIMENSION DC(5),FG(5),F(5),TP(5,8,9),TCOV(5,9),CCOEF
     1(9),TGA(5,9),TGP(5,9),B1(5),H(5)
      CALL RADATA(DC(M),DCOV,DREF,E2,EXAIR,TFURN,TERM)
      PTH=.01
      AIR=17.05*EXAIR
      HMD=DCOV-DC(M)
      IF(M .EQ. 1) GOTO 4
      FG(M)=FG(M-1)-F(M)
      GOTO 5
    4 FG(M)=FLOW-F(M)
    5 D1=.0279*DCOV/((DCOV+DC(M))**(1.8)*HMD)
      D0=.0279*DCOV/((DREF+DCOV)**(.8)*(DREF-DCOV)*DC(M))
      IF (M .EQ. 1) GOTO 6
      BM=B1(1)
      HM=0.
      DO 3 MM=2,M
      BM=BM+2.*B1(MM)
    3 HM=HM+H(MM-1)
      HCUM=BM+HM+FLOAT(M)*PTH+FLOAT(J-1)*DZ
      GOTO 8
    6 HCUM=B1(1)+PTH+FLOAT(J-1)*DZ
    8 X=HCUM/HMD
      IF ((X .GT. 1.).AND.(X .LT. 24.)) GOTO 10
      IF (X .GE. 24.) GOTO 9
      Y=.25
      GOTO 15
    9 Y=1.
      GOTO 15
   10 Y=.418+.204*ALOG(X)
   15 CALL GASPHEAT(TGP(M,J),FS)
      CALL GASPROP(TGP(M,J),FY)
      CALL SPHCOMPROD(TFURN,FO)
      CCOEF(J)=D1*FY*FG(M)**(.8)/Y
      D3=EXP((0.7854*(DCOV+DC(M))**2*DZ*CCOEF(J))/(DCOV*
     1FG(M)*FS))
      C1=CCOEF(J)
      C2=5.671E-11/((1.-E2)/E2+DC(M)/DCOV*(1.-E1)/E1+1.)
      C3=D0*FY*((1.+AIR)*FRATE)**(.8)
      C4=5.671E-11/TERM
      DEL=-FG(M)*FS*DCOV*(1.-1./D3)/(FO*(1.+AIR)*FRATE*
     1(DCOV+DC(M)))
```

```
      TCOV(M,J)=600.
      IF (CYCLE .LT. 0) GOTO 16
      CALL NEWRAPH1(C1,C2,C3,C4,DEL,TCOV(M,J),TFURN,TP
     1(M,IL,J))
      GOTO 17
   16 C5=0.429*DCOV/DC(M)
      C6=7.371E-11*E2
      CALL NEWRAPH2(C1,C2,C5,C6,TCOV(M,J),TFURN,TP(M,IL,J))
   17 EQ=C1+4.*C2*TP(M,IL,J)**3
      QOUT=C1*TCOV(M,J)+C2*(TCOV(M,J)**4+3.*TP(M,IL,J)**4)
C  CALCULATE THE TEMP. OF THE GAS IN THE ANNULUS
      IF (M .EQ. 1) GOTO 18
      IF (J .EQ. 1) GOTO 19
      GOTO 20
   18 IF (J .EQ. 1) GOTO 21
      GOTO 20
   19 TGA(M,J)=TOPG/D3+(1.-1./D3)*(DCOV*TCOV(M,J)
     1+DC(M)*TP(M,IL,J))/(DCOV+DC(M))
      GOTO 25
   20 TGA(M,J)=TGA(M,J-1)/D3+(1.-1./D3)*(DCOV*TCOV(M,J)+DC
     1(M)*TP(M,IL,J))/(DCOV+DC(M))
      GOTO 25
   21 DTG=30.
      IF (CYCLE .LT. 0) DTG=0.
      TGA(M,J)=TDIF+DTG
   25 TGP(M,J)=TGA(M,J)
      IF (J .EQ. JL) TOPG=TGA(M,J)
      RETURN
      END
C
      SUBROUTINE NEWRAPH1(C1,C2,C3,C4,X,TC,TF,TP)
   10 F1=C1*(TC-TP)+C2*(TC**4-TP**4)
      F2=C3*(TF-TC)+C4*TF*(TF**3-TC**3)
      E=F2-F1
      DE=-C1-C3-3.*C4*TF*TC**2-4.*C2*TC**3+(C3+4.*C4*TF**3
     1-C4*TC**3)*X
      ER=E/DE
      TC=TC-ER
      IF (ABS(ER) .GT. 1.) GOTO 10
      RETURN
      END
C
      SUBROUTINE NEWRAPH2(C1,C2,C5,C6,TC,TA,TP)
   10 TM=(TC+TA)/2.
      C5=C5/TM
      F1=C1*(TP-TC)+C2*(TP**4-TC**4)
      F2=C5*(TC-TA)**(4./3.)+C6*(TC**4-TA**4)
      E=F1-F2
      DE=-C1-4.*(C2+C6)*TC**3-4./3.*C5*(TC-TA)**(1./3.)
      ER=E/DE
      TC=TC-ER
      IF (ABS(ER) .GT. 1.) GOTO 10
      RETURN
      END
```

```
C
C   ***************************************************
C   *  THIS PROGRAM CALCULATES THE EMISSIVITY OF THE  *
C   *  COMBUSTION GAS BY HADVIG'S CORRELATION AND THEN *
C   *  COMPUTES THE RADIATIVE COEFFICIENT IN THE HEAT  *
C   *  FLUX TO THE COVER SIDE.                         *
C   ***************************************************
      SUBROUTINE RADATA(DIAM,DCOV,DREF,E2,EXAIR,T,TERM)
      F(Z)=.02668+1.236*Z-5.676*Z**2+17.46*Z**3-30.31*Z
     1**4+26.71*Z**5-9.291*Z**6
      TOTMOL=10.879+9.868*(EXAIR-1.)
      PCO2=1.017/TOTMOL
      PSUM=2.978*PCO2
      PR=0.85*PSUM*(DREF-DCOV)
      Z=PR
      F1=F(Z)
      Z=2.*PR
      F2=F(Z)
      E3=(2.7-T/1000.)*F1
      A=E3/(2.-F2/F1)
      B=A/E3-1.
      C=B*DCOV/DREF
      D=1.3*E2*DCOV/DIAM
      TERM=(1.3*E2*(1.+C)/((1.+B+C)*E3)+(1.-1.3*E2)/A)/D
      RETURN
      END
C
C   ***************************************************
C   *  THIS ROUTINE CALCULATES THE MINIMUM AND MAXIMUM *
C   *  TEMPERATURES IN EACH COIL OF THE STACK          *
C   ***************************************************
      SUBROUTINE TLIMIT(M,L,IL,JL,II,JJ,T,TL)
      DIMENSION T(5,8,9)
      II=1
      JJ=1
      TL=T(M,II,JJ)
      DO 30 I=1,IL
      DO 30 J=1,JL
      IF (L .GT.0) GOTO 10
      IF (TL .LE. T(M,I,J)) GOTO 30
      GOTO 20
   10 IF (TL .GE. T(M,I,J)) GOTO 30
   20 TL=T(M,I,J)
      II=I
      JJ=J
   30 CONTINUE
      RETURN
      END
```

```
C
C   ****************************************************************
C   *  THIS SUBPROGRAM COMPUTES THE OVERALL MEAN TEMP              *
C   *  IN THE WHOLE STACK OF STEEL COILS.                          *
C   ****************************************************************
      SUBROUTINE TMEAN(NCOILS,T,DC,DCOR,DR,DZ,H,TM)
      DIMENSION T(5,6,9),DCOR(5),DC(5),H(5),DR(5),DZ(5)
      TTOT=0.
      TVOL=0.
      DEN=0.
      DO 20 M=1,NCOILS
      IL=IFIX((DC(M)-DCOR(M))/(2.*DR(M))+.1)+1
      JL=IFIX(H(M)/DZ(M)+.1)+1
      DO 10 I=1,IL
      DO 10 J=1,JL
      TTOT=TTOT+T(M,I,J)
   10 CONTINUE
      DEN=DEN+FLOAT(IL*JL)
      TVOL=TVOL+.7854*(DC(M)**2-DCOR(M)**2)*H(M)
   20 CONTINUE
      TAV=TTOT/DEN
      CALL STEELCAP(TAV,FP,FR)
      HIN=TVOL*FP*TAV
      TM=400.
   30 FN=0.6352*TM+2.146E-3*TM**2-3.813E-6*TM**3+3.135E-9*
     1TM**4-HIN/TVOL
      FD=0.6352+4.291E-3*TM-1.144E-5*TM**2+1.2538E-8*TM**3
      TM=TM-FN/FD
      IF (ABS(FN/FD) .GT. 1.) GOTO 30
      RETURN
      END
      FINISH
****

LLLLLLLLLLLLLLLLLLLLLLLLLLLLLLLLLLLLLLLLLLLLLLLLLLLLLLLLLLLLLLLLLLL
L                                 LLLLLLLLLLLLLLLLLLLLLLLLLLLLLLLLLL
L      NUMBER OF PAGES   24       LLLLLLLLLLLLLLLLLLLLLLLLLLLLLLLLLL
L                                 LLLLLLLLLLLLLLLLLLLLLLLLLLLLLLLLLL
LLLLLLLLLLLLLLLLLLLLLLLLLLLLLLLLLLLLLLLLLLLLLLLLLLLLLLLLLLLLLLLLLLL
```

REFERENCES

1. Lihou, D.A., 'Heaters for Chemical Reactors' an industrial survey, IChemE, 1975.

2. Hottel, H.C. and Sarofim, A.F., 'Radiative Transfer, McGraw-Hill Book Co., 1967.

3. Hottel, H.C. and Cohen, E.S., AIChE Journal, 4, 3, 1958.

4. Gill, D.W., Loveridge, J.D. and Thurlow, G.G., 12th Int.Symp. on Combustion, The Comb. Inst., p.1239, 1969.

5. Lucas, D.M. and Lockett, A.A., 4th Simp. on Flame and Industry, paper 15, Brit. Flame Res. Comm. and Inst. Fuel, 1972.

6. Lobo, W.E. and Evans, J.E., Trans. AIChE, 24, 743, 1939.

7. Hottel, H.C., J.Inst.Fuel, 34, 220, 1961.

8. Roesler, F.C., Chem.Engng.Sci., 22, 1325, 1967.

9. Campbell, P.M., Int.J.Heat and Mass Transfer, 10, 519, 1967.

10. Howell, J.R., 'Adv. in Heat Transfer', 5, 2, Academic Press, London, 1968.

11. Hadvig, S., J.Inst. of Fuel, 129-135, 1970.

12. Kennett, S.J. and Owen, S.W., 'Some Metallurgical Aspects of Annealing of Mild Steel Strip and Sheet', Conference on Recent Developments in Annealing, The Iron and Steel Institute, 1963.

13. Rosier, C., 'Analog Study of Heat Transfer into a Steel Coil during Annealing', Conference in Metallurgical Process Development, The Iron and Steel Institute, 1969.

14. Hawdon, G.A., 'Conventional Methods in Batch Annealing', The Iron and Steel Institute Conference, 1963.

15. Lihou, D.A., Trans.IChemE, 55, 225-242, 1977.

16. British Gas Data Book, Vol. 1, 1974.

17. Gilchrist, J.D., 'Fuels, Furnaces and Refractories', Pergamon International Library, 1977.

18.. Gray, W.A. and Müller, R., 'Engineering Calculations in Radiative Heat Transfer', Int. Series on Materials Science and Technology Vol. 13, Pergamon Press, 1974.

19. McAdams, W.H., 'Heat Transmission' 3rd edn., International Student Edition, McGraw-Hill Co., 1954.

20. Spiers, H.M., 'Technical Data on Fuel', 5th edn., The Brit. National Comm., World Power Conference, London, 1955.

21. Engineering Science Data Unit, item no. 68007, 1968.

22. Jenson, V.G. and Jeffreys, G.V., 'Mathematical Methods in Chemical Engineering', 2nd edn., Academic Press, 1977.

23. Collier, W.D., 'Heatran', A Finite Element Code for Heat Transfer Problems, special report.

24. Spiers, H.M., 'Technical Data on Fuel', 6th edn., The Brit. National Comm., World Power Conference, London, 1961.

25. Abdelsalam, T.M., Lihou, D.A. and Gay, B., Annual Res. Meeting, IChemE, 1978.

26. La Fara, R.L., 'Computer Methods for Science and Engineering,' International Textbooks Co., 1973.

27. Barakat, H.Z. and Clerk, J.A., J. Heat Transfer, Trans. of ASME, 421-427, 1966.

28. Smith, J.H., J.Computational Phys., 17, 181-191, 1975.

29. Crank, J. and Nicolson, P., Proc.Camp.Phil.Soc., 43, 50-64, 1947.

30. Perry, R.H. and Chilton, C.H., 'Chem.Engineers' Handbook', 5th edn., McGraw-Hill Book Co., 1973.